Department of
Architecture and Built Environment

The University of Nottingham

INVESTIGATION OF NOVEL EVAPORATIVE COOLING MATERIAL FOR CYPRUS CLIMATE

PERVİN ABOHORLU DOĞRAMACI

B. Arch, M. Arch

Thesis submitted to the University of Nottingham for the degree of Doctor of Philosophy
August 2018

INVESTIGATION OF NOVEL EVAPORATIVE COOLING MATERIAL FOR CYPRUS CLIMATE

Pervin Abohorlu Doğramacı

B. Arch, M. Arch

Contents

Contents **1**
Abstract **7**
Publications **9**
Acknowledgements **10**
Dedication **11**
Nomenclature **12**
List of Figures **15**
List of Tables **23**

CHAPTER 1: Introduction **25**

1.1 Background and problem definition 25
1.2 Research aims and objectives 33
1.3 Methodology of the research 35
1.4 The novelty of the research 38
1.5 The scope and limitations of the research 39
1.6 The layout of the thesis 39

CHAPTER 2: A Review of Thermal Comfort and Evaporative Cooling **41**

2.1 Introduction 41
2.2 Thermal Comfort 42
2.2.1 Psychrometric Chart 42
2.3 Passive Cooling 43
2.3.1 Basic Building Design Parameters (Principles or Strategies) for Cooling 45
2.3.2 Ventilative Cooling 47
2.3.3 Radiative Cooling 47
2.3.4 Earth Cooling 48
2.3.5 Dehumidification with a Desiccant 49
2.4 Evaporative Cooling (EC) 49
2.4.1 Architectural Background of Evaporative Cooling 53

2.4.2 Direct Evaporative Cooling (DEC) 55
2.4.2.1 Mechanical Evaporative Cooling Systems 57
2.4.2.2 Homemade Passive Direct Evaporative Cooling Devices 57
2.4.2.3 The Cooling Tower of Cunningham and Thompson 58
2.4.3 Indirect Evaporative Cooling (IEC) 59
2.4.3.1 Ventilated Roof Ponds with Fixed Insulations 59
2.4.3.2 Roof Ponds with Floating Insulation 60
2.4.3.3 Insulation Embedded within the Pond 60
2.4.4 Desiccant Evaporative Cooling 60
2.4.5 Direct/Indirect Combinations 64
2.4.6 Application of Direct and Indirect Evaporative Cooling 65
2.4.7 Advantages and Disadvantages of Evaporative Cooling 67
2.5 Architectural Integration of Evaporative Cooling 68
2.5.1 Functional Integration 75
2.5.2 Constructive Integration 75
2.5.3 Formal Integration 76
2.6 Evaporative Cooling Pads 77
2.6.1 Wood Materials (Eucalyptus Tree) 78
2.6.2 Stone Materials (Yellow Stone) 79
2.6.3 Polymer Hollow Fibre 80
2.7 The Performance of Evaporative Cooling 81
2.7.1 Temperature Difference 81
2.7.2 Cooling Efficiency 82
2.7.3 Cooling Capacity 82
2.7.4 Coefficient of performance (COP) 83
2.7.5 Evaporation Rate 83
2.7.6 Specific Cooling Capacity 84
2.7.7 Uncertainty analysis 85
2.8 Water Harvesting Technology 85
2.8.1 Rainwater Harvesting 86
2.8.2 Ground water Harvesting 88
2.8.3 Water Desalination 89
2.8.4 Atmospheric Water Harvesting 93
2.8.5 Summary of Water Harvesting Technology 96

2.9 Conclusion 100

CHAPTER 3: Experimental measurements of local materials of evaporative cooling performance 102

3.1 Introduction 102

3.2 Experimental investigation of the potential of local materials for evaporative cooling application 103

3.2.1 Experimental Methodology 105

3.2.2 Testing of materials 108

3.2.2.1 Eucalyptus fibres 110

3.2.2.2 Yellow stone 111

3.2.2.3 Cyprus marble 112

3.2.2.4 Ceramic pipes 113

3.2.2.5 Dry bulrush basket 114

3.2.3 Comparison of the performance of testing results 115

3.3 The wind tunnel experiment for performance comparison of eucalyptus fibres and yellow stone for evaporative cooling 119

3.3.1 System description for local materials 120

3.3.2 Test procedure for unit 124

3.3.3 Experimental results 126

3.3.3.1 The effect of air velocity on temperature difference 130

3.3.3.2 The effect of air velocity on outlet relative humidity 133

3.3.3.3 The effect of air velocity on cooling efficiency 134

3.3.3.4 The effect of air velocity on cooling capacity 135

3.3.3.5 The effect of air velocity on COP 136

3.3.3.6 The effect of air velocity on evaporation rate 138

3.3.3.7 The effect of air velocity on specific cooling capacity 140

3.3.4 Determinations of optimum operating parameters for eucalyptus fibres 141

3.4 Numerical analysis of eucalyptus fibres based evaporative cooling system 146

3.4.1 Mathematical Formulation 146

3.4.2 The effect of inlet dry bulb temperature on performace of the system 147

3.4.3 The effect of inlet air velocity on performance of the system 152

3.5 Conclusion 157

CHAPTER 4: Conceptual Design Ideas of Integrated Eucalyptus Fibres Based Evaporative Cooling Panel (EFECP) into Building Elements 158

4.1 Introduction 158
4.2 Sizing and structural system of eucalyptus fibres based evaporative cooling Panel 159
4.3 Comparison matrix for building elements integrated eucalyptus fibres evaporative cooling panel and building requirements 163
4.4 Shutter integrated EFECP 168
4.5 Window and door integrated EFECP 170
4.6 Toplighting integrated EFECP 172
4.7 Wind-solar tower integrated EFECP 176
4.8 Wall integrated EFECP 178
4.8 Conclusion 180

CHAPTER 5: Application of evaporative cooling for a house in Cyprus 182

5.1 Introduction 182
5.2 Building Simulation Programmes 182
5.3 Autodesk Ecotect 182
5.4 Description of Modelled House in Kyrenia, Cyprus 183
5.4.1 Climatic Zones of Cyprus 183
5.4.2 Climatic Data of Cyprus 185
5.4.3 Environmental Conditions of Modelled House 186
5.4.4 Geometrical Model of House 189
5.4.5 Building Components and Constructional Conditions 190
5.4.6 Thermal Conditions 192
5.4.7 Zoning of Modelled Building 193
5.5 Analyses of Modelled House in Nicosia, Cyprus 194
5.5.1 Hourly Temperatures for all Visible Thermal Zones 195
5.5.2 Hourly Gains and Losses for all Visible Thermal Zones 197
5.5.3 Gains Breakdown for all Visible Thermal Zones 198
5.5.4 Monthly Heating and Cooling Loads 199

5.5.5 Simulation Results 203
5.5.6 Economic and Environmental Analyses 205

CHAPTER 6: Hollow fibre used for evaporative cooling performances through experimental investigations 215

6.1 Introduction 215
6.2 Hollow fibre integrated evaporative cooling system with bundles in a horizontal cylinder test module 217
6.2.1 Test rig description for hollow fibre material 217
6.2.2 Procedure of the test rig 222
6.2.3 Results of the test for hollow fibres 222
6.2.3.1 Temperature difference at different air velocity 223
6.2.3.2 Relative humidity at different air velocity 226
6.2.3.3 Cooling efficiency at different air velocity 227
6.2.3.4 Cooling capacity at different air velocity 229
6.2.3.5 COP at different air velocity 230
6.2.3.6 The effect of air velocity on evaporation rate 231
6.3 Hollow fibre integrated evaporative cooling system with bundles in circular module 232
6.3.1 System description for hollow fibres material 232
6.3.2 Procedure of the test rig 238
6.3.3 Results of the test for hollow fibre 238
6.3.3.1 Outlet temperature at different air velocity 240
6.3.3.2 Relative humidity at different air velocity 241
6.3.3.3 Cooling efficiency at different air velocity 243
6.3.3.4 Cooling capacity at different air velocity 244
6.3.3.5 COP at different air velocity 245
6.4 Hollow fibre integrated evaporative cooling system with potassium formate desiccant dehumidification 246
6.4.1 System description for hollow fibres material 246
6.4.2 Procedure of the test rig 252
6.4.3 Results of the test for plastic fibre 253
6.4.3.1 The effect of different inlet air temperature and RH at different air velocity 254

6.4.3.2 The effect of different inlet RH at different air velocity 259
6.4.3.3 The effect of different solution concentration at different air velocity 262
6.5 A comparison of experimental study on eucalyptus fibres and hollow fibres 264
6.6 Conclusion 269

Chapter 7: Conclusion and Recommendations..... 273

REFERENCES 279

Abstract

Energy consumption by human enhanced activities has led to distinctive environmental problems; in particular, climate change and global warming. In hot regions, the main reason for energy consumption comes from the cooling of many buildings. The intensity and duration of the sunshine in hot regions have a direct relation with the usage of cooling systems. The energy used for cooling purpose is continuously increasing and expected to increase in the following years.

Evaporative cooling is one of the passive cooling method which has been used throughout history. As it is cheaper, environmentally-friendly and simpler compared to vapour compression systems, it is more widely used in residential, commercial and industrial buildings in hot and dry regions. Since this method is less efficient and limited under hot and humid climate, the desiccant based evaporative cooling system is preferred in such areas in order to dehumidify the air.

The pad material used for evaporative cooling system is important as it helps to evaporate the water. Therefore, the material should be porous enough to absorb water which enhances the rate of evaporation. Moreover, the material should be available and cheap. This study shows the potential of using different materials for evaporative cooling systems.

The aim of this study is to investigate the feasibility, suitability and potential of using local materials such as eucalyptus fibres, as cooling pads for evaporative cooling system in hot and dry regions. In addition to this, the liquid desiccant evaporative cooling systems by using potassium formate is also studied for hot and humid areas in Cyprus. Since Cyprus has multi-climate regions due to the topography and different weather condition, different cooling systems can be used for each region. The results are reported in terms of temperature difference, cooling output, COP, etc.

The wind tunnel is used to test the eucalyptus fibres with an inlet air temperature of 35 °C to simulate the climate in Cyprus. It was found that the maximum reduction of air temperature was between 11.3 °C and 6.6 °C, while

the maximum cooling efficiency was in the range of 71% and 49% at 0.1 and 0.6 m/s air velocity respectively. Corresponding cooling capacities were also calculated as 108 and 409 W indicating a directly proportional relation between air velocities and cooling performance.

Following this, the conceptual design ideas of integrated eucalyptus fibres based evaporative cooling panel (EFECP) into building elements are considered to meet the demand for cooling and the architectural requirements of the building. These design ideas were developed for shutter, fenestration, toplighting elements, wind catcher-solar chimney and wall design of the building.

The cooling performances of the hollow fibre integrated by using potassium formate desiccant based evaporative cooling system were experimentally investigated under the incoming air temperature in the range of 35 ˚C to 40 ˚C. The cooling capacity is increased as the air velocity is increased. At 3.5m/s, the cooling capacity is 1340 W, 1530 W and 1920 W respectively for incoming air relative humidity of 60%, 65% and 70%. Both evaporative cooling systems performances are discussed and clearly presented in this study.

From the experimental testing in this thesis, it is concluded that local eucalyptus fibres can be used for hot-dry areas and liquid desiccant evaporative cooling systems can be used for hot-humid areas of Cyprus. Since using of eucalyptus fibres for evaporative cooling system is locally available, simple construction and easy to apply, the design ideas for integrating eucalyptus fibres with evaporative cooling system are developed within the scope of the thesis.

The usage of local eucalyptus fibres and Polyvinylidene fluoride (PVDF) hollow fibres as evaporative cooling pad, the evaporative cooling process designed by using fibres and the conceptual building design ideas integrated local eucalyptus fibres combined with evaporative cooling system are all the novel ideas of this thesis.

Publications

Journal Papers

Abohorlu, P., Kurt, S., (2017). Traditional Earth Sheltered Buildings on Five Finger Mountain (Cyprus) Evaluation of the Energy Efficiency by Computer Simulating the Rectangular Plan Typology, Prostor: a scholarly journal of architecture and urban planning, Vol. 25, No. 1(53), 98-111.

Abohorlu Doğramacı, P., Riffat, S., Gan, G., Aydın, D., (2018). Experimental Study of the potential of Eucalyptus Fibres for Evaporative Cooling, Renewable Energy. https://doi.org/10.1016/j.renene.2018.07.005 (In press)

Conference Presentations (with paper)

Abohorlu, P., Riffat, S., (2015). Architectural Design Principles for Passive Cooling in Cyprus Climate, Sustainable Energy for a Resilient Future: Proceedings of the 14th International Conference on Sustainable Energy Technologies, 25-27 August 2015, Nottingham, UK. University of Nottingham: Architecture, Energy & Environment Research Group. Volume III, pp 587-594, ISBN 9780853583158.

Abohorlu, P., Riffat, S., Gan, G., (2016). Experimental Investigation of a New Material for Evaporative Cooling, Proceedings of the 15th International Conference on Sustainable Energy Technologies SET 2016, 19th 22nd of July 2016, National University of Singapore, Singapore, ISBN 978-981-11-0451-0.

Acknowledgements

I am very grateful to a number of people, who have been instrumental in getting this thesis to completion.

I would like to express the deepest appreciation to my supervisor, **Prof. Saffa Riffat** for his constant encouragement, scientific support and kind guidance throughout this PhD research journey.

I am very much indebted to my supervisor, **Dr. Guohui Gan** who gave tireless efforts through discussion and valuable suggestions ensured the success of this undertaking.

I would like to thank my examiners, **Dr. Yuehong Su** and **Dr. Andrei Chamchine** for their insightful comments and encouragement to widen my study from various perspectives.

I would like to express my extreme sincere gratitude and appreciation to **Dr. Devrim Aydın** for his kind endless help, creative advice and support during the study. Without his support, it would not be possible to conduct this study.

I express my sincere thanks to my friend, **Dr. Hasila Jarimi** for her encouragement and generous advice. Without her guidance and persistent help, this study would not have been possible.

I owe my sincere thanks to **Dr. Xiangjie Chen** who provided me an opportunity to join her team, and who gave access to the laboratory and research facilities.

I express my heartfelt thanks to my beloved teacher, **Prof. Dr. Sevinç Kurt** who is always there to stretch her helping hands. She inspires me to open the path for higher knowledge. She is my role model and will always be in my heart. Thank you for your critical suggestions and valuable support.

This study would not have been materialized without the financial and technical support of the University of Nottingham, Cyprus International University and Middle East Technical University Northern Cyprus Campus.

I would like to thank all **my friends** for their continuous support and valuable contributions towards the successful completion of this thesis.

I want to express my love and my regards to **my mother** and **my father** for their valuable love, encouragement and support throughout this journey.

Dedication

All my work is dedicated to my husband, Kazım

who inspires, supports and believes.

I couldn't have done it without you…

and also dedicated to my son and daughter, Atlas and Peri

to inspire them:

"*Where there is a will, there is a way*"

Nomenclature

A	Heat transfer area (m^2)
c_p	Specific heat at constant pressure (kJ/kg°C)
c_{pda}	Specific heat of dry air (kJ/kg°C)
COP_s	System coefficient of performance
d	Fiber diameter (m)
h	Specific enthalpy (kJ/kg)
h_k	Specific enthalpy of humid air (kJ/kg)
h_1	Specific enthalpy of inlet air (kJ/kg)
h_2	Specific enthalpy of outlet air (kJ/kg)
L	Length of hollow fibre bundle (m)
$\dot{m}_a$	Mass flow rate of air (g/s)
m_w	Evaporation rate (g/s)
N	Number of fibres inside the heat exchanger
Q_c	Sensible cooling capacity (kW)
Q_{total}	Total cooling capacity (sensible + latent) (kW)
T	Temperature (°C)
T_1	Inlet temperature (°C)
T_2	Outlet temperature (°C)
T'_1	Inlet wet bulb temperature (°C)
V	Velocity of air (m/s)
W_p	Pump electric power (kW)
w	Absolute humidity of air (kg_{wv}/kg_{da})
w_2	Outlet absolute humidity (kg_{wv}/kg_{da})
w_1	Inlet absolute humidity (kg_{wv}/kg_{da})

Abbreviations

ASHRAE	American society for Heating Ventilation Refrigeration and Air conditioning Engineer
CC	Cooling capacity (kW)
COP	Coefficient of performance
DBT	Dry bulb temperature (°C)
DEC	Direct evaporative cooling
EC	Evaporative cooling
ECC	Evaporative cooling cavity
EF	Eucalyptus fibres
EFECP	Eucalyptus Fibres Based Evaporative Cooling Panel
ER	Evaporation rate (g/s)
GHGs	Greenhouse gases
HF	Hollow fibres
MRR	Moisture removal rate (g/s)
RH	Relative humidity (%)
SC	Solar chimney
SCC	Specific cooling capacity (kWh/kg)
S_{CO_2}	Carbon dioxide savings
SFC	Standard Fog Collector
WBT	Wet bulb temperature (°C)
YS	Yellow stone

Greek Letters/Subscripts

a	air
ΔT	Temperature difference (°C)
in	Inside
ξ	Total yearly energy consumption (kWh)
H	Heat transfer

M	Mass transfer
ης	Cooling efficiency
ρ	Density of the fluid (kg/m^3)
ςe	Conversion factor of electricity
out	Outside
s	surface
sol	desiccant solution
v_1	saturated water vapour at the entrance of the hollow fibre manifold
v_2	saturated water vapour at the exit of the hollow fibre manifold
v	incoming air velocity, m/s

List of Figures

Figure 1. NASA graphs showing CO_2 and CH_4 concentrations (Riebeek, 2010) 26

Figure 2. Energy performance of buildings (Directive 2010/31/EU)..... 27

Figure 3. Electricity Authority of Northern Cyprus (Chart adapted from KIBTEK, 2013) 27

Figure 4. Electricity generation and consumption in North Cyprus (KIBTEK, 2013-2016)..... 28

Figure 5. The total energy generation (E_g) and consumption (E_c) for North Cyprus (KIBTEK, 2013-2016) 29

Figure 6. Traditional and Industrial Evaporative Cooling Solution 30

Figure 7. Evaporative cooling (modelled by author)..... 31

Figure 8. The structure of the methodology 37

Figure 9. Psychrometric chart (ASHRAE, 1997) 43

Figure 10. Cooling strategy (Baker, 1987) 44

Figure 11. Good cross ventilation (Lechner, 2009)..... 45

Figure 12. Different kind of overhangs (Lechner, 2009)..... 46

Figure 13. Earth-Sheltered Design Strategies (Moore, 1993) 48

Figure 14. (Up) Evaporative Food Coolerand (Down) Cooling the surrounding of the building..... 52

Figure 15. Air flows around jars creating cool breeze (Moore, 1993) 53

Figure 16. Muscatese evaporative cooling system (Phan, 2004)..... 54

Figure 17. Wind-Catcher (Moore, 1993). 54

Figure 18. Direct Evaporative Cooler (Musa, 2008). 55

Figure 19. Porch for DEC (Givoni, 1994). 58

Figure 20. Vapour pressure of potassium formate at different mass concentration (Beyer and Steiger, 2016) 63

Figure 21. Diagram of desiccant evaporative cooling (Elsarrag et al., 2016) .. 64

Figure 22. Direct/ Indirect Combination (Musa, 2008)..... 65

Figure 23. Direct and Indirect Combination (ASHRAE, 2000) 65

Figure 24. (a) DEC for inner land (b) IEC for coastal region (Baca et al., 2011) 66

Figure 25. Evaporative cooling system for Iran 67

Figure 26. The integration of the vaulted roof and evaporative cooling technique (Haghighi et al., 2015) 70

Figure 27. Evaporative cooling facade (Naticchia et al., 2010) 70

Figure 28. Porous plate integrated into wall (Chen, 2011)..... 71

Figure 29. Passive Evaporative Cooling Wall (He and Hoyano, 2011) 72

Figure 30. Water recirculation for evaporative cooling system (Franco et al., 2011)..... 72

Figure 31. Solar chimney and evaporative cooler (Miyazaki et al., 2011)..... 73

Figure 32. SC and ECC (Maerefat and Haghighi, 2010)..... 73

Figure 33. Schematic view of wind catcher integrations (Poshtiri and Mohabbati (2017); Calautit et al., (2017); Khani (2017)..... 74

Figure 34. Vegetal Facade (Ojembarrena et al., 2013)..... 76

Figure 35. Cross section of Akrotiri Aquifer (Demetriou and Georgiou, 2004) 89

Figure 36. Solar still desalination unit (Shatat et al., 2013) 90

Figure 37. New v-trough solar concentrator (Riffat and Mayere, 2013)..... 91

Figure 38. The fog collector screens (Karkee, 2005; Klemm et al., 2012; Brown, Bhushan, 2016) 94

Figure 39. Warka Water Towers, Ethiopia (Nguyen, 2014)..... 96

Figure 40. Water consumption by sector and water source supply (Savvides et al., 2001) 99

Figure 41. Testing local materials used in preliminary experiment for evaporative cooling..... 104

Figure 42. Structure of the experimental methodology 105

Figure 43. View of insulated box 106

Figure 44. Plan of experimental design 107

Figure 45. Photographs of the inside of the insulated box 107

Figure 46. The process of containing eucalyptus fibres 110

Figure 47. Yellow Stones with Different Types (10/18/25 mm holes) 111

Figure 48. Materials used in the experiments 112

Figure 49 Ceramic pipes 113

Figure 50. Dry bulrush basket 114

Figure 51. Test model plan of dry-bulrush basket 115

Figure 52. Cooling efficiency of local materials 118

Figure 53. Testing materials 119

Figure 54. Open Wind Tunnel (HM170) schematic 120

Figure 55. Integrated water pipe onto the meshed eucalyptus fibres 123

Figure 56. Integrated water pipe onto the yellow stone 123

Figure 57. (a) Schematic diagram of the experimental testing rig and (b) thermocouple locations 124

Figure 58. Schematic diagram and general view of the experiment (eucalyptus fibre) 125

Figure 59. Schematic diagram of the experiment (yellow stone) 125

Figure 60. Temperature difference of eucalyptus fibre and yellow stone 127

Figure 61. Outlet RH of eucalyptus fibre and yellow stone 127

Figure 62. Cooling efficiency of materials at 0.1m/s 128

Figure 63. Cooling capacity of eucalyptus fibre and yellow stone 129

Figure 64. COP of eucalyptus fibre and yellow stone 129

Figure 65. Effect of air velocity to outlet temperature at T_{in}= 35.5 °C 131

Figure 66. The variation of outlet air temperature for different air velocities (T_{in}= 35.5 °C) 131

Figure 67. Inlet, outlet DBT and water temperature difference at 0.1 m/s 132

Figure 68. Effect of air velocity on outlet relative humidity 134

Figure 69. Cooling efficiency trends at 0.1 - 1.2 m/s 135

Figure 70. Cooling capacity trends at 0.1 - 1.2 m/s 136

Figure 71. COP trends at 0.1 - 1.2 m/s 137

Figure 72. Correlation of outlet dry bulb temperature and COP 138

Figure 73. Evaporation rate trends at 0.1 - 1.2 m/s..... 139

Figure 74. Specific cooling capacity trends at 0.1 - 1.2 m/s..... 140

Figure 75. Combined effects of SCC and CC at different mass flow rate 142

Figure 76. Combined effects of COP and SCC at different mass flow rates.. 143

Figure 77. CC and SCC at different evaporation rates 144

Figure 78. Numerical results on (a) dry bulb temperature (b) evaporation rate and (c) cooling capacity (at 35°C and 0.6 m/s) 148

Figure 79. Numerical results on (a) dry bulb temperature (b) evaporation rate and (c) cooling capacity (at 40°C and 0.6 m/s) 150

Figure 80. Numerical results on (a) evaporation rate at 0.9 m/s (b) evaporation rate at 1.2 m/s (at 35°C)..... 153

Figure 81. Numerical results on (a) cooling capacity at 0.9 m/s (b) cooling capacity at 1.2 m/s (at 35°C) 154

Figure 82. Numerical results on (a) evaporation rate at 0.9 m/s (b) evaporation rate at 1.2 m/s (at 40°C)..... 155

Figure 83. Numerical results on (a) cooling capacity at 0.9 m/s (b) cooling capacity at 1.2 m/s (at 40°C) 156

Figure 84. Structural system of EFECP a) perspective b) system detail (designed by author) 162

Figure 85. 3D view of Eucalyptus fibres evaporative cooling system 163

Figure 86. Building requirements for comparison matrix 164

Figure 87. Evaporative cooling system integrated shutter a) horizontally folded evaporative shutter b) vertically folded evaporative shutter c) sliding evaporative shutter d) pivot evaporative shutter..... 169

Figure 88. Evaporative cooling system integrated into window 171

Figure 89. Evaporative cooling system integrated into door..... 171

Figure 90. Evaporative cooling system integrated into window 172

Figure 91. Skylight, Sawtooth at clerestory, Monitor (Kadir et al., 2015)..... 173

Figure 92. Evaporative cooling system a) integrated baffles and b) monitor in summer and winter condition 174

Figure 93. Evaporative cooling system integrated a) sawtooth and b) clerestory 176

Figure 94. Evaporative cooling system “wind-solar tower” 177

Figure 95. Glazing with shading device facing south-west..... 178

Figure 96. Evaporative cooling system facing north-west 179

Figure 97. Combined evaporative cooling system and curtain wall..... 179

Figure 98. Cyprus 184

Figure 99. Average Annual Temperature for July (Table adapted from Department of Meteorology, TRNC, 2014) 186

Figure 100. Aerial view of Modelled House in Kyrenia (Source: Google Earth) 187

Figure 101. Monthly average temperature, relative humidity, wind analysis and incident solar radiation for Cyprus (Kyrenia) generated from Ecotect 188

Figure 102. General view of apartment block 189

Figure 103. Sun path diagram of the case area with Ecotect v 5.50..... 190

Figure 104. Floor plan layout of modelled house..... 194

Figure 105. Hourly Temperature for all Thermal Zones 196

Figure 106. (a) Hourly Temperature for Zone 1 (Bedroom) and (b) 2 (Living Room and Kitchen)..... 197

Figure 107. Hourly gains and losses for the hottest month 198

Figure 108. Gains breakdown for all thermal zones..... 199

Figure 109. Monthly cooling and heating loads for Zone 1 and 2 201

Figure 110. Monthly cooling and heating loads of AC system for all thermal zones 202

Figure 111. Payback period of the integrated eucalyptus fibre based evaporative cooling panel (EFECP) 209

Figure 112. CO_2 savings using EFECP in comparison with AC 214

Figure 113. Diagram of the hollow fibre integrated evaporative cooling system 217

Figure 114. The flow cross section of aluminium tunnel 218

Figure 115. Detailed 3D model of testing 219

Figure 116. The actual testing prototype 219

Figure 117. General view of the test rig 220

Figure 118. The cross section of the duct showing thermocouple locations as T1-T4 221

Figure 119. Temperature difference trends for hollow fibres at 0.6 - 1.5 m/s at 30°C 224

Figure 120. Temperature difference trends for hollow fibres at 0.6 - 1.5 m/s at 36°C 225

Figure 121. Temperature difference trends for hollow fibres at 0.6 - 1.5 m/s at 40°C 225

Figure 122. Outlet relative humidity trends at 1.2 m/s 226

Figure 123. Cooling efficiency trends for hollow fibres at 0.6 - 1.5 m/s at 30°C 227

Figure 124. Cooling efficiency trends for hollow fibres at 0.6 - 1.5 m/s at 36°C 228

Figure 125. Cooling efficiency trends for hollow fibres at 0.6 - 1.5 m/s at 40°C 229

Figure 126. Cooling capacity trends at 1.2 – 2.5 m/s 230

Figure 127. COP trends 231

Figure 128. Water consumption trends at 1.2 - 2.5 m/s 232

Figure 129. Diagram of the hollow fibre manifold 233

Figure 130. Detailed view of the glass box 234

Figure 131. The actual testing prototype 235

Figure 132. Detailed 3D model of testing 235

Figure 133. Side image of the system 236

Figure 134. The cross section of the duct showing thermocouple locations as T1-T4 237

Figure 135. Outlet air dry temperature at 0.25 - 3.5 m/s at 35°C 241

Figure 136. Outlet relative humidity at different air velocities for different inlet air humidity conditions 242

Figure 137. Absolute humidity change at different velocities for different inlet air humidity conditions 242

Figure 138. Cooling efficiency at different air velocities 243

Figure 139. Cooling capacity at different air velocities 244

Figure 140. COP at different air velocities 245

Figure 141. Schematic diagram of polymer hollow fibre integrated evaporative cooling system with desiccant dehumidification 247

Figure 142. Detailed view of the glass box 248

Figure 143. The actual and 3D view testing prototype 249

Figure 144. The cross section of the duct showing thermocouple locations as T1-T4 251

Figure 145. The dehumidifier moisture removal rate trends at different air temperature (T_{in}= 35-40ºC at 70%RH) 255

Figure 146. The dehumidifier moisture removal rate trends at different relative humidity (RH=55-75%, velocity: 0,7m/s) 255

Figure 147. The cooling capacity trends at different air temperature and relative humidity (T_{in}= 35-40ºC, RH=70%) 256

Figure 148. The cooling capacity trends at different relative humidity (RH=55-75%, velocity: 0,7m/s) 257

Figure 149. The dehumidifier effectiveness trends at different air temperature (T_{in}= 35-40ºC, RH=70%) 258

Figure 150. The dehumidifier effectiveness trends at different relative humidity (RH=55-75%, velocity: 0,7m/s) 258

Figure 151. The dehumidifier moisture removal rate trends at different air velocity (T_{in}= 35ºC, sol=62%) 259

Figure 152. The cooling capacity trends at different air velocity (T_{in}= 35ºC, sol=62%)..... 260

Figure 153. The dehumidifier effectiveness trends at different air velocity (T_{in}= 35ºC, sol=62%)..... 261

Figure 154. The dehumidifier moisture removal rate trends at solution concentration (T_{in}= 35ºC, RH=60%)..... 262

Figure 155. The cooling capacity trends at different solution concentration (T_{in}= 35ºC, RH=60%)..... 263

Figure 156. The cooling capacity trends at solution concentration (Tin= 35ºC, RH=60%)..... 264

List of Tables

Table 1. Previous studies on evaporative cooling material 32

Table 2. Summary of advantages and disadvantages of evaporative cooling .. 68

Table 3. Various fog harvesting installed worldwide 95

Table 4. Type of water resources of Cyprus (Farmer et al., 2006) 97

Table 5. Some water harvesting technologies 98

Table 6. Performance comparison of local materials 116

Table 7. Temperature reduction through different type of yellow stones at 30°C inlet air 117

Table 8. Characteristics of experimental sensors 121

Table 9. Errors for uncertainty analysis 122

Table 10. Temperature drop and cooling efficiency of materials at 0.1 m/s .. 128

Table 11. Readings at 0.1 m/s 133

Table 12. Results of eucalyptus fibres under experimentation 141

Table 13. Optimum conditions for using eucalyptus fibres 145

Table 14. Numerical simulation at three various inlet RH 151

Table 15. Numerical simulation at two various inlet DBT 151

Table 16. Numerical simulation at three various inlet air velocity 152

Table 17. Questions to evaluate the performance of the building elements integrated evaporative cooling system 165

Table 18. Comparative table between the building elements integrated evaporative cooling system and building requirements 167

Table 19. Implemented Settings for Modelled House 191

Table 20. Implemented Zoning for Modelled House 193

Table 21. Gains breakdown for period 1st January to 31st December 199

Table 22. Annual cooling load of each zone 200

Table 23. Monthly cooling loads of modelled house 202

Table 24. Monthly cooling loads of AC system for all thermal zones with cooling capacity of system operation 204

Table 25. Optimum design conditions for using 1 m² eucalyptus fibres 206

Table 26. The cost of system components 207

Table 27. The results of economic analysis of AC 210

Table 28. The results of economic analysis of EC 211

Table 29. The results of CO_2 Emissions of EFECP and AC 213

Table 30. Properties of experimental sensors used in the test 221

Table 31. Testing data for three different experimental conditions 223

Table 32. Data for three different experimental conditions 239

Table 33. Properties of experimental sensors used in the test 251

Table 34. Testing data of dehumidifier performance for various experimental conditions 254

Table 35. Testing results of the experimentations 267

Table 36. Comparative summary of evaporative cooling systems 268

CHAPTER 1: Introduction

1.1 Background and problem definition

The climate of the Earth changes by natural means; the location and duration of the sun, the geographic structure of the earth and the atmospheric conditions. However, today human activities are largely responsible for the warming of the earth. This particularly started after the Industrial Revolution in the 18th century (Riebeek, 2010). The average temperature of the earth gradually increased by 0.6 – 0.9 °C in the period between 1906-2005. It is expected to further rise 2 – 6 °C by the end of the 21st century. It is claimed that the increased has doubled for the last 50 years. However this does not mean that it is started in that time period (Riebeek, 2010). According to Fourier (1824), Tyndall (1863), Arrhenius (1896) and Chamberlain (1897), one of the greenhouse gases, carbon dioxide emission had already warmed the Earth (Grundmann, 2013).

"Throughout its long history, the Earth has warmed and cooled. Climate has changed when the planet received more or less sunlight due to subtle shifts in its orbit, as the atmosphere or surface changed, or when the Sun's energy varied. But in the past century, another force has started to influence Earth's climate: humanity" (Riebeek, 2010).

The greenhouse gases such as methane, nitrous oxide, carbon dioxide and so on are increased by the electricity, transportation, industry, agriculture, residential and commercial building sector. The CO_2 levels have increased by 38% and CH_4 by 148% until 2009 (Figure 1).

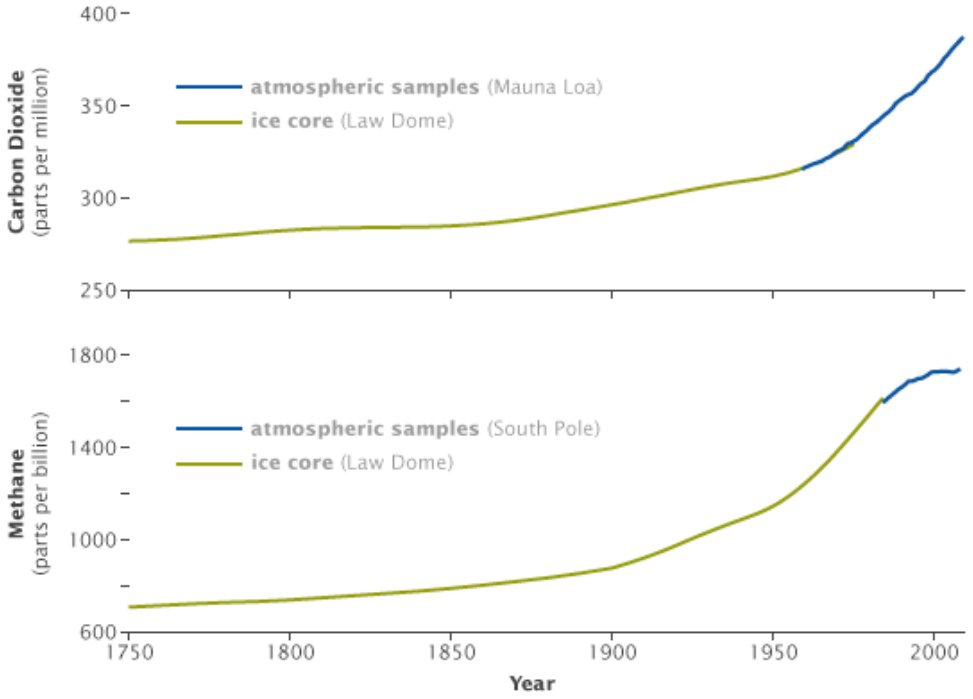


Figure 1. NASA graphs showing CO_2 and CH_4 concentrations (Riebeek, 2010)

Buildings in European Union are responsible for 40% of CO_2 emissions and total energy consumption (Figure 2). By 2020, the greenhouse gases emissions can be reduced by 20%. Therefore, energy performance of building is a key factor for reducing gas emissions and climate change. Energy consumption can be reduced and renewable energy usage can be increased in order to supply safe energy, technological growth and to provide employment opportunity (Directive 2010/31/EU). According to the Directive 2010, energy consumption is mostly used for heating (31%) residential buildings. The next largest consumption is cooling demand at 12%. However, the results vary according to the location of the country. The heating demand is lower in hot regions, whereas it is higher in the cold northern regions.

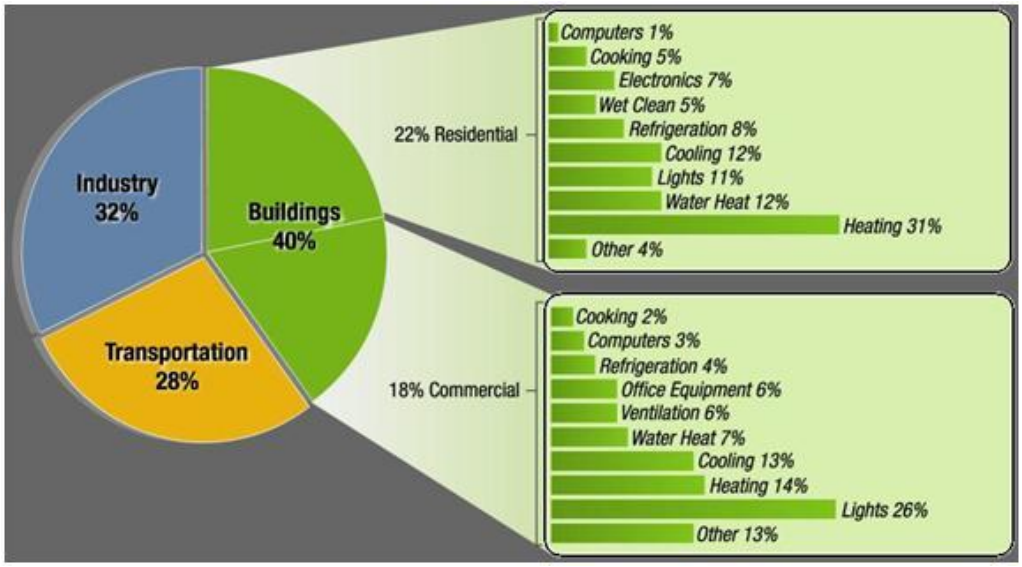


Figure 2. Energy performance of buildings (Directive 2010/31/EU)

As Cyprus has a subtropical climate, the energy consumption in the building (residential and commercial) is caused by the usage of heating, daylighting, and mostly, for cooling (Figure 3). Compared to the energy consumption in the UK, space and water heating accounted for 44.89% of domestic use of energy in 2013. Since the climate in the UK is generally cool, energy is consumed to maintain warmer indoor temperature (Dukes, 2017).

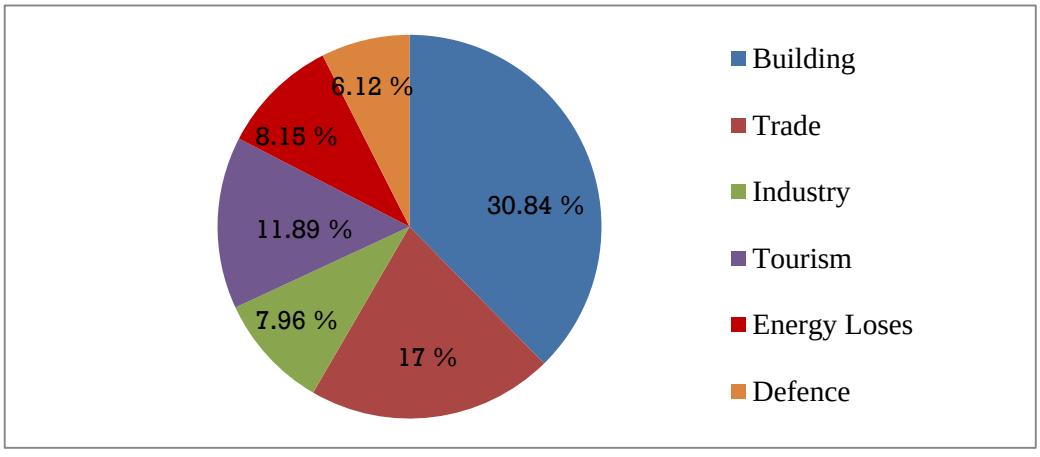


Figure 3. Electricity Authority of Northern Cyprus (Chart adapted from KIBTEK, 2013)

In Cyprus, electricity is mainly produced and consumed during summer (Figure 4). Therefore, the energy demand and electricity production for cooling are increased in summer. Due to the extreme weather conditions, a mechanical way of cooling, i.e. air-conditioning is mostly used.

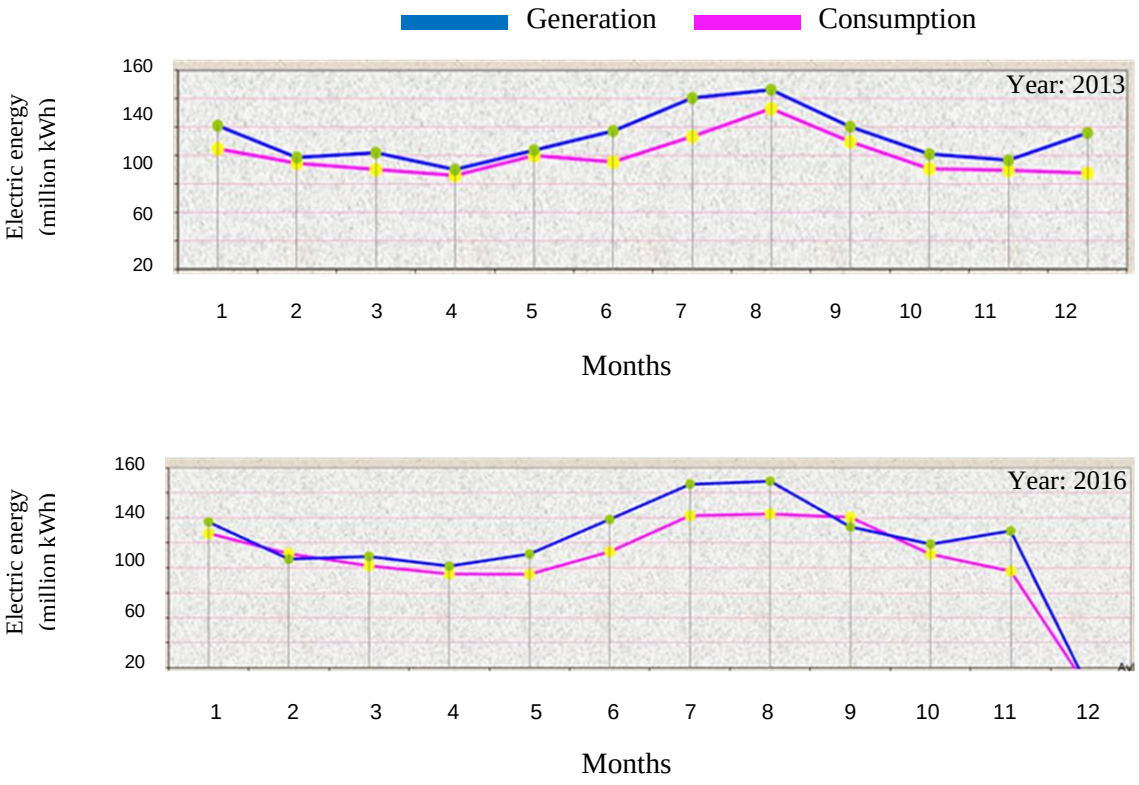


Figure 4. Electricity generation and consumption in North Cyprus (KIBTEK, 2013-2016)

The population of North Cyprus is 313.626 thousand people in 2014 (286.257 in 2011). As the population of Cyprus is increased, the demand for new housing and thus, the energy consumption is also increased. The total energy consumption for North Cyprus was 1195 GWh in 2013 whereas for 2016, it was increased to 1275 GWh by 6% increase as seen in Figure 5.

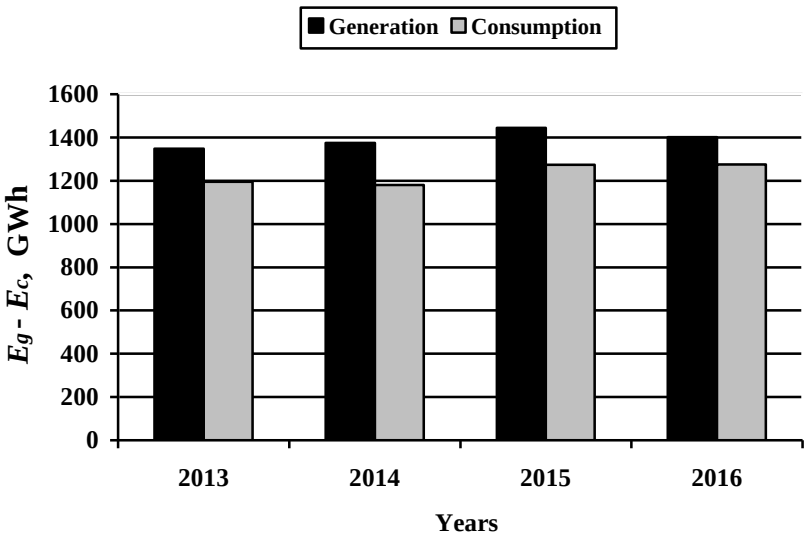
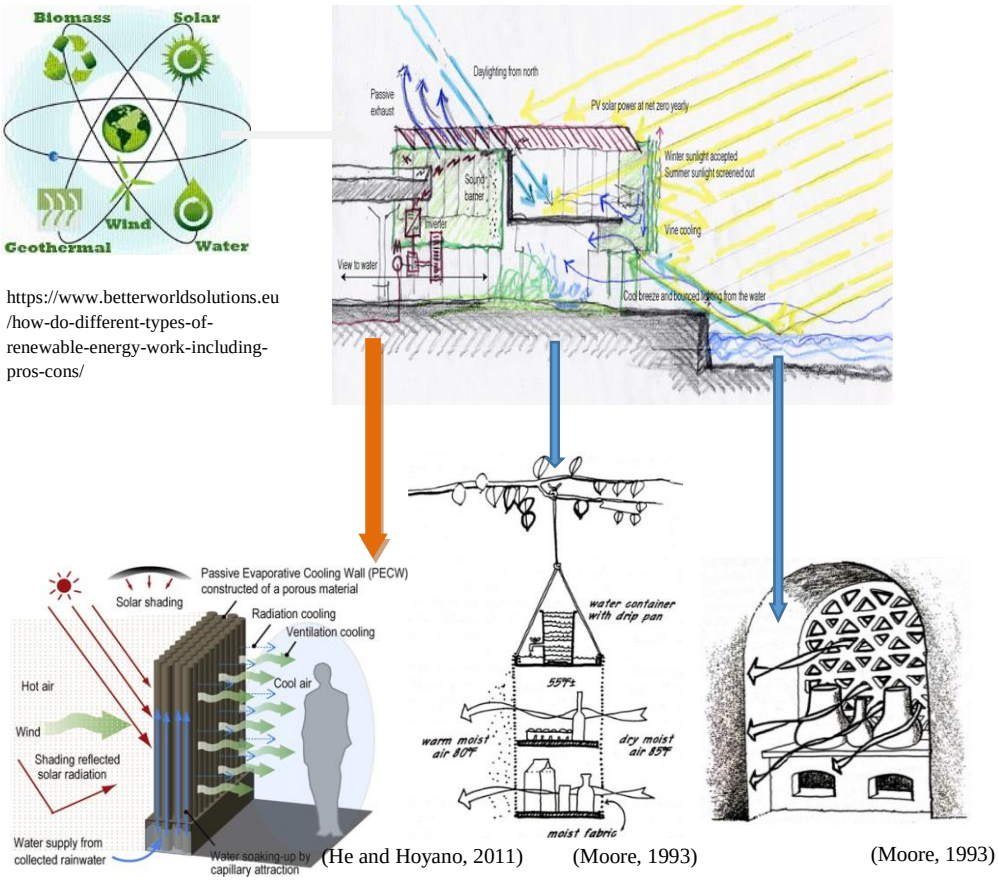


Figure 5. The total energy generation (E_g) and consumption (E_c) for North Cyprus (KIBTEK, 2013-2016)

It should be concluded that the high use of fossil fuels, as non-renewable resources can lead to environmental pollution, the need to import energy and an effect on climate change.

The renewable energies such as solar energy, wind energy, ocean energy, etc. have been passively used for lighting, cooling and heating buildings since ancient times. Many buildings, especially those nearer to the sea, have the advantage of taking cool breezes inside of the building due to the different atmospheric pressure created by the land and sea. This is called **evaporative cooling** and is a very old way of cooling method. According to a number of studies, it can be divided into two parts: *traditional* and *industrial solution* (Figure 6). As seen in building section, renewable energy such as sun and wind are used directly to create cool breeze coming from the sea which enhances cooling effect by evaporation of water. The method of evaporative cooling is divided into two sections: active and passive evaporative cooling. These passive methods (blue arrow) are not currently applied to the building. However, there is a huge number of research to study the active (orange arrow) way of evaporative cooling for building element.



https://www.betterworldsolutions.eu/how-do-different-types-of-renewable-energy-work-including-pros-cons/

(He and Hoyano, 2011) (Moore, 1993) (Moore, 1993)

Figure 6. Traditional and Industrial Evaporative Cooling Solution

As seen in Figure 7, in evaporative cooling, dry air is passed via an evaporative pad; it gets cooled and is then passed to the indoors (Wu et al., 2009; Rogdakis et al., 2013; Kabeel et al., 2017; Kovačević and Sourbron, 2017). It utilizes latent heat of evaporation of water to create cooling effect and can be direct, indirect or a combination of these. The combination types are also known as hybrid or integrated types. Misting or drip systems, cool cells/wetted pads and fogging systems are three main methods of evaporative cooling (Musa, 2008).

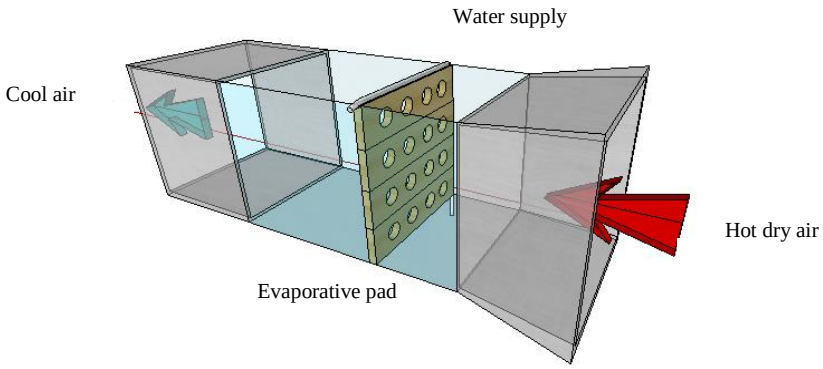


Figure 7. Evaporative cooling (modelled by author)

Material used in the evaporative cooling method has been widely investigated by many researchers for hot climate conditions. According to the studies, these materials can be fibre, ceramic, plastic and paper which show good performances in reducing temperature as it is shown in Table 1.

Different fibre pads are also used as a cooling pads such as jute fibres (Kulkarni and Rajput, 2010), coconut fibres (Rawangkul et al., 2008), luffa fibre (Al-Sulaiman, 2002), rice husk (Soponpongpipat and Kositchaimongkol, 2011).

Jain and Hindoliya (2011) conducted studies using Palash Fibre which provided 14°C temperature difference. Celdek, straw and sliced wood pads were tested for greenhouses for optimizing greenhouse temperature and humidity for crop growth. The results revealed that sliced wood pads showed better performance compared to other evaporative cooling materials (Ahmed et al., 2011). Wanphen and Nagano (2009) have found that siliceous shale absorbs more vapour due to the higher pore volume and pore size which provided 6.8-8.6°C temperature differences. Gunhan et al., (2007) studied the potential of pumice stones, volcanic tuff and greenhouse shading net at four different levels of air velocity and two different levels of RH. As a result, it was obtained that volcanic tuff pads perform best at 0.6 m/s air velocity. Atikol and Hacışevki (2001) have studied the suitability of evaporative cooling systems in Cyprus, particularly in Nicosia. According to their feasibility study, it is suggested that evaporative cooling can be used in May and September without any need of an additional cooling system. It was also found that in

June, effective cooling can be achieved only between 12.00 pm-15.00 pm hours. Since the evaporative cooling is not sufficient in July and August, an auxiliary cooling system is needed during that period. Although a lot of researchers studied to find better local materials for evaporative cooling, there is a lack of research to be done in Cyprus in terms of local materials for evaporative cooling process.

Table 1. Previous studies on evaporative cooling material

Researcher	**Material**	ΔT (°C)	Air Velocity (m/s)	Cooling Efficiency (%)
Sulaiman (2002)	**Jute**	-	-	62
Liao and Chiu (2002)	**Coarse Fabric PVC Sponge**	-	1.0-1.5	63-86
Wanphen et al., (2009)	**Siliceous Shale**	6.8-8.6	-	-
He et al., (2010)	**Porous Ceramic**	2-4	1-3	-
Jain et al., (2011)	**Palash Fibre**	13.94	-	81-84
Dagtekin et al., (2011)	**Cellulose based pad**	4-7	0.5-1.5	75-85
Shrivastava et al.,(2014)	**Coconut coir**	13	-	60

The humidity content (absolute humidity) of ambient air could directly affect the performance of an evaporative cooling system. When the ambient humidity is increased, the cooling efficiency becomes lower due to the limitations in the amount of vapour that could be added to the air. In order to increase the evaporative cooling performance in humid condition, desiccant materials can be used to reduce the air humidity level (Ma and Guan, 2015; Sohani et al., 2016). This is called desiccant enhanced evaporative cooling. Rafique et al.,

(2016) developed a mathematical model for solid desiccant cooling system under humid conditions of Dhahran, Saudi Arabia. It was found that this system can be applied to provide cooling demands for Dhahran. Banik and Ganguly (2017) developed a desiccant assisted distributed fan-pad ventilated greenhouse system for the cultivation of varieties of Gerbera for the plains of Gangetic Bengal in Indian sub-continent. It was found that the outlet temperature drops below 27 °C with the use of desiccant, while it was nearly 29 °C without using the desiccant.

This research includes the experimental investigations of local materials (porous, fibres materials) for evaporative cooling process in order to increase thermal comfort of the occupants for building indoors in particular, dry regions of Cyprus. In addition to this, an artificial material such as polymer hollow fibre is experimentally investigated for evaporative cooling system (by using water and desiccant liquid) to provide the desired air for indoor environments in dry and humid regions of Cyprus.

1.2 Research aims and objectives

Evaporative cooling is one of the cooling method, which consumes less energy, maintains indoor comfort conditions and gives less harm to the environment. The main aim of this study is to investigate the testing of the performance of local and artificial materials for evaporative cooling method as a wet pad. It is focused to enhance cooling the spaces in hot-dry and hot-humid climates in particular for Cyprus island. In addition to this, it is necessary to propose new ideas of evaporative cooling process in hot-dry and hot-humid parts of Cyprus. Therefore, the following specific objectives of this study are established in order to achieve this aim:

1. The gap of literature of Cyprus including evaporative cooling methods is highlighted for Cyprus. A thorough literature researches show that local materials have not been investigated for evaporative cooling process in Cyprus which are necessary for hot and dry regions in order to reduce energy consumption through the cooling demand of the buildings. Furthermore, an

artificial material of hollow fibre have not been studied or proposed for evaporative cooling system for humid parts of Cyprus based on liquid desiccant cooling system. Desiccant is used as a sorbent in order to absorb water vapour from the humid air to provide cooling effect. As regards investigating the potential of evaporative cooling by using aforementioned processes, it is taken as main studies of this thesis due to the lack of research to be done in Cyprus.

2. The performance of some materials such as eucalyptus fibre, yellow stone, etc. which could be used as a new material for the evaporative cooling process are tested in order to choose better performance of cooling material for hot and dry regions of Cyprus.

3. The conceptual design ideas of integrated evaporative cooling system into architectural building elements are developed for building design in order to enhance cooling effect with architectural requirements. The various conceptual design ideas are illustrated by using three-dimensional modelling.

4. Ecotect Analysis 2011 is used as it is architect-friendly simulation software in order to investigate the monthly cooling load of an existing residential building located in Northern Cyprus by predicting the saving of annual energy consumption of the existing building. Using the data obtained from Ecotect Analysis 2011, economic and environmental emissions savings with the use of evaporative cooling system compared to vapour compression air conditioning have performed.

5. The cooling performance of artificial material, the hollow fibre, is experimentally investigated by using water and potassium formate (KCOOH) as a working fluids for evaporative cooling system for hot-dry and hot-humid regions of Cyprus. It is used for the system since it is cheaper, less corrosive and non-volatile.

1.3 Methodology of the research

This study is started from the cooling requirements of occupants in summer for Cyprus climate since there is a high impact of temperature for indoor space. As the electrical energy and greenhouse gases (GHGs) emissions are higher in order to operate cooling systems (eg. AC) in Cyprus, it is important to study the alternative material and method for cooling process. It is also necessary to develop new design ideas in order to integrate cooling system into building design. Therefore, the methodology of the study is presented in this section.

The first method used in this study was based on literature review in Chapter 2. The experimental studies carried out at the laboratory were another method in this study in order to investigate the cooling performance of evaporative cooling pad. Based on the results, the use of eucalyptus fibres as a local material was studied by Ecotect Analysis 2011 to find the emissions savings. Following this, the conceptual design ideas of integrated system were developed. The final method was the testing carried out at the laboratory by using artificial, hollow plastic fibres.

Different laboratory experiments have been conducted in Cyprus and Nottingham between the years 2013-2017 (as a part-time project) in order to improve cooling effect of evaporative cooling pads. As seen in Figure 8, the structure of the methodology was demonstrated to provide better understanding of the thesis.

The laboratory testing is divided into two parts. The first column represents the testing by using local materials for hot-dry regions in Cyprus. Regarding the testing, two different testing conditions were used as preliminary (insulated box) and main experiments (wind tunnel). These testing are focused on investigating better cooling performance of local materials in Cyprus for evaporative cooling process in terms of some parameters such as temperature difference, relative humidity, cooling efficiency, cooling capacity, COP, evaporation rate (ER) and specific cooling capacity (SCC).

In the second column, the experimental testing in the Nottingham were based

on the investigation of the cooling performance of the plastic hollow fibres (HF) integrated evaporative cooling system (manufactured by ZENA Ltd.). In this respect, three different testing were conducted by using water and potassium formate as a working fluids in different testing modules. In the first and second test modules, water was used for hot-dry regions. Potassium formate was used as a desiccant for hot-humid regions of Cyprus in the second testing module.

It is thought that the laboratory experiments will provide new contribution to evaporative cooling phenomenon for Cyprus climatic conditions. This study will enlarge the vision of the development of this process for buildings in Cyprus.

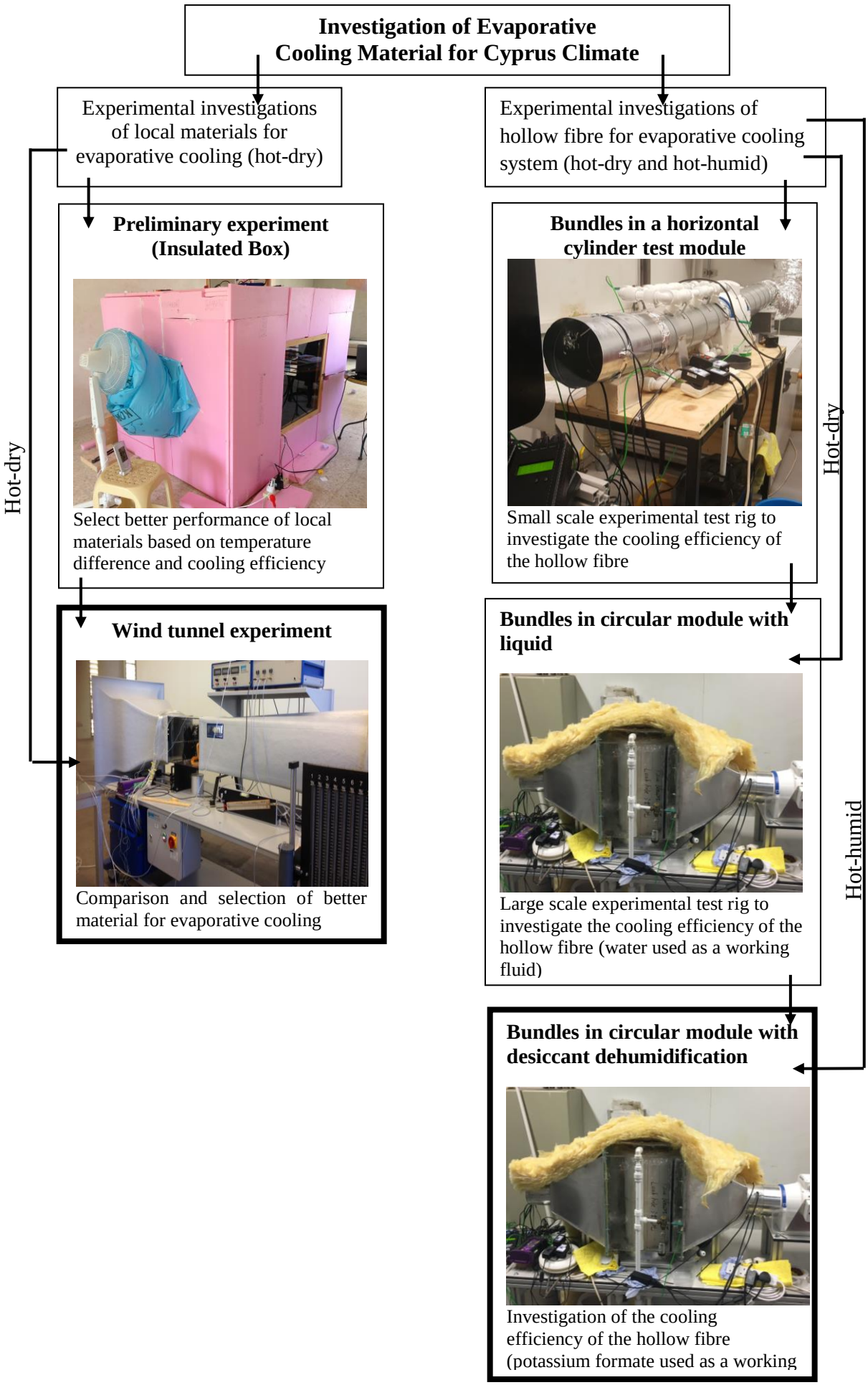


Figure 8. The structure of the methodology

1.4 The novelty of the research

A thorough literature research have been done in order to investigate previous studies on evaporative cooling system for Cyprus climatic conditions, however it was found that there are some gaps in this research area for Cyprus climate. The novel features of the study are summarized as following:

- It is important to emphasize that both direct and desiccant based evaporative cooling processes have been studied for hot-dry and hot-humid regions in Cyprus in this research method. It should be noted that there is no any research which has been conducted for desiccant assisted evaporative cooling system for Northern Cyprus.

- The local materials have been studied for the research since commercial pads are more expensive than local materials. Therefore eucalyptus fibres which is locally available, cheap and easily constructed material, is essential for using in evaporative cooling technology. It is also worth mentioning that this material has not been investigated before for evaporative cooling.

- In addition to this, the experimental investigations have not been carried out in order to evaluate the local materials in Cyprus that might be used as a pad material for direct evaporative cooling process.

- It should also be emphasized that this proposed evaporative cooling system is integrated into building elements such as wall, window, door, etc. to promote cooling effect. The various conceptual design ideas are developed to combine both cooling and architectural requirements in a single building element.

1.5 The scope and limitations of the research

This thesis focused on the investigation of evaporative cooling pad for hot-dry and hot-humid climate in Cyprus. The testing of cooling performance was conducted in the wind tunnel for eucalyptus fibres and the polymer hollow fibre in the test rig named bundles in circular module.

Both numerical and experimental analysis of the performance of evaporative cooling system were provided in this study.

Conceptual design ideas of building integrated evaporative cooling system were developed, however, theoretical or experimental studies about these integrated ideas were not included within the scope of the study.

Desiccant based studies limited only for dehumidification. Regeneration of desiccant has not been investigated.

The feasibility study of eucalyptus fibres was investigated. The artificial material, plastic fibres was excluded since eucalyptus fibre is natural, cheap and abundant.

During this study, the limitation factor was the duration of the laboratory experiments. Due to the limited time during the laboratory, it became difficult to study more. Moreover, since the laboratory in Cyprus is larger, it is difficult to adjust the environmental conditions by using environmental chamber.

1.6 The layout of the thesis

The layout of the thesis was organised as follows in order to summarize the content of the study:

Chapter 1 presents the general layout of the study with the background and problem definitions, research aims and objectives, the methodology of the research and as well as the novelty of the thesis.

Chapter 2 reviews the literature review of the evaporative cooling process with the existing methods, pad material used for the process and the integrated

system for hot-dry and hot-humid regions around the world. The performance of evaporative cooling is presented for experimental methodology. The water harvesting technologies are also described.

Chapter 3 describes the preliminary and main experiments in details which have been carried out both in and out of the laboratory. It includes the comparison of local materials in Cyprus based on the cooling efficiency performance calculations. It concludes with the conceptual ideas of integrated evaporative cooling panel into building elements.

Chapter 4 presents the conceptual design ideas of integrated evaporative cooling system into building element for building design. Eucalyptus fibres is used as a pad material for evaporative cooling system for the architectural integration of the building. The various conceptual ideas are modelled by using three-dimensional illustrations.

Chapter 5 represents the application of evaporative cooling of a house in Cyprus. Ecotect Analysis 2011 was used to find the monthly cooling load of an existing building. It also consists of the economic and environmental analyses by comparing the evaporative cooling system and vapour compression AC.

Chapter 6 includes the different indoor laboratory testing in the University of Nottingham regarding the hollow fibre used for evaporative cooling performances. As a working fluids, water and potassium formate were used in order to be suggested for evaporative cooling process. It concludes with the suggestion of using water and potassium formate in the water and desiccant based evaporative cooling system for hot–dry and humid regions of Cyprus.

Chapter 7 covers the summary of the all chapters and the contributions of the study to the research area. It concludes with the recommendations for further study by researchers in order to improve new ideas for evaporative cooling process in Cyprus.

CHAPTER 2: A Review of Thermal Comfort and Evaporative Cooling

2.1 Introduction

People always try to become adapted to the surroundings they live in. They build a "shelter" in order to protect themselves from the outer environment, such as wild animals, severe weather and climate conditions. Shelter is very important to man in terms of the struggle for survival (Rapoport, 1969). Shelter was a cave or tree hollow for the early people, but now it is called a house or home.

According to Louis Kahn (1901-1974), "architecture is what nature cannot make" (in Roth, 2007). A chambered nautilus creates a hard shell around itself as protection; architecture is that chambered nautilus shell for the human beings. It is the environment that we create to adapt to our surroundings.

"In architecture as in all other operative arts, the end must direct the operation. The end is to build well. Well-building hath three conditions: Commoditie, Firmeness and Delight." (Roth, 2007, p.5)

The elements of architecture identified by the ancient Roman architect Marcus Vitruvius (25 B.C.) have not changed from the early times until now/today (Roth, 2007). Architecture should provide utility, firmness and delight. Vitruvius explained the "utility" as spaces being used easily. By firmness, he meant the building should be strong and by beauty, the appearance of the building should be likeable. Besides all the elements of architecture, climate is also a very essential parameter in terms of comfort conditions for the occupants. All of these factors must be considered together by designers (Abohorlu, 2010).

Climatic determinism viewed that the primitive people firstly look for shelter and then adapt to climatic conditions of the surroundings (Rapoport, 1969). They all built their house to keep out from the enemies and then feel thermally comfortable in any climate.

In order to achieve thermal comfort especially in summer, heat gain strategies and passive cooling methods should be taken into consideration. There are a number of passive cooling systems which lower the temperature and shift the comfort zone to higher temperatures.

2.2 Thermal Comfort

The human environment should provide aesthetic, light, air, acoustic and hygienic comfort. Besides these factors, thermal comfort of the space is also very important in order to provide a comfortable and healthy environment for the occupants. People feel uncomfortable as a result of enclosed spaces being too hot or cold, humid or dry. Comfort conditions have direct contact with the human senses, in particular the eyes, ears, nose and tactile (Bradshaw, 2006).

According to ASHRAE, thermal comfort is "that condition of mind in which satisfaction is expressed with the thermal environment". It is obvious that maintaining a pleasant environment in buildings is very important for the occupants. It is the basic physical and biological needs for humans and is related with the thermal balance between heat gains and heat losses. Heat is gained by the metabolism of the body and losses from the body to the environment by heat transfer methods.

2.2.1 Psychrometric Chart

The psychrometric chart is used to show the relationship between temperature and humidity which affects thermal conditions of the environment (Figure 9). The dry bulb air temperature (DBT) is plotted on the horizontal axis of the chart, the moisture content/humidity ratio (specific humidity) is shown on the vertical axis and relative humidity (RH) is found on the curved lines. The bottom line shows that the RH is 0%. The upper curve is the saturation line that shows the air is saturated with water (100%). The RH changes when the moisture and temperature of the air change.

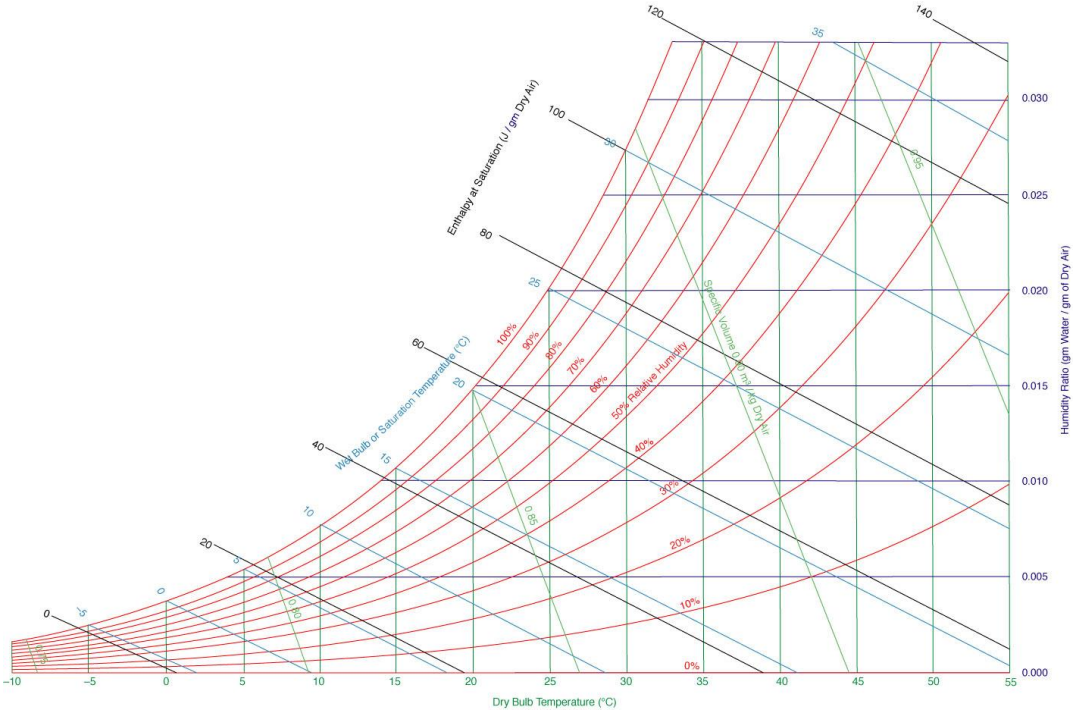


Figure 9. Psychrometric chart (ASHRAE, 1997)

2.3 Passive Cooling

Passive cooling is not only the removal of latent or sensible heat from the building, but also the reduction of heat gain and minimisation of its physiological effect. This structure is shown in cooling strategy where buildings can be cooled by these passive methods (Figure 10).

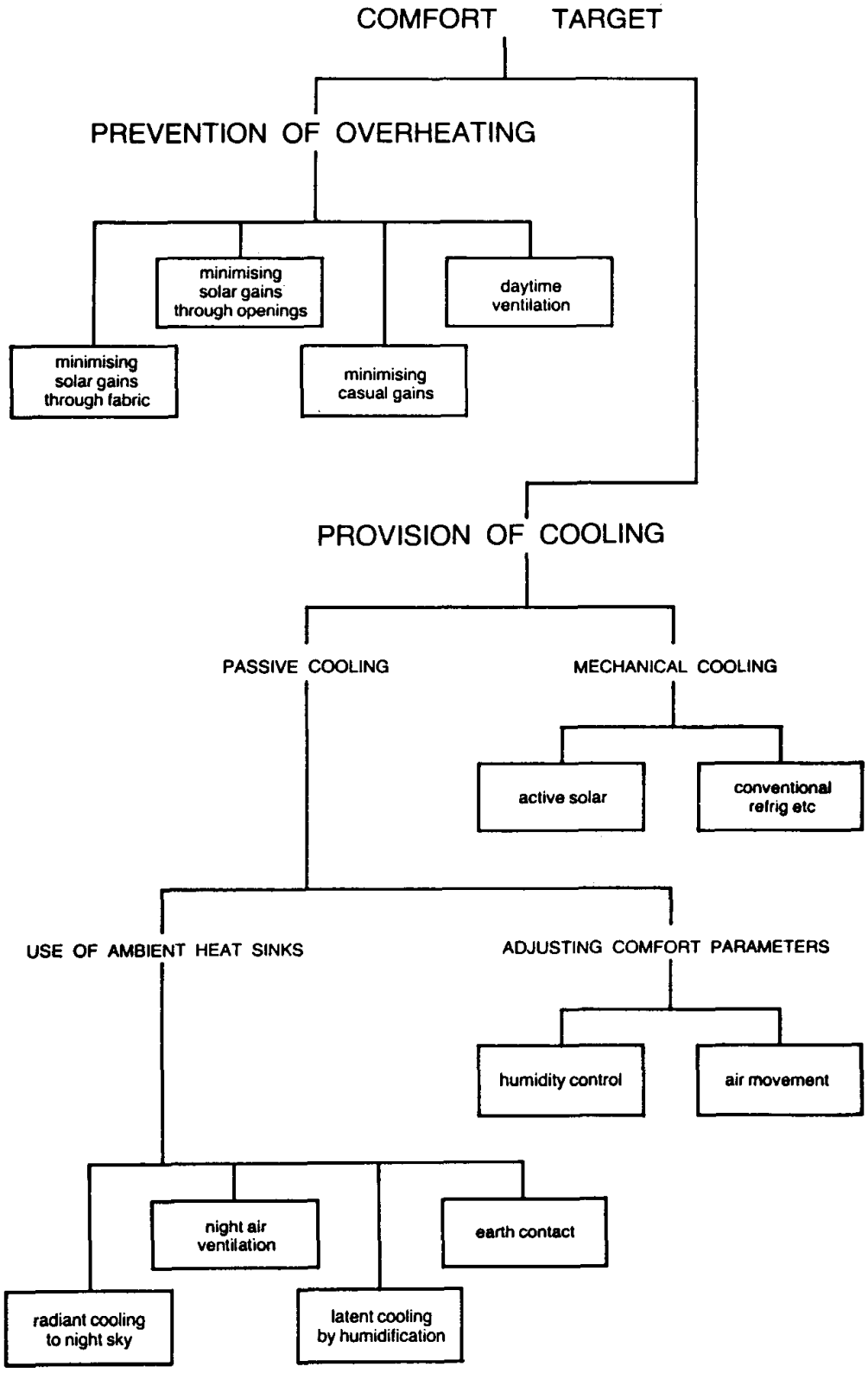


Figure 10. Cooling strategy (Baker, 1987)

2.3.1 Basic Building Design Parameters (Principles or Strategies) for Cooling

The cooling rate of a building, in particular during summer nights is dependent on the **building form**: minimum the surface area affects both the amount of solar radiation and wind effect. Compact buildings, such as square or rectangle-shaped ones, have a minimum surface area which reduces heat gain and heat loss. The **orientation** of a building is related to the wind orientation of the windows and wall areas. It is a well-known fact that the effective cross ventilation reduces the indoor temperature. **Windows** have multiple functions when required, such as the intake of daylight, sun and wind. In passive cooling strategies, windows play a vital role. The placement of windows affects the air movement. If the openings are placed opposite to each other and oriented to the prevailing wind direction, this leads to the creation of air movement by cross ventilation. If the window size is larger, indoor air movement will also be greater. When the sizes of inlet and outlet windows are equal, good air exchange is obtained (Figure 11).

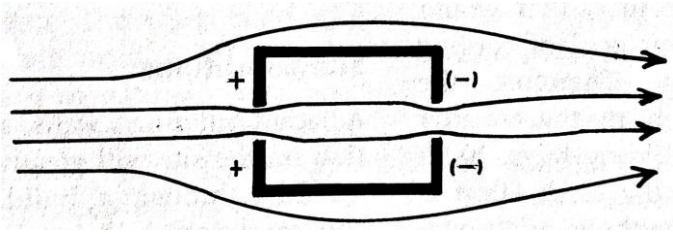


Figure 11. Good cross ventilation (Lechner, 2009)

Overhangs above the inlet window increase the wind velocity that flows into the building. The wind is directed towards the ceiling. On the other hand, if a 15 cm gap is created between the overhang and the building, the wind flows out of the room. In both ways, a comfortable level of good cooling is obtained (Figure 12).

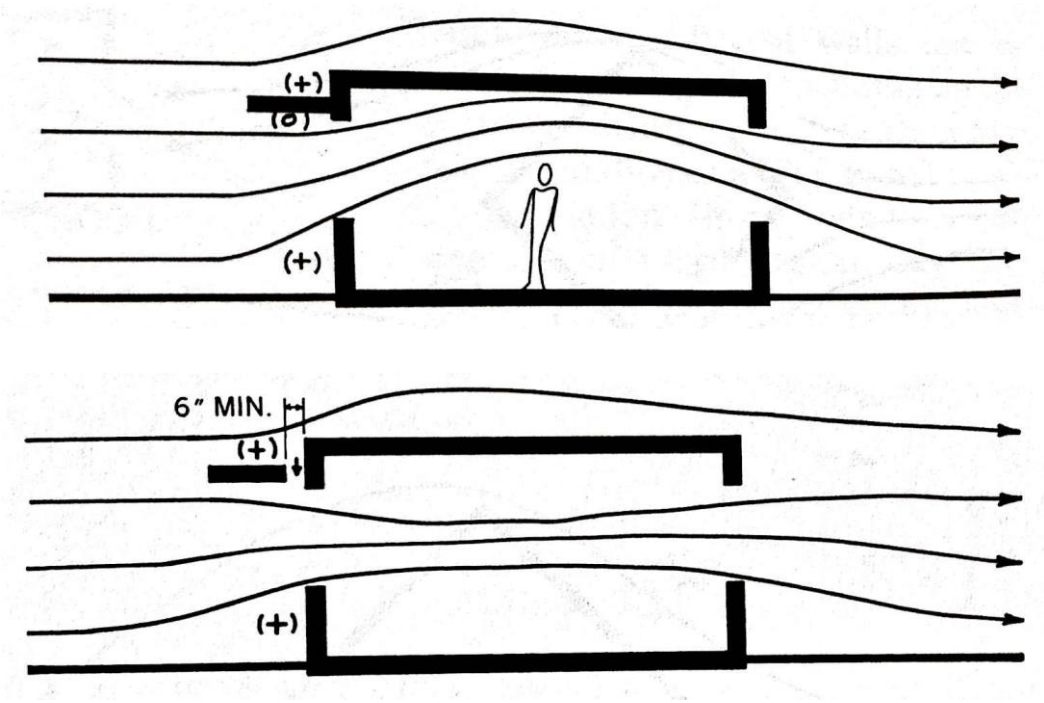


Figure 12. Different kind of overhangs (Lechner, 2009)

The **stack effect** is a phenomenon which induced by the temperature and moisture difference between the air inside of a building and outside conditions. As the pressure difference is becoming more with the height of the structure, greater buoyancy force is occurred and thus, the stack effect. In **cross ventilation**, wind is essential to create effective cooling. However, if there is no wind or the climate is calm, cross ventilation will not be effective. Thus, stack ventilation will be better in terms of providing a cooling effect. The rate of air movement is also increased by the size of the windows, temperature differences between indoors and outdoors and the height of the room.

Sun protection is absolutely vital in hot summer climates. If no **shading** is used, more sun energy is stored by the surface of the building, causing an increase in inner temperature. Thus, shading at the overheated time of the year is essential (Olgyay & Olgyay, 1957). Shading devices such as deciduous trees, overhangs, shutters, pergolas, arcades and so on can be used to prevent heat gain of the building.

Vegetation has many positive effects for a building, such as the prevention of air pollution, noise and excess sunlight. Beside this, it also provides good shading both for the roof and wall. This means that deciduous trees should be used in summer in order to protect the building from excess sun energy (Bradshaw, 2006). In addition, deciduous vines can be horizontally used on trellises for shading and insulation.

Green areas are cooler than the dense building areas due to evapotranspiration, reflection and shading (Brown, 2001). This enhances the cooling effect by water and wind. In doing this, water will increase the **evaporative effect** of plants by keeping them wet. The role of wind is to increase the evaporation rate. However, in humid areas, the rate of evaporation is decreased due to excess humidity.

2.3.2 Ventilative Cooling

Comfort ventilation works best in hot and humid climates. Therefore, this cooling strategy is simply defined as ventilation during the day and night to enhance evaporation from the skin and improve thermal comfort of the occupants. Maximum air should flow at the level of occupants since there is a high level of moisture in hot and humid climates. The moisture will be evaporated by air passing over the occupant's skin, causing a physiological cooling effect (Lechner, 2009). On the other hand, ventilation in the evening increases the cooling rate and improves the comfort of the occupants in hot dry climates.

2.3.3 Radiative Cooling

As the laws of physics demonstrate, the energy is transferred from a warmer object to a cooler object until it reaches the equilibrium means that two bodies have the same temperature. It is also known that darker object gets more energy than the light colour object. However, as shiny and rough surfaces reflect energy more, they cannot absorb energy compared to darker surfaces.

These principles form the general idea of radiation cooling. If radiative cooling is not occurred in the whole earth, it will be warmer since the trapped energy will not be released to the atmosphere (Santamouris and Asimakopoulos, 1996). Heat is radiated and thus, a cooler environment is created.

2.3.4 Earth Cooling

Earth sheltering involves the covering of some part of the building, such as one or more wall or roof, with soil or as an underground building (Moore, 1993). It may be built into an excavated earth, fully or semi-bermed, built into hillside or combining rooms below and above ground (Figure 13).

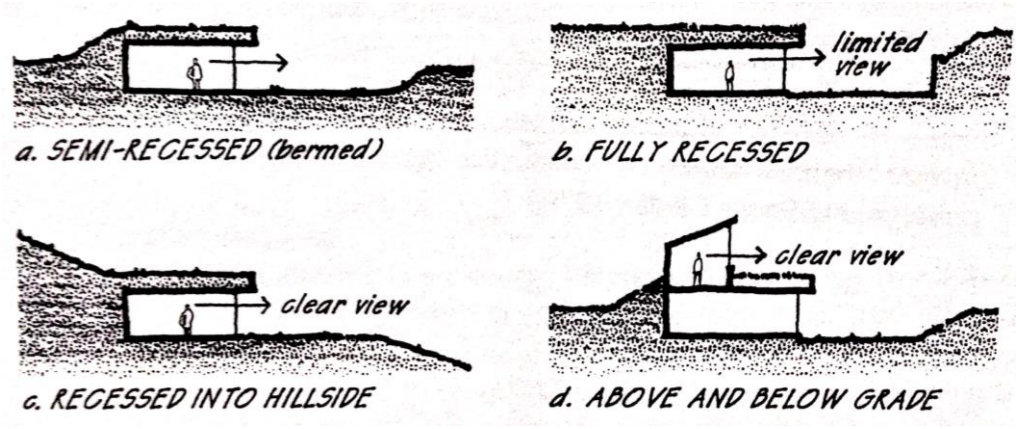


Figure 13. Earth-Sheltered Design Strategies (Moore, 1993)

Earth-sheltered building plays a vital role in passive cooling methods because of reduced energy requirements for cooling. It is caused by minimizing the need for a mechanical cooling system and thereby, reducing the cooling bill. It was found that the earth sheltered buildings have better energy efficiency and passive heating and cooling capacity (Abohorlu and Kurt, 2017).

2.3.5 Dehumidification with a Desiccant

The term “dehumidifying” represents to remove moisture from the air to increase the comfort conditions, in particular humid areas. There are some methods to condense out the moisture from the air. The first method is to cool the air below dew point and then, air is condensed out. Secondly, some desiccant such as silica, calcium chloride, etc. can be used to remove the moisture by absorbing the water vapour from the air.

2.4 Evaporative Cooling (EC)

Heat is a form of energy and appears in two forms, as sensible and latent heat. Sensible heat is the heat energy released from or absorbed by a substance during a change in temperature. This heat is named as “sensible” due to its relation with the senses. That is why the change of temperature can be measured by thermometer (McMullan, 2007). Latent heat is the energy used to change the state of the matter without altering the temperature. As heat of water is increased, the temperature of water is also increased until it reaches its boiling point. Latent heat is absorbed by water in the later stage to allow water to change its state into steam (Pohl, 2011). A liquid may change to a gas by evaporation instead of supplying heat. The latent heat is taken from the surroundings in order to make this change. Thus, an effective cooling effect will be produced (McMullan, 2007). When water evaporates into the air, it is made to reduce its temperature and this process continues until the humid air becomes more saturated (Martinez, 2010).

While water is evaporating, it absorbs heat from the air which leads to a decrease in the temperature of the surroundings. After water evaporates, the state of water is changed into water vapour and this enters into the air in the form of latent heat. Then the air is humidified and the enthalpy or total heat of the air remains the same. This process is called evaporative cooling and it can be used for cooling the space by direct, indirect or combined (direct/indirect) methods. These were used for many years ago in hot arid regions, like in ancient Egypt (Fathy, 1986) where there is high temperature and very low

humidity ratio. They can also be used in desert and Mediterranean zones (Konya, 1980). In dry climates, direct evaporative cooling works best. An indirect evaporative cooling can be used in humid climates because it does not add moisture to the surroundings. However, a combination of the two methods is sometimes the best (Lechner, 2009).

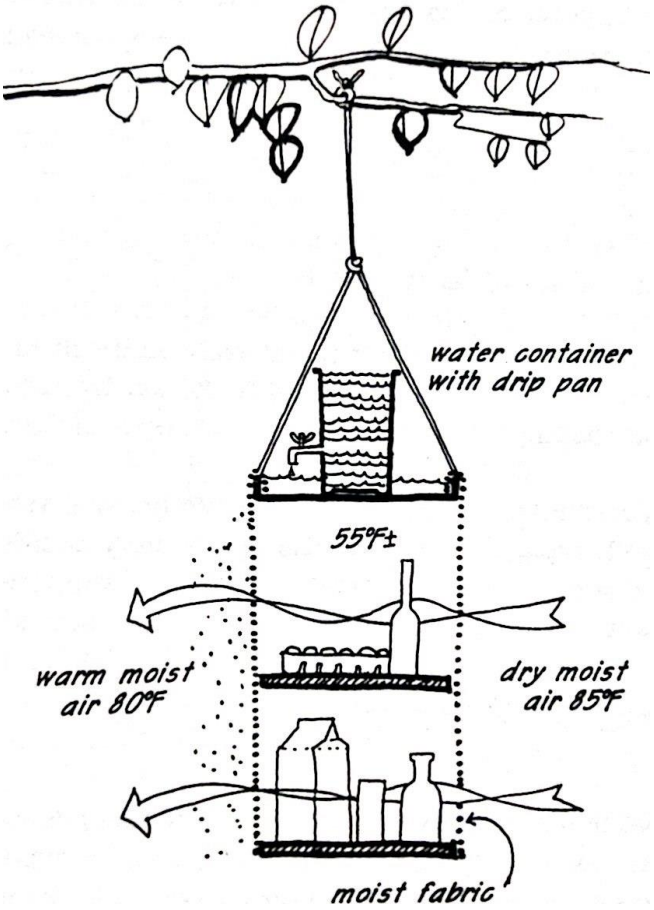
Energy should be absorbed from the surroundings when water changes from liquid to vapour during evaporation. When energy is taken from surroundings, sensible heat is converted to latent heat and the temperature becomes cooler. This is the same as when sweat evaporates from the skin. The heat is taken from the skin and then cooled. As a result, the sensible heat in the skin is turned into the water vapour as latent heat (Lechner, 2009). Absorption of energy is very important during evaporation. The temperature of 1 litre of water from 0 °C to 100 °C is increased by 4.2 J of energy. 1 litre of water at 100 °C is changed into water vapour at 100 °C by 2260 J/g of energy.

There are a number of different ways to cool buildings by evaporation of water. The first is to evaporate the water in the building or the outdoor air intake; air in the surrounding will then be cooled. As the air is humidified, the moisture level is raised above the outdoor level. This method is called “direct evaporative cooling”. The second is to cool the indoor air without raising the humidity. This is termed “indirect evaporative cooling”. Lastly, both processes can be combined together as “direct/indirect combinations”. The first indirect stage cools the air which is then passed to the direct stage and is cooled further (ASHRAE, 2000).

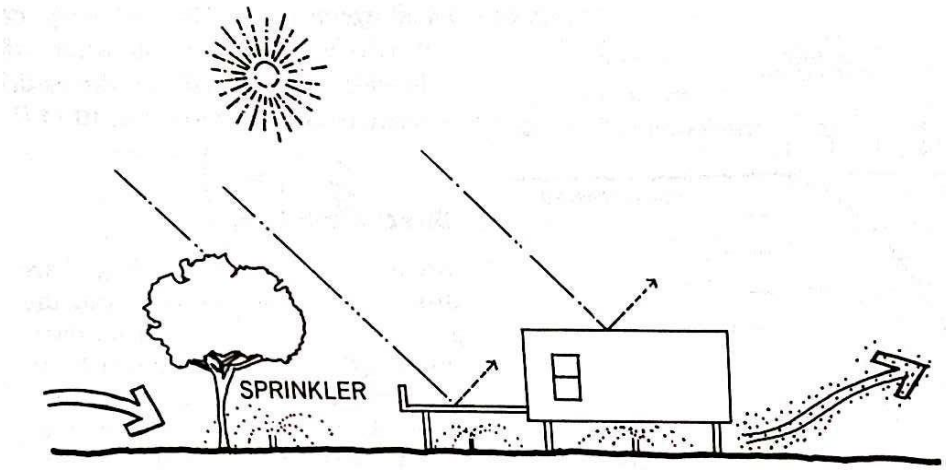
Air Movement is an important factor as natural or artificial air movement. Velocity of air has an obvious effect on heat loss. The comfortable range of air velocity is between 0.1 and 0.3 m/s (Lechner, 2008). It is known that during water evaporation, the humidity level of the air is increased. If the humid air is not moved away from the space, the evaporation rate and the cooling effect will be low. So air movement is required during the evaporation process; This is done by replacing the dry air with humid air. The last factor is *Surface Area*. When it is larger, more water can evaporate and create a cooling effect. In

general, the cooling capacity of a system is affected by the rate of water evaporation which relies on relative humidity, air temperature, air movement and surface area. For that reason, evaporation can be increased by reducing relative humidity or increasing air movement. To create a large surface area between air and water is very common since evaporation takes place in the liquid-air interface (Sodha, 1986).

Evaporative cooling method has been used since pre-scientific eras in very hot regions. It is used for example to keep food cooler. The hanging of open-weaves to the trees was kept moist while dripping water from the top. Therefore, the fabric remains wet and creates a dry breeze towards the food which enables it to be kept drier (Figure 14). Evaporative cooling was not only used only for cooling food, but also for cooling the garden of the buildings (Figure 14). Simple passive cooling techniques were used, in particular, watering the courtyard floors, putting wetted surfaces or terracotta pots filled with water in front of a window facing the prevailing wind. Spraying water over the roof or some other building surface was also used to reduce the temperature of the surroundings (Szokolay, 2008). It is obvious that it is better to describe examples of this technique in order to understand the main idea of the evaporative cooling method.



(Moore, 1993)



(Lechner, 2008)

Figure 14. (Up) Evaporative Food Cooler and (Down) cooling the surrounding of the building

2.4.1 Architectural Background of Evaporative Cooling

Evaporative cooling method occurs in nature near water surfaces such as waterfalls, lakes and oceans. It is also historically used in vernacular architecture with natural resources such as a fountain, pool, vegetation, tree or by splashing the garden floor and roof. This causes the humidity level of the air to increase and thus, provides a cool breeze particularly in hot and arid regions. This occurs when dry air is blown over a wetted surface. The Egyptian architect, Hassan Fathy (1900-1989) placed porous clay and pottery jars filled with water in front of windows to create cool ventilation when air flows around the jars (Figure 15). The porosity of clay allows the surface to remain wet and the air is cooled by evaporation. In India, old tatties covered with sweet-smelling dried khuss-khuss grass were hung in the door or window and were kept wet by pumping water. There was also a wooden grille to cover the window which had a porous pot filled with water in front of it. Air blew via the grille and then pottery caused the air to be cool and more humid. Thus, cooling was created by an evaporative cooling method (Figure 16).

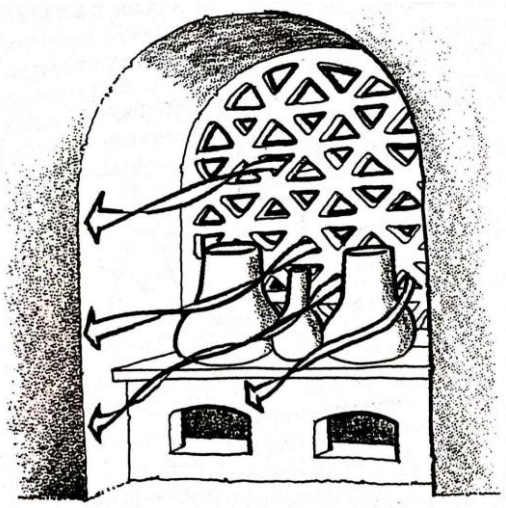


Figure 15. Air flows around jars creating cool breeze (Moore, 1993)

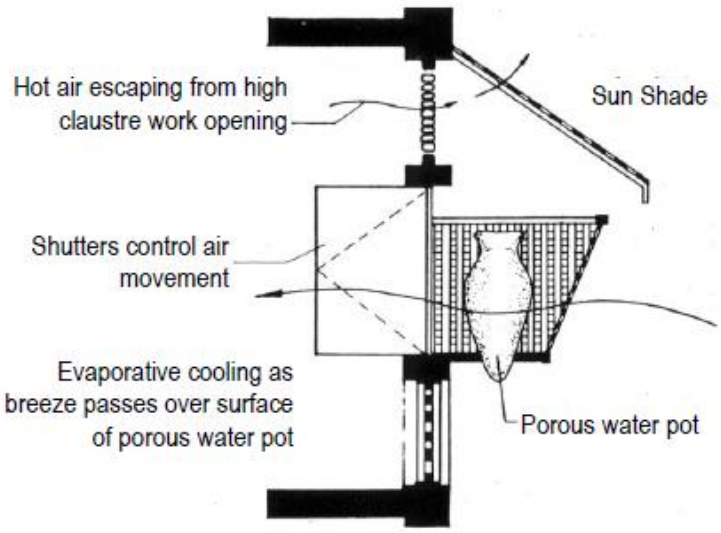


Figure 16. Muscatese evaporative cooling system (Phan, 2004)

A courtyard pool is very common in hot arid regions. When air flows into the surrounding rooms during the day, it is blown over a fountain or pond before entering a building. This system provides air cooled by the evaporation of water. Another way of creating a cooling breeze is to use porous earthenware pots filled with water in the building design. A wind-catcher (Malkaf) in old houses traps the wind which is taken from a shaft facing the prevailing wind direction. This trapped air is passed over a fountain which is then cooled by evaporation (Figure 17).

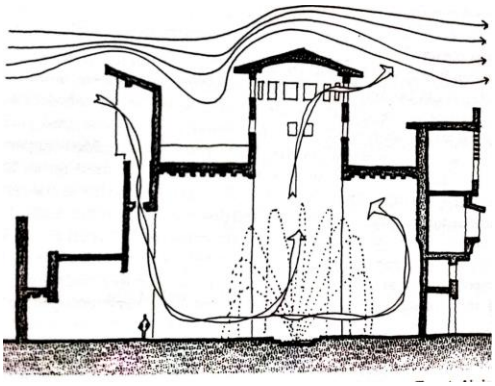


Figure 17. Wind-Catcher (Moore, 1993).

2.4.2 Direct Evaporative Cooling (DEC)

The room air is cooled by forcing the air via a water surface area for evaporation by the use of fans. This process is called *direct evaporative cooling* (Figure 18). It directly cools the air by contacting with the water, by the use of wetted-surface material or sprays and then sensible heat energy of the air evaporates the water. Thus water vapour diffuses into air by latent heat (Camargo, Ebinuma, Silveira, 2005). This leads to an increase in humidity and reduction in the dry-bulb temperature of the room by the heat and mass transfer between the air and water (ASHRAE, 2000). The wet-bulb temperature remains the same and therefore, enthalpy remains constant. An example may be a fountain in the courtyard. A wind blowing via a fountain will cause the temperature of the surroundings to decrease, the humidity level to increase and therefore, the area to cool by direct evaporative cooling. Increasing humidity creates thermally comfortable conditions. This process is more efficient when the temperature is higher. However, it is not suitable for hot and humid regions, due to the excess humidity ratio that the system produces.

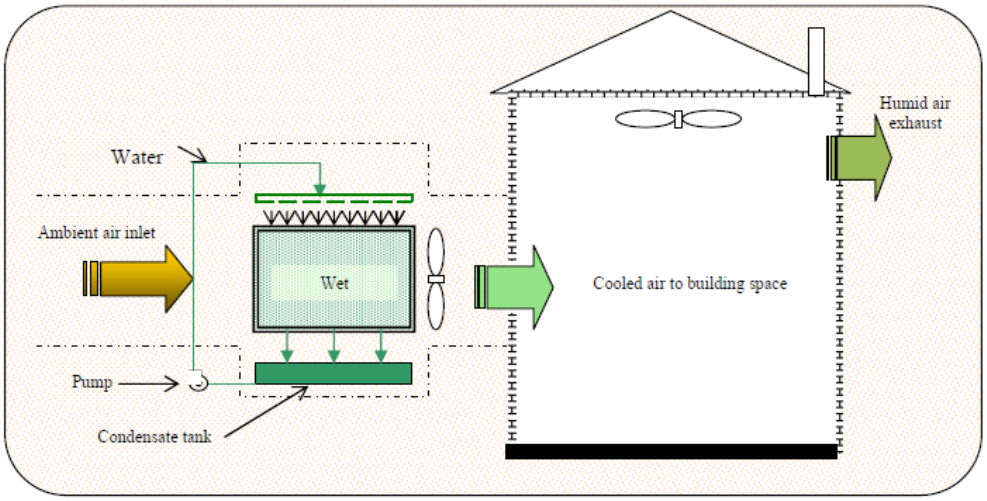


Figure 18. Direct Evaporative Cooler (Musa, 2008).

Direct evaporative cooling is adiabatic which means no exchange of heat (addition and extraction) of a system with its environment and also constant total energy content of the air (sensible and latent). So, heat must be supplied to the system in order to evaporate water. The air that is given into the system for

water evaporation supplies the heat causing the decrease of air temperature and hence cooling. The amount of heat removed from the air will then become equal to the amount of heat absorbed by the water evaporation. If the water is recirculated by pump in the system and evaporation takes place by this recirculated water, its temperature in the tank will become nearer to the wet-bulb temperature of air entering (ASHRAE, 1999).

It is very common to evaluate the performance of various evaporative (cooler) cooling materials. The cooling efficiency or (direct) saturation efficiency/effectiveness is a key factor in rating the performance of the coolers. When the leaving air temperature of the DEC is nearer to the wet-bulb temperature of the entering air, this means saturation is approached. However, it does not mean that it causes complete saturation. Cooling efficiency is also known as “saturation efficiency” because it is due to the amount of moisture that is packed in the air. It is defined by the following equation, as mentioned in ASHRAE (2000).

$$\eta\varsigma = \frac{(T_1 - T_2)}{(T_1 - T'_1)}$$

$\eta\varsigma$ = direct evaporative cooling or saturation effectiveness, %

T_1 = dry-bulb temperature of entering air, °C

T_2 = dry-bulb temperature of leaving air, °C

T'_1 = wet-bulb temperature of entering air, °C

The cooling efficiency is the percentage of the depression of the dry-bulb temperature of the air leaving the media compared to (divided by) the wet-bulb depression (dry-bulb less wet-bulb temperature) of the entering air. WBT is very important in all evaporative cooling systems. The direct evaporative cooling is adiabatically less than 100% effective theoretically. However, 100% saturation is impossible for DEC because some materials are not closely packed so the air can easily escape without making enough contact with water

and contact time between air and water is short. Saturation depends on not only contact between air and water, but also media depth/density, air velocity and using higher spray density (ASHRAE, 2000). The type of material used as a cooler (pad), the size of perforations, and relative humidity of air and volume of water are also essential in the efficiency of evaporative pads (Malli et al., 2011).

Air is humidified in direct evaporative cooling in three ways: using recirculated water, preheating the air or heating recirculated water during the process. There are also some factors that affect the temperature difference between leaving air and leaving water. Firstly, it is related with the temperature differences between entering dry and wet-bulb temperature (WBT depression). The length and height of water supplying, velocity of air, the amount of water and the way of giving water (spray pattern) are other common factors (ASHRAE, 1999).

The air in the direct evaporative cooling can be introduced by:

- Mechanical ways (fans, heat exchanger)
- Natural ways (temperature differences, water spraying into the system, orienting to the wind)

2.4.2.1 Mechanical Evaporative Cooling Systems

The mechanical evaporative system was first developed in the United States in 1906. Such systems are not passive system, although some systems consume less energy. These include single-stage direct evaporative cooler, two-stage indirect evaporative cooler and multiple-effect direct coolers (Givoni, 1994).

2.4.2.2 Homemade Passive Direct Evaporative Cooling Devices

Evaporative pads in windows and the use of porches in buildings are two types of homemade approaches to provide natural direct evaporative cooling. Wetted pads are used in windows facing to the wind, watered from the top; water is

collected and recirculated from the bottom of the pads. In this way, dust from the wind is also filtered. Afterwards, temperature decreases by 40-50%. On the other hand, the view from the window and the air flow will be prevented by this pad. This problem can be solved by designing a fixed frame in front of the window with a lightweight pad, water supply, pump and water tank. In winter, this frame can be easily removed.

Evaporative pads can be put in front of the porch facing the windward direction (Figure 19). Windows in the porch can also provide a view. Air passing via the wet pads will allow the building to become cooler (Givoni, 1994).

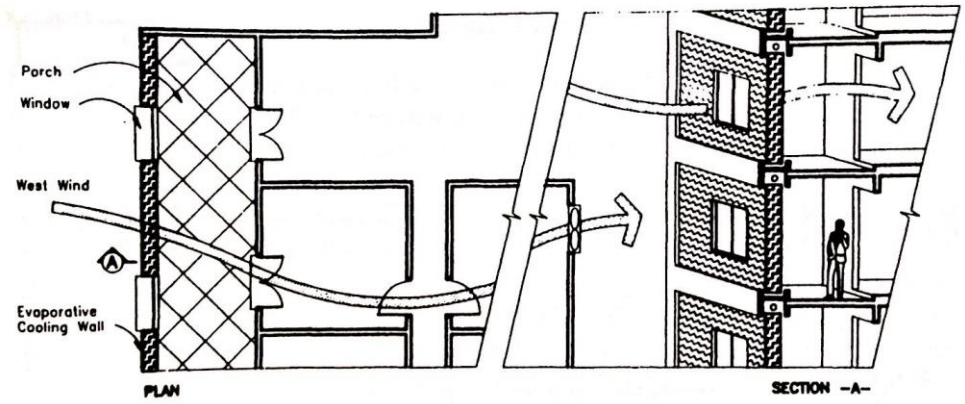


Figure 19. Porch for DEC (Givoni, 1994).

2.4.2.3 The Cooling Tower of Cunningham and Thompson

Cunningham and Thompson developed a downdraft passive evaporative cooling tower in 1986 (Givoni, 1994). It can be used to cool a building without the use of wind or mechanical devices such as a fan. Hot air is taken from the high opening of tower which is covered with wet pads, causing the temperature to reduce and humidity to rise. As the cooler air becomes denser, it falls to the lower part of the tower. As a result, air starts to flow through the building (Brown, 2001).

2.4.3 Indirect Evaporative Cooling (IEC)

Cooled air is very humid in direct evaporative cooling (DEC). So, DEC is not suitable for hot humid regions because there is already high humidity. Indirect evaporative cooling has an advantage when compared with DEC. Indoor air humidity is not raised and DBT is reduced by evaporating the exterior surface of the element of the building in particular roofs and walls in indirect evaporative cooling. This cooled building element then becomes a heat sink and absorbs heat from the interior in order to cool the indoor air. A shaded water pond over an uninsulated roof can be used in this system in order to take the heat from the air by the heat transfer method of convection. Heat can also be obtained by conduction and radiation. When heat flows from the indoor space to the pond, the temperature of the water rises. This will cause to the water pressure and evaporative cooling rate to rise which results in a reduction of the temperature elevation. As the roof has a high conductivity and contact with water, it acts as a "cold" sink leading to a lowering of the room temperature. In this shaded pond system, the water temperature is lower when compared with the unshaded pond. When water is protected, it plays a vital role in the cooling potential.

In dry climates, the cooling potential of a roof pond is higher than the other passive systems (Givoni, 1994). There are three types of shading of roof pond that provide winter insulation.

2.4.3.1 Ventilated Roof Ponds with Fixed Insulations

Water is used to cool the building indoors by evaporation during the night; this cooled water is used during the daytime by heat exchangers (Givoni, 2011). In summer, wind is passed over the pond. When the water evaporates, it is cooled down and acts as a heat sink for the interior. In winter, the water should be drained and openings closed in the roof.

2.4.3.2 Roof Ponds with Floating Insulation

Another alternative to the roof pond is to use floating insulation, so water can be protected from excess sun. In this system, water is sprayed over the insulation which is then cooled by convection, evaporation and radiation at night (Lechner, 2009). In the morning, water below the insulation remains protected and acts as a heat sink to cool the interior of the building.

2.4.3.3 Insulation Embedded within the Pond

Givoni designed this system for reinforced concrete flat roofs in desert regions (Givoni, 1994). In summer, the drains at the bottom of the pond must be closed to keep the water for thermosyphon circulation. The gaps between the impermeable insulation materials can allow warm air to leave the building at night. The sun rays are reflected over the upper layers of pebbles and some are emitted; however, insulation of the roof will protect the building from the sun.

2.4.4 Desiccant Evaporative Cooling

Desiccant material is used to dry the air by absorbing water vapour from the air. Since firstly developed by Gog (1955), desiccant dehumidification system has been widely applied in industrial and agricultural application. Recent few decades, desiccant dehumidification incorporated with air conditioning system has been intensively studied by researchers. There are some advantages of using desiccant cooling system compared to conventional vapour compression system. Conventional vapour compression air conditioning systems is operated in order as shown below while leads to higher energy requirement:

- cooling air below its dew point,
- removing moisture from the air,
- reheating the dehumidified air to the desired temperature.

However, desiccant could dehumidify the air with the help of its hygroscopic properties. Therefore, the energy required for desiccant cooling process is less

compared with conventional vapour compression system. In addition to this, the refrigerants (CFCs, HFCs) used in vapour compression system have relatively high Global Warming Potentials (Montreal Protocol, 1987; UNEP, 2007a). Finally, conventional vapour compression system is generally driven by electricity however, desiccant cooling system has the ability to be operated by low grade energy such as solar energy.

Desiccant cooling system is occurred by the water vapour pressure difference between air and desiccant surface (Daou et al., 2006). The moisture transfer between the air and the desiccant is generally driven by the difference in vapour pressure. When the vapour pressure of the air is greater than that of the desiccant, the moisture will be transferred from the air to the desiccant.

Desiccants are categorized under two systems: liquid and solid desiccant dehumidification systems. Although solid desiccant material is less corrosive and compact, liquid desiccant material provides more advantages such as lower energy consumption compared to conventional air conditioning, lower humidity thus reduce cost of humidity damage, flexible in utilisation, lower regeneration temperature, the lower pressure drop of air, high quality of supply air since it filters viruses, bacteria and moulds (Elsarrag et al., 2016; Rafique, 2016; Chen et al., 2017).

While selecting the best desiccant material, it should has a high adsorption capacity, easily reaction capability, low cost and high availability. A desiccant material can dry the humid air by the methods of absorption or adsorption (Rafique, 2016). As an examples, lithium bromide (LiBr), lithium chloride (LiCl), potassium formate (KCOOH), calcium chloride ($CaCl_2$) can be used for drying air (Elmer et al., 2016; Chen et al., 2017). LiCl, LiBr and other salts are corrosive and can give harm to the system. However, KCOOH is less corrosive, cheaper and non-volatile (Sahlot, Riffat, 2016). $CaCl_2$ solution is the cheapest and most widely available desiccant, but it has the disadvantages of being unstable performance, depending on the air inlet conditions and the solution concentration rate (Dai and Zhang, 2004). Lithium bromide (LiBr) solution offers similar characteristics during dehumidification and regeneration process,

but the cost of LiBr is about 20% higher than LiCl (Iu et al., 2015). LiCl solution is the most stable liquid desiccant, which offers the lowest water vapour pressure and dehydration concentration 30-40% (Fumo and Goswami, 2002). Koronaki et al., (2013) developed a theoretical model for an adiabatic structured dehumidifier with three different desiccant solutions (LiCl, CaCl2 and LiBr). It was found that LiCl has the best dehumidifier efficiency and the highest dehumidification mass rate in comparison to LiBr and $CaCl_2$.

Longo and Gasparella, (2015) examined the energy saving effect of three different liquid desiccants (LiCl, KCOOH and LiBr) in a real flower greenhouse application during three years' time span. The greenhouse equipped with such desiccant based air conditioning system exhibited the energy saving of 9.6%, 11.7% and 15.1% respectively for using the desiccants of LiCl, KCOOH and LiBr. The above mentioned three salts have the disadvantages of corrosive feature, which can cause significant damage to air conditioning system. As a less corrosive and more environmental friendly solution, potassium formate (KCOOH) solution has recently been applied in desiccant cooling unit. KCOOH solution has the advantages of low toxicity and viscosity, and they are neither corrosive nor volatile (Elmer et al., 2016). However, the cooling and dehumidification performance of KCOOH was hardly revealed by researchers experimentally.

KCOOH is a liquid desiccant and thus, not much research is available currently. Qiu and Riffat (2010) investigated a novel air dehumidifier using potassium formate. A highly concentrated solution was used, which effectively dehumidified the air with high moisture content (75% RH), but was rather ineffective at low moisture content (43% RH). Qiu et al., 2008 investigated an evacuated tube was used to regenerate the weak potassium formate. Results indicated that 45°C–50°C was optimum desiccant temperature for solution regeneration, when the mass concentration was between 51.3% and 69.9% by weight.

The vapour pressure of potassium formate can be seen in Figure 20 at different mass concentration. It can be concluded that the vapour pressure is reduced

with decreasing in temperature and increasing mass concentration. Although high concentration is good for dehumidification, desiccant solution can cause some harm to the system. Thus, some concentration ranges are determined for vapour pressure. According to this, the mass concentration is chosen at 65% to 70% for potassium formate at temperature 30-35°C. Elmer et al., 2016 also found that as the solution of concentration is increased with temperature decreasing, the vapour pressure of solution began to decrease. Meaning, the potential of dehumidification is increased due to the higher vapour pressure difference in between hot humid air and desiccant solution. They suggested to use 60-70% solution mass concentration at 20-30°C air temperature in the dehumidifier and 55°C in the regenerator.

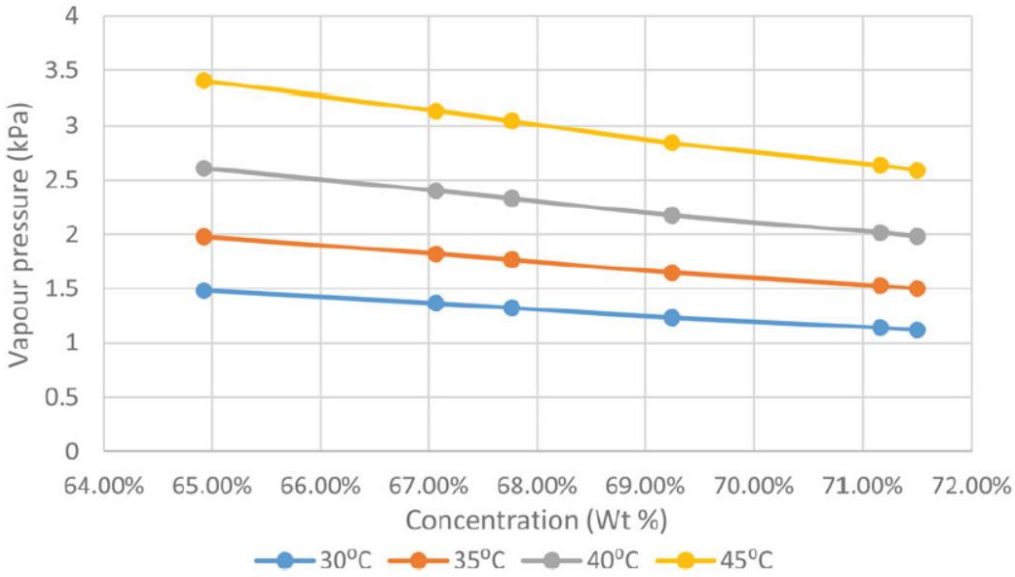


Figure 20. Vapour pressure of potassium formate at different mass concentration (Beyer and Steiger, 2016)

Regarding the desiccant evaporative cooling system process, the Figure 21 shows the system which consists of regenerator (heat source), dehumidification (desiccant material), evaporative cooler (cooling unit). Moisture from the inlet air is forced to the dehumidification process via a desiccant material to reduce the moisture content and temperature. When moisture is absorbed by a desiccant material, it becomes more dilute and loses its ability to absorb more moisture. Therefore, regenerator is used to increase the concentration of the

solution and thus, increase the capacity of dehumidification of the solution and provide cooling (Elmer et al., 2016). During desiccant evaporative cooling system, latent (by changing the state of the matter) and sensible heat are removed by dehumidifier and cooling device.

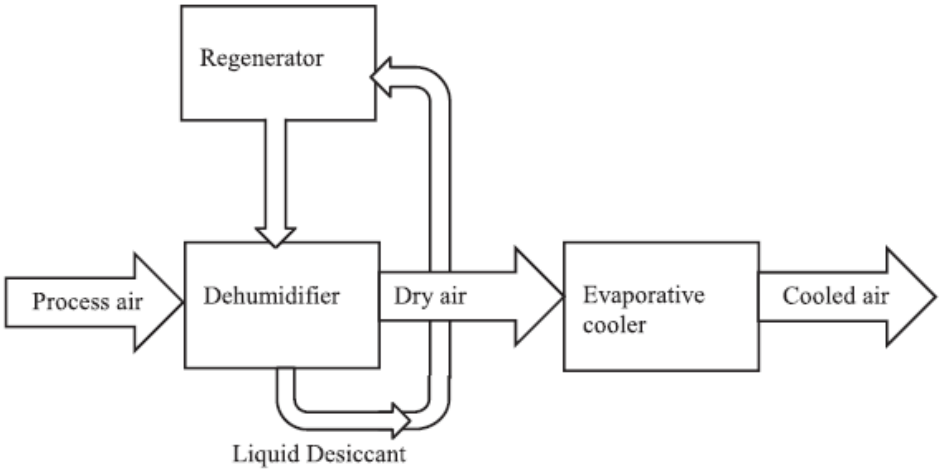


Figure 21. Diagram of desiccant evaporative cooling (Elsarrag et al., 2016)

Combined system of desiccant evaporative cooling and direct evaporative cooling also studied by many researchers for hot and humid regions. Mohammed et al., (2013) found that evaporative cooler can be used with desiccant dehumidifier to provide better thermal condition for humid region of Kuala Lumpur.

2.4.5 Direct/Indirect Combinations

Both indirect and direct evaporative systems can be combined for cooling the building. Air can be cooled by an indirect method and then further cooled by a direct method (Figure 22). Wet bulb and dry bulb temperatures of the air are reduced by the indirect process at the first stage. As no moisture is added to the air, the humidity ratio remains constant (ASHRAE, 2000). This air then passes through the second stage; the direct evaporative cooler causes the humidity level of the surrounding to increase. In figure 23, the psychrometric chart for

combined evaporative system is shown. The use of direct/indirect evaporation process depends on the climatic conditions of the region. The best choice is sometimes to use combinations (Lechner, 2009).

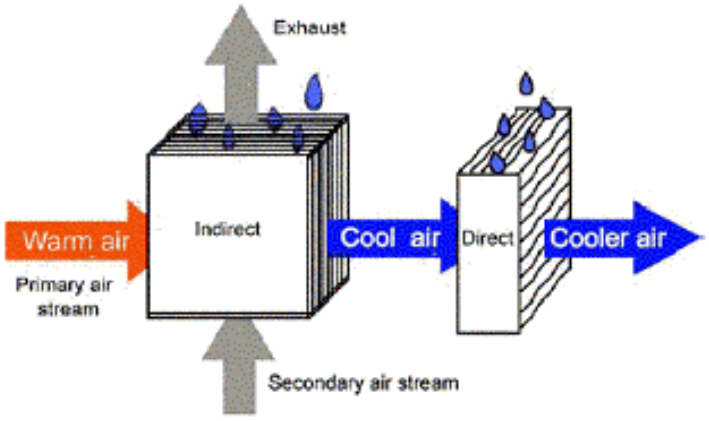


Figure 22. Direct/ Indirect Combination (Musa, 2008)

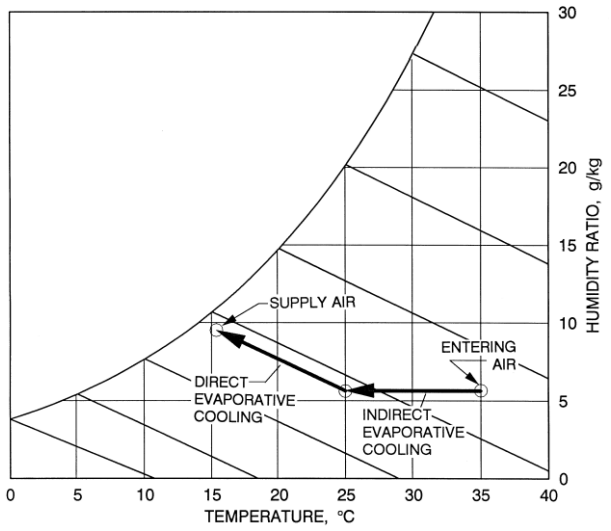


Figure 23. Direct and Indirect Combination (ASHRAE, 2000)

2.4.6 Application of Direct and Indirect Evaporative Cooling

The Maisotsenko cycle (an improved version of IEC) has been investigated for Mediterranean climate of Greece. Rogdakis, Koronaki, Tertipis (2014) have found that it had good performance in terms of water and electricity consumption. They used 40 W fan which prevented the system from becoming passive. This system was not suitable for humid climates due to the high level of demand for electricity and high water consumption.

Baca et al., (2011) have developed a methodology in order to evaluate the potential of EC strategy (Direct and Indirect) as required in different climatic conditions in Spain. They found that the performance of EC was directly dependent on geographic location. In this method, the EC strategies had been suggested depending on the location, and the improvement of comfort was calculated hourly. It was found that the DEC is good in the continental climates which has less relative humidity as seen in Figure 24(a); the IEC is more efficient on the Mediterranean coast which has a higher level of relative humidity and temperatures as seen in Figure 24(b).



Figure 24. (a) DEC for inner land (b) IEC for coastal region (Baca et al., 2011)

Heidarinejad et al., (2008) studied in multi-climatic regions of Iran, where there is plenty of water for an evaporative cooling system. Four cooling processes (DEC, DW with DEC, DEC/IEC, DW with DEC/IEC, and mechanical cooling systems) were investigated. Consequently, 53% of people comfort was provided by using DEC (Figure 25).

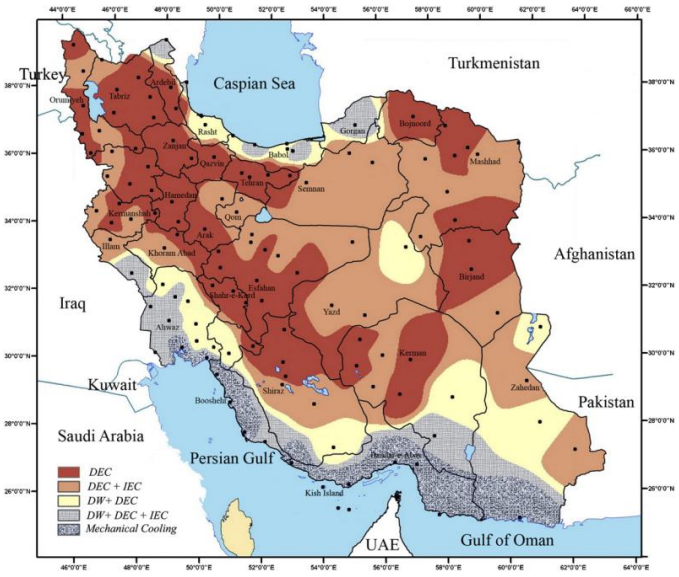


Figure 25. Evaporative cooling system for Iran

Jaber and Ajib (2011) designed the Indirect Evaporative air conditioning system for Jordan where there is a scarcity of water. This system was used for 500,000 Mediterranean residential buildings. It was concluded that legionella bacteria did not produced if the system was regularly maintained, cleaned and dried out.

2.4.7 Advantages and Disadvantages of Evaporative Cooling

There are some disadvantages of evaporative cooling systems (Musa, 2008 and Jaber and Ajib, 2011). However, these disadvantages can be prevented if the system is designed well. For example, humidification or dehumidification can be provided according to the climatic conditions of the environment. The production of bacteria can be prevented if the system is dried out. For water consumption, water can be re-used in order not to use excessive water. As seen in Table 2, the advantages and disadvantages of evaporative cooling method is presented.

Table 2. Summary of advantages and disadvantages of evaporative cooling

Advantages	Provide better indoor air quality
	Reduce energy consumption and cost
	Reduce harmful gases emission to the environment (no chlorofluorocarbon usage)
	Improve life-cycle cost effectiveness
	Easily integrated into the system or building
	Humidity level can be regulated
	Local materials can be used
Disadvantages	Need water supply which increased water consumption
	Dust mites effects
	Add moisture to the air which is not suitable for humid regions

2.5 Architectural Integration of Evaporative Cooling

When the heating or cooling systems are integrated into a building, they act as one of the elements of the building. It is crucial to determine these systems during the early stage of the design process and not to regard them as separate from the building. Building integration is simply defined as the integration of the component of any systems into the part of the building by creating a connection with the architectural design concept. Although the building integration is related with the physical integration, aesthetics are mainly another main issue for the architects to consider. If the integration of the system is done with the conceptualization of architectural elements (functional, constructive and (aesthetic) formal), then it becomes architecturally integrated. This means that the system should also be aesthetically integrated into the building in order to create good architectural quality. If the heating or cooling

system is functionally or constructively integrated into the building, the system is then named as building integrated (Munari Probst and Roecker, 2012).

Architectural integration technology is used for architectural design in order to improve the thermal comfort conditions of the occupants within the occupied area by using low energy. Therefore, economic feasibility is also another important aspect. This is achieved by integrating the system for both cooling and heating requirements into the roofs, fenestration (window, door), facades, shading systems and urban furnitures (Reddy, 2010). Building integrated evaporative cooling can cause the temperature of the surface of the material and the surroundings to be reduced by using specific materials. These are classified as Natural (palash fiber), Porous (porous ceramic), Metal organic framework (Zeiler and Vissers, 2012).

Roof is one of the building integrated evaporative cooling element. It can also be used as porous roof for indirect method of evaporative cooling. Wanphen and Nagano (2009) have conducted the experimental test to identify porous roofing material in order to reduce surface temperature and thereby, the building. The result has showed that siliceous shale showed good performance in terms of lowering the temperature.

Accordingly, the rain water is collected and allows evaporation to take place during sunny day. After, the temperature of the material and air become lower because of the release of latent heat. On the other hand, there are some researchers who integrated evaporative cooling system into roof. Haghighi et al., (2015) have conducted an experiment regarding the integration of the vaulted roof and evaporative cooling technique together. Due to the pressure differences created at the roof and the bottom of the room, the air at the roof was forced upward and inside air was drawn. The results showed that the relative humidity should be lower and the temperature should be higher with more than 0.4 m/s wind velocity (Figure 26).

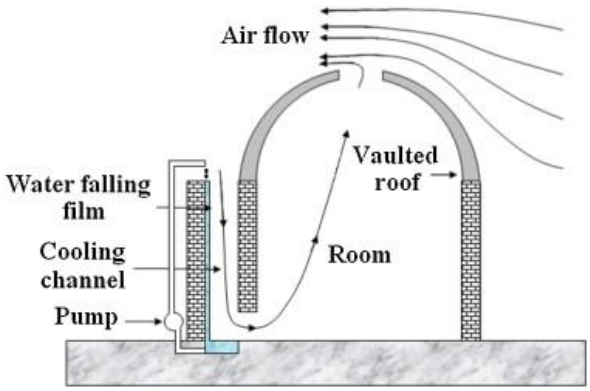


Figure 26. The integration of the vaulted roof and evaporative cooling technique (Haghighi et al., 2015)

The other building integrated method for direct evaporative cooling is the usage of porous materials in the **walls**. The system is passive since it is not essential to use pump or fan. Porous material can absorb water due to their capillary action and continuously become wet to allow evaporation.

The water-evaporative walls are developed as novel evaporative cooling technique (Figure 27) which prevent the energy flow to the inside and reduce wall temperature (Naticchia et al., 2010).

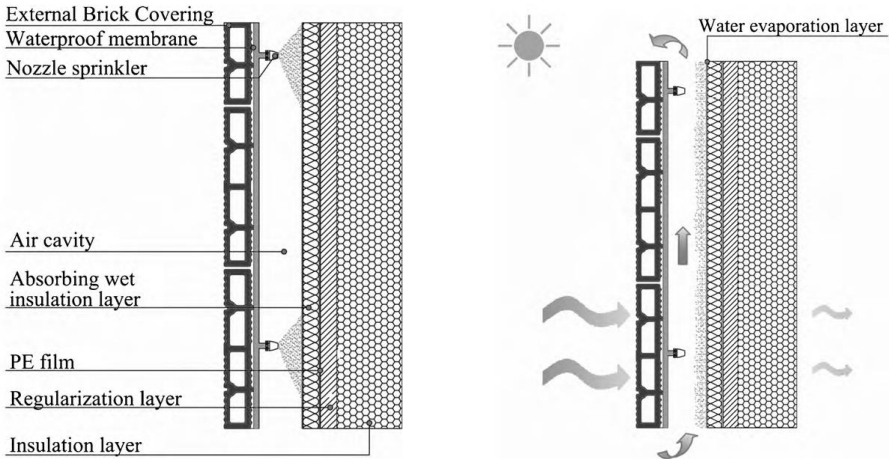


Figure 27. Evaporative cooling facade (Naticchia et al., 2010)

Active and passive evaporative cooling strategies are all used in many studies. Chen (2011) has studied wet porous cooling plate in order to create cooling by evaporation within porous plate for building wall. The system is inserted to the northern wall of the space. The water which is used for evaporation is given from top of the porous plate and thermal insulation is placed to the top and bottom of it (Figure 28).

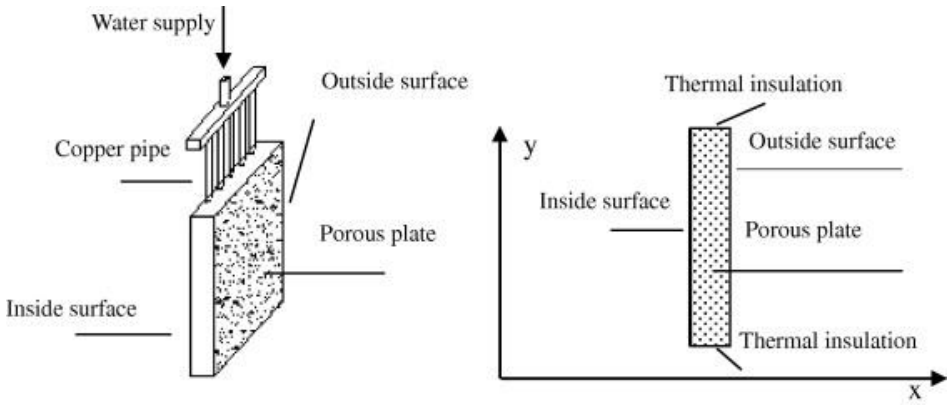


Figure 28. Porous plate integrated into wall (Chen, 2011)

He and Hoyano (2011) improved passive evaporative cooling wall (PECW) and constructed into porous ceramics (Figure 29). Therefore, it allows wind penetration and water absorption afterwards reducing the surface temperature by means of water evaporation. This method does not need any source of water supply to make the surface continuously wet. The water soaking-up method for evaporation is used in order to reduce the temperature of the surrounding. The lower end of the porous material is placed into water which has a high water soaking-up ability. Therefore, water rises up by capillary action which means the surface becomes wet to a high level.

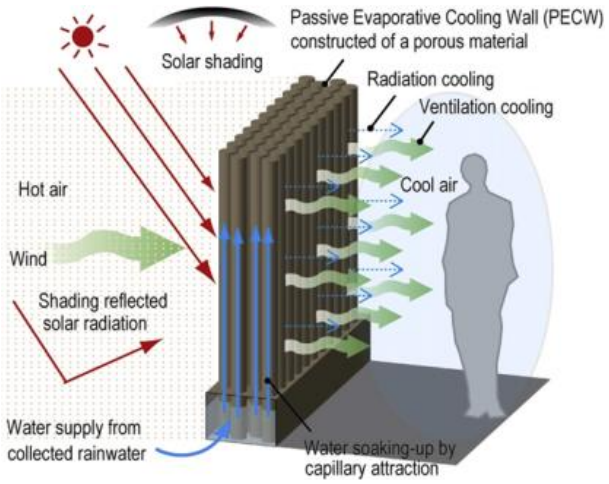


Figure 29. Passive Evaporative Cooling Wall (He and Hoyano, 2011)

There are also many experimental investigations regarding the EC system in the Mediterranean climate. Franco et al., (2011) used corrugated cellulose paper for evaporative cooling pads for greenhouses in Spain (Figure 30).

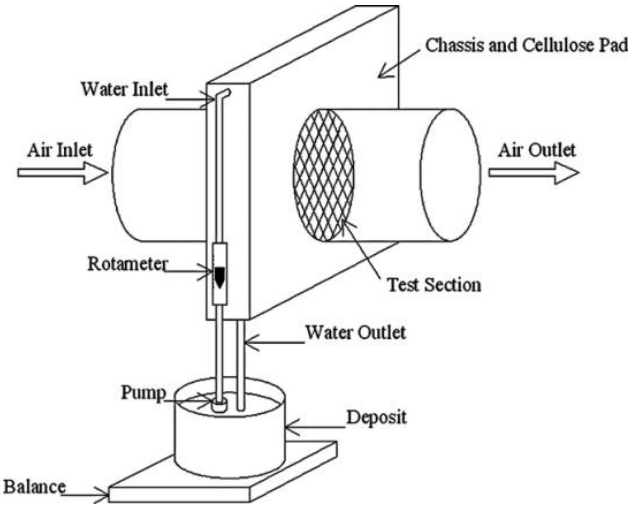


Figure 30. Water recirculation for evaporative cooling system (Franco et al., 2011)

A **solar chimney** is integrated into a south-facing wall and an evaporative cooler (M-Cycle) is integrated into the ceiling panel as shown in Figure 31 (Miyazaki et al., 2011). An evaporative cooling cavity (ECC) and solar

chimney (SC) have also been considered as shown in Figure 32 to provide natural ventilation and passive cooling (Maerefat and Haghighi, 2010).

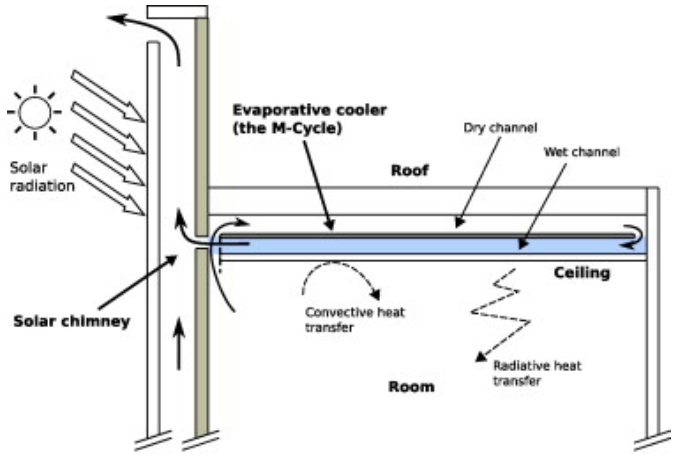


Figure 31. Solar chimney and evaporative cooler (Miyazaki et al., 2011)

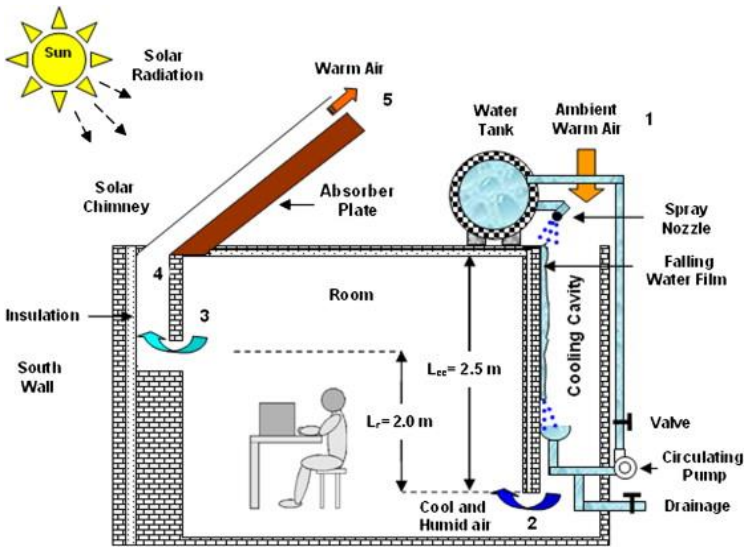


Figure 32. SC and ECC (Maerefat and Haghighi, 2010).

Wind tower or wind catcher is an element of the building which is installed on top to allow more natural ventilation in order to reduce energy consumption. It is used in many hot-arid and hot-humid regions such as Egypt, Iran, coast of Persian Gulf and Oman Sea to create cool and ventilated indoors (Bahadori et al., 2014; Gharakhani et al., 2017). There are some limitations of the performance of wind tower such as (Dehghani-sanij et al., 2015):

- Reducing wind speed by fixed air inlet
- Entering of any animals and dust
- Not enough to cool the indoor in hot days
- The effect of wind tower is low at low wind speed

Although there are some problems of the performance of wind tower, some important parameters should be considered to overcome these problems such as: height, cross section of the tower and position, place of the openings (Montazeri, 2011). Some researchers studied to increase the performance of wind tower by investigating some factors as aforementioned above. Poshtiri and Mohabbati (2017) proposed wind catcher where a shower system is attached in order to reduce the ambient air temperature resulting lower electrical energy consumption. Calautit et al., (2017) studied wind catcher by integrating vertically-arranged heat transfer devices to provide natural ventilation, to reduce air temperature and to maximise cooling effect. It was found that the inlet air was reduced by 12K which creates good cooling effect. Khani (2017) studied the modular wind tower with wetted surface which reduces the air temperature by 10°C and increases the relative humidity by 36%. These integrations can be seen in Figure 33.

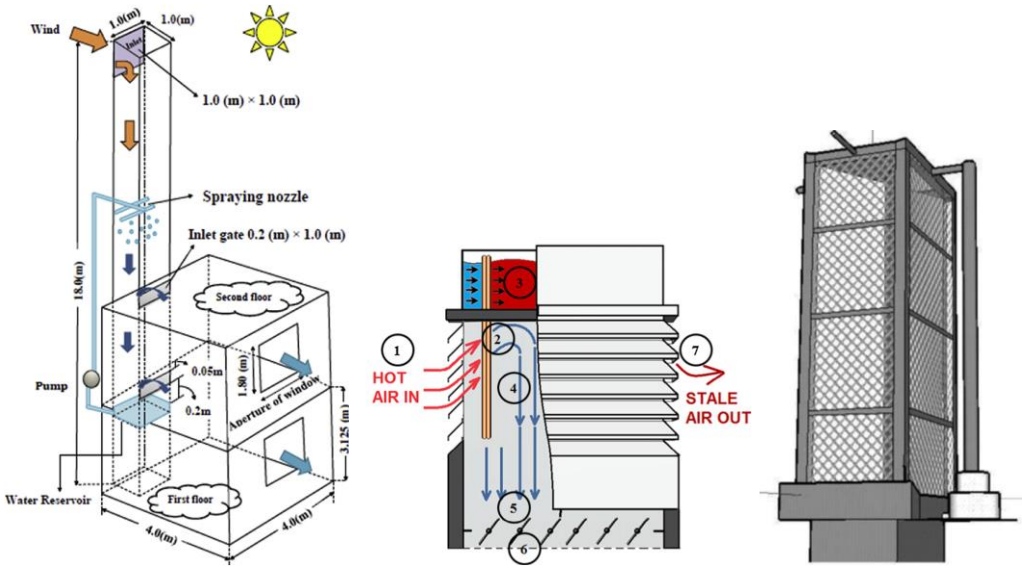


Figure 33. Schematic view of wind catcher integrations (Poshtiri and Mohabbati (2017); Calautit et al., (2017); Khani (2017)

2.5.1 Functional Integration

One fundamental requirement for human comfort is to cool the building in extreme summer. From this point of view, a cooling system should be identified as one of the functionalities of the building envelope (Munari, Roecker, 2011). It is a well-known fact that architectural integration refers the multi-functionality. The integration of the system is used for cooling in the external skin of the building. Wong (2010) studied vertical greenery systems to reduce surface temperature, to provide shading and to insulate the facade.

The building envelope is not only formed by the facade. As the envelope is the external skin of the building, it separates the exterior part of the building from the interior space. If it is well designed, a comfortable indoor environment is provided using little energy. In consideration of this, a cooling system can also be integrated into the shading devices and roof. The functional aspects of architectural integration, can be classified together in terms of their common objectives. These functions can be grouped as;

- The protection from climatic elements (sun, wind, rain) and climatic conditions (cold, hot)
- Noise protection
- Visual control
- To provide daylighting, ventilation and fresh air
- To provide energy.

2.5.2 Constructive Integration

While integrating the cooling system technology into the building, features of the structural system should also be considered. These systems are related with fire protection, transfer of the system load uniformly, prevent thermal bridges and withstand wind load.

Ojembarrena et al., 2013 designed a vegetal façade composed of translucent green wall. They used recyclable and reusable materials in the constructive

components of the vegetal façade (Figure 34). It helps to minimize the indoor temperature by providing shading.

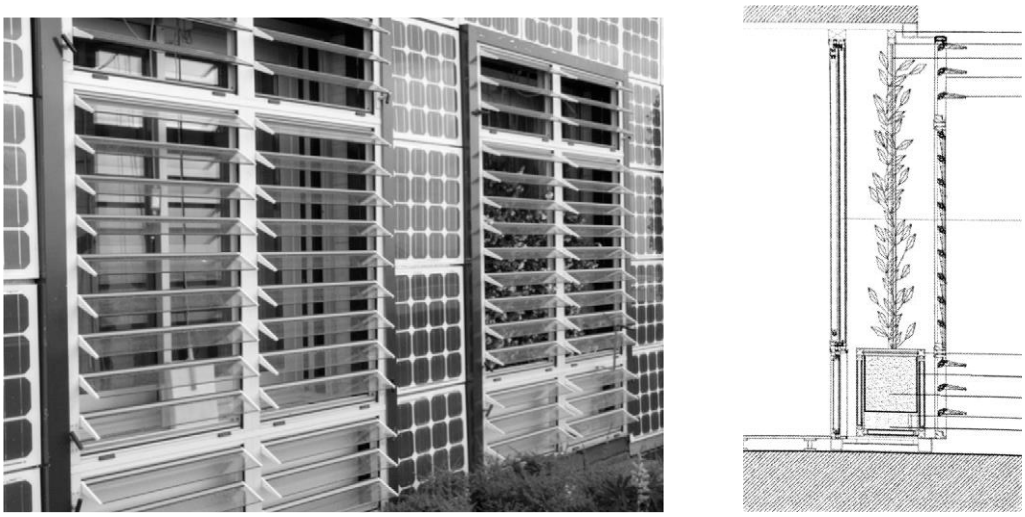


Figure 34. Vegetal Facade (Ojembarrena et al., 2013)

2.5.3 Formal Integration

The functional and constructive issues were well considered. However, since aesthetic is a subjective aspect, it is not exactly easy to define. On the other hand, formal composition of the system should also be coherent with the functional and constructive requirements of the whole building. There are some formal properties such as (Munari, Roecker, 2011):

- The size and position
- Material and texture
- Colour, shape, size of the modules
- Types of jointing

Additionally, in the design process, a well aesthetic integration should also be treated as required situation as a well physical integrated system.

2.6 Evaporative Cooling Pads

The evaporative cooling pad material plays a vital role for increasing the cooling efficiency of the evaporative cooling system. This is obtained by keeping the surface of the material wet which causes to enhance the performance of cooling efficiency.

Several researchers are studying to search and develop new pad material for evaporative cooling system which is aimed to improve the efficiency and cooling potential of the system. Currently metal, wood, plastic, ceramics, celdek pads, cellulosic pad, aspen pad and rigid medium pad are used as a pad for evaporative cooling system (Warke, 2017; Vala, 2016). Nowadays, manufacturers have been used pads made from cellulose based paper or plastic fibres in order to obtain more efficient evaporative cooling system for extreme climatic conditions and for different applications such as industrial sector.

Despite these materials are efficient, they are complicated and expensive due to the fabrication and processing costs. Therefore, the locally available materials can be significant alternatives for evaporative cooling system. Since local materials are easy to find and abundant in most locations, it could be a low cost opportunity to be utilized in less developed hot countries. Besides of being low cost, light in weight, abundant and environmentally friendly, it should also have high water holding capacity and long life span which can be used as an alternative material for evaporative cooling systems.

In this section, locally available materials in particular, eucalyptus fibres and yellow stone are briefly described in order to evaluate the performance under different operating conditions. In addition to this, the commercial pad material, such as, polymer hollow fibre is also explained in section 2.6.3. Although the hollow fibre is not easy to manufacture, it has large surface area which is essential for heat and mass transfer.

2.6.1 Wood Materials (Eucalyptus Tree)

Local materials which are easily obtainable were used in the production of traditional buildings in Cyprus before 1960 in particular. In deciding which material can be employed in building construction, the availability of the material plays a vital role. As stones are extracted from the mountainous areas, it is necessary to use them with wood or earth. Due to the construction techniques and selection of natural materials, the buildings are easily adapted to the nature. For the inland region (Mesario) earth, straw, bushes are used as available materials which are environmentally friendly, cheap and provide better thermal conditions.

Moreover, wood is another local and constructional material used in the island. Particularly pine, oak, poplar and cypress are widely known for supporting the Roofs and wall openings. On the contrary, the eucalyptus species are not used in the structural or constructional material. It is one of the genera of Eucalypts with Angophora and Corymbia which is native to Australia and some Pacific regions. As eucalyptus tree grows fast, it could be utilized in many industries for timber, fibrewood, pulp, charcoal, etc. production (Simberloff & Rejmánek, 2011). According to Couppis (1956), eucalyptus grows to a diameter of 6 feet (1.8288 m) within 40 years. However, it can drain a huge amount of water from underground and thus, the level of underground water is declined. As they have water-sucking capabilities and high level of productivity, they had been brought to Cyprus during the British Colony (1878-1960) by one of the English M. Madon in 1879 to defeat malaria. They were planted in marshy land in order to dry out it, because of causing malaria diseases. Evapotranspiration and direct evaporation occurred in particular, marshland areas. In 1970s, since it was the drought period, it is cited that water level was reduced although water levels were higher than sea level in between 1940-1986 (Milnes, 2011). Now as they dried out underground water resources, this leads to be scarcity of water in Cyprus.

Due to the fact that eucalyptus consists of hemicelluloses inside, it has a flexible structure. Accordingly, this types of fibre plays a vital role for the production of absorbent paper; in particular toilet paper and tissue (Garcia et

al., 2012). Together with pine, fir, hemlock, etc. are crucial raw materials for the production of paper pulp.

Eucalyptus is also one of the common example for woody biomass production and thus, lowering the greenhouse gases (Garcia et al., 2012). It saves the energy since it is needed less water.

2.6.2 Stone Materials (Yellow Stone)

The natural stones began to be used in the Neolithic Age by the starting of first settlement in Cyprus. They were firstly used as stone tools for daily life and hunting. Then, it was started to use in residential, religious, government, many cultural heritage sites, decorative purpose and for restoration of old buildings in the island. Throughout history, it is clearly seen that the most durable buildings are made from stone such as Giza Pyramids in Egypt, Machu Picchu in Peru, etc. In Cyprus, there are many stone heritages and buildings which were built in the early history. Tholos houses (singular tholoi) in Khirokitia were the first settlement where the settlement is listed as a World Heritage Site by UNESCO since 1998. The ancient city of Salamis was built by the Romans where the theatre has been still using by the public. The types of stones used in these settlements are different since they are in different locations. Although it is thought that there are not many types of stones in the island because of being in the same area. However, the island has four different types of geological terranes as: the Keryneia Terrane, the Troodos Terrane, the Mamonia Terraneand and the Circum Troodos Sedimentary Succession. Therefore, it involves different kinds of stones which are extracted from different quarries in particular Limassol, Larnaca, Nicosia, Karpasia, Five Fingers Mountain Ranges, etc.

One of the porous natural stone is called “yellow stone” (locally named) which is extracted from Gerolakkos village (in Turkish Alayköy). As it is a kind of sandstone, it can be easily used as cut blocks for construction and restoration purposes. This vuggy limestone had been used in many historical monuments (for the Venetian fortification) and churches in Nicosia (Ioannou, et al., 2009).

Modestou, et al. (2015) had made a thorough investigation about carbonate stones found in Cyprus. According to their findings, yellow stone has high open porosity (ratio of holes area to total surface area) and low density (< 1.8 g cm^{-3}). It is found that capillary absorption coefficient is the highest compared to other carbonate stones (1000 $g.m^{-2}.s^{-1/2}$). From this point of view, yellow stone has been still used at the wall of the sewage well of the house to absorb any liquid for long time. It is continued to absorb water until the stones become saturated. It is also studied that uniaxial compressive strength is low, thus its mechanical strength is weak.

2.6.3 Polymer Hollow Fibre

Since water is directly in contact with the incoming air in the evaporative cooling system, there is a potential for microbial growth due to the supply of stagnant water. This may provide an opportunity for the spread of liquid phase-born bacterial diseases for occupants (Johnson et al., 2003).

In order to solve this problem, a hollow fibre can be suggested to use for evaporative cooling system since there are some advantages. The size of Polyvinylidene fluoride (PVDF) hollow fibres (manufactured by ZENA Ltd.) is 0.8mm of outside diameter and 0.6mm of inside diameter with the pore size of 0.5μm and a porosity of 50%. Compared with porous pad media, hollow fibre materials provide several advantages as follows:

- allow selective permeation of moisture: with pore sizes less than 0.1μm, hollow fibre material will allow the water vapour transfer but eliminate the bacteria and fungi penetration (Chiari, 2000);

- provide large surface area per unit volume (Wickramasinghe, 1993) which is favourable for enhanced heat and mass transfer.

The hollow fibre materials and their applications are summarized in the literature (Chen et al., 2016). According to Chen et al., (2016) the overall heat transfer coefficients could reach 1675W/m^2K with a fibre diameter of 550μm. Kachhwaha and Preahhakar (2010) analysed heat and mass transfer

performance for a direct evaporative cooler using a thin plastic plate. The experimental testing results indicated that the outlet air temperatures were between 21°C and 23°C, at the inlet dry bulb temperature of 24.8-28.4°C, the air humidity ratio of 2.3-5.8g/kg and air mass flow rate of 0.13, 0.2, 0.3 and 0.4g/s. Zhang (2012) proposed the theoretical investigations on a rectangular cross-flow hollow fibre membrane module for air humidification. With 2600 fibres (fibre outside diameter 1.5mm) inside the module, the outlet air temperature could reach 21.5°C when the inlet dry bulb temperature was 30°C. The above publications are mainly concentrated on the theoretical analysis on the polymer hollow fibre integrated evaporative cooling system. The available experimental results were limited to the variation of outlet air temperatures with respect to different air flow rates.

2.7 The Performance of Evaporative Cooling

Considering the material for evaporative cooling process, the performances of evaporative cooling pad were evaluated by using some mathematical expressions. The performance of eucalyptus fibres was evaluated according to the following equations:

2.7.1 Temperature Difference

The temperature difference between the inlet and outlet air temperature is a common factor for evaluating the material performance based on the cooling performance as given in the following expression:

$$\Delta T = T_1 - T_2 \tag{2.1}$$

Where, T_1 and T_2 represent the inlet and outlet air temperature while passed through the material.

2.7.2 Cooling Efficiency

The cooling efficiency is an important parameter in order to evaluate the material based on air saturation capacity. Therefore, it is the ratio between temperature difference of material while air is passing through it to the difference between inlet dry and wet bulb temperature named as wet bulb depression. Meaning that the ratio between the thermal difference on passing through the material (T_1 - T_2) and the maximum thermal difference that would occur if the air were saturated (T_1 - T'_1). When the cooling efficiency becomes 100%, it is meant that the temperature reduction is equal to the wet bulb depression.

The cooling efficiency (saturation effectiveness) of eucalyptus is calculated with Eq. 2.2 given by ASHRAE (2001):

$$\eta\varsigma = \frac{(T_1 - T_2)}{(T_1 - T'_1)} \tag{2.2}$$

Where T_1 is the dry bulb temperature of inlet air, T_2 is the dry bulb temperature of outlet air and T'_1 is the wet bulb temperature of inlet air. From the equation, the efficiency of an evaporative cooling system could be calculated as the ratio of the difference between inlet - outlet DBT and difference between inlet DBT - outlet WBT. The temperature levels of inlet air for testing in the laboratory were regulated according to the temperature of the days in summer when cooling is most needed.

2.7.3 Cooling Capacity

The cooling capacity in an evaporative cooling process is the function of the mass flow rate, the specific heat capacity of air, temperature difference between inlet and outlet air. The mass flow rate of air through the material is

calculated by density, ρ and velocity of air, V, of the air, and cross section area, A_C of material sample which is defined as:

$$\dot{m}_a = \rho V A_C \tag{2.3}$$

The sensible cooling capacity is an important parameter for performance analysis as given by:

$$Q_c = \dot{m}_a \, C_P \, (T_1 - T_2) \tag{2.4}$$

Where, $\dot{m}_a$ is the mass flow rate and C_P is the specific heat capacity of air.

2.7.4 Coefficient of performance (COP)

The coefficient of performance is crucial term based on the efficiency of evaporative cooling process. The power consumption for evaporative cooling process is based on the power used by electrical equipment. The performance analysis was also carried out using the coefficient of performance (COP), which is the ratio of the cooling capacity, Q_c to electric input power, W_p and W_f were used during the experimentation. These were the water pump and fan.

$$COP = \frac{Q_c}{W_p + W_f} \tag{2.5}$$

2.7.5 Evaporation Rate

Evaporation rate is calculated with the Eq. 2.6 to ascertain the amount of water required for the system. Absolute humidity can be determined through the psychometric chart by plotting the intersection point of DBT and RH of air. It

is defined as the water vapour content per kg of air flow at the inlet, w_2 and at the outlet, w_1:

$$m_w = \dot{m}_a (w_2 - w_1) \tag{2.6}$$

The specific enthalpy of humid air is written by the following equation:

$$h_k = 1.006T + w(2501 + 1.85T) \tag{2.7}$$

Where t is the temperature in °C. w is the absolute humidity of air in kg_{wv}/kg_{da}. The specific heat of dry air (c_{pda}) is 1.006 kJ/kg°C.

Absolute humidity w, can be defined as the mass of water vapour per kg dry air, which could be calculated with the following equation (8):

$$w = \frac{c_{pda}(T'_1 - T_1) + w_2 h_{fg_2}}{h_{g_1} - h_{f_2}} \tag{2.8}$$

2.7.6 Specific Cooling Capacity

The specific cooling capacity (*SCC*) is determined to find the amount of cooling capacity (*CC*) obtained per kg of water evaporated. The specific cooling capacity did not used in the literature before. It is the ratio of cooling capacity to evaporation rate (*ER*). It is used to show the amount of water used at different air velocities and defined with the Equation (9):

$$SCC = \frac{CC}{ER} \tag{2.9}$$

2.7.7 Uncertainty analysis

It is necessary to find the experimental error of the measured values during experimentations. Uncertainty analysis could be performed by the use of the propagation of error formula (Moffat, 1988; Taylor, 1997). By this method, the source of errors which are the variables used in experimental analysis (*e.i.* temperature difference, cooling efficiency, relative humidity, etc.) are identified. The experimental uncertainty can be obtained by the Eq. (16):

$$Y = f(X_1, X_2 \dots X_n)$$

$$\delta Y = \sqrt{\left(\frac{\partial Y}{\partial X_1}\delta X_1\right)^2 + \left(\frac{\partial Y}{\partial X_2}\delta X_2\right)^2 + \cdots + \left(\frac{\partial Y}{\partial X_n}\delta X_n\right)^2} \quad (2.16)$$

Where δY is the overall uncertainty in the result. $(X_1, X_2 \dots X_n)$ are the set of measurement which are directly measurable parameters. δX_1, $\delta X_2 \dots \delta X_n$, are the overall uncertainty of parameters. Each term represents the same calculation: The partial derivative of Y with respect to X_1 is multiplied by the uncertainty value for that variable.

2.8 Water Harvesting Technology

In the previous sections, the concept of evaporative cooling systems has been introduced. An important point to note is that a typical evaporative cooling system would require water source for the cooling process to take place. Following to that, this section will provide insights into various water collection or harvesting technologies reported in literature. This section gives an overview to the various water harvesting technologies and finally potential technologies that may be applied in Cyprus are proposed and briefly discussed, which play a vital role for the proposed evaporative cooling system.

The increasing demand for water is led to the depletion of the aquifer thus, causing water scarcity. It is aimed to protect and provide more water for better living standards. Therefore, some non-conventional water resources should be

identified in order to meet the requirements of freshwater. These are: harvesting of rainwater, ground water harvesting, desalination of seawater, atmospheric water harvesting (Murad, 2010; Tsiourtis, 2003).

2.8.1 Rainwater Harvesting

One of the alternative water sources for water management is the rainwater harvesting (RWH). It is mostly used for drinking and non-drinking water as the population and need for water are increased, in particular in regions where there are water shortage problems. It is one of the alternative methods as it can be easily collected in rainy days and do not need to be treated for non-drinking use. This method also acts like a zone where prevents the degradation of streams and flooding where there is a damaging impact of excess rainfall (Farreny et al., 2011). Despite several advantages of collecting water by rainwater, there are some disadvantages of using the system. The collected water from the roof or in a place where exposed to polluted air, may be contaminated due to the air pollution, animal faeces. Thus, the collected water needs to be treated before use. However, the using of non-drinking water is used for public interest such as fire fighting, washing of pavement, irrigation in Portugal (Silva et al., 2015).

It is shown that the potential of rainwater harvesting system provides a key source for domestic, farmland and industrial purposes in many countries. Take some application around the world for instance, rainwater collecting system has been using in the residential buildings. A 10 m^3 of rainwater storage tank should be used for each house in order to use the collected water for toilets and gardens (Domènech et al., 2013). A 16 m^3 of collected rainwater can provide drinking and non-drinking water for a drought in semi-arid Brazil (Gomes et al., 2012). In Atlantis (South Africa), the drinking water can be supplied to many millions humans by dune infiltration. Due to the sandy soils, 15%-30% of the rainwater fill up the groundwater. In order to increase the groundwater, the artificial recharge through dune infiltration supplies more water since the

groundwater is the only source of water of the town (Van Steenbergen et al., 2009).

As proven by Rashidi Mehrabadi et al., (2013) rainwater harvesting system is not sufficient enough in hot and arid regions since the annual precipitation does not meet the demand of water. However, Mahmoud et al., (2014) found that the rainwater harvesting through the roof provides an alternative source of water in the arid region, Khartoum (the capital of Sudan). The rainfall level shows variables in Khartoum as few rainy days and intense rainfall. Due to this, some buildings were selected for potential sites for rainwater collection in certain times of the year. It was found that approximately $0.033m^3$ water can be harvested per unit area from the rooftop.

Cyprus is categorised as a semi-arid areas (Cyprus Department of Meteorology, 2014; Pashardes and Christofides, 1995; Harb, 2015) where has low precipitation and high temperature. Nowadays, rainwater harvesting is described as useful method for collecting water from roofs or other parts of the urban structures. It can be used in regions where there is water shortage problem such as western United States and African countries (Ling and Benham, 2014). In this light, using of water from underground can be minimised.

In a research conducted by Harb (2015), the potential of rainwater harvesting system was assessed in the Middle East Technical University in Cyprus (METU-NCC). It was not aimed to optimize the rainwater harvesting system. It was aimed to study if there is a rainwater harvesting potential in the campus. Thus, it was found that the system can meet the campus irrigation demand by 41.2%. The reservoir volumes were calculated as 2300 m^3, 3500 m^3 and 1100 m^3 with efficiencies of 37.8%, 41.3% and 90.5% respectively.

Since this study represents the preliminary study for assessing the potential of the system, more study can be conducted to ascertain other factors of the system. It has been also reported that the rain falling on Limassol city (Cyprus) was doubled than potable water supplied in the years 2003/04-2008/09 (Water Research and Management - The Cyprus Institute., 2017). Meaning that

rainwater harvesting system can be applied in rooftops of any buildings in Cyprus.

2.8.2 Ground water Harvesting

Groundwater is a main source of fresh water. Generally speaking, the fresh water is supplied by underground around 20% of world (Dube et al., 2013). It is stored in rocks called aquifers where the water is filled by precipitation melting of snow, evaporating of water. The first water layer which has contact with the soil can easily evaporate. Between the first layer and aquifers, there is a layer which includes small amount of water. Below this layer, the water table is existed where excess water is filtrated into it. Underneath of the water table, water is moved to the aquifers where the groundwater is pumped from. This natural filling of water is occurring slowly since there are layers where water has to pass through.

Due to the growth of population, lack of water management, over exploitation, and global warming, the groundwater is depleted which resulting the lack of water and the salination of water. Thus, groundwater recharge can be suggested by directing surface water towards the aquifers.

Groundwater harvesting is clean and cheap methods of obtaining reliable water from the aquifers. However, these are at risk since the water in aquifers is overexploited beyond their efficiency (Socratous, 2011). The excessive use of groundwater due to the higher demand of water in Cyprus is led to deplete the aquifer, thus causing water scarcity. It is searched that the biggest part of the Akrotiri Aquifer has become salted because of the seawater intrusion and over pumping (Demetriou and Georgiou, 2004). In Figure 35, the cross section of the aquifer on 2003 is shown, indicating that the amount of fresh water is almost low shown in blue colour. The colours from red to blue represent the amount of saline water due to the seawater intrusions. As the ground water in the aquifer flows inside, the water becomes less saline. The darker blue arrows represent the flow of sea water.

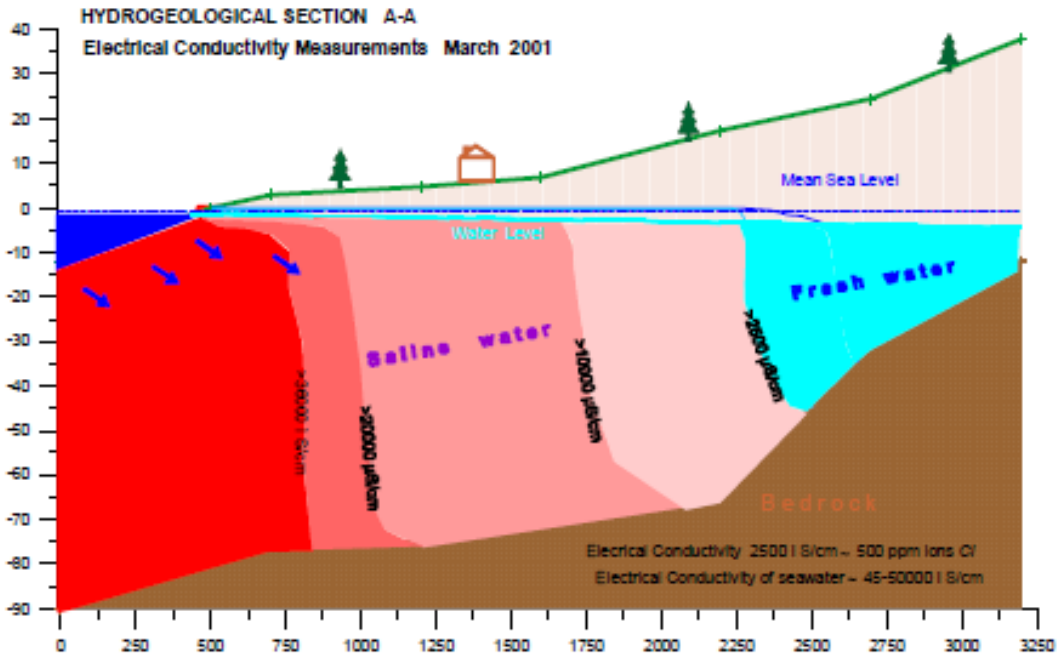


Figure 35. Cross section of Akrotiri Aquifer (Demetriou and Georgiou, 2004)

2.8.3 Water Desalination

Water desalination is concerned as a method of water production for all living organisms. It has been reported that 14,000 desalination plants are existed around the world which supply huge amounts of water (Shatat et al., 2013). However, since fossil fuels are used for operating this system, this leads to create negative impact on environment and therefore, to the ecosystem. Nowadays, these impacts are tried to be minimized by integrating of renewable energy resources such as sun into the desalination process. This leads to reduce the emissions of greenhouse gasses and the cost of energy consumption.

The energy required to desalinate salt water is 0.86kWh/m^3. However, the energy required for desalination plants use 5-26 times more of this energy (Manju and Sagar, 2017). The energy sources such as coal, gas or oil have negative impacts on environment. Renewable sources can be integrated into the desalination process to purify the water without compromising the natural environment as a sustainable solution for driving the plants.

The desalination systems that use renewable energy sources can be divided into three categories: wind, solar (photovoltaic or solar collectors) and geothermal energy. These renewable energy sources can be coupled with thermal distillation or membrane desalination system to produce water (Ali, Fath, & Armstrong, 2011; Mathioulakis, Belessiotis, & Delyannis, 2007). The solar still desalination is one of the solar desalination technology which uses solar energy. It is used to trap sun energy which passes via the glass or plastic surface same as the greenhouse phenomenon (Figure 36). The black-coloured basin containing salt water is existed in the unit. It is black-painted in order to increase the amount of solar radiation hitting on the surface. Due to this, the temperature of saline water is increased and the evaporation is occurred. The water vapour is then rose up and contacted with the sloped surface. It is then condensed into water and slide down the slope surface into the tank. This system produced 3-4L fresh water per m^2. It is worth mentioning that this system can be used for domestic use (Shatat et al., 2013).

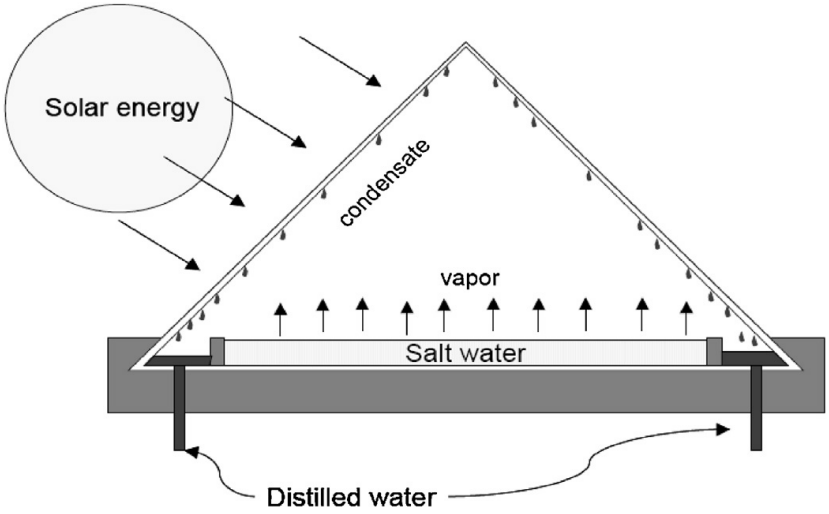


Figure 36. Solar still desalination unit (Shatat et al., 2013)

The “v-trough” collector was demonstrated by Tabor (1966) to expose more sunlight compared to flat plate collector. Nowadays, this collector has taken attention in terms of energy consumption. This is suggested by Riffat and Mayere (2013) for energy required in the desalination application. They demonstrated a new concentrating solar collector for water desalination. As

seen in Figure 37, two parabolic troughs are formed a V-shape which provide easy installation and insulation together with preventing shadow on the receiver. Different solar collectors such as flat plate collector, compound parabolic collector compared to v-trough solar collector is studied in terms of land requirement and cost. It was concluded that v-trough solar collector is more economical than the other collectors for incorporating with the desalination system for obtaining water.

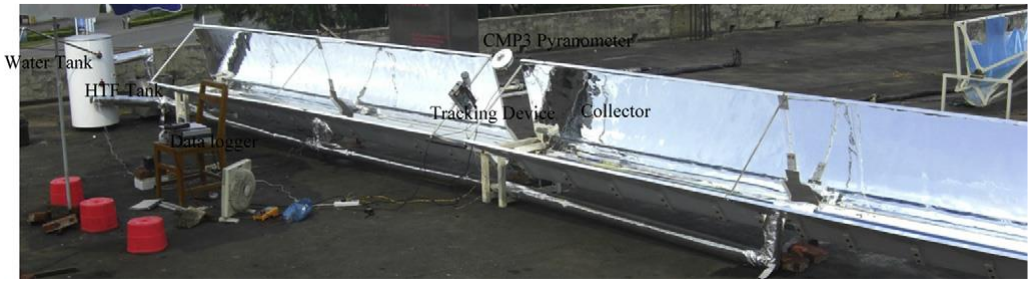


Figure 37. New v-trough solar concentrator (Riffat and Mayere, 2013)

Technical improvement, increasing of fossil fuels prices, low cost equipment and locally available materials, can reduce the water desalination cost (Karagiannis and Soldatos, 2008; Chandrashekara and Yadav, 2017). Although the renewable energy is environmental friendly energy to be used in the desalination process, it causes some limitations such as efficiency and the cost of equipment. The equipment of the plant is required to consume less energy and be low cost together with the higher performance in order to provide clean water (Chandrashekara and Yadav, 2017). Take an example of a low cost solar still, it can be sufficiently used for small houses near the coastal regions in an island for water harvesting. It can also remove the fluoride from the water since it may create anatomic problems for humans. In addition to this, the performance of this system can be improved to heat the water by integrating evacuated tubes or parabola trough (Chandrashekara and Yadav, 2017).

The government of Cyprus has decided to harvest the water by construction of desalination plants in Cyprus (Marangou and Savvides, 2001). *Desalination of seawater* is the separation of water from seawater (salt) under some specific

process which play a vital role in producing water without salt. According to this decision, the first desalination plant was built in Dhekelia, 1997 which provides drinking water to Nicosia, Larnaca and Famagusta (Koutsakos et al., 2005). However, according to the EIA of the Cyprus Department of Fisheries and Marine Research, this plant has negatively affecting the marine environment within a radius of 200 m outfall point. It is cited that the size of the desalination plants on the island does not exceed 2000m^3/day, however the size of Dhekelia Plant is 60,000 m3/day (Mentis et al., 2016).

The price of desalinated sea water in Dhekelia Plant was €0.92/m^3 for a number of years in 1997. The price was then changed at €0.64/m^3 when the plant was bought by the government in 2005 (Fylaktos et al., 2014). Following this, Larnaca Desalination Plant was built in 2000. Another plant was built after the drought in 2008. The mobile seawater desalination unit at Moni was built in 2008 and the Garyllis brackish water plant in Limassol and the mobile seawater desalination unit at Kouklia, Paphos were built in 2011. The last desalination plants were built in the Vasilikos EAC's power station and the other at Limassol in 2013 (Loucaides and Koutsakos, 2015). The mobile desalination units are selling the desalinated water around 1.3 €/m3 and the last unit in Limassol is selling for €0.872/m^3 (Fylaktos et al., 2014).

With the increasing size of water desalination plants, the cost of desalination is also increased therefore; the cost analysis is required to estimate the effect of using different type of water and energy (Karagiannis and Soldatos, 2008). When compared the desalination of seawater and brackish, seawater contains more contaminates than brackish water. The energy consumption and thus, the carbon footprint by the brackish water desalination is lower than the seawater desalination (Miller, et al., 2015).

Hot and dry regions mostly have more solar energy which can be used for desalination concept to provide water (Chaibi, 2000; Shatat et al., 2013). However, using of solar thermal energy in particular for larger-scale plant causes some problems such as: the low productivity and thermal efficiency and

significant larger area is also required (Qiblawey, Banat, 2008; Shatat et al., 2013; Shalaby, 2017)

2.8.4 Atmospheric Water Harvesting

According to the Food and Agriculture Organization, the fog collection may be a cheaper way of harvesting water for portable drink, irrigation, livestock and forest in particular in dry regions (Park et al., 2013).

In foggy regions such as coastal regions, mountain areas where there is a water shortage problem, the water can be collected by demonstrating a mesh for fog harvesting. The fog is occurred by the formation of low-level Stratus clouds while contacting of humid or hot air with cold body. The water vapour is condensed into tiny water droplets suspending in the air. Foggy air is used as a water source by the saturation of air with water vapour as water droplets. The water droplets moved in the air and then, collected on any surface (Brown, Bhushan, 2016).

There is a truth that the water shortage is mostly seen in hot and arid regions since the annual rainfall is low. Thus, the fog water collection is a significant method for the people who are living in hot regions. Nowadays, the fog harvesting is done by using nets in highlands to obtain water from the air. As seen in Figure 38, screen of mesh fog collectors are vertically placed towards the wind in order to face with water droplets in the foggy air. These water droplets create larger water drops which are then fall down to the water tank by the gravity. A 1 m^2 mesh of Standard Fog Collector (SFC) was perpendicularly used which has 1 x 1 m^2 surface to the wind direction as seen in Figure 38a. In Figure 38b, the mesh of Large Fog Collector (LFC) was used in Spain which was supported by cable frame. It is generally used when the water yield is higher to extract more water. The difference between SFC and LFC is the supporting of the mesh. The mesh is supported by cables that are attached to the frame for LFC design; however the mesh in the SFC design is strained over the metal. A registered charity with the Government of Canada, FogQuest, is planning and implementing water projects for people since 1987. They provide

meshes for water collection in America, Africa and Asia by use of natural atmospheric sources of water (Figure 38c).



a b c

Figure 38. The fog collector screens (Karkee, 2005; Klemm et al., 2012; Brown, Bhushan, 2016)

By taking countries of similar climate as examples, fog harvesting methods were reported to produce water as much as 118 L/m² and 51.0 L/m² per day in Nepal and Canary Island, respectively. For semi-arid region of Al-sooda in Saudi Arabia 6.215 L/m² water was produced. For sub-tropical Mpumalanga area, 11 L/m² water was produced. The lists of various fog harvesting methods and the water produced by this methods are shown in Table 3.

Table 3. Various fog harvesting installed worldwide

Fog Harvesting	6.215 L/m²	Al-sooda – Saudi Arabia	Al-hassan, (2009)
Fog Harvesting	11 L/m²	Mpumalanga area-S.Africa	Olivier, (2004)
Fog Harvesting	3 L/m²	Chile	Batisha, (2003)
Fog Harvesting	9 L/m²	Peru	Batisha, (2003)
Fog Harvesting	30 L/m²	Oman	Batisha, (2003)
Fog and Rainwater Harvesting	118 L/m²	Nepal	Karkee (2005)
Fog Harvesting	51.0 L/m^2	Canary Islands	Marzol Jaén, M. V. (2002)

Regarding the potential of fog over Cyprus, it has been reported from the Department of Meteorology in Cyprus that the fog is not occurring often but generally seen in the early mornings. However, it is also mentioned that there are long periods of foggy areas in particular on the mountains when the clouds cover the highest part of the mountains. There is a lack of information about the potential of fog-harvesting in Cyprus in particular the Troodos Mountains where it is the highest part of the island. It is cited that it can be determined by annual cloud frequency, wind regime and topography of the site (Anon, 2017).

In recent years more advanced technologies have been proposed in water harvesting. This section will discuss some of the technologies which are found attractive and promising. One of them is Warke Water Towers as shown in Figure 39 were designed by Arturo Vittori in order to provide clean potable water in some parts of Ethiopia, Africa. This is formed by a lightweight Juncus effusus stalks as an outer housing of the tower to allow air to pass. A mesh net which hangs inside is made of polypropylene or nylon to harvest water droplets from dew. When the air gets cooler, it condenses and thus, the water droplets slide down into the water tank found below. The significant finding from the study is that more than 25 gallons of water (93 L) is daily collected (Nguyen, 2014).

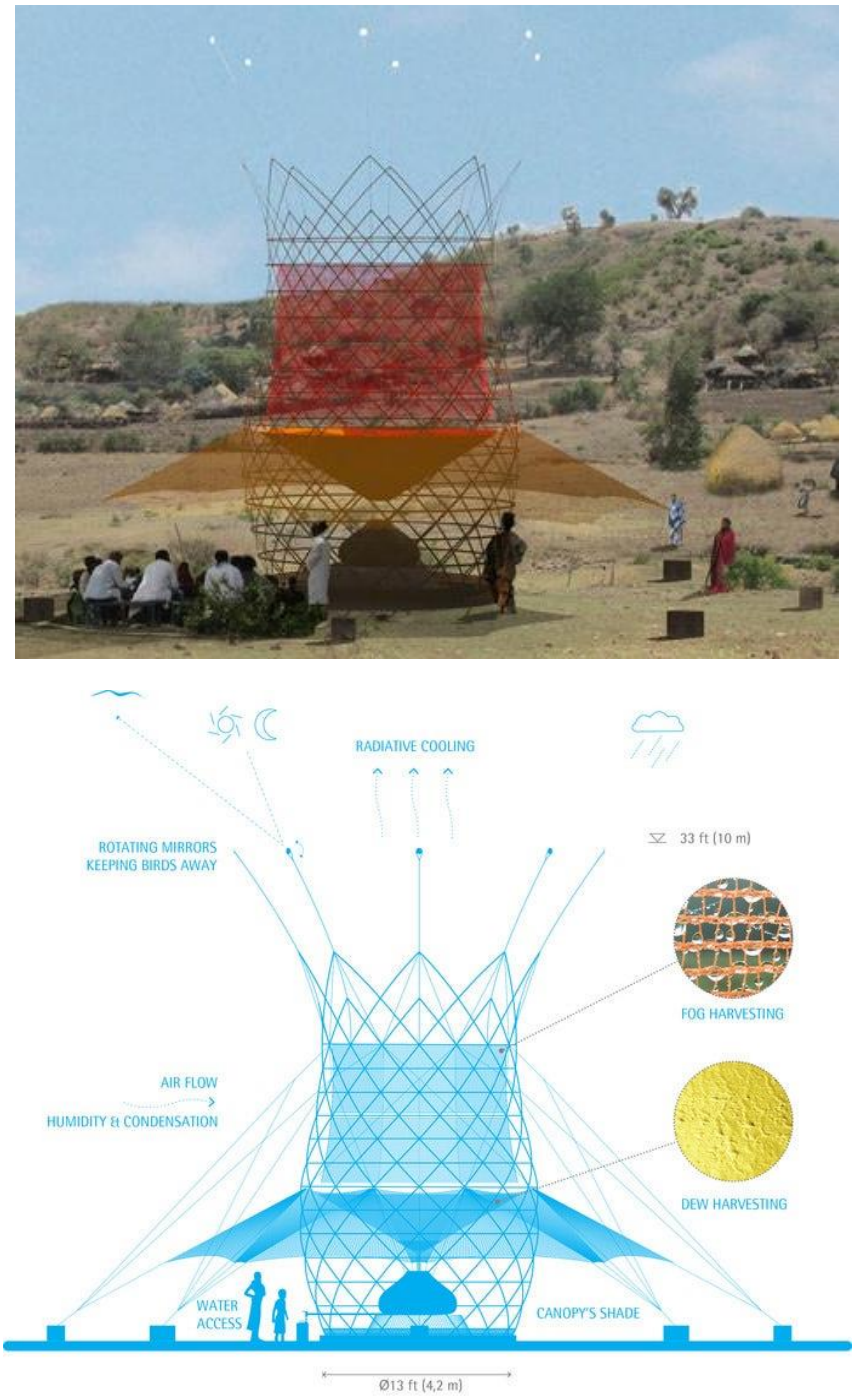


Figure 39. Warka Water Towers, Ethiopia (Nguyen, 2014)

2.8.5 Summary of Water Harvesting Technology

Water shortage is not only a problem of small or poor regions. It affects all parts of the earth since humankind is facing with climate change. For Cyprus in particular, one of the issues in regard to the water scarcity is the rainfall

shortage. As can be seen in Table 4, is the amount of water resource or availability in Cyprus from 1997 to 2002.

Table 4. Type of water resources of Cyprus (Farmer et al., 2006)

Year/ Water Resource	1997	1998	1999	2000	2001	2002
Dams	63.7	33.0	67.4	52.7	62.4	151.0
Deposits	2.0	2.0	2.0	2.0	2.0	2.0
Desalination	6.4	11.0	13.1	13.1	24.9	30.0
Wastewater Treatment	0	2.0	3.0	3.0	1.7	4.0
Total	201.2	177.1	214.6	199.9	220.1	316.1

In this section, the alternative methods such as desalination, groundwater, transportation of water and rainfall harvesting were described for Cyprus and other regions in the world. As mentioned, the rainfall is mostly occurred in Cyprus during winter and filled the aquifers. However, the water in summer is lost through the evaporation. In addition to this, the underground water level is also reduced due to the unconsciously over-pumped of water.

Regarding the desalination of seawater or brackish, some countries such as Greece, Spain or Italy depend on desalinated water for combating water shortage. As seen in Table 5, the amount of water collected by seawater desalination in Rhodes is around 5.000 m^3/day with the cost of 0.425€/m^3. The amount of water produced by brackish water desalination is 1.000 m^3/day with 0.79€/m^3 in Aegean Islands. In Cyprus, 40.000 m^3 of water is produced per day with the cost of 0.9€/m^3. Although the cost of imported water by desalination of seawater is five times cheaper than transportation of water from Greece to Cyprus, it is highly cost and consumes more energy (Sofroniou, Bishop, 2014).

Nevertheless, very limited literature was published in the discussion of the cost or the economic aspect of the water harvesting system. Table 5 shows the summary of the amount of water produced per day and the cost of some water harvesting technologies.

Table 5. Some water harvesting technologies

Water Harvesting Technology	Amount of water per day etc.	Cost	Site	Ref
Seawater Desalination	1000-100.000m^3/day	0.55-2.50 $/$m^3$		Karagiannis and Soldatos (2008)
	<5.000 m^3/day	0.425€/m^3	Rhodes, Greece	Manoli et al., (2004)
	40.000 m^3/day	0.9€/m^3	Dhekelia Cyprus	World Bank, (2004)
Brackish water Desalination	1000 m^3/day	0.79€/m^3	Aegean Islands in Greece	Karagiannis and Soldatos (2007)
	<5.000 m^3/day	0.14-0.32€/m^3		Ortiz et al., (2008)
Fog Harvesting	51.0 L/m^2		Canary Islands	Marzol Jaén, M. V. (2002)
Dew Harvesting	0.46 L/m^2		Lebanon	Tomaszkiewicz et al., (2017)

In relation to the comparison of water harvesting methods, some ideas can be presented to determine the potential of water harvesting for Cyprus. Regarding the potential of water harvesting by fog and dew have not been studied for Cyprus climate. These data can be obtained by long term historical observations and meteorological sources.

The groundwater is a natural way of obtaining fresh water however, the water is salty and polluted due to the climate change and commonly the overexploited beyond its efficiency level. Therefore, it is not recommended for domestic use in Cyprus. As seen in Figure 40, the groundwater is highly used for agriculture.

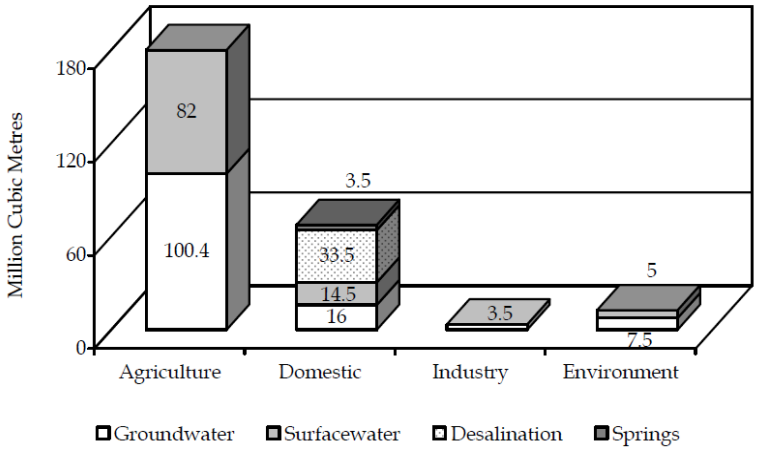


Figure 40. Water consumption by sector and water source supply (Savvides et al., 2001)

Transportation of water via pipes is required advanced engineering solutions. The cost of transported water from Turkey is highly cost (1.18€/m^3) compared to desalination of sea water (0.64€/m^3). Although it is highly expensive, it solves the problem of water shortage of domestic usage.

Desalination of sea water method can be used in Cyprus since it is not dependent on rainfall and drought. It provides fresh water however, it causes harm to the marine environment and also dependent on intensive use of energy which affects the global warming. It is also highly cost (0.64€/m^3), but it is available to use for Cyprus situation. In regards for different sectors, such as for farmers, this water should be subsidized since they can hardly afford the tariffs of water. As seen in Figure 40, desalination water is mostly used for domestic demand.

Regarding the rainwater harvesting system can provide alternative water supply for Cyprus conditions by applying this system into large surface buildings such as educational buildings, commercial/public building, museums or multi-functional buildings and also housing projects. However, in terms of flexibility and cost of buildings, this method requires larger water storage tanks, different materials and architectural details. Although this method has some disadvantages, it is mostly available for Cyprus.

However, it is important to be emphasized here that the scope of this research is limited to the review on the water harvesting technology including both traditional and advanced methods. This section adds insights into the different technologies that have the potential to be incorporated into the evaporative cooling system which will be discussed in the following chapters. A very important conclusion that can be made from this review is that, with many advanced technologies and continuous research in water harvesting, water resources for the proposed evaporative cooling system will not be an issue to be implemented in Cyprus. The review of different kind of water harvesting technology will create a platform to further research the potential technology that may be applied or incorporated for the proposed evaporative cooling system in the future.

2.9 Conclusion

A thorough and detailed literature review is presented to emphasize the study of evaporative cooling for Cyprus climate. The subjects reviewed in Chapter 2 are based on the background, knowledge, application and previous studies of an evaporative cooling method. Due to this, passive cooling methods, studies about architectural integration of evaporative cooling system into building design, the performance of evaporative cooling as mathematical expressions (including cooling capacity, evaporation rate, cooling efficiency, COP, specific cooling capacity) and recent water harvesting technologies are presented.

In the first stage of the Chapter 2, the basic passive cooling methods are illustrated for different climates to show that these strategies do not provide sufficient comfort to the occupants under excessive summer heat. Thus, typical evaporative cooling systems such as direct evaporative cooling system, desiccant based evaporative cooling systems, etc. are presented. In addition to this, the various evaporative cooling system pads (natural and artificial) and integration into building design are highlighted. Following that, the cooling performance of evaporative cooling system is indicated by using mathematical expressions. As a result, the important necessity of evaporative cooling system

are reviewed in regards to water harvesting methods. It is aimed to show that there is a potential to collect water in Cyprus which plays a vital role for providing required water for evaporative cooling system.

Based on the literature review and study of the author, it is seen that the passive cooling strategies of building design are not sufficient for excessive summer heat, in particular for Cyprus climate. Thus, the direct evaporative cooling method which electrically powered to operate should be considered in the building design.

In addition to this, it is also observed that the researchers are currently studying to develop new evaporative cooling material pad in order to increase the cooling performance of the system. Due to this, the commercial materials are mostly used as evaporative cooling pad, although they are expensive.

From this point of view, the study of this PhD work has been developed to create new ideas and materials for one of the cooling method, the evaporative cooling, for Cyprus climate. Since the island is hot-dry in inland region and hot-humid in coastal regions, the direct evaporative cooling system and desiccant based evaporative cooling should be studied for the following Chapters 3 and 6.

In the following chapter, the local materials are investigated for direct evaporative cooling system. The various local materials are tested under different testing module and environmental conditions. Finally, the numerical analysis have been conducted to validate the experimental results.

CHAPTER 3: Experimental measurements of local materials of evaporative cooling performance

3.1 Introduction

Research designs can be qualitative, quantitative or mixed methods. In this study, a quantitative method was used to gather data by experimental design. It was important to test the hypothesis under certain conditions. In this way, data were collected and analysed.

In this chapter, the experimental testing is based on to investigate the potential of local materials in Cyprus for evaporative cooling and to choose the better performance of material. Local materials such as eucalyptus fibre, yellow stone, Cyprus marble, ceramic pipes and dry bulrush basket were tested. The materials used in the test can be grouped as porous stone, non-porous stone and fibre.

The general processes of experimental setups on different local materials are presented as preliminary and main experiments. These processes are explained in this chapter based on how to achieve better performance for evaporative cooling, which is mentioned in Chapter 2. In this light, local materials were studied and compared by investigation in different experimental units - *insulated box as a preliminary experiment* and *wind tunnel as a main experiment* - in order to obtain correct results. These tests were allowed to have alternative materials for the evaporative cooling pad which resulting in energy conservation through the cooling of buildings. In the preliminary testing, different size and configuration of materials was tested. Afterwards, better performances of materials were selected for testing and comparing in the wind tunnel unit. During the preliminary testing, the incoming air temperature was kept constant at 30°C and relative humidity of 35%. After selecting better performance of local materials in the preliminary experiment, the best candidate materials were experimentally investigated at the wind tunnel under the inlet air dry bulb temperature of 35-36°C and relative humidity of 20%. The effects of different air velocity on temperature difference, relative

humidity, cooling efficiency, cooling capacity, COP, evaporation rate and specific cooling capacity were analysed in the wind tunnel unit.

3.2 Experimental investigation of the potential of local materials for evaporative cooling application

The tests for local materials such as eucalyptus fibre, yellow stone, Cyprus marble, ceramic pipes and dry bulrush basket were tested due to the advantages of being cheaper, easily abundant, higher water holding capacity and environmentally friendly. They were run as a preliminary test in order to ascertain better cooling performance of materials. The aim of doing this is to select best material before doing testing under more improved experimental condition (in the wind tunnel unit).

As seen in Figure 41, the testing local materials used in preliminary experiment were configured in different size and shape. The insulated box was designed for preliminary testing to obtain a rough estimation for the potential of local materials. As the material's geometrical configuration and size are different from each other, it was not possible to develop a standard testing unit. However, all testing were done under constant environmental conditions.



Cyprus marble



Ceramic pipes



Dry-bulrush



Yellow stone (10mm)



Yellow stone (18mm)



Yellow stone (25mm)



Eucalyptus fibres

Figure 41. Testing local materials used in preliminary experiment for evaporative cooling

3.2.1 Experimental Methodology

In order to determine the materials used for the evaporative cooling process, some measurements were carried out for preliminary experimental testing unit. Two testing conditions were prepared for this chapter. The aim of first testing (preliminary) is to find the better cooling performance of materials in small scale experiment and select best materials before doing more controlled and large scale experimental unit. The small scale experimental arrangement was developed in order to evaluate the potential of the local materials based on evaporative cooling process. The measurements was done to determine the cooling efficiency of the materials. Afterwards, better cooling performance of materials were chosen to be tested in the wind tunnel in order to compare the performance of materials in terms of some parameters such as temperature difference, relative humidity, cooling efficiency, cooling capacity, COP, evaporation rate and specific cooling capacity. The structure of the methodology of the study can be seen in Figure 42.

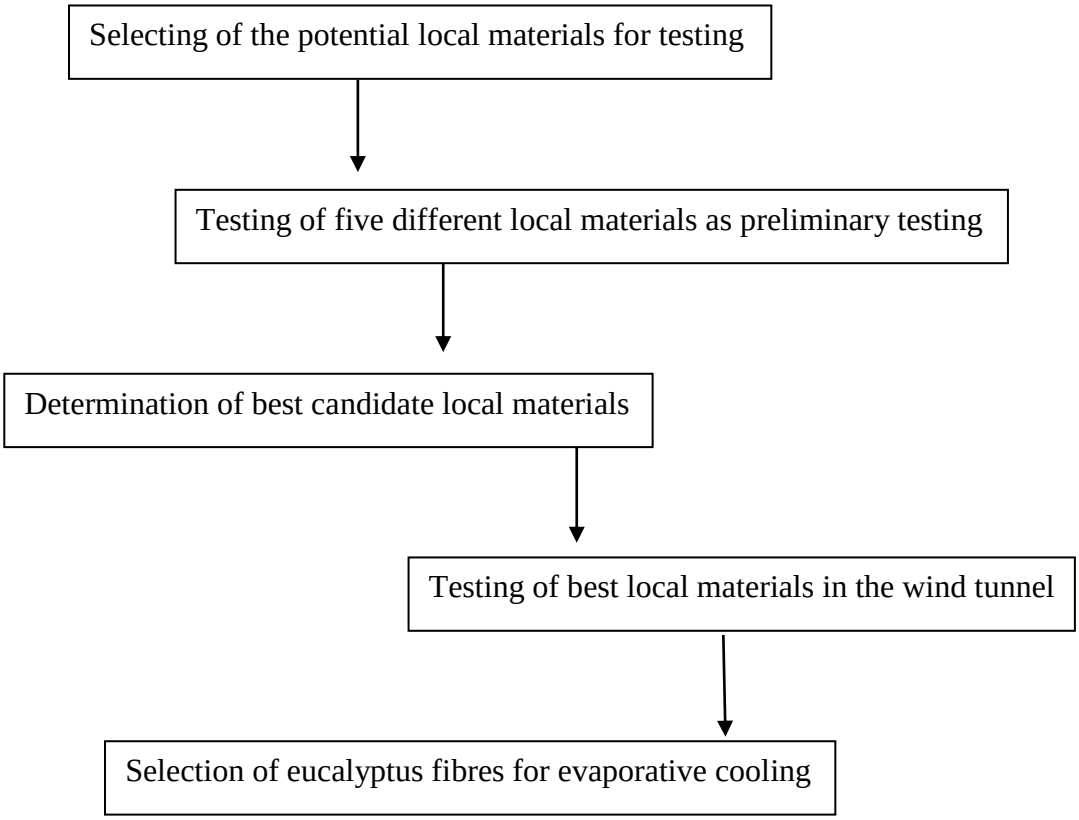


Figure 42. Structure of the experimental methodology

Description of the preliminary experimental design

The insulated box was designed to use local materials to test the cooling effect, which was provided by the evaporative cooling method. The box was 180×140×140 cm and each wall was composed of medium density, 6 mm thick fibreboard (MDF), as shown in Figure 43.

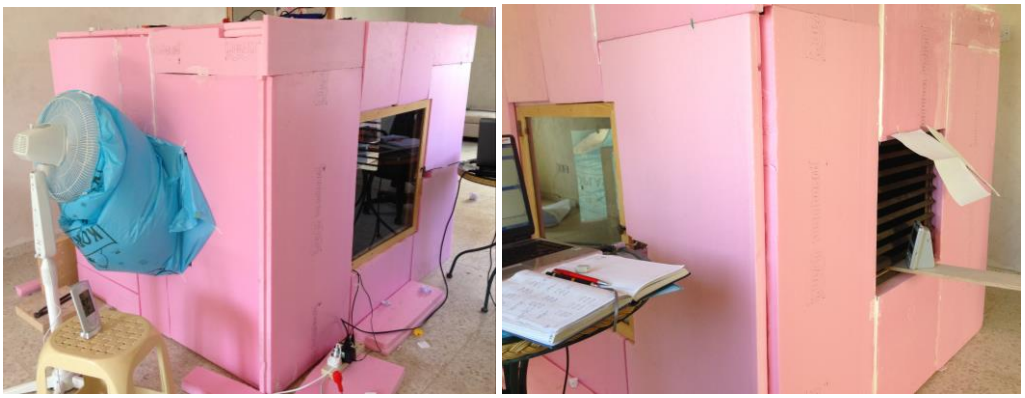


Figure 43. View of insulated box

In order to keep the indoor temperature constant, the model test box was highly insulated with 50 mm thick extruded polystyrene boards (XPS). Regarding the four sides of the box, there were two openings for the inlet and outlet of air on opposite sides. A fan was installed on one side of the wall and a 50x50 cm louvre was placed in the opposite wall to the fan in order to allow air to leave. Thus, the air could be forced over the materials and then flowed through the louvre. One side wall contained a glass window for controlling the water temperature and placing the material. There was no opening on the fourth side. Inside the box, there was a wooden frame to support the materials to be tested. The surrounding of the frame was covered by cardboard to create a chamber for uniform air flow (Figure 44). On top of the chamber, the water supply was provided through pipes; this was provided by a 20W water pump. Water dripped from the pipes onto the top of the material. In Figure 45, water dripping, chamber and water tank are shown. During the experiment, mainly local materials such as eucalyptus fibre, yellow stone, Cyprus marble, ceramic pipes and dry bulrush basket were used as samples of testing (Figure 44). All materials were soaked in water for 24 hours to become saturated. During

experimentation, various types of stone were positioned next to each other or back to back in order to provide materials fully faced with air flow.

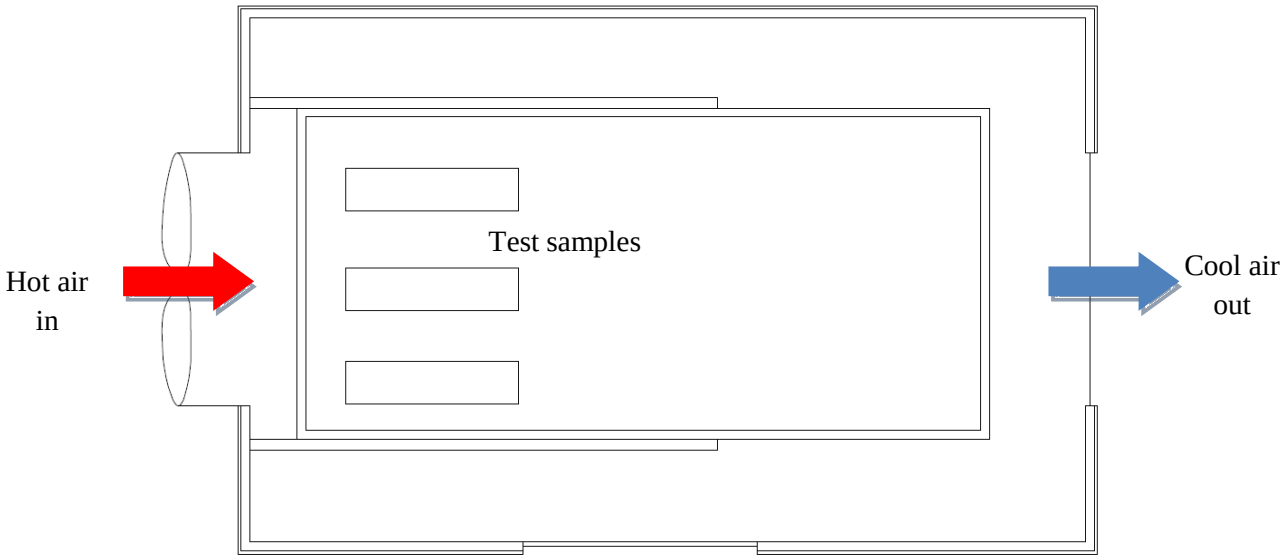


Figure 44. Plan of experimental design



Figure 45. Photographs of the inside of the insulated box

Procedure for experimental design

Air temperature was simulated by using a 2kW heater during experimentation. This air was then forced over the materials by a 20W fan. DT500 data taker was used to record dry bulb temperature, surface temperature and also wet bulb temperatures. WBT for inlet and outlet air were measured by wrapping wet cotton around thermocouples. An anemometer with 0 m/s to 10 m/s measurement accuracy was used to measure air flow. The manual TT TECHNIC hygro-thermometer, which has a measurement range -20°C to 50°C with ± 1°C accuracy, was also used to measure RH in order to check WBT through the psychrometric chart. Overall, three types of measuring instruments were used to ascertain WBT and RH. The psychrometric chart was then used to check the results.

Before starting to record measurements, it is ensured that the system is operating under steady state conditions. In the preliminary experiments, the tests were conducted at different air temperatures between 29.7°C-31.4°C, with RH between 33.9% and 35.2%.

The measurements were recorded 1 hour after starting the test, and then readings were recorded every 15 seconds.

3.2.2 Testing of materials

Local materials collected by author, (eucalyptus fibre, yellow stone, Cyprus marble, ceramic pipes and dry bulrush basket) were tested to evaluate their behaviour and performance under different environmental conditions. At this stage of the study, the temperature difference (Eq. 1 mentioned in Chapter 2) and cooling efficiency (Eq. 2 mentioned in Chapter 2) were both calculated for cooling performance of materials in order to develop initial ideas about these materials, since it was necessary to ascertain the type of materials which would be tested in the main experiments of the study. The preliminary experiments were conducted under the incoming air dry bulb temperature at 30°C and 35% incoming RH. In this light, the results showed that some materials showed higher temperature differences. It should be also mentioned that reliability was

necessary in order to check the test conditions and materials. According to this, **ceramic pipes and dry-bulrush** were used for testing since they were tested before (He and Hoyano, 2010).

In order to keep meshed fibres wet during the experimentation, a water dripping was provided with an 18 mm water pipe which has been placed on top of the meshed structure. A 20W water pump was also used to provide water circulation between the water tank and pipeline. When water from the pipe was dripped onto the material, the excess water was collected in the water tank and reused in the system in order to minimize water consumption.

3.2.2.1 Eucalyptus fibres

Eucalyptus fibres were collected from the barks of the eucalyptus tree. They were soaked into the water in order to create thin fibres easily. The fibres were then separated and embedded into a 28x28x2 cm mesh wire frame. The preparation stages of the meshed eucalyptus fibres is illustrated in Figure 46.



Figure 46. The process of containing eucalyptus fibres

3.2.2.2 Yellow stone

The porous yellow stones were cut to 28x28x3cm (cross sectional area 0.0784 m^2) and small holes were then drilled. The size of holes was 10, 18 and 25 mm. In Figure 47, three different yellow stones with three different sizes of holes can be seen. Some grooves were also created in order to increase the surface areas of the stones in order to absorb more water for evaporative cooling process.



Figure 47. Yellow Stones with Different Types (10/18/25 mm holes)

3.2.2.3 Cyprus marble

Cyprus marble was cut into 28x28x5 shapes for experimental testing (cross sectional area of 0.0784 m^2). Three marbles were prepared for preliminary testing and placed in 5cm intervals. Before testing, these were soaked into water to absorb water. However, it was observed that they become drier while the fan was turned on during the experimentation (Figure 48).



Figure 48. Materials used in the experiments

3.2.2.4 Ceramic pipes

Local porous clay was used to make 12 cylinder-shaped pipes as testing material for the experiment, shaped as 12 pipes. These ceramic pipes were 300mm in height. The inner and outer diameters were 18 and 25 mm, respectively. Grooves were created in each pipe in order to increase surface area. They were dried and put into a kiln in order to be hardened. When they were taken from kiln, they soaked into water until fizzing stop. The wooden structure was then formed to hold them up during the test (Figure 49).



Figure 49 Ceramic pipes

3.2.2.5 Dry bulrush basket

The bulrush is a natural fibre collected from the farms, river or dams. It is traditionally used to carry and store the food. In the manufacturing process, the bulrushes are firstly dried out and they are then woven by hands to make baskets.

Before testing, dry bulrush basket were put into the water to make them wet. Due to the properties of material, not being porous, they were tested by superposing two of them in three columns. They were faced to the fan and water was dripped onto the baskets (Figure 50 and 51).



Figure 50. Dry bulrush basket

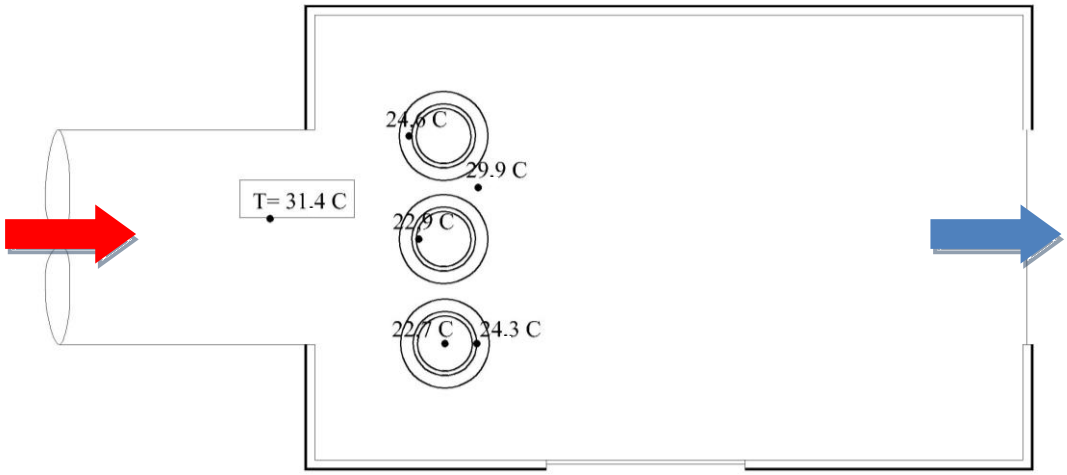


Figure 51. Test model plan of dry-bulrush basket

3.2.3 Comparison of the performance of testing results

Preliminary experiment were conducted in order to analyse the cooling performance of local materials and to choose better performance of materials. The inlet air temperature was kept constant at 30°C with the RH of 35%.

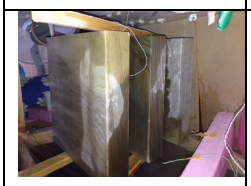
A **dry-bulrush basket** was tested for temperature difference. It is traditionally accepted that these baskets are used to keep food products fresh. People cover the fresh product with a wet fabric in the basket. The cooling efficiency of dry bulrush basket was 19%. As was expected, the air temperature inside the basket was lower compared to the outside air temperature (Figure 51). When air left the baskets, it was seen that the temperature drop became lower by around 1.7 °C, which was not efficient enough with 19% cooling efficiency.

As seen in Table 6, local materials are shown in terms of temperature difference and cooling efficiency. The cooling efficiency of **ceramic pipes** was 28% which was higher than the cooling efficiency of dry bulrush basket. It also caused 3.2°C temperature drop in the experiment at 29.7°C inlet air temperature. Even though fan speed was changed in order to accentuate any cooling effect, there was no significant change over 4 hours testing.

Cyprus marbles showed lower performance, with a temperature drop of 1-2°C during experimentation at 29.9°C inlet air temperature. In addition, it was

observed that the marbles started to dry quickly. Although they absorbed water when soaked into the water, they dried out quickly. When the marbles were also faced with air, they dried quickly although water was continuously added onto it.

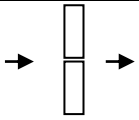
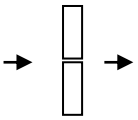
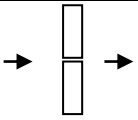
Table 6. Performance comparison of local materials

Test Configuration	Material	WBT_{in} (°C)	DBT_{in} (°C)	RH_{in} (%)	DBT_{out} (°C)	ΔT (°C)	υ (m/s)	ης (%)
	Dry bulrush basket	19.9	31.4	34.6	29.7	1.7	0.8	19
	Ceramic pipes	18.4	29.7	33.9	26.5	3.2	0.8	28
	Cyprus marble	19	29.9	35.2	28.8	1.1	0.8	15
	YS	19.1	30.4	34.8	28	2.4	0.8	21
	EF	18.9	30.1	34.1	26	4.1	0.8	36

Yellow stones with different holes sizes were tested after ensuring the steady state conditions at 30°C inlet air dry bulb temperature. After one hour testing, it was concluded that the higher temperature drop occurred at the lowest air velocity with 10 mm diameter-hole yellow stone. The results can be seen in

Table 7. As was expected, the narrower the gap in the stone, the higher the air velocity and thus, evaporative cooling.

Table 7. Temperature reduction through different type of yellow stones at 30°C inlet air

Air flow rate (m/s)	**Ø 10**	**Ø 18**	**Ø 25**
			
0.8 m/s	2.4 °C	1.5 °C	1.4 °C
1 m/s	2.2 °C	1.6 °C	1.4 °C
3 m/s	1.7 °C	1.5 °C	1.3 °C

Yellow stones with 10 mm holes in the stones showed around 2.4°C temperature reduction while the inlet dry air bulb was 30.4°C. When compared to dry bulrush basket and Cyprus marble, the cooling efficiency of yellow stone was higher (21%). However, it was not higher than the cooling efficiency of ceramic pipes as seen in Table 6. It should be also mentioned that the yellow stone with 10mm holes size were heavier compared to the other local materials. Being heavier of the stone can create some problems to the structure of the evaporative cooling system by applying additional forces to the system. Since the water holding capacity of yellow stone is higher, it becomes heavier while absorbing more water during the evaporative cooling process.

Eucalyptus fibres showed the highest temperature difference at 4.1°C which was higher than yellow stone. The cooling efficiency was also 36% which was the highest amongst other local materials. As seen in Figure 52, the cooling

efficiency for dry bulrush basket, ceramic pipes, Cyprus marble and yellow stone are 19%, 28%, 15% and 21%, respectively.

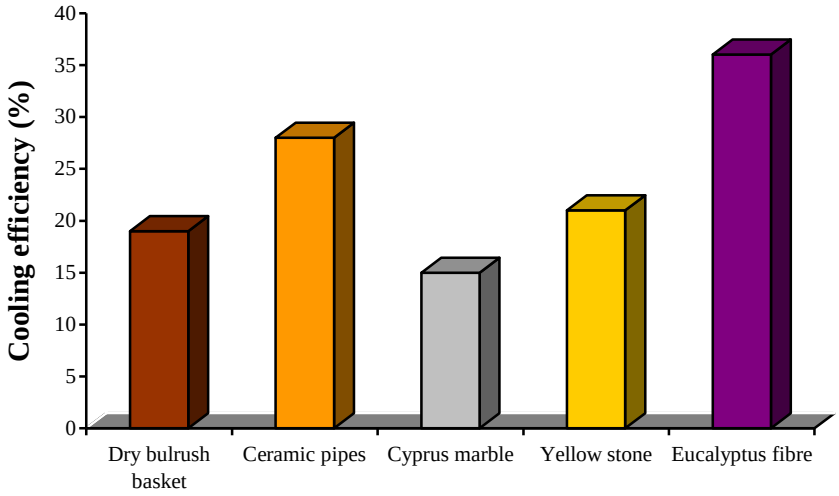


Figure 52. Cooling efficiency of local materials

During the experiment, it was observed that the rate of air flow is decreased while passing through material. This might be due to the pressure drop of air across the fibres. Since the fibres covered the whole meshed structure, this affected the air flow through the material surface. The outlet air flow in front of the fibre is lower than inlet air dry bulb temperature. As the air goes away from the material, the temperature is reduced.

In summary, eucalyptus fibres and yellow stone can be chosen to be tested in more controlled experimental condition in order to investigate the cooling performance of these materials. Although ceramic pipes had higher cooling efficiency than yellow stone, it is not experimentally used in the wind tunnel as it was tested by many researchers before. In addition to this, yellow stone can easily obtained than ceramic pipes since the manufacturing of ceramic pipes takes longer time. Eucalyptus fibres is also easily found from the nature without harming the nature. Since the eucalyptus tree causes water shortage problem in Cyprus, it can be suggested to test for evaporative cooling process.

3.3 The wind tunnel experiment for performance comparison of eucalyptus fibres and yellow stone for evaporative cooling

After the preliminary experiments, the main experiment was carried out by an Open Wind Tunnel (HM170). The tunnel is used at the Engineering Laboratories of the Middle East Technical University Northern Cyprus Campus (METU NCC). In this experimental unit, eucalyptus fibres and yellow stone with 25 mm holes size were tested in a more controlled environment and larger scale experiment.

The experiments were conducted in two stages: in the first stage of the experiment, eucalyptus fibres and yellow stone were tested under the same conditions in order to ascertain which material creates a better cooling performance for the evaporative cooling process (Figure 53). In the second stage, eucalyptus fibres were studied to identify their behaviour under different conditions for the evaporative cooling process.

Material tested in the Wind Tunnel



Eucalyptus fibres



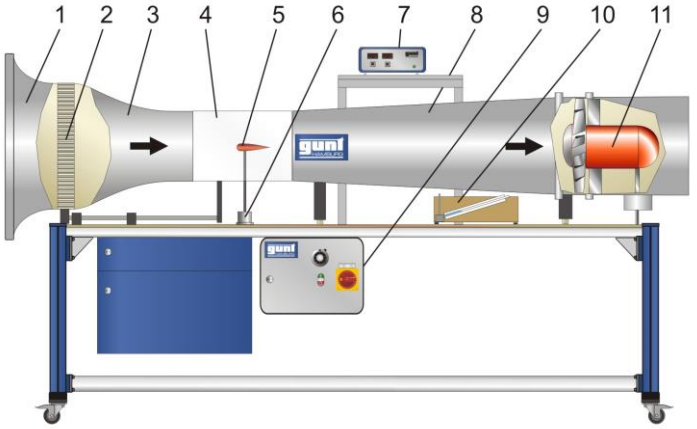
Yellow stone (Φ25mm)

Figure 53. Testing materials

3.3.1 System description for local materials

The Open Wind Tunnel (HM170) was used as the main rig for laboratory testing under controlled environmental conditions (Figure 54). The dimensions of the tunnel are 2870x890x1540 mm and the cross section area for sample measurement is 292x292 mm as shown in Figure 54. The tunnel consists of a measuring section, air blower and exhaust zones. The material is placed in the measuring section which is 420 mm in length. In the air blower section, the inlet air was heated with a 2kW heater in order to increase the air temperature.

The experiment was carried out in the laboratory in February, March and April in 2016. Dry and wet bulb temperatures and relative humidity were controlled during the experiment in order to provide steady environmental conditions. Uniform airflow was provided by the honeycomb structure which is located at the entrance of the duct.



1 inlet contour
2 flow straightener
3 nozzle
4 measuring section
5 drag body
6 force sensor
7 display and control unit
8 diffuser
9 switch cabinet
10 inclined tube manometer
11 axial fan

Figure 54. Open Wind Tunnel (HM170) schematic

The instruments such as datalogger and anemometer were provided by the University of Nottingham. A DT500 model data taker which was connected to a computer was used to record the air temperatures, WBT and surface temperatures of the material continuously. K-type thermocouples, which were connected to the datalogger, were used to record data of the inlet and outlet measurements. An anemometer was used to measure the inlet and outlet air

velocity which was controlled during the test. The microclimate probe and pocket weather meter were used to measure the relative humidity and wet bulb temperature. The sensors used in the experiments are listed in Table 8.

Table 8. Characteristics of experimental sensors

Sensor type	**Sensor model**	**Sensor accuracy**	**Specification range**
Temperature	Type-K Thermocouple	± 0.2 %	-50 ~ + 250 °C
Relative humidity	Kestrel 4000 weather meter	± 3 %	5 ~ 95 %
WBT	Kestrel 4000 weather meter	± 2 °C	-29 ~ 70 °C
Air flow	Testo 405 V1 anemometer	± 5 % ± 0.1 m/s	0 ~ 10 m/s
Relative humidity	Metrel 6201 multinorm	± 2 %	0 ~ 60 %
Temperature	Metrel 6201 multinorm	± 0.2 %	20 ~ 60 °C
Water temperature	Multi-thermometer	± 1 °C	-50 ~ + 300 °C

Uncertainty analysis

According to the uncertainty range for each instruments shown in Table 8, the overall uncertainty results for each measured variables are seen in Table 9. The largest error occurred at relative humidity.

Table 9. Errors for uncertainty analysis

Variable	Temperature difference (°C)	Cooling efficiency (%)	Relative humidity (%)
Error	**1.3%**	**7.1%**	**8.3%**

It was crucial to keep the material wet for evaporative cooling during the test. Therefore, some components were added to the meshed fibres and yellow stone.

Eucalyptus fibres were collected from the tree and soaked into the water to create thin fibres using the same as the method used in the preliminary stage of the experiment (in Insulated Box). Water was supplied by using 20W water pump through the 18 mm perforated circular water pipe which was integrated to the meshed eucalyptus fibres. The air flow was provided by using the fan of the wind tunnel which has different power at different air velocity (63.92W at 0.1 m/s, 68.56W at 0.3 m/s, 82.48W at 0.6 m/s, 96.4W at 0.9 m/s and 108W at 1.2 m/s). When water from the pipe was dripped onto the material, excess water was collected in a water tank, it was then re-circulated through the pipe onto the material. The preparation stages of the meshed eucalyptus fibres is illustrated in Figure 55.



Figure 55. Integrated water pipe onto the meshed eucalyptus fibres

The porous yellow stones which had been used in the preliminary stage of the experimental study were used as the size as 28x28x3cm and the same surface area of 0.0784m² in the Open Wind Tunnel. In this stage of the experiment, yellow stones with 25mm holes were used for testing. Although yellow stone with 10mm holes sizes created better performance (1°C lower of temperature difference) compared to yellow stone with larger holes sizes on the surface, 25mm holes of yellow stone was used due to it becomes lighter while creating larger holes sizes than yellow stone with smaller sizes (10mm).

The material should be kept wet during the experiment for evaporative cooling process. Therefore, a gap was created at the upper part of the yellow stone for replacing 18mm plastic water pipe (Figure 56). This water pipe at the upper part of the stone was drilled to provide water during the test which was connected to the water pump. The other end of the water pipe was sealed with silicone gel.

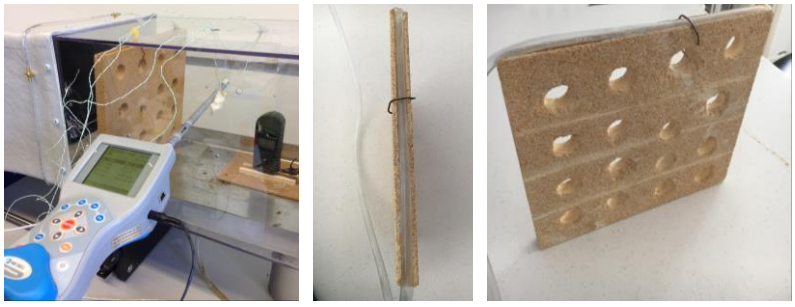


Figure 56. Integrated water pipe onto the yellow stone

3.3.2 Test procedure for unit

The performance of the materials were studied by setting the inlet air temperature to around 35-36°C, which is the average temperatures of Cyprus in the hottest month of the year, August. To measure the temperatures, thermocouples were placed in the outlet and inlet sections with the same distance from the material to measure the DBT and WBT of the air. Figure 57, 58 and 59 show the schematic diagram of the experiment for both materials (eucalyptus fibres and yellow stone). The moistened cotton was wrapped around the thermocouples to record the WBT of the aforementioned positions. RH was also measured by a microclimate probe for both sides of the material. Finally, the results were checked in the psychometric chart. The 2kW heater was positioned in front of the blower in order to keep the inlet air temperature constant at the set point (35-36°C). The inlet relative humidity was also kept at around 20% during the experimental testing.

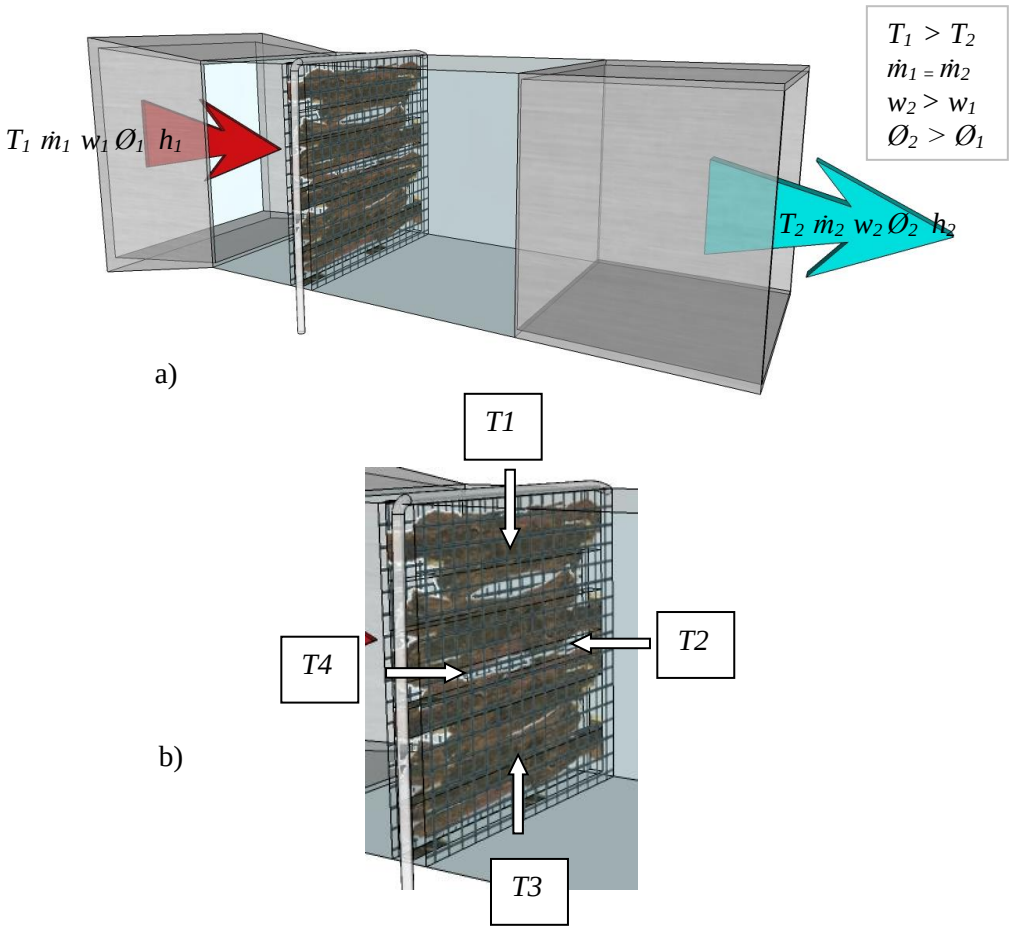


Figure 57. (a) Schematic diagram of the experimental testing rig and (b) thermocouple locations

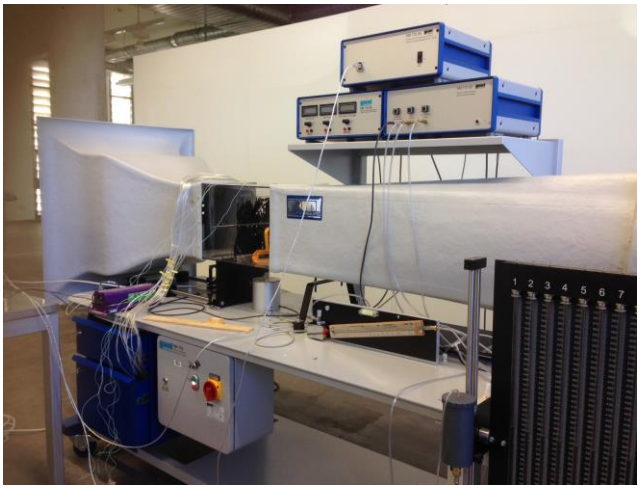


Figure 58. Schematic diagram and general view of the experiment (eucalyptus fibre)

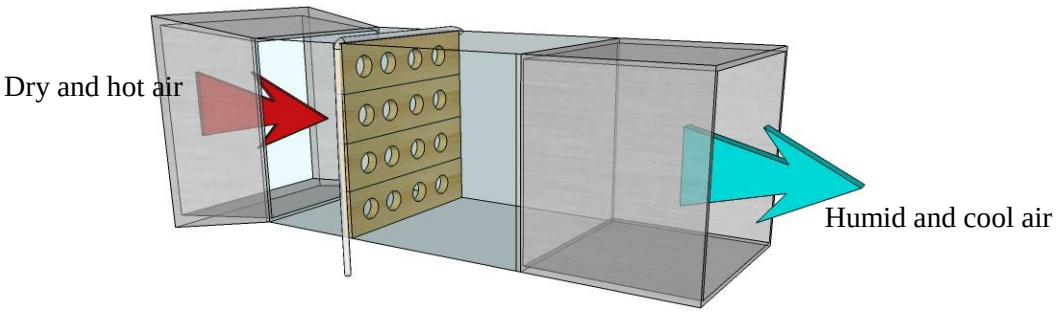


Figure 59. Schematic diagram of the experiment (yellow stone)

The data recording has begun after 30 minutes of the start of the experiment to ensure that the system is operating under steady state conditions (Malli, 2011).

In the first part of the experiment, 120 readings were recorded for two hours in every minute. In the second stage, the measurements were also recorded once in every minute and totally, 240 readings were recorded for four hours testing duration. When the water level decreased in the water tank, additional water was added.

In regards to the cooling efficiency of an evaporative cooling system, the air flow rate is a key parameter, significantly influencing the system performance. Therefore, air velocity was chosen as the variable during the tests to ascertain its impact of on the cooling effectiveness obtained with the eucalyptus fires. Accordingly, air velocity was set to 0.1, 0.3, 0.6, 0.9 and 1.2 m/s to compare the evaporative cooling performance of the system at different air velocities.

Repeatability and reliability are crucial for the test result. Therefore, the experiment was run more than four times in order to ensure near steady state condition and to obtain correct readings. All tests were conducted in almost at the same environmental conditions. The measured and calculated results were illustrated by graphical explanations in order to gather data and make comparison.

3.3.3 Experimental results

Comparison of the eucalyptus fibres and yellow stone through experimental investigations

The evaluation of cooling performance is based on some important parameters such as inlet DBT and air velocity. In this context, eucalyptus fibres and yellow stone were tested under same conditions at 35.5 - 35.8 °C inlet air temperature and 0.1 m/s air velocity to evaluate the materials performance at the first stage of the experiment. This evaluation included temperature difference, relative humidity, cooling efficiency, cooling capacity, COP and evaporation rate of both materials.

The cooling effect is directly proportional to temperature reduction. When comparing the temperature drop of materials, it was seen from the Figure 60 that the outlet temperature of testing by eucalyptus fibres dropped from 35.6°C to 26°C, whereas the outlet temperature dropped from 35.6°C to 32°C for yellow stone testing.

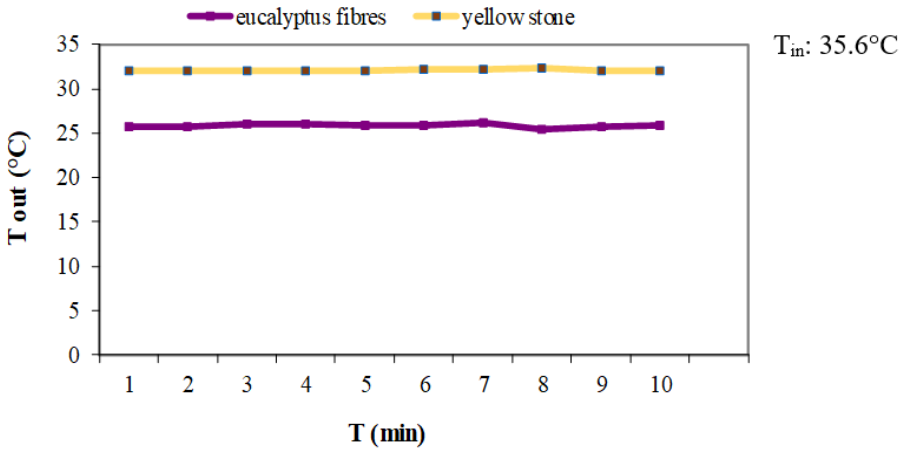


Figure 60. Temperature difference of eucalyptus fibre and yellow stone

The average outlet RH of eucalyptus fibres was increased from 20% inlet RH to 57%; however, the RH for yellow stone was increased to 35% from 20% inlet RH as seen in Figure 61. The all testing in the previous sections showed that by increasing of inlet temperature, the temperature difference between inlet and outlet is higher.

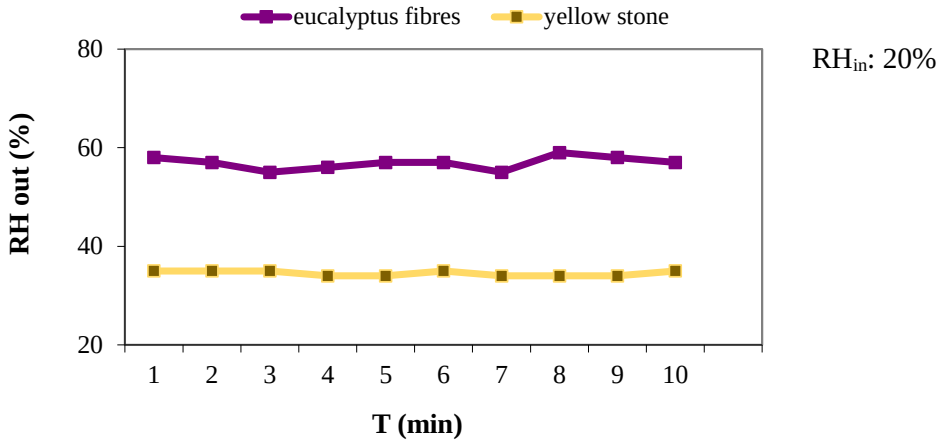


Figure 61. Outlet RH of eucalyptus fibre and yellow stone

Figure 62 represents the cooling efficiency (Eq. 1) of both materials at 0.1 m/s air velocity. As seen from the graph, cooling efficiency of eucalyptus fibres is

higher than yellow stone. The temperature difference for yellow stone and eucalyptus fibres were 3.6°C and 10.4°C, respectively as shown in Table 10. Due to the better performance, eucalyptus fibres were chosen for further testing for this study.

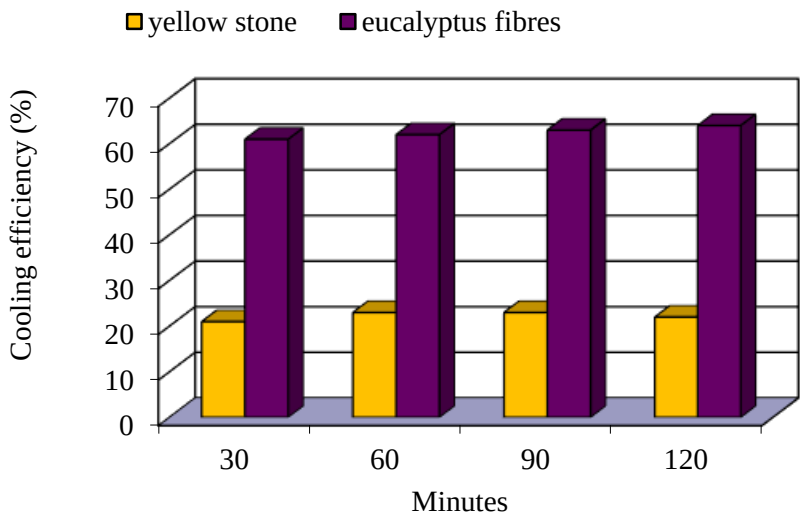


Figure 62. Cooling efficiency of materials at 0.1m/s

Table 10. Temperature drop and cooling efficiency of materials at 0.1 m/s

Material	υ (m/s)	DBT_{in} (°C)	WBT_{in} (°C)	DBT_{out} (°C)	ΔT (°C)	nς (%)	Facing Area (m^2)
Yellow stone	0.1	35.5	19	31.9	3.6	21	0.0784
Eucalyptus fibres	0.1	35.8	19.1	25.4	10.4	62	0.0784

Figure 63 demonstrates the cooling capacity of eucalyptus fibres and yellow stone under same environmental condition. As it is seen in the graph, the cooling capacity of eucalyptus fibres is 2.7 times higher than yellow stone. The average cooling capacity of eucalyptus fibres was 95W. However, it was 35W for yellow stone.

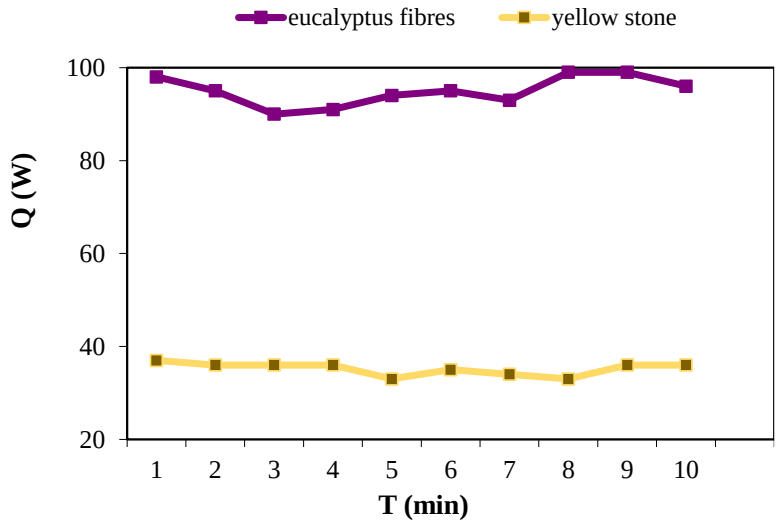


Figure 63. Cooling capacity of eucalyptus fibre and yellow stone

In Figure 64, the COP value for both materials are shown. At 0.1 m/s, the COP value for eucalyptus fibres was 1.14 and 0.42 for yellow stone. As seen in the graph, the COP is higher for eucalyptus fibres. The evaporation rate of both eucalyptus fibres and yellow stone was nearly the same at 0.049 g/s and 0.043 g/s, respectively.

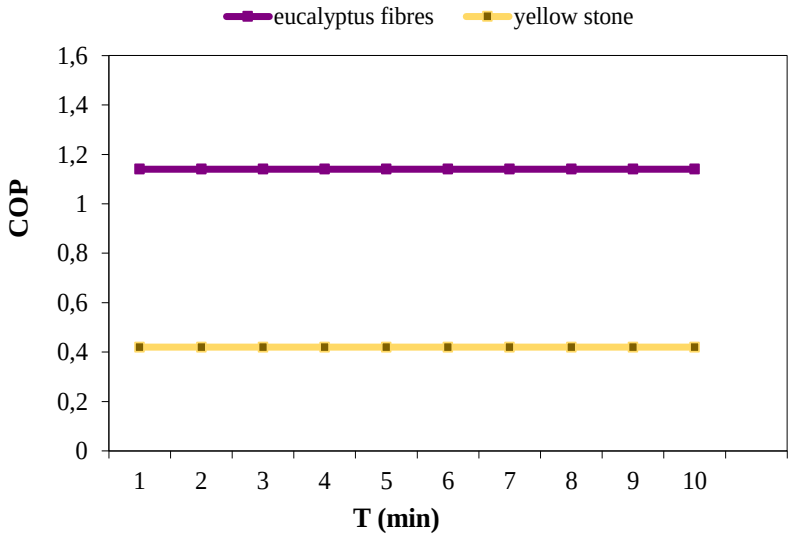


Figure 64. COP of eucalyptus fibre and yellow stone

Investigation of the effect of operating parameters for eucalyptus fibres performance

As aforementioned above, experimentations at the second part of the laboratory experiment were repeated by changing inlet DBT and air velocity. The temperature differences, cooling efficiency, mass flow rate, cooling capacity, water consumption, COP and specific cooling capacity of the eucalyptus fibres were measured and calculated in this study.

The meshed eucalyptus fibres were tested under the same environmental conditions except what was supplied to the material. At first, the meshed eucalyptus fibres were tested without continuous water supply, and then, the tests were continued by adding water to find the effect of evaporative cooling. Temperature difference of eucalyptus fibres at constant inlet temperature of 35.5°C remained unchanged at around 35.5 °C during without adding water.

3.3.3.1 The effect of air velocity on temperature difference

The outlet temperature at different air velocities are shown in Fig. 65. It is obvious that at 0.1 m/s speed, the temperature difference was higher compared to higher air velocities. This is because that the more time the air is exposed to material at lower air velocity, the more water is evaporated. Therefore, more temperature reduction is achieved. Besides, as the mass flow rate of air is less at low air velocities, more temperature drop is obtained for the same rate of cooling capacity. According to the testing results, the average temperature drop of air at 0.1 m/s, 0.3 m/s, 0.6 m/s, 0.9 m/s and 1.2 m/s air velocities were 9.8 °C, 8.1 °C, 5.7 °C, 4.1 °C and 3.1 °C respectively. In Figure 66, the correlation between outlet dry bulb temperature and air velocity is shown. The trend line supports the data given in the graph. As seen, temperature difference is indirectly proportional with the increased air velocity.

Consequently, eucalyptus fibres showed a better performance at low air velocity operating conditions in terms of providing higher ΔT. However in order to determine the overall impact of air velocity on system performance; cooling efficiency, cooling capacity and COP parameters should also be

investigated. These analyses are presented in the following sections of the study.

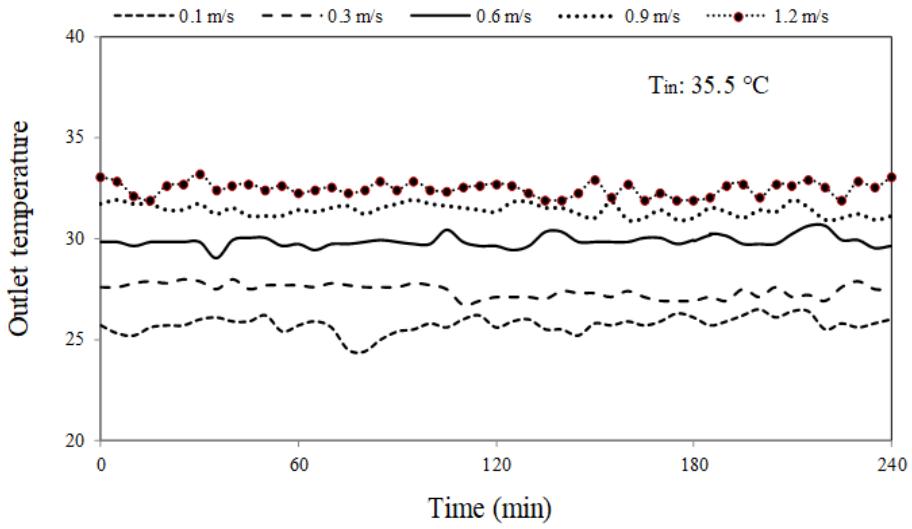


Figure 65. Effect of air velocity to outlet temperature at T_{in}= 35.5 °C

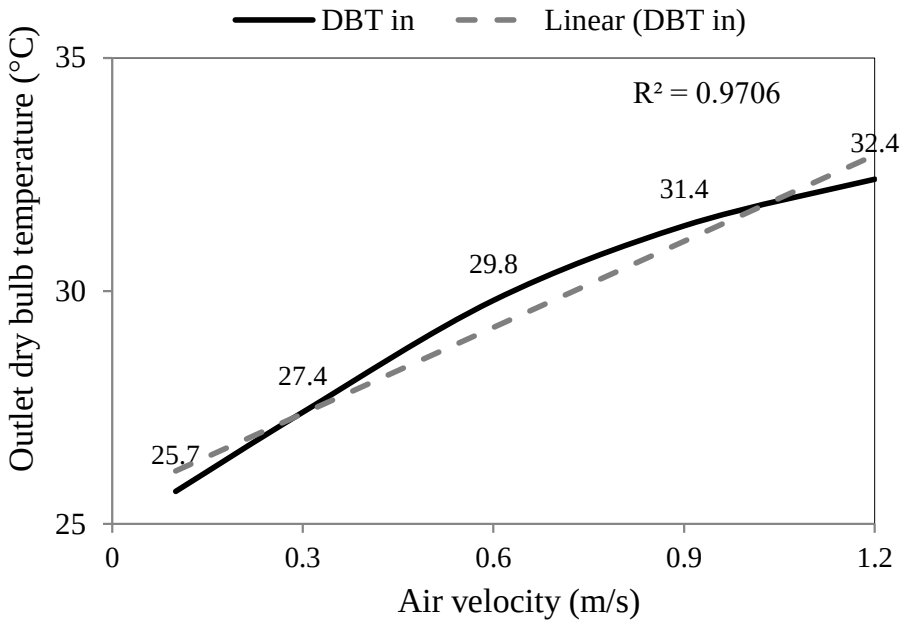


Figure 66. The variation of outlet air temperature for different air velocities (T_{in}= 35.5 °C)

Fig. 67 shows the entering and leaving DBT and water temperature of the meshed eucalyptus fibres for four hours. During the testing, DBT at the inlet

fluctuated between 35°C and 37°C as it was supplied by 2kW heater. According to this, RH also fluctuated around 16-23%. The DBT at the outlet fluctuated between 25.2-26.2°C. Overall, the average DBT and RH at the outlet were 25.7°C and 60% respectively. From the Table 11, the readings of air temperatures, wet bulb temperature and cooling efficiency are indicated. As regards the water temperature, it was measured as 18.2°C. Afterwards, it was increased by 2.6°C to 20.8°C.

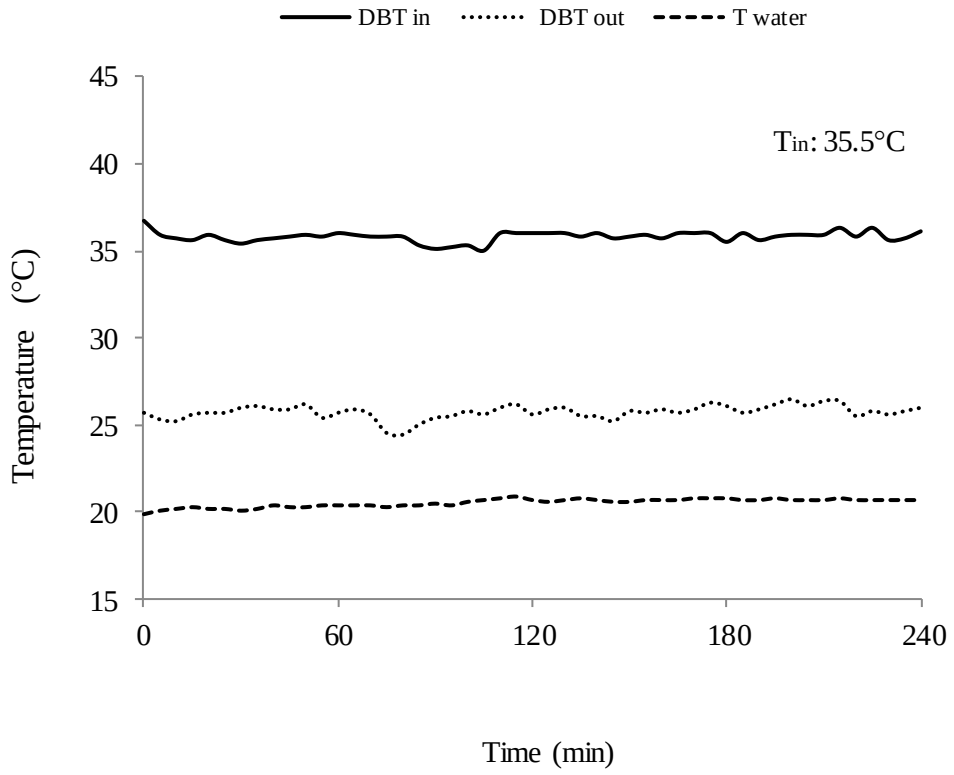


Figure 67. Inlet, outlet DBT and water temperature difference at 0.1 m/s

Table 11. Readings at 0.1 m/s

DBTin	**WBTin**	**DBTout**	n_{ς} **(%)**
35.4 °C	19.0 °C	26.0 °C	57
35.3 °C	19.7 °C	25.8 °C	61
35.7 °C	19.7 °C	25.2 °C	66
35.7 °C	19.9 °C	25.9 °C	62
35.6 °C	19.9 °C	25.9 °C	62
35.6 °C	20.0 °C	25.6 °C	64

3.3.3.2 The effect of air velocity on outlet relative humidity

Fig. 68 shows the variation of the outlet air relative humidity over 4 hours testing period for the air velocities in the range of 0.1-1.2 m/s. As seen in Fig. 68, the rise in air velocity causes a reduction in relative humidity difference between inlet and outlet (Malli, 2011). This is due to the contact time of air with material surface. As the contact time of air with the wetted surface of material is reduced with the increasing velocity, less evaporation occurs.

During the testing at 0.1 m/s air velocity, RH of the outlet air was fluctuated around 60%. On the other hand, RH for the first two hours at 0.3 m/s remained nearly constant at around RH of 50% whilst it was increased to 55% in the following period due to the slight rise in ambient humidity. This was followed by a uniform increase of 12% after 120 minutes to 180 minutes at the highest RH of 55%. For 0.6 m/s and 0.9 m/s, the outlet RH's were remained nearly stable at around 41% and 25%, respectively.

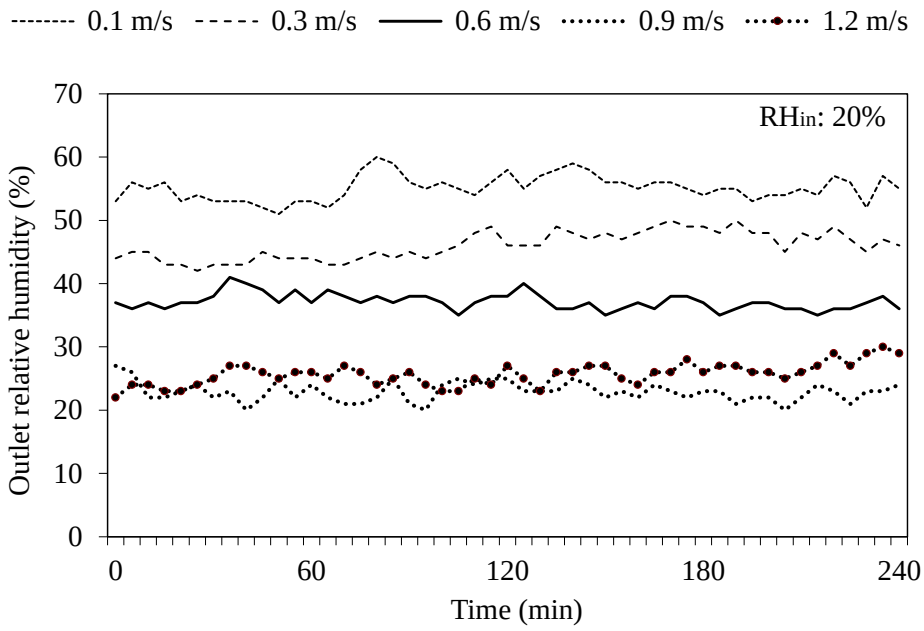


Figure 68. Effect of air velocity on outlet relative humidity

3.3.3.3 The effect of air velocity on cooling efficiency

In Fig. 69, the variation in cooling efficiency is shown for different air velocities. The inlet air temperature varied between 35-36°Cover the four hours testing and the average highest cooling efficiency was obtained as 62% at 0.1 m/s air velocity, corresponding to a cooling capacity of 96 W.

According to the testing results, an inversely proportional relation was found between the cooling efficiency and air velocity, which is in accordance with the literature (He, et al., 2014). For the variation of air velocity in the range of 1.2 → 0.1 m/s, cooling efficiency was calculated between 20% → 71%. This is due to the reduced contact time between air and wet evaporation pad (eucalyptus fibre) which results with limited heat and mass transfer. The average cooling efficiency for 0.1 m/s, 0.3 m/s, 0.6, 0.9 and 1.2 m/s air velocities were 62%, 52%, 42%, 24% and 27% respectively.

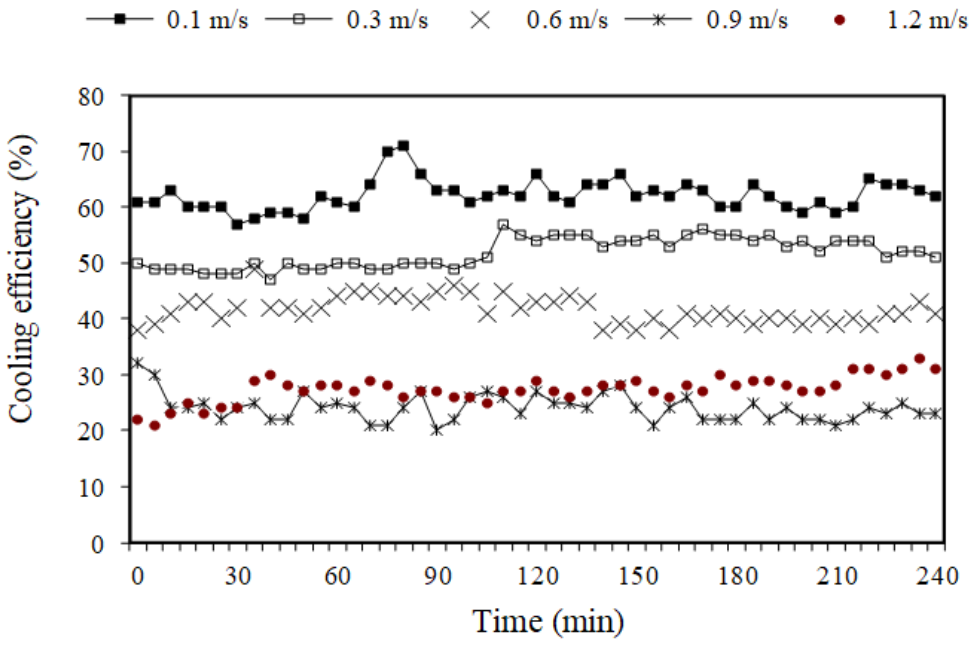


Figure 69. Cooling efficiency trends at 0.1 - 1.2 m/s

3.3.3.4 The effect of air velocity on cooling capacity

The cooling capacity of material is crucial to measure the release of heat energy during the evaporative cooling process. The variation of cooling capacity versus air velocity for meshed eucalyptus fibres is represented in Fig. 70. The figure shows that cooling capacity was raised with the increasing air velocity. This is due to the increasing evaporation rate of water at higher air velocity levels. In addition to this, cooling capacity is inversely proportional to cooling efficiency (Kulkarni and Rajput, 2013). The average cooling capacity was 96W, 239W, 350W, 404W and 518 W for air velocities of 0.1, 0.3, 0.6, 0.9 and 1.2 m/s, respectively.

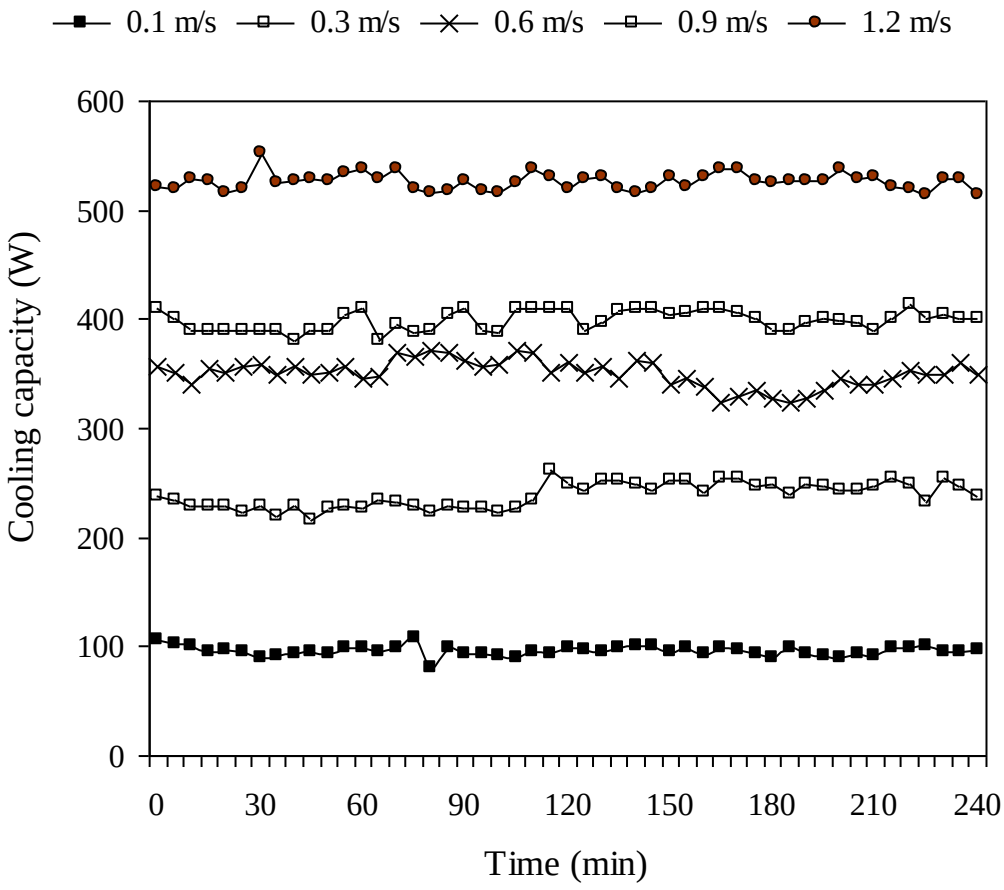


Figure 70. Cooling capacity trends at 0.1 - 1.2 m/s

3.3.3.5 The effect of air velocity on COP

Fig. 71 demonstrates the overall COP, which is crucial to evaluate the energy consumption of the evaporative cooling material at different air velocities. This figure illustrates that the COP value was obtained at 1.2 m/s air velocity with 4.05 and it dropped to 1.14 at 0.1 m/s air velocity. In accordance, evaporation rate showed a decreasing trend in the range of 0.55→ 0.049 g/s with the drop in air velocity. This condition demonstrates the impact of water evaporation rate on cooling COP.

Although evaporation rate and COP values were higher at 1.2 m/s air velocity, the cooling efficiency was the lowest at 24% for the eucalyptus fibre test sample utilized in the testing rig. It could be concluded that, such a small size

(2 cm thickness) eucalyptus fibre is not enough for evaporative cooling at 1.2 m/s air velocity.

It can also be concluded that COP value and cooling capacity are increased with the increase of the velocity of air up to a certain value (~0.9 m/s). Since COP is also the function of fan power, at higher velocity levels (>0.9 m/s) COP shows a decreasing trend resulting with lower evaporative cooling performance.

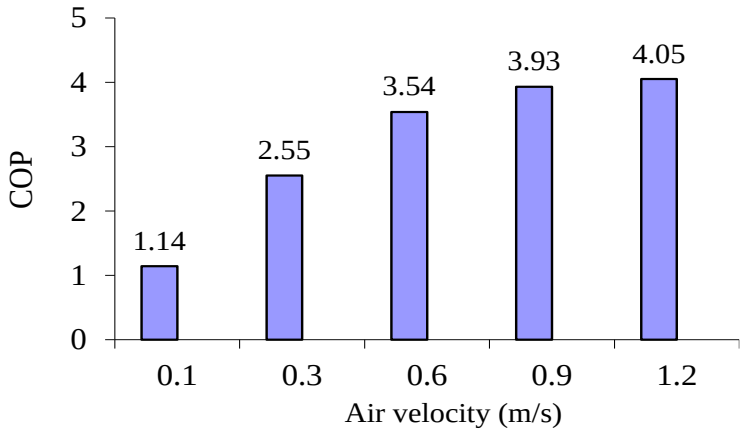


Figure 71. COP trends at 0.1 - 1.2 m/s

The correlation between outlet dry bulb temperature and air velocity (blue line) and the correlation between COP and air velocity (red line) were shown in Figure 72. As seen, temperature difference is inversely proportional with increased air velocity. Despite the temperature difference gets lower with the increasing air velocity, the rate of the cooling capacity to the consumed power (fan + pump) increases. As a result, COP shows an increasing trend.

In addition to this, there is a second order correlation between air velocity and COP. As seen from the same figure, there is a sharp increase in COP (1.2-3.5) for the change of air speed in the range of 0-0.6 m/s. However, the variation of COP becomes gradual at higher air speeds (0.6-1.2 m/s). This condition

demonstrates that air speed >0.6 m/s should be used in order to obtain a high evaporative cooling performance.

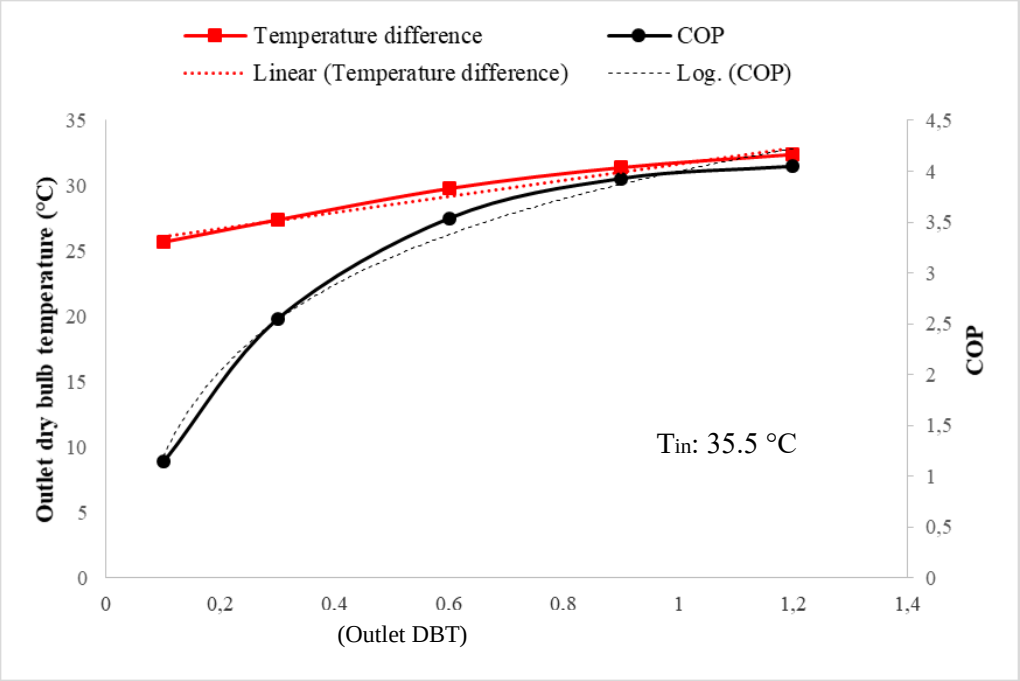


Figure 72. Correlation of outlet dry bulb temperature and COP

3.3.3.6 The effect of air velocity on evaporation rate

The trend of evaporation rate (ER) for different air velocities is shown in Fig. 73. As seen in the graph, the maximum evaporation rate of 0.55 g/s was obtained at 1.2 m/s and it showed a gradual drop with the reduced air velocity. At 0.1 m/s, ER was ~10 times lower than the ER at 1.2 m/s. This condition demonstrates that the ER is directly proportional with the air velocity and should be optimized during the system operation depending on the cooling demand (Franco et al., 2014).

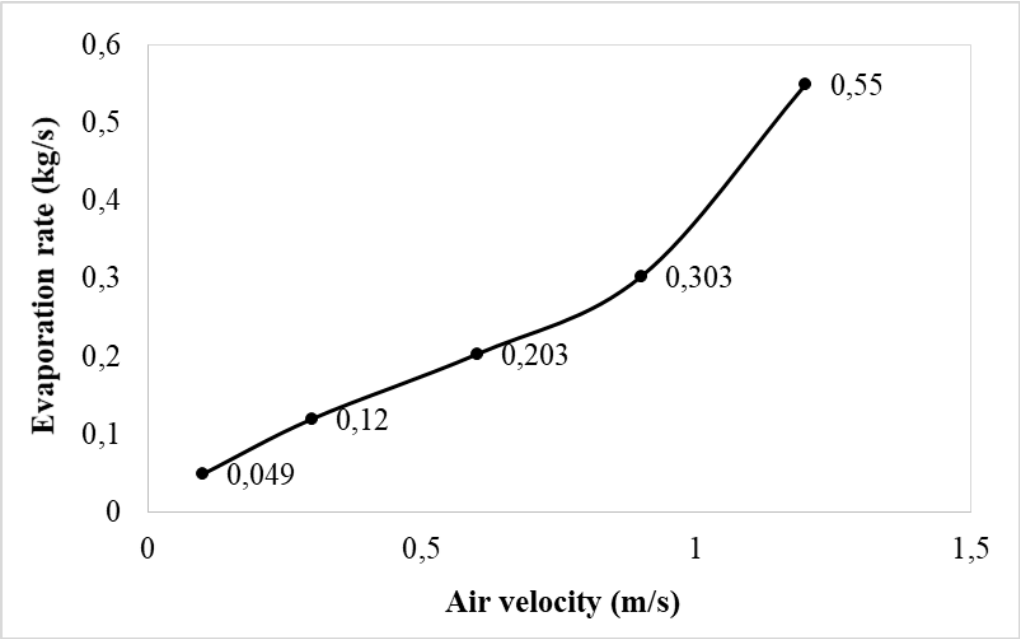


Figure 73. Evaporation rate trends at 0.1 - 1.2 m/s

It can be concluded that eucalyptus fibres at lower air velocity shows better performance in terms of cooling efficiency compared to higher air velocity, in accordance with the literature data. The values for appropriate air velocity were 0.1 and 0.3 m/s with the highest cooling efficiency at 71% and 57% respectively. The cooling efficiency results for 0.9 and 1.2 m/s were close in close approximation with an average in the range of 24-18%. The highest cooling COP value were obtained with the air velocity of 0.6 m/s, 0.9 m/s and 1.2 m/s with 3.54, 3.93 and 4.05, respectively. In this light, the performance of eucalyptus fibre is evaluated according to the different air flow rate.

Although it is obvious that the cooling efficiency at 0.6 m/s is not as high as the values at 0.1 and 0.3 m/s air velocity, COP value at that velocity was higher (3.54). The water consumption at 0.6 m/s air velocity was also lower (0.084 g/s) than the water consumption at 0.9 and 1.2 m/s while providing higher average cooling efficiency of 42%. For that reason, it could be concluded that, in terms of cooling COP, 0.6 m/s is an optimal air velocity for the tested evaporative cooling system with the eucalyptus fibres.

3.3.3.7 The effect of air velocity on specific cooling capacity

As specific cooling capacity is the ratio of cooling capacity to evaporation rate, it represents the cooling performance of material according to different air velocities. In other words, the specific cooling capacity is the amount of cooling capacity obtained per evaporated kg of water.

As seen in Figure 74, specific cooling capacity is dropped with the increasing of air velocity. According to the test results provided in Figure 74, the drop in SCC is minimal (0.54→0.49 kWh/kg) for the range of air velocities 0.1→0.6, whereas a sharp drop (0.49→0.26 kWh/kg) is observed for the air velocities between 0.6→1.2 m/s. This finding shows that system operation is most efficient at ~0.6 m/s, when both COP and SCC parameters are considered.

Cooling capacity and evaporation rate are two factors that affect the specific cooling capacity. Therefore, they are both the function of velocity. But the rate of the increase of ER is greater than the CC with the increase of the velocity. Therefore, SCC gets lower at high air velocity. According to this, the velocity of the air should be kept lower in order to use water in more effective manner and to minimize water consumption.

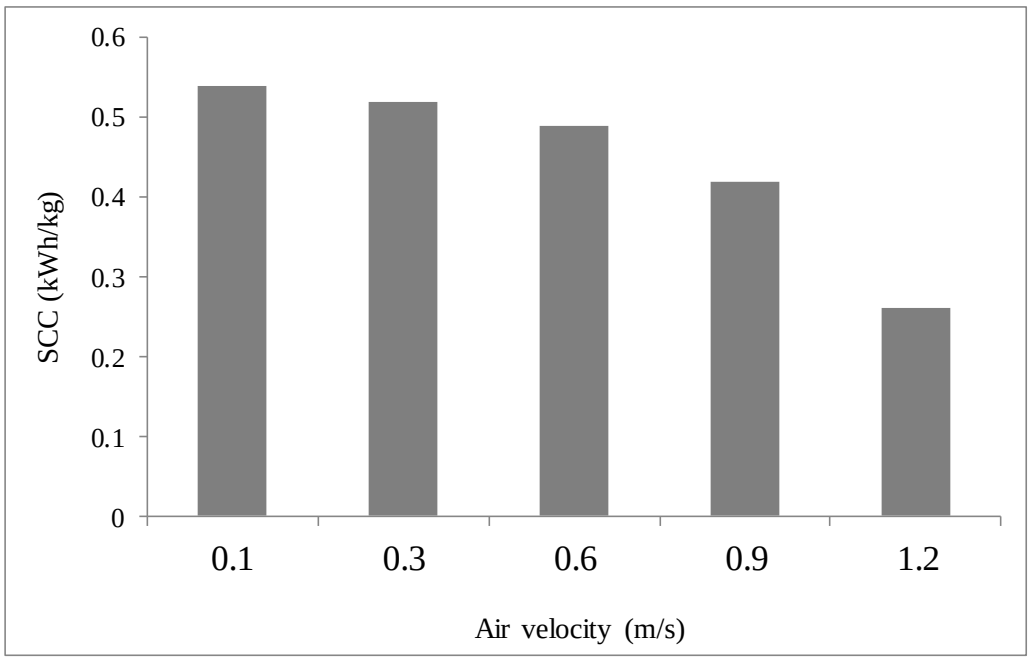


Figure 74. Specific cooling capacity trends at 0.1 - 1.2 m/

3.3.4 Determinations of optimum operating parameters for eucalyptus fibres

The performance of eucalyptus fibres is compared in terms of specific cooling capacity, cooling capacity, COP, mass flow rate and evaporation rate. Moreover, the optimum design conditions are indicated in the graph. The summary of the testing results of eucalyptus fibres are shown in Table 12.

Table 12. Results of eucalyptus fibres under experimentation

Velocity (m/s)	Mass flow rate (kg/s)	Evaporation rate (g/s)	SCC (kWh/kg)	Cooling capacity (kW)	COP
1.2	0.115	0.55	0.26	0.518	4.05
0.9	0.0864	0.303	0.42	0.458	3.93
0.6	0.058	0.203	0.49	0.363	3.54
0.3	0.029	0.12	0.52	0.226	2.55
0.1	0.0096	0.049	0.54	0.096	1.14

As seen in Figure 75, the cooling capacity gets higher with the increase of the mass flow rate since these two parameters are directly proportional to each other.

In contrast, specific cooling capacity was dropped with the increase of the mass flow rate. This indicates that, at higher air velocities more water is evaporated during the process and thus more water vapour is added to the air. As a result, water consumption rate becomes higher for the same cooling generated. This is a significant factor especially for region where there is water scarcity.

As seen from the Figure 75, SCC and CC are indirectly proportional to each other during the evaporative cooler operation. It is desirable to have both high SCC and high CC. Therefore, the intersection point can be considered as optimum operational conditions for the use of eucalyptus fibres as evaporative cooling pad.

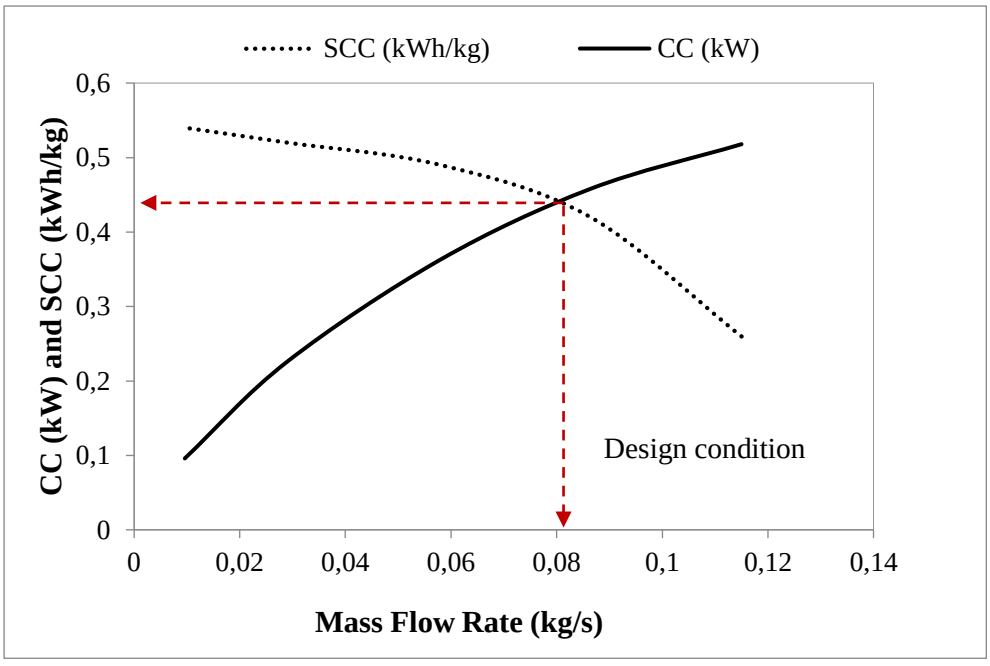


Figure 75. Combined effects of SCC and CC at different mass flow rate

In contrast to SCC, cooling COP showed an increasing trend with the rise of mass flow rate (See: Figure 76). COP sharply increased up to mass flow rate of ~0.06 kg/s and then, it showed a gradual change. On the other hand, specific cooling capacity was dramatically decreased for the change of mass flow rate in the range of 0.0096-0.058 kg/s and the drop became more gradual at higher mass flow rates. The intersection point of two curves gives the optimum conditions as seen Figure 76.

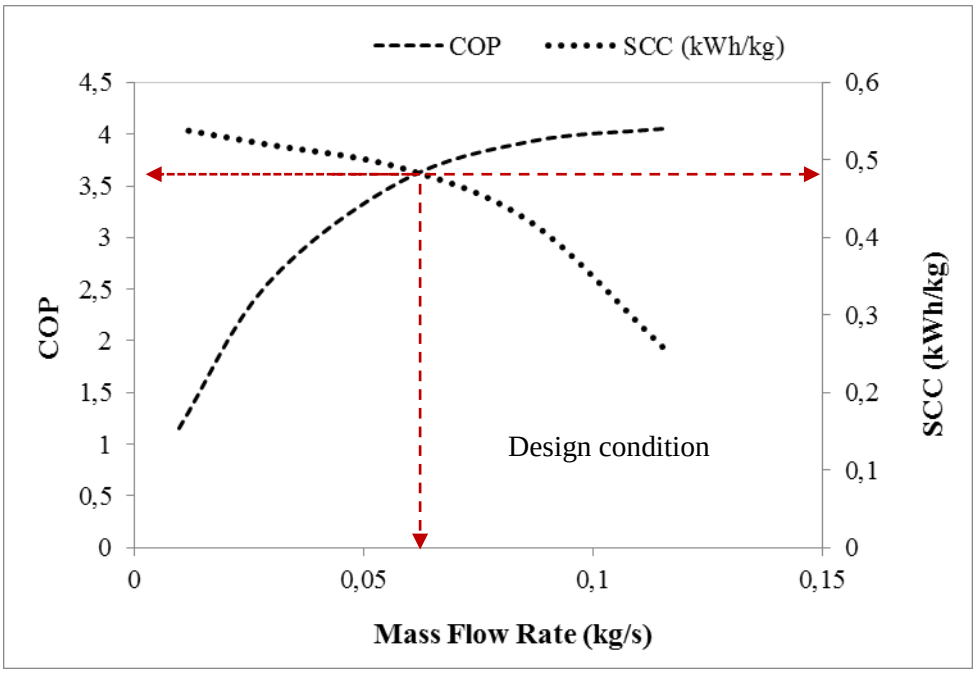


Figure 76. Combined effects of COP and SCC at different mass flow rates

In this part of the study, the variation of cooling capacity and specific cooling capacity versus evaporation rate are represented in Fig. 77. As indicated in the graph, the cooling capacity increases linearly until 0.2 g/s evaporation rate. This is due to the increase of the mass flow rate and thus, the convection rate. After that point, the increase in cooling capacity falls as the effect of the evaporation on air temperature difference is minimal due to the reason that the air humidity is close to saturation point. According to the graph, there is also an indirect relation between CC and SCC. This is because that the ratio of the increase of ER is higher than the CC with the increasing mass flow rate.

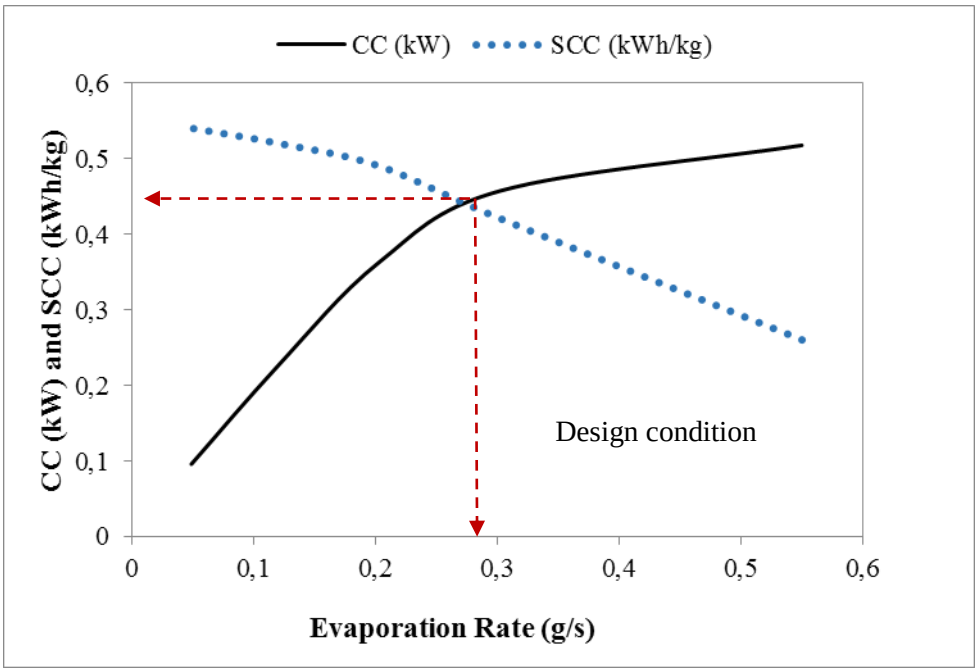


Figure 77. CC and SCC at different evaporation rates

The intersection point of the two curves indicates the optimum condition of the eucalyptus fibres for evaporative cooling pad as given in Table 13.

Table 13. Optimum conditions for using eucalyptus fibres

Parameter	**Value**
Mass flow rate, $\dot{m}$	0.06 – 0.08 kg/s
Specific cooling capacity, *SCC*	0.44 - 0.48
Coefficient of performance, *COP*	3.65
Cooling Capacity, *CC*	0.44 kW
Air velocity, ϑ	0.6 – 0.9 m/s
Evaporation rate, *ER*	0.27 g/s

3.4 Numerical analysis of eucalyptus fibres based evaporative cooling system

This part of the thesis shows the numerical investigation of the eucalyptus fibre based evaporative cooling system with regard to outlet dry bulb temperature, evaporation rate and cooling capacity at different environmental conditions. Experimental results have been used for numerical study in order to validate the experimental results. This includes two various cases of simulation conducted in order to investigate the performance of the system:

- The effect of different dry bulb temperature (35°C and 40°C) on the outlet dry bulb temperature, evaporation rate and cooling capacity.
- The effect of different air velocity (0.6 m/s - 0.9 m/s - 1.2 m/s) on the outlet dry bulb temperature, evaporation rate and cooling capacity.

3.4.1 Mathematical Formulation

The aim of the numerical analysis is to study the performance of the eucalyptus fibres based evaporative cooling system under various conditions in order to enhance the knowledge of the system. Therefore in this part of the thesis, the mathematical model is described to investigate the system performance by indicating the following assumptions:

- The inlet DBT is 35°C and 40°C
- The inlet RH is 10%, 30% and 50%
- The air velocity is 0.6 m/s, 0.9 m/s and 1.2 m/s
- The outlet RH is 60%, 80% and 100%.

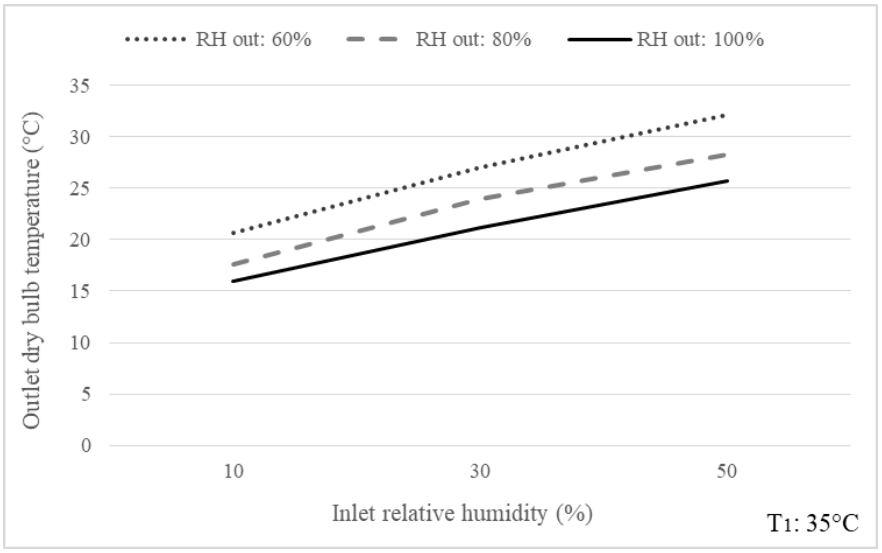
As described in section 2.7, the cooling capacity of the eucalyptus fibres based evaporative cooling are given by Eq. 2.2 and 2.3. Evaporation rate is represented with the Eq. 2.6, 2.7 and 2.8.

3.4.2 The effect of inlet dry bulb temperature on performance of the system

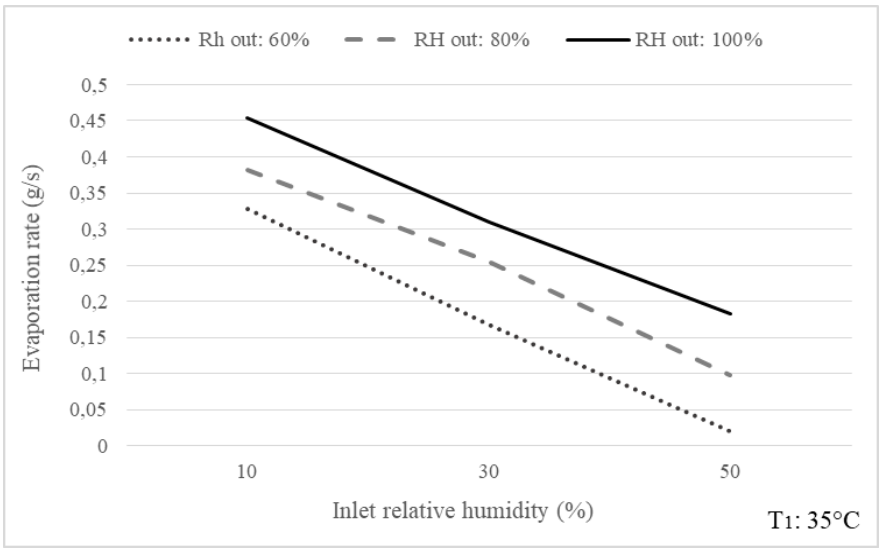
The effect of inlet dry bulb temperature at 35°C and 40°C is numerically studied when the velocity of the intake air is set to 0.6 m/s, on the performance of the eucalyptus fibre based evaporative cooling system. The validation of the numerical simulations is shown in Figure 78 at constant inlet dry bulb temperature (35°C), outlet relative humidity (60-80-100%), air velocity (0.6 m/s) and variable inlet relative humidity (10-30-50%) on the performance of outlet dry bulb temperature, evaporation rate and cooling capacity. In Figure 79, the simulation is presented under constant inlet dry bulb temperature (40°C), outlet relative humidity (60-80-100%), air velocity (0.6 m/s) and variable inlet relative humidity (10-30-50%).

The graph in Figure 78(a) show that show that the inlet RH is directly proportional to outlet DBT. As the inlet RH is lower (10%) and the outlet RH is higher (100%), the outlet temperature is 15.9°C when the inlet DBT is 35°C. Whereas, evaporation rate is reduced with increasing inlet RH. In accordance with the literature, as the inlet RH is higher, the air has less potential to absorb moisture from the air. As seen in Figure 78(b), the evaporation rate is the lowest at 0.45g/kg at 10% inlet RH and %100 outlet RH.

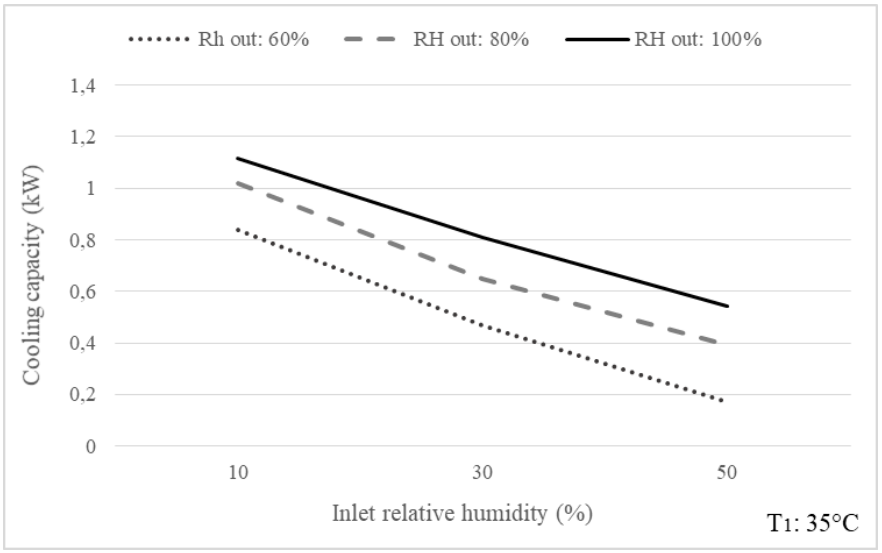
The simulations show that the cooling capacity and evaporation rate are directly proportional to each other. The CC is higher (1.12kW) at 10% inlet RH and at %100 outlet RH. When the inlet RH is 10% and outlet RH is 60%, it is reduced to 0.84kW. When the supply RH increases from 10% to 50%, it is reduced to 0.17kW as seen in Figure 78(c).



(a)



(b)



(c)

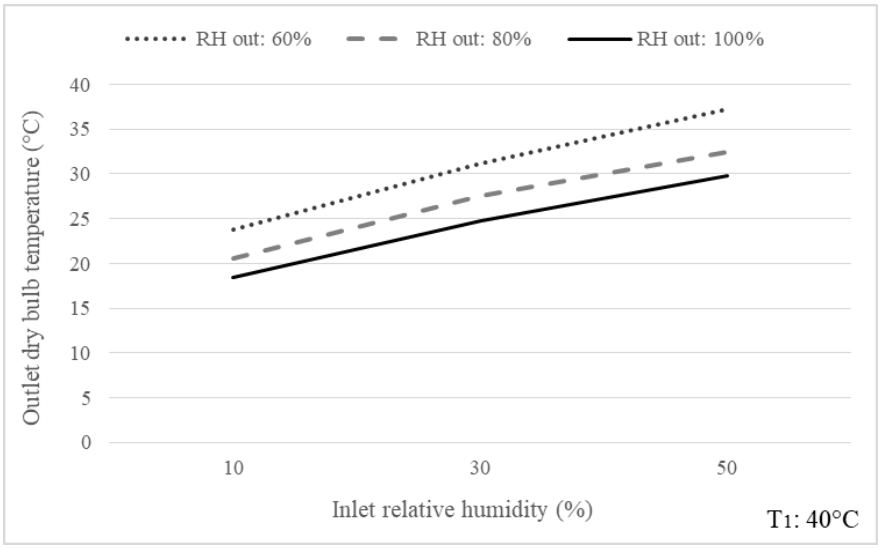
Figure 78. Numerical results on (a) dry bulb temperature (b) evaporation rate and (c) cooling capacity (at 35°C and 0.6 m/s)

The increasing inlet DBT from 35°C to 40°C causes to the rise of temperature difference between inlet and outlet DBT in Figure 79(a). The change of 5°C inlet DBT gives about 2°C temperature difference when the inlet RH is 10% and outlet RH is 80%. The increasing of inlet RH from 10% to 50% also leads to the rise of the temperature difference. The temperature difference is 2°C, 1.4°C and 0.8°C when the inlet RH is 10%, 30% and 50%, respectively. It is clearly seen that the significant factor affecting the outlet DBT is the inlet RH.

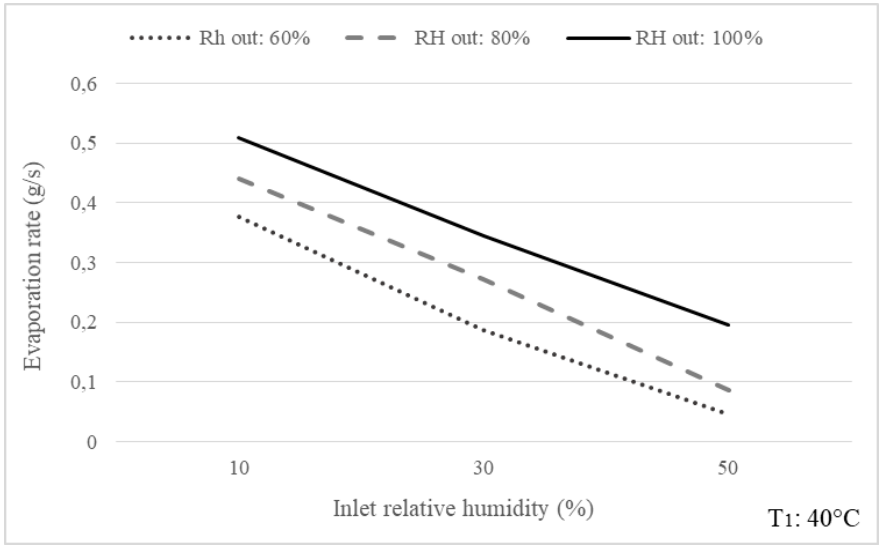
Based on the numerical simulations, the evaporation rate is higher as the inlet DBT is higher in Figure 79(b). Compared to the inlet DBT (35°C), the evaporation rate is 0.509 g/s at 40°C DBT when the inlet RH is 10% and outlet RH is 100% (Table 14). It is reduced to 0.196 g/s as the inlet RH is lower at 50%. The evaporation rate is the lowest at 0.046 g/s when the inlet RH is 50% and outlet RH is 60%.

The increasing evaporation rate tends to increase the cooling capacity since they are directly proportional to each other. The cooling capacity is 1.257kW at 10% inlet RH and 100% outlet RH. It is reduced 0.596kW when the inlet RH is increased to 50% (Table 14). This is due to the air has less potential to absorb moisture which causes to reduce the cooling capacity as seen in Figure 79(c).

a)



b)



c)

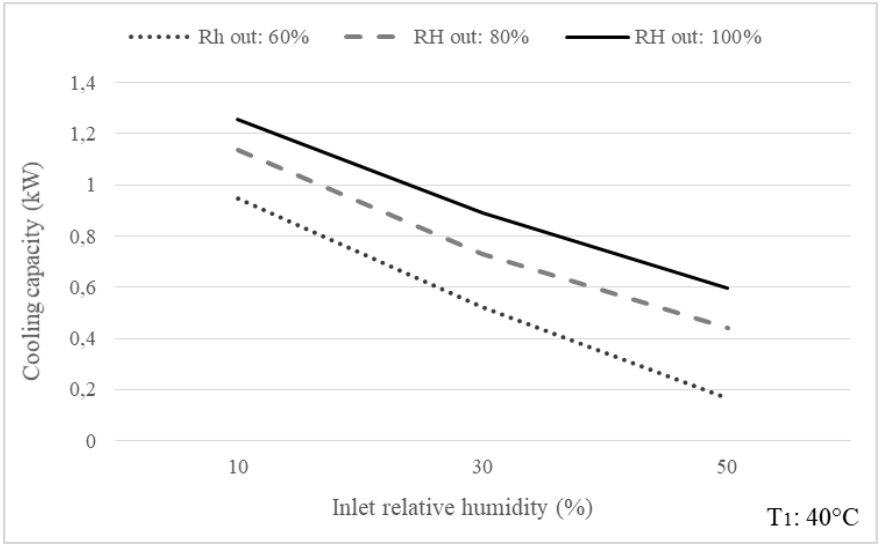


Figure 79. Numerical results on (a) dry bulb temperature (b) evaporation rate and (c) cooling capacity (at 40°C and 0.6 m/s)

Table 14. Numerical simulation at three various inlet RH

Inlet relative humidity (%)	10	30	50
Inlet air temperature (°C)	40	40	40
Inlet air velocity (m/s)	0.6	0.6	0.6
Outlet air temperature (°C)	18.5	24.8	29.8
Outlet relative humidity (%)	100	100	100
Evaporation rate (g/s)	0.509	0.344	0.196
Temperature difference (°C)	21.5	15.2	10.2
Cooling capacity (kW)	1.257	0.889	0.596

The effect of inlet dry bulb temperature at 35°C and 40°C is also numerically studied at 1.2 m/s inlet air velocity. As seen in Table 15, the evaporation rate is slightly higher at 40°C compared to evaporation rate at 35°C. The cooling capacity is also higher at 1.182kW at 40°C. These are due to the mass flow rate is the function of both evaporation rate and cooling capacity.

Table 15. Numerical simulation at two various inlet DBT

Inlet air temperature (°C)	35	40
Inlet air velocity (m/s)	1.2	1.2
Inlet relative humidity (%)	50	50
Outlet relative humidity (%)	100	100
Evaporation rate (g/s)	0.363	0.389
Cooling capacity (kW)	1.078	1.182

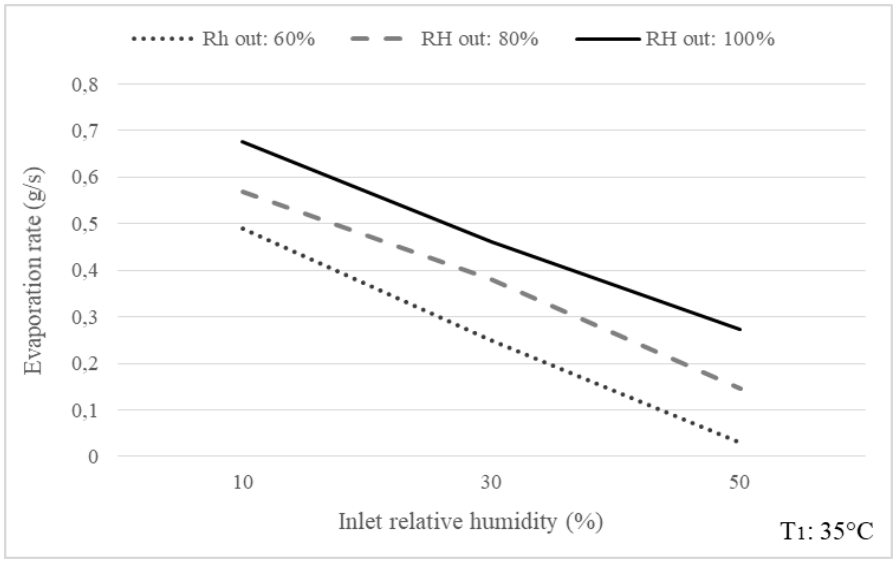
3.4.3 The effect of inlet air velocity on performance of the system

The simulations are carried out in order to investigate the effect of air velocity at 0.6 m/s, 0.9 m/s and 1.2 m/s on the performance of the system. In Table 16, the results of evaporation rate and cooling capacity is seen at different air velocities. It is presented that the evaporation rate and cooling capacity are directly proportional to increasing inlet air velocity. By increasing air velocity, the mass flow rate is also increased. As can be seen in Figure 80 and 81, the evaporation rate and cooling capacity are higher by increasing air velocity from 0.9 m/s to 1.2 m/s. The evaporation rate is the lowest around 0.029 g/s when the inlet air velocity is 0.9 m/s at 50% inlet Rh and at 60% outlet RH since air is more humid to absorb water vapour from the surrounding as seen in Figure 80(a). At 1.2 m/s inlet air velocity as seen in Figure 80(b), the evaporation rate becomes slightly higher around 0.039 g/s which is due to the increasing mass flow rate. In both graphs, these are higher at 10% inlet and 100% outlet RH at 0.68 g/s and 0.89 g/s evaporation rate at 0.9 m/s and 1.2 m/s air velocities, respectively.

Table 16. Numerical simulation at three various inlet air velocity

Inlet air velocity (m/s)	0.6	0.9	1.2
Inlet air temperature (°C)	40	40	40
Inlet relative humidity (%)	50	50	50
Outlet relative humidity (%)	100	100	100
Evaporation rate (g/s)	0.196	0.292	0.389
Cooling capacity (kW)	0.596	0.888	1.182

a)



b)

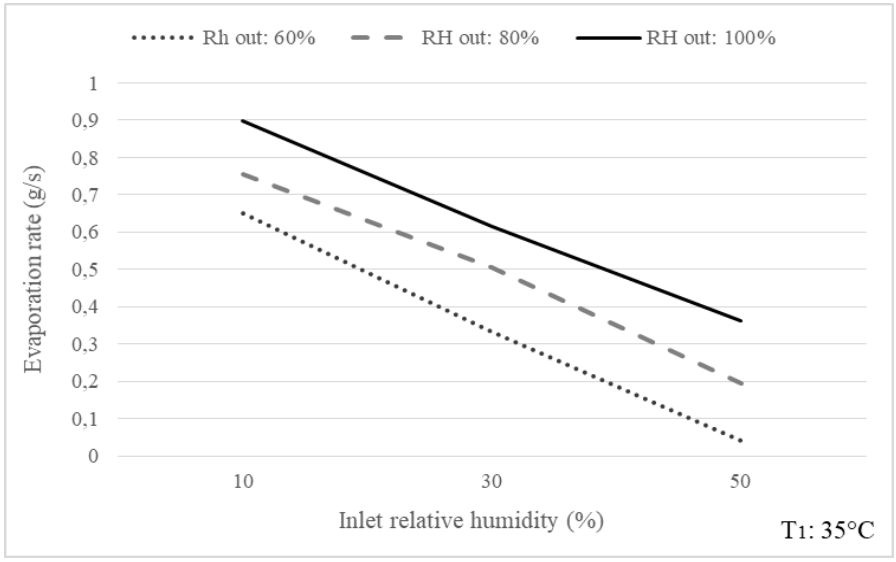
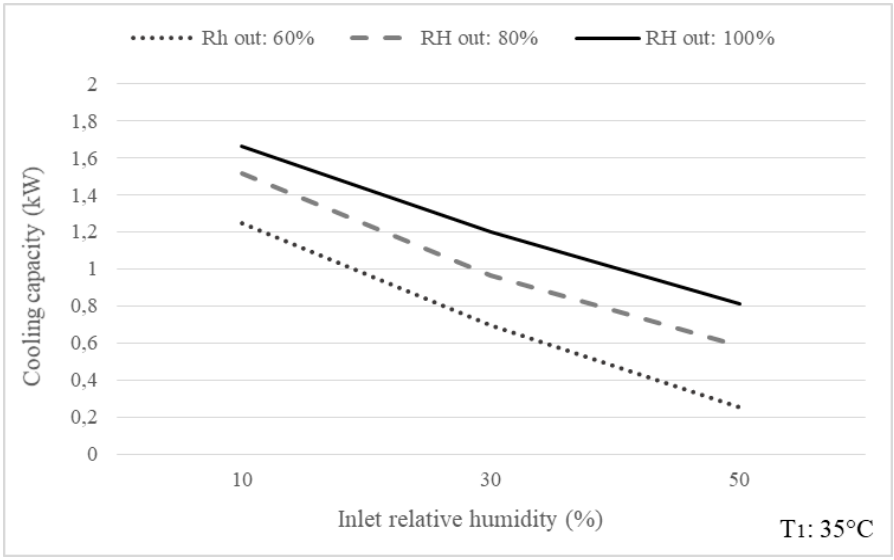


Figure 80. Numerical results on (a) evaporation rate at 0.9 m/s (b) evaporation rate at 1.2 m/s (at 35°C)

The cooling capacity shows the same trend as evaporative cooling at 0.9 m/s and 1.2 m/s when the inlet DBT is 35°C as seen in Figure 81. In both conditions, the cooling capacities are higher when the inlet RH is lower compared to higher inlet RH. The cooling capacities are higher around 1.66kW and 2.21kW at 0.9 m/s and 1.2 m/s inlet air velocities when the inlet RH is 10% and outlet RH is 100%.

a)



b)

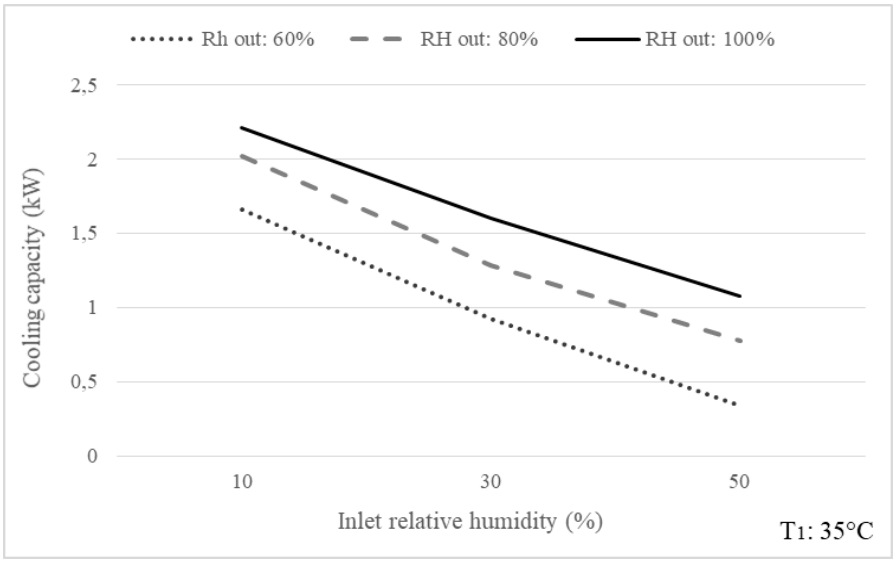
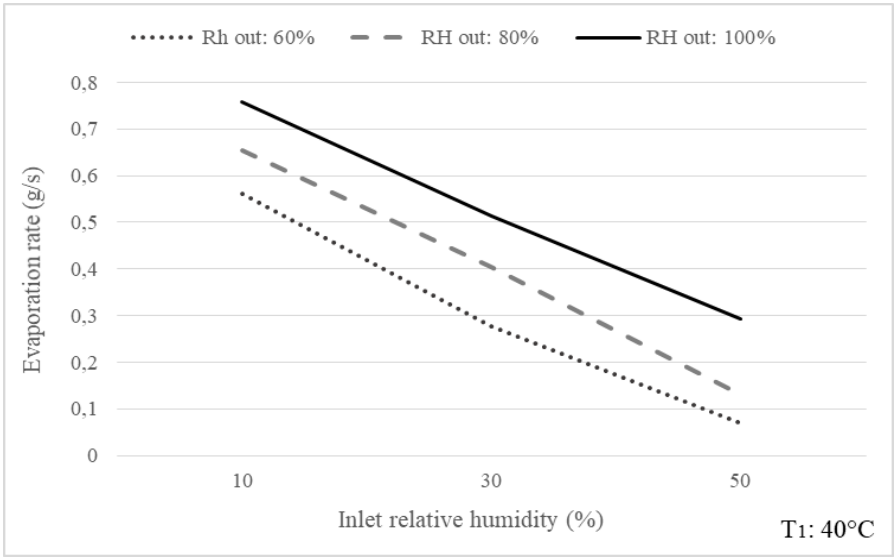


Figure 81. Numerical results on (a) cooling capacity at 0.9 m/s (b) cooling capacity at 1.2 m/s (at 35°C)

It is also clear that the evaporation rate and cooling capacity are increased when the inlet DBT is increased from 35°C to 40°C as seen in Figure 82 and 83. The evaporation rates at 40°C inlet DBT are higher around 0.759 g/s and 1.009 g/s at 0.9 m/s and 1.2 m/s inlet air velocity, respectively (Figure 82).

a)



b)

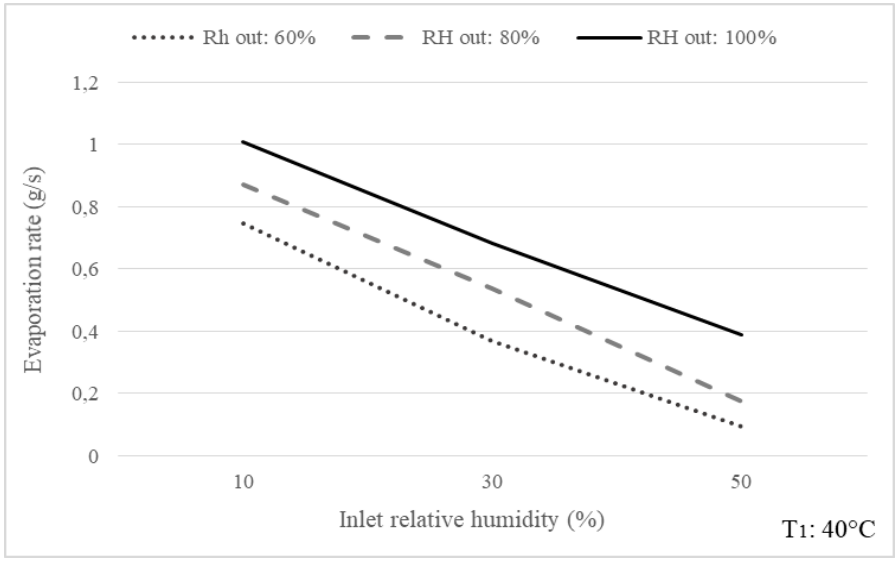
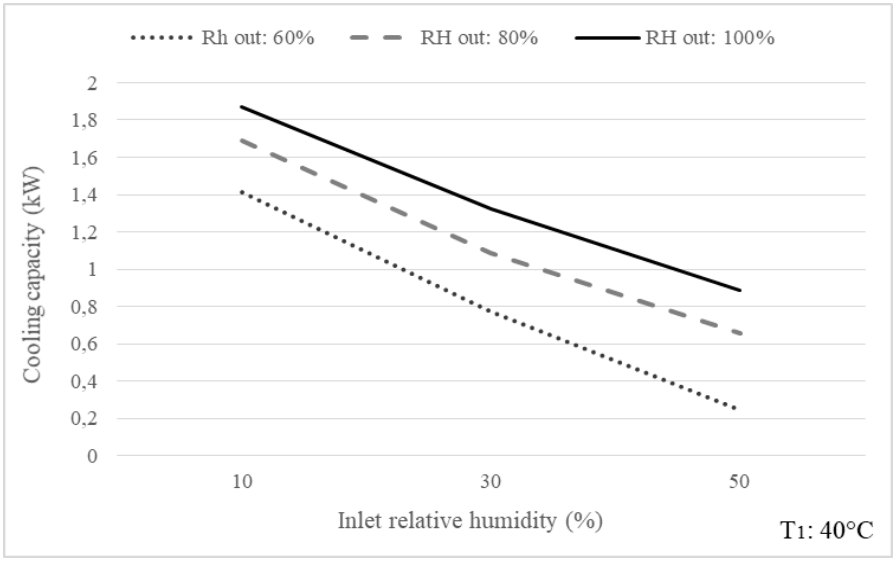


Figure 82. Numerical results on (a) evaporation rate at 0.9 m/s (b) evaporation rate at 1.2 m/s (at 40°C)

The cooling capacities are 1.87kW and 2.49kW at 40°C inlet DBT when the air velocities are 0.9 m/s and 1.2 m/s, respectively (Figure 83). It is obvious that by increasing inlet DBT, the higher evaporation rate and thus, the cooling capacity is obtained. However, it is the lowest at 0.24kW when the inlet RH is 50% and inlet air velocity is 0.9 m/s

a)



b)

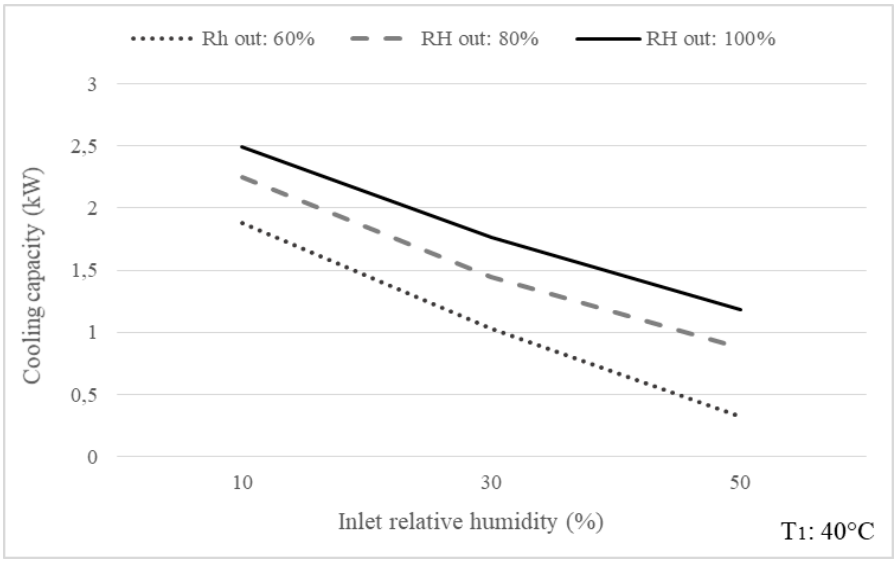


Figure 83. Numerical results on (a) cooling capacity at 0.9 m/s (b) cooling capacity at 1.2 m/s (at 40°C)

3.5 Conclusion

In this chapter, the eucalyptus fibres and yellow stones are experimentally studied under different test conditions. Each testing conditions were tested at 35-36°C which is the average temperature of Cyprus climate. The RH is set up as 20% since at higher lands (mountainous areas) the average RH is lower compared to inlands. It was found that the temperature drop was 9.6°C for eucalyptus fibres and 3.6°C was recorded for yellow stones. The outlet relative humidity was higher for eucalyptus fibres (57%) compared to yellow stones (35%).

It was then followed by the further experimental investigation by using eucalyptus fibres. It was aimed to study the performance of eucalyptus fibre pads under different conditions in order to gather information about the cooling efficiency and cooling capacity of eucalyptus fibres based evaporative cooling system and to analyse the effect of air temperature and air velocity on the material performance.

This chapter showed that a novel organic and environmentally friendly material; eucalyptus fibres can be used as an alternative evaporative cooling pad instead of vapour compression system which has high operational costs. According to the study results, it can be concluded that the eucalyptus fibres at low air velocity, provides better performance in terms of cooling efficiency, in accordance with the literature data.

In the following chapter, the conceptual design ideas of integrated evaporative cooling system into building elements are developed by using three-dimensional illustration in order to give brief explanation about architectural integration of eucalyptus fibres as an evaporative cooling pad. In this respect, it is aimed to show that the cooling effect can be provided by creating simple design ideas for building.

CHAPTER 4: Conceptual Design Ideas of Integrated Eucalyptus Fibres Based Evaporative Cooling Panel (EFECP) into Building Elements

4.1 Introduction

The idea of building integration with energy efficient system is a significant factor when the main aim is to reduce the energy consumption since the buildings are responsible for 40% of CO_2 emissions and total energy consumption (Directive 2010/31/EU).

Integration of eucalyptus fibre based evaporative cooling system into building element is important not only for providing clean energy, but also for meeting the architectural requirements of a building. Architectural design elements such as wall, wind catcher, solar chimney, shutter, etc. become the multifunctional elements of the building components based on cooling approach.

Considering the elements that form the building design, they play a vital role for low energy design strategies. According to Santamouris (2006) the building form has the highest role for low-energy design by 67%. It is then followed by façade design (52%). Thus, the form and façade design of the building should be considered in the design stage of the building in order to reduce the energy consumption caused by heating and cooling loads.

The heating and cooling systems are typically integrated into the envelope of the building (roof or façade) such as, awning, wall, balcony and shading element of the building (Chan et al., 2010). Implementing of any heating or cooling system as a conventional way into façade meet the requirement of a single function which is just to cool or heat the indoor space. By considering the combination of both thermal and architectural requirements, the multi-functionality is provided for each integration approach. Meaning that, the integration of the cooling system into shutter can provides shading, cooling and lighting. An architect plays a vital role for designing the shutter with evaporative cooling material in order to provide shading and cooling. This integration protects the building from the direct sun and thus, climate-

responsive building element is obtained. Depending on the economic feasibility of the integrated evaporative system into building envelope, it is also necessary for reducing energy consumption of the building.

In this chapter, the conceptual design ideas of integrated evaporative cooling system into building element are developed for building design. In this respect, the new material, eucalyptus fibres is used as a pad material for evaporative cooling system for the architectural integration of the building. The integrated building design should be aimed to meet the requirements of cooling, heating, ventilation and daylighting strategies to meet the demand of these loads (Torcellini, 2006). Thus, it is aimed to focus on conceptual design idea of integrated eucalyptus fibres for evaporative cooling in building elements in order to provide cooling, heating, ventilation and daylighting. Improved or new conceptual ideas are implemented into building elements such as:

- shutter,
- window,
- door,
- toplighting element,
- wind catcher and solar chimney,
- wall,

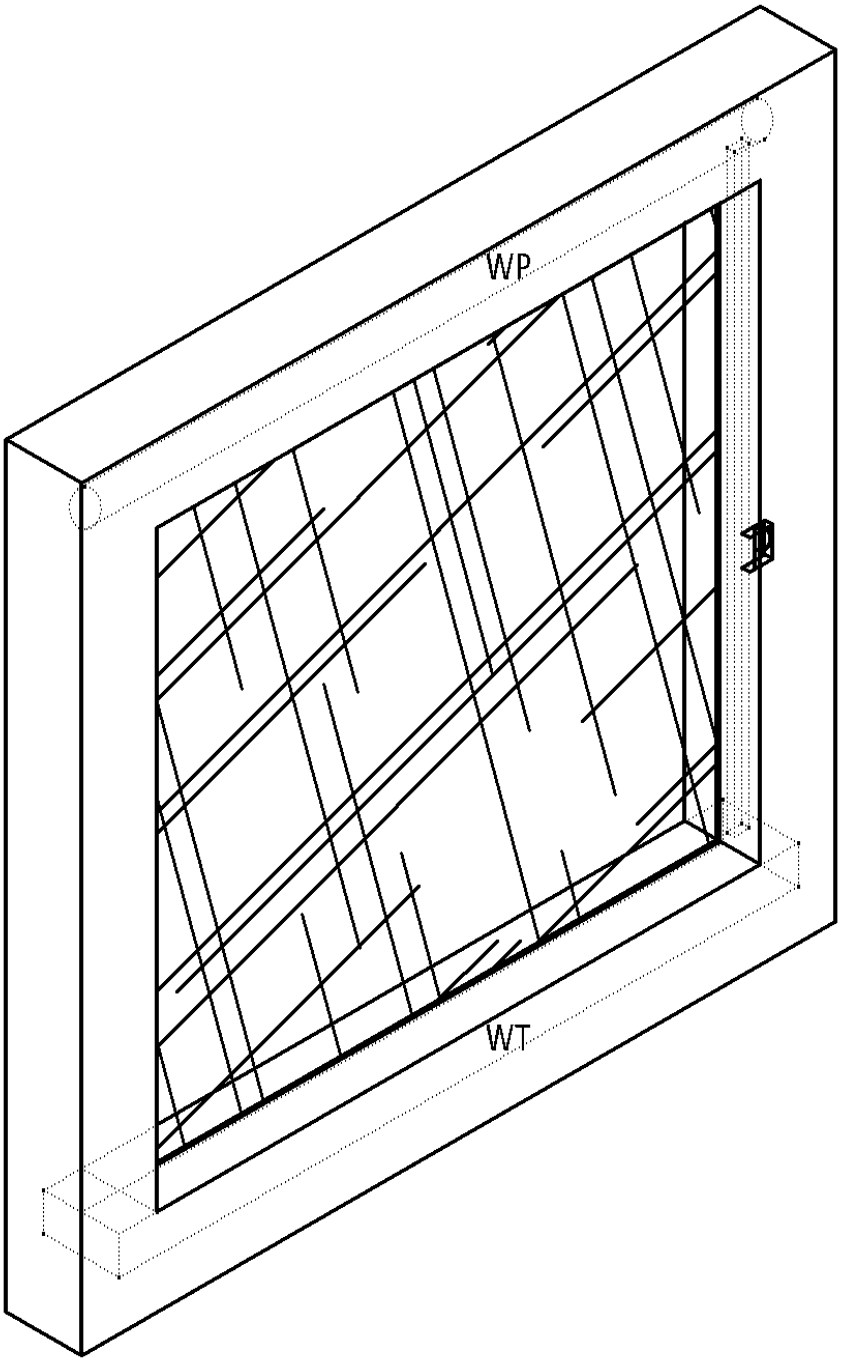
in order to reduce indoor air temperature and energy consumption by mechanical cooling.

4.2 Sizing and structural system of eucalyptus fibres based evaporative cooling Panel

As aforementioned above, the eucalyptus fibres were tested for 28X28cm panel (with 0.0784m² surface area) and the cooling capacity was calculated as 0.44kW for this specific panel. The monthly cooling capacity for this panel was found as 120kWh. To increase the amount of cooling capacity, the panel size should be increased. Thus, 1m² EFECP is proposed for increasing the performance of the material. It was calculated that 1m² EFECP provided

5.7kW cooling capacity. The monthly cooling capacity of 1m² EFECP was found as 1710kWh. The structural system and 3D view of the panel are detailed as seen in Figure 84 and 85.

As it is shown, the panel consists of the rectangular-shaped frame, water tank, water pipes and evaporative panel. The evaporative panel is formed by the plastic mesh filled with eucalyptus fibres. The water is supplied to the plastic mesh passed through the plastic pipe from water tank at the bottom and then, upper part. The water is dripped from the upper pipe which is drilled for water dripping in order to keep the pad wet. It is then dripped over the fibres and collected at the water tank.



a)

PERSPECTIVE

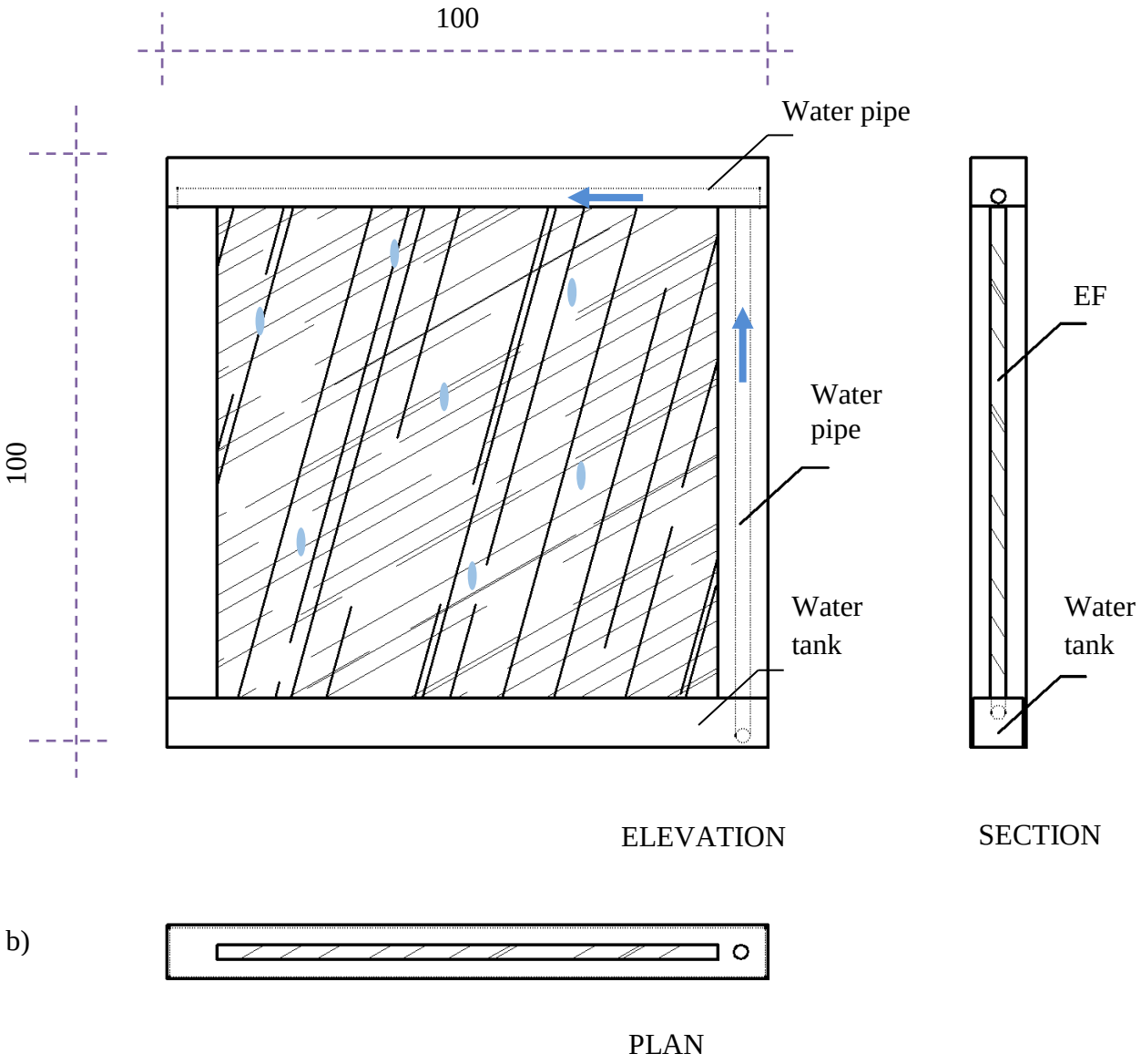


Figure 84. Structural system of EFECP a) perspective b) system detail (designed by author)

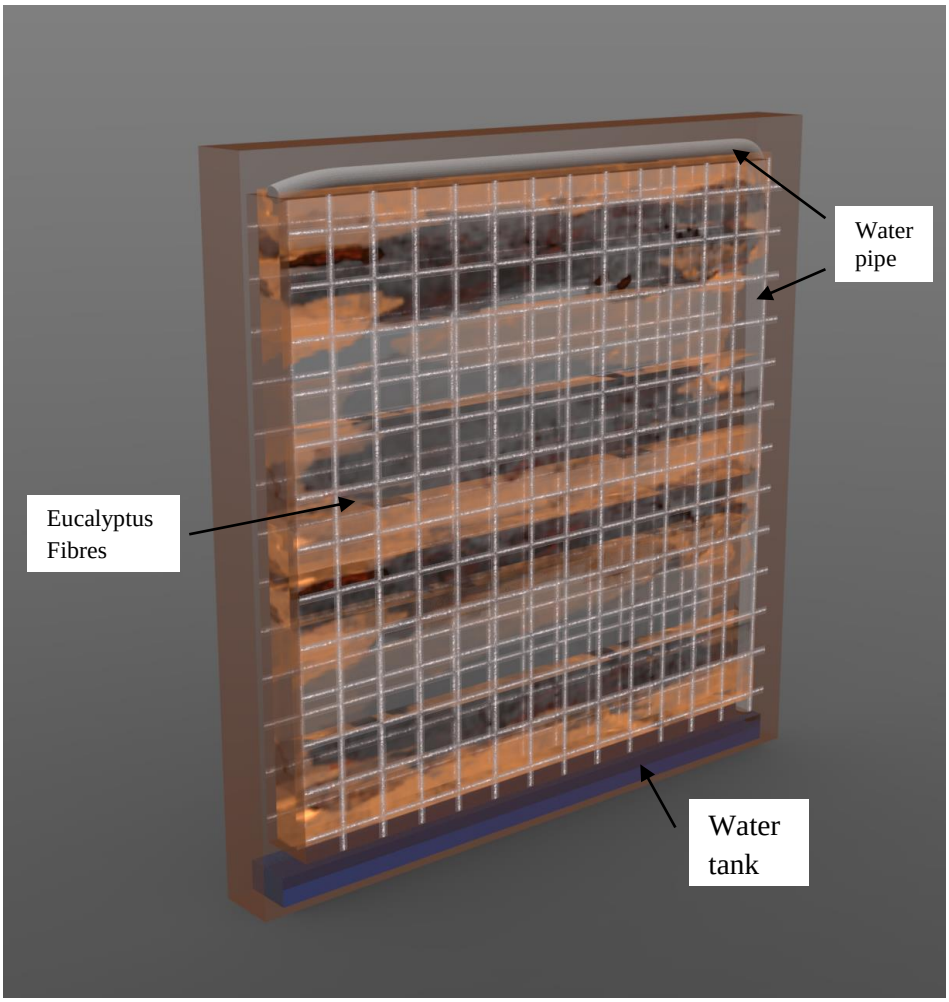


Figure 85. 3D view of Eucalyptus fibres evaporative cooling system

4.3 Comparison matrix for building elements integrated eucalyptus fibres evaporative cooling panel and building requirements

A comparison matrix was developed to compare the building elements integrated eucalyptus fibres based evaporative cooling system with building requirements in order to identify the characteristics of proposed evaporative cooling integrated building elements. In addition to this, it is aimed to incorporate evaporative cooling process as a significant architectural element for the building.

The building elements represent the various configuration of the implemented evaporative cooling system into shutter, window, door, toplighting element, wind catcher-solar chimney and wall. The building requirements are also

analysed in terms of building physics, construction, application & usage, functional and economical aspects (Figure 86).

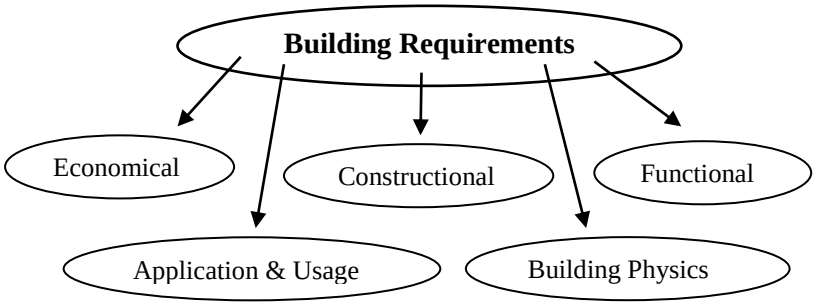


Figure 86. Building requirements for comparison matrix

Conceptual design ideas of eucalyptus fibres integrated evaporative cooling into building elements are analysed in relation to questions about building requirements in order to evaluate the performance of the proposed design concepts. These questions are shown in Table 17. It is aimed to show the potential strength and weaknesses of the proposed ideas in the building and to decide which integrated system meets the building and occupant's requirements. Thus, the designer can decides which design idea is suitable for required conditions. During conceptual design ideas, it was assumed that the integrated panels are facing to the prevailing wind. However, it should be noted that the fan can also be integrated to the system to promote air ventilation.

Table 17. Questions to evaluate the performance of the building elements integrated evaporative cooling system

Building Physics	Protection from climatic elements	1. Is this system provide protection against climatic elements such as precipitation, snow, wind and the sun?
	Supply of fresh air	2. Is this system introduce fresh air to indoor?
	Perform well towards prevailing wind	3. What is the role of orientation towards the prevailing winds?
	Visual relation between in &outside	4. Does this system provide visual relation between indoor and outdoor?
	Allowance of daylight	5. What is the level of daylight allowance?
	Shading	6. Can this system control the effect of the sun by shading?
Constructional	Additional structural system for exposing live loads	7. Does this system require additional structural systems for exposing live loads?
	Simple structure	8. Is this system easy to install?
	Easy integration into existing building elements	9. Is this system able to be integrated into existing building?
Application and Usage	Maintenance & easy cleaning	10. What is the level of maintenance and cleaning of the system?
	Feasibility	11. Can this system be feasibly integrated to any part of the building?
Functional	Multi-functionality	12. Does this system provide multi-functionality?
	Extra space	13. Does this system need extra space in the building?
Economical	Construction cost	14. What is the level of construction cost of this system?

Considering the building elements, shutter is a simple construction for night and day insulation which controls the heat gain and loss of the building. Wall openings such as window and door, play a vital role for heat gain and loss between indoor and outdoor environment.

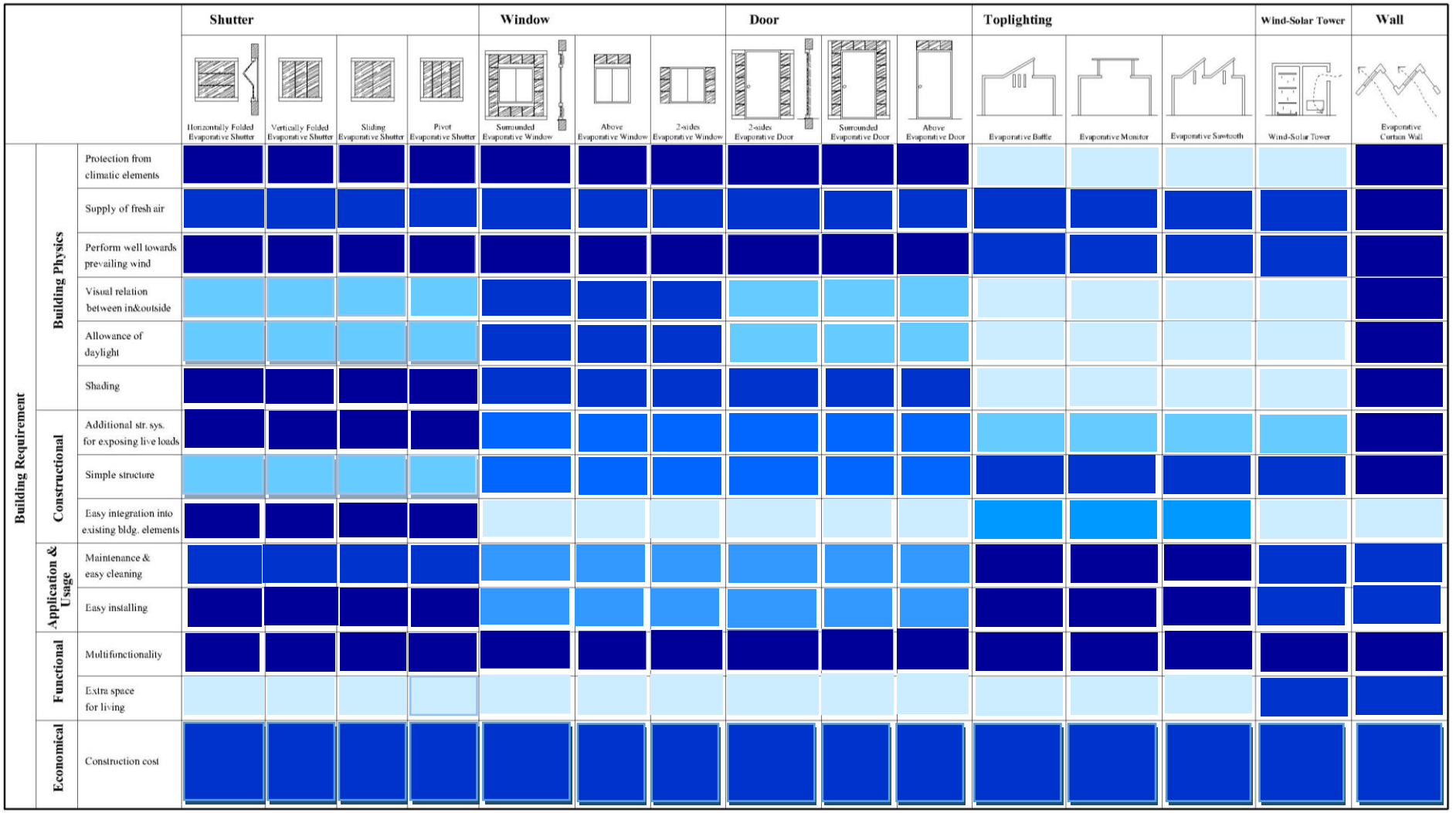
Toplighting elements allow natural lighting from ceiling level which creates more and homogenous lighting. However, it also allows more sunshine in winter and summer. For summer conditions the shading strategies should be considered to prevent sunlight. Moreover, the cooling purpose should also be implemented into toplighting elements. The wind-catcher and solar chimney provide natural ventilation in the building. The wind-catcher faces the prevailing wind to catch it and provide air flow inside. However, in solar chimney, sun heats up the air causing pressure difference in the chimney. The air then rises up and sucks the air from inside by convection.

As a part of the envelope, wall of the building divides the relation between outside and inside. The shape of the wall can also be considered in the design stage to get benefit from the environmental conditions.

As these building elements aforementioned above create openness between inside and outside, they can be used with the combination of evaporative cooling process. This approach helps to guide the design, develops new architectural integration idea and provides knowledge of architectural details for further study which is significant for researchers and designers.

During the comparison of the building elements integrated evaporative cooling system, the colour grading was used to compare the building element integrated evaporative cooling panel with building requirements as seen in Table 18. For grading, blue colour is chosen to show the low and high effect by using light and dark blue. It should be also known that this colour grading results can be changed if the new technology or material is used.

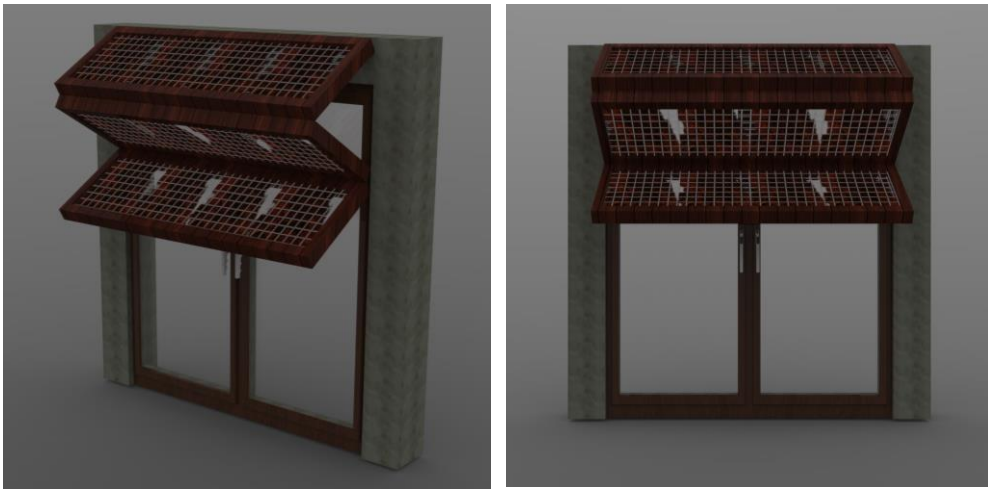
Table 18. Comparative table between the building elements integrated evaporative cooling system and building requirements



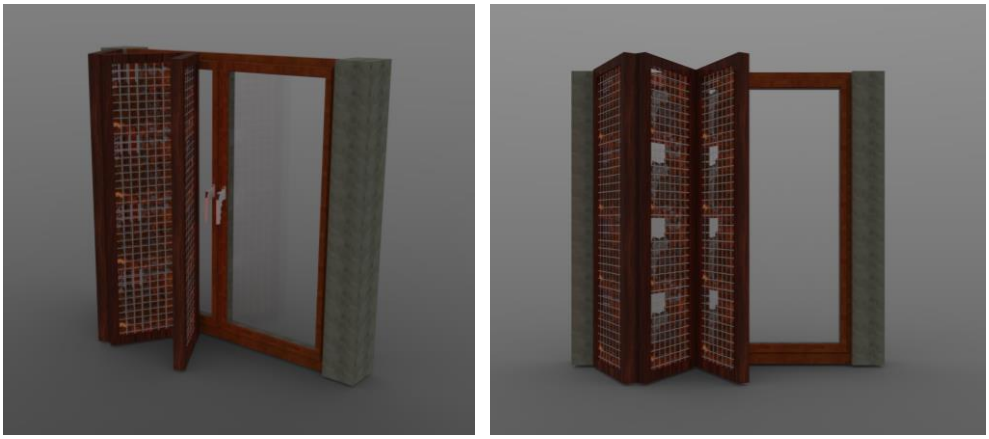
4.4 Shutter integrated EFECP

In many hot countries, the glazing facade should be covered with shutter to reduce sunlight penetration and glare in order to prevent heat gain in particular for summer. When the sunshine is required in winter, the shutters can be opened in order to increase heat gain.

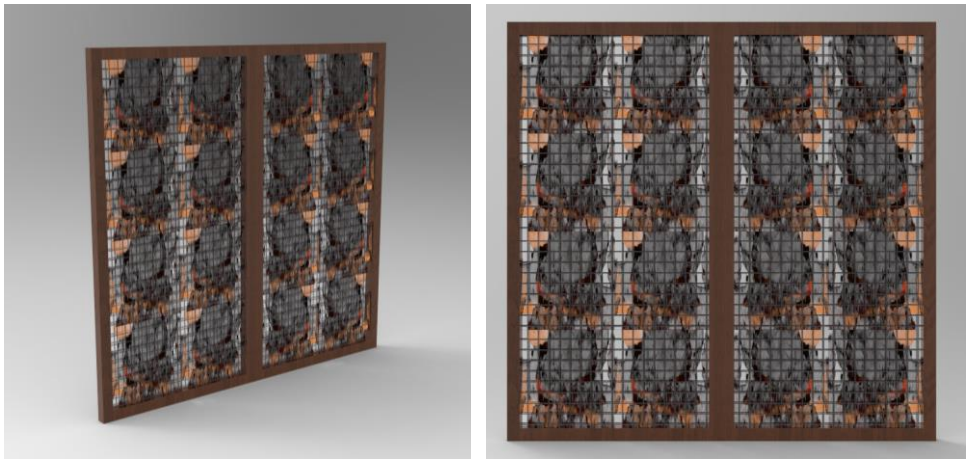
As seen in Figure 87, the different types of shutters are made from eucalyptus fibres pad for evaporative cooling process. The water is supplied from the top frame through the pad and collected at the water tank located at the lower frame. This shutter can be better faced to west direction in order to control heat gain in summer since the sun from the west direction is disturbing. In addition to this, the shutter can also allow warm air movement from outside to inside since the strongest wind is mostly coming from the west or north-west in Cyprus. The warm air is then passed through the wet surface of the shutter resulting to cool the indoor air by evaporation effect. When the sun is required in winter, the shutter can be totally opened to allow heat gain through the glass window. Therefore, shutter as a shading device and evaporative cooling panel can be faced to the west and north-west façade.

a) 

b)



c)



d)

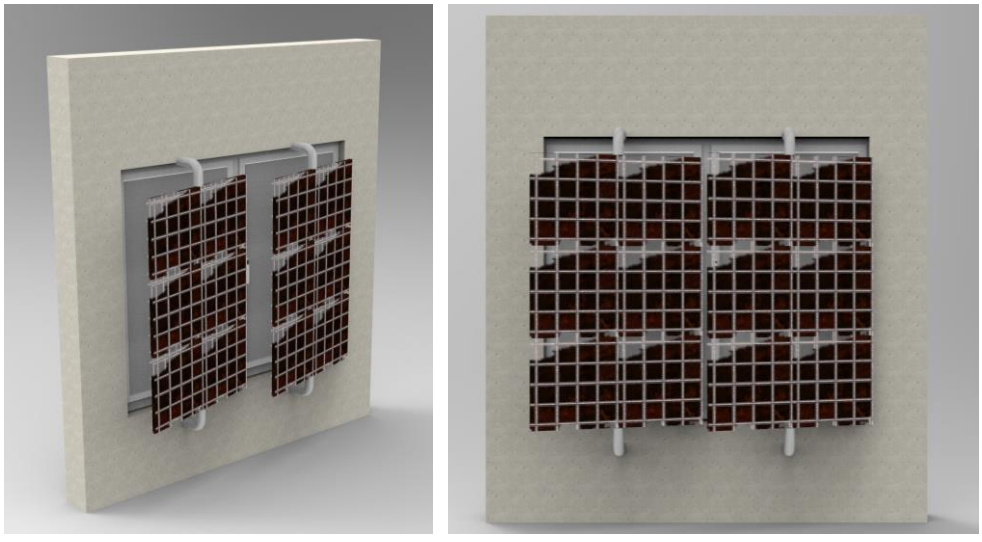


Figure 87. Evaporative cooling system integrated shutter a) horizontally folded evaporative shutter b) vertically folded evaporative shutter c) sliding evaporative shutter d) pivot evaporative shutter

The ideas of integrated shutters seen in Figure 87, provide protection from environmental conditions and shading when they are used to cover the window area. The visual relation between inside and outside, daylight and fresh air can also be provided and controlled since they are moveable structure. Since it is moveable, it is not easily constructed. As the shutter is a separate element, it can be easily integrated into existing window without any additional space in the building. When compared to plastic or metal shutter, the cost of the construction with local material is lower during the construction and operation of the system. However, the local material should be changed when it starts to deteriorate.

4.5 Window and door integrated EFECP

Regarding the **fenestration** of the building, windows or doors are the important part of the building for thermal comfort requirements. The orientation of window and door should facilitate air ventilation in the buildings. They are also used to provide thermal requirement, visual communication and daylighting purposes if required. The heat transmissions for indoor space can be controlled by fenestration both for winter and summer condition. The system is suggested to integrate at the top of the window and door as seen in Figure 88 and 89. For better air supply, the fan assisted integrated system can be also proposed. In Figure 90, fan assisted evaporative cooling system for window can be seen. The PV module can also be integrated for powering the fan used in the cooling system. According to the literature, the glazing is mostly integrated with photovoltaic panels for solar energy application. The windows are integrated with PV panels (Han et al., 2010; Connelly et al., 2016; Leite Didoné, Wagner, 2013).

Since the proposed system is placed within the cavity of the wall at the top of the door and window, it does not affects the visual relation, fresh air and solar allowance. On the other hand, it is not easy to integrate into the existing building. It is also easy to clean and maintain which reduces the installation costs.



Figure 88. Evaporative cooling system integrated into window



Figure 89. Evaporative cooling system integrated into door

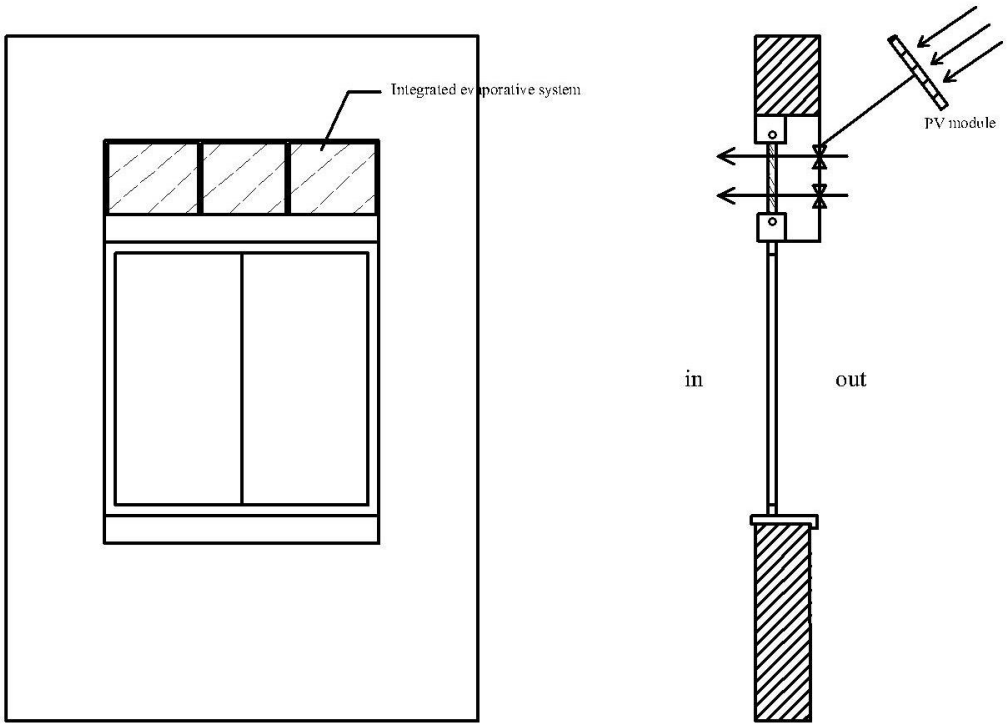


Figure 90. Evaporative cooling system integrated into window

4.6 Toplighting integrated EFECP

Daylighting allowance from openings is a significant architectural necessity for the building design. Openings do not only provide daylighting, but also air ventilation and visual communication between inside and outside (Reinhart and Wienold, 2011; Ahmad et al., 2016).

When the air ventilation do not meet the demand of cooling by openings from the top, some other methods can be proposed to enhance cooling effect and to lower energy consumption. Thus, evaporative cooling system is suggested through the use of toplighting devices.

Toplighting elements are especially used in large and compact building where some spaces have no facade to the outside. Monitor, sawtooth, clerestory and skylight are mostly used architectural elements in providing natural daylighting since the elements can allow light from the roof (IESNA Lighting Handbook, 1984; Freewan, 2015). When these elements face to south or north, they

provide better performance of daylighting. As seen in Figure 91, these elements are incorporated on top of the building.

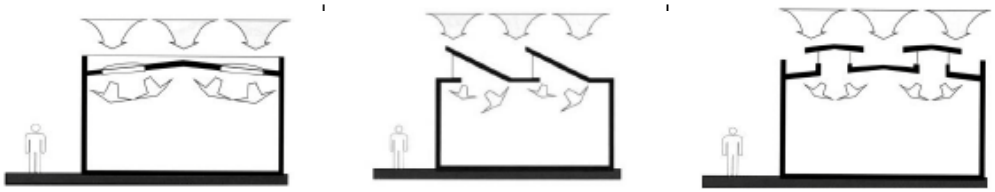


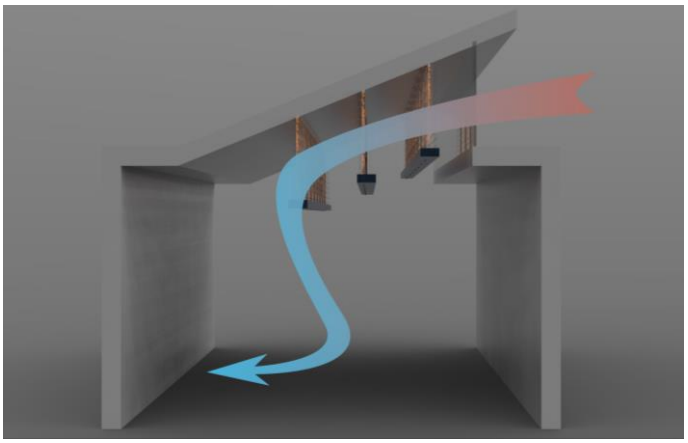
Figure 91. Skylight, Sawtooth at clerestory, Monitor (Kadir et al., 2015)

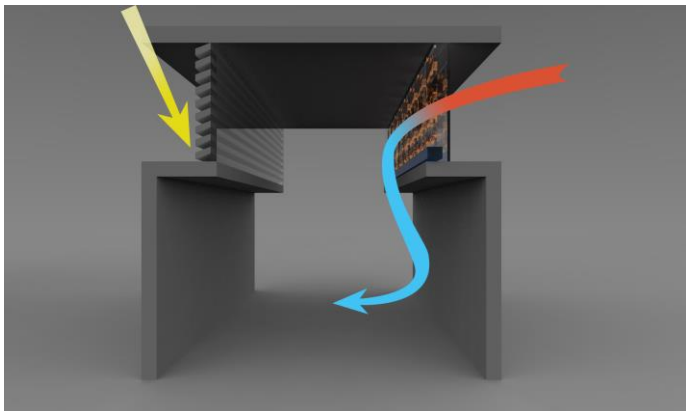
The integration of evaporative cooling system into toplighting elements provide the combinations of daylighting, cooling and air ventilation. The evaporative cooling integrated toplighting element is suggested to face prevailing wind in order to enhance cooling effect and natural lighting. This orientation also prevents the disturbing effect of direct sunlight from south direction. Although north-facing toplighting minimizes the effect of lighting compared to south-facing orientation, a suncatcher baffle can be used on the outside of the clerestory to increase natural daylighting (Choi et al., 2004).

Since these elements are both used for solar radiation in winter and natural air ventilation in summer, the integration of evaporative cooling system into these elements can also provide cooling effect by the evaporation of the water process. These are directed to the prevailing wind to promote air ventilation. If these are faced to the south, east or west facade, night insulation or shading devices can be used to prevent overheating.

As seen in Figure 92, the evaporative cooling system is integrated into baffle and monitor element. The baffles are covered with eucalyptus fibres for cooling effect and used to diffuse sunlight. For summer condition in Figure 85(b), the panel is directed to the prevailing wind direction to allow more air for evaporative cooling process. Due to the size of the south-facing overhang and the shutter, the penetration of the direct sunlight is controlled. In addition to this, if wall opening is created at the other side or adjacent of the wall, more air ventilation and cooling effect are created due to the cross ventilation phenomenon. For winter condition, the evaporative cooling system should be

closed by covering the monitor by curtain or louvers as seen in Figure 92(b). The heat gain is provided from the south-facing monitor since the angle of the sun is lower in winter.

a) 

b) summer 

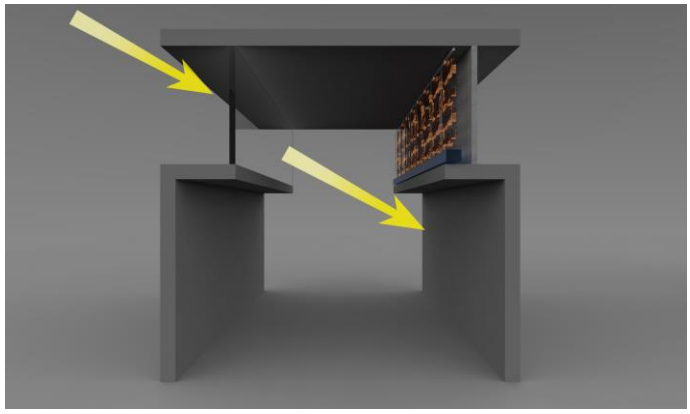
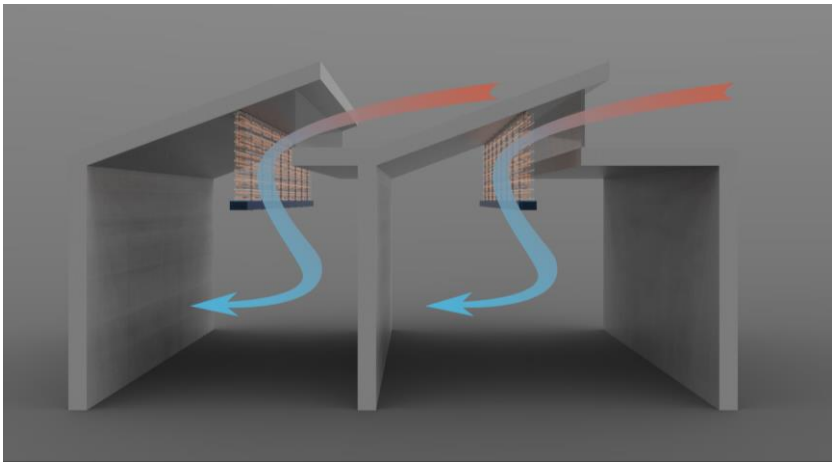
b) winter 

Figure 92. Evaporative cooling system a) integrated baffles and b) monitor in summer and winter condition

The integration ideas in Figure 93(a), the evaporative cooling integrated vertical roof glass, sawtooth, facing to the prevailing wind direction capture more air blow. Thus, more evaporation of water is obtained. Generally, the sawtooth is good at distributing natural light evenly. However, as the eucalyptus fibres panel is located in front of sawtooth, the amount of light diffused inside is minimised.

In Figure 93(b) the evaporative cooling integrated clerestory is shown. It is both used to illuminate interior space and allow air ventilation. Although the toplighting element is generally used for lighting purpose from the ceiling of the building, it also allows air ventilation when facing prevailing wind. The daylight is diffused from the panel as it is situated in front of the clerestory window.

a) 

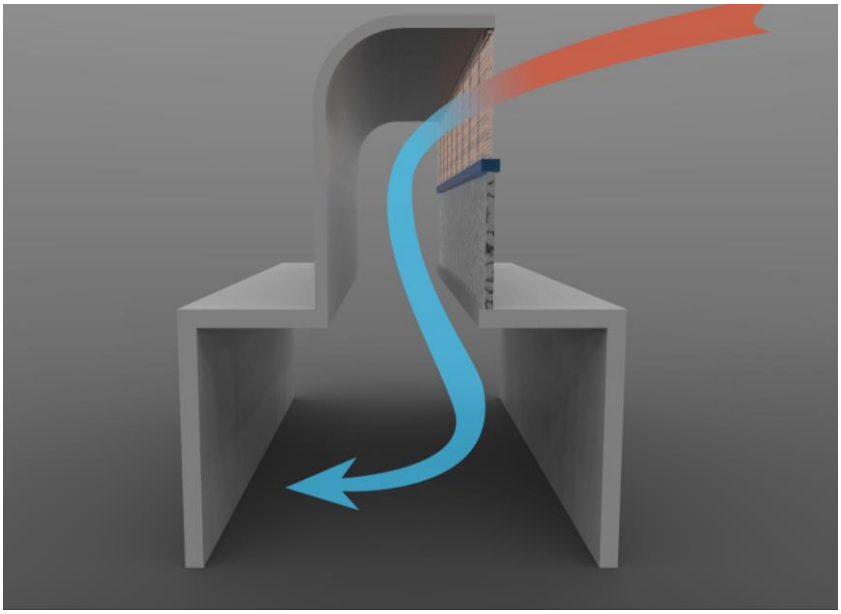
b) 

Figure 93. Evaporative cooling system integrated a) sawtooth and b) clerestory

The integrated evaporative cooling panel into toplighting element provides well performed towards prevailing wind if the elements are facing towards prevailing wind. On the other hand, the allowance of daylight is minimised since the panel is situated in front of the toplighting element. As it is not directly combined with the element, it can be easily integrated into the existing building. It also provides easy maintaining and cleaning.

4.7 Wind-solar tower integrated EFECP

"Wind-solar tower" is proposed which representing the combination of wind catcher and solar chimney. Wind catcher is used during hot seasons to cool the indoor by capturing wind whereas solar chimney is used to induce air ventilation. Generally, solar chimney is also used for heating by using fan (Xue, 2014). It is heated by glazing surface where absorbs solar radiation. According to this, difference air pressure is created at the inlet and outlet openings resulting to increase stack effect (Khani, 2017).

These systems are suggested as two separate rectangular-prisms which share a single wall. In one channel, the cooling effect is created by placing evaporation

pad material into the channel as seen in Figure 94. The water is sprayed from the top part through the materials and collected at the bottom. The water is then re-circulated through the system to provide water for increasing evaporation effect. The other channel is used to increase wind effect and stack effect in order to ventilate building. The upper part is made of glazing surface to heat the air inside the channel and to increase updraft by stack effect in order to exhaust hot air inside during hot season. Thus, it can meet the requirements of cooling and air ventilation of the buildings in hot regions (Figure 88). These channels can be both used together if additional cooling effect is required for extreme conditions.

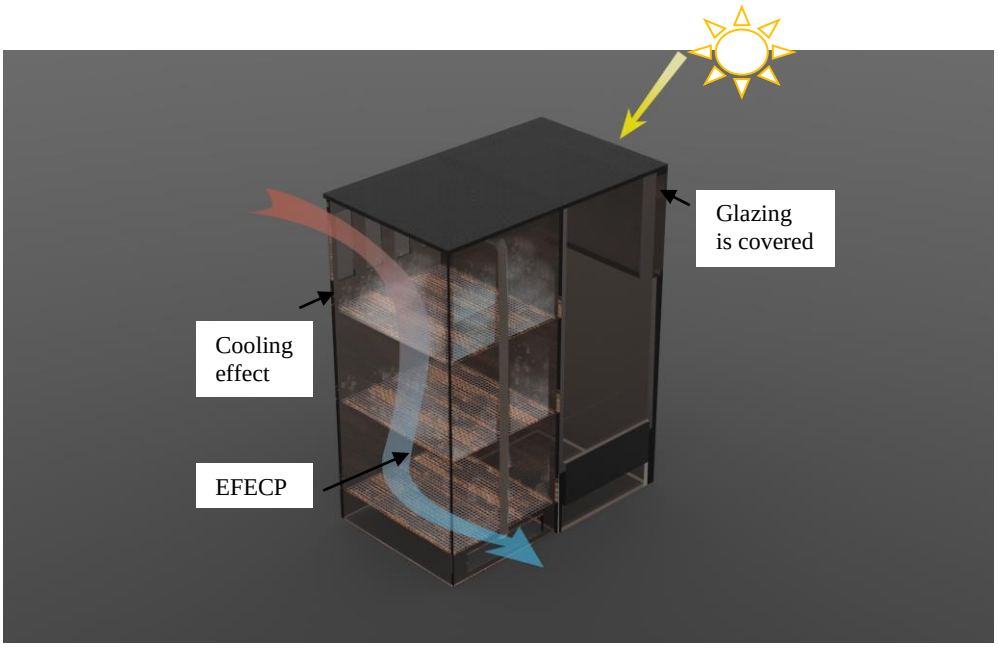


Figure 94. Evaporative cooling system “wind-solar tower”

The integrated evaporative cooling panel into wind-solar tower does not provides building physics requirements such as daylighting, visual relation. Regarding the constructional factors, it is not easy to be integrated into existing building. Due to the height and width of the tower, it is not easy to install panels and thus, to maintain them regularly.

4.8 Wall integrated EFECP

The evaporative cooling system can be integrated into a wall structure in order to meet the demand of lighting, heating and cooling. This type of integration can be named as *combined wall*.

As sun is rising in the south-east/east and setting in the south-west/west in northern hemisphere, the evaporative cooling system can be integrated into wall facing to the sun. Regarding the prevailing wind direction in Cyprus, the strongest wind is coming from west or north-west direction. Thus, the integrated system can be used in facade facing west or north-west to provide both shading, lighting and cooling effect.

One side of combined wall where large openings with shading elements are located, allows the sun comes in from the openings facing south-west providing clear visual sights, penetration of sunlight and daylight. During summer, the shutters can be used to prevent heat gain (Figure 95).

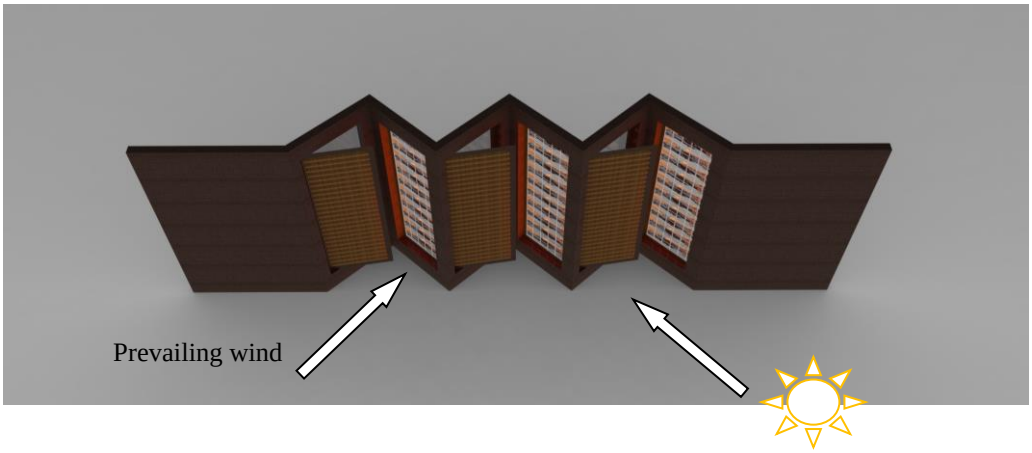


Figure 95. Glazing with shading device facing south-west

The other side of combined wall where evaporative cooling system is integrated, faced to the prevailing wind direction to allow maximum air flow which leads to create more evaporation by the evaporative cooling panel (Figure 96). In this respect, this wall provides cooling, heating, shading and daylighting when required. In Figure 97, the evaporative curtain wall with which is lower-angle evaporative cooling system integrated wall can also be

proposed for cooling process. In this approach, the sun penetration can be prevented by providing curtain wall. The evaporative cooling system integrated into wall perform well in terms of building physics, constructional and functional factors. It should be mentioned that additional space would be necessary in building elements.

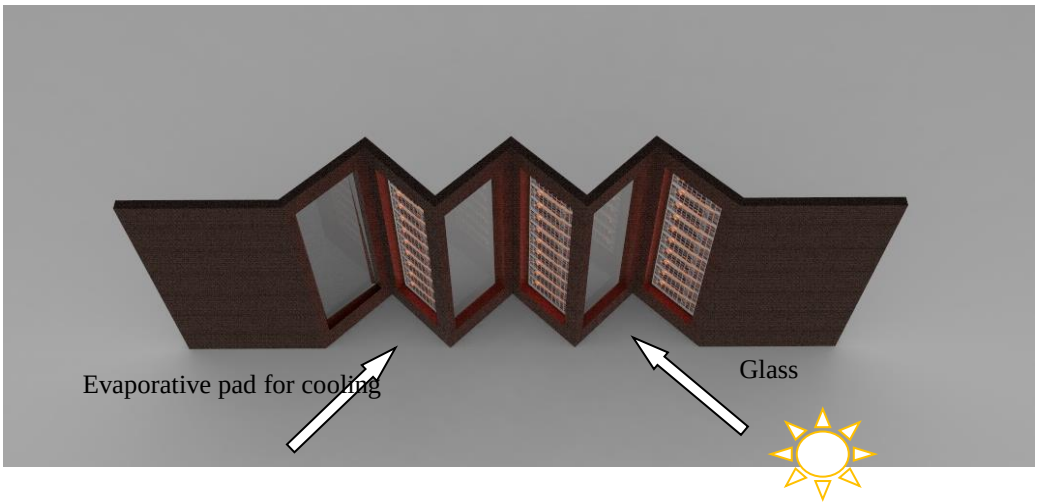


Figure 96. Evaporative cooling system facing north-west

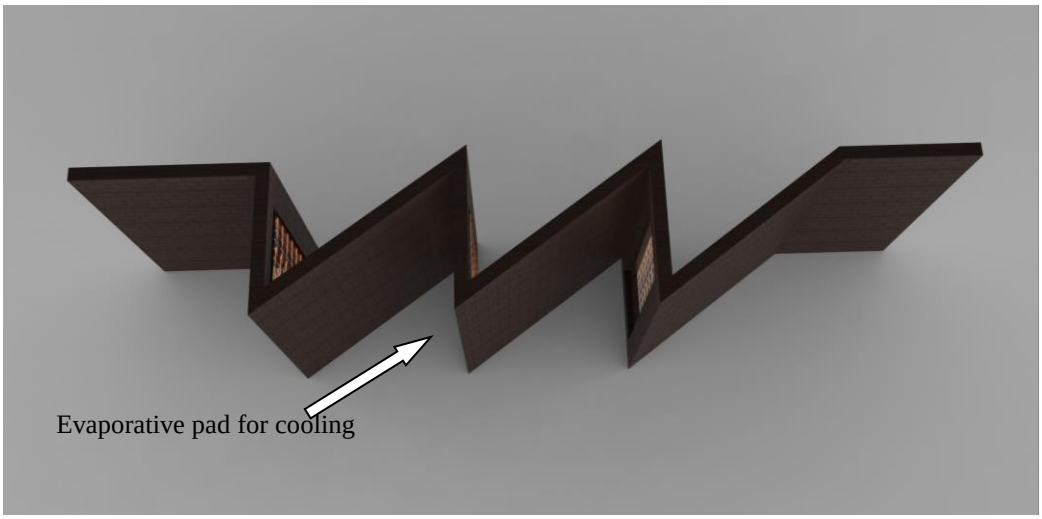


Figure 97. Combined evaporative cooling system and curtain wall

4.8 Conclusion

The conceptual design ideas of integrated eucalyptus fibres based evaporative cooling panel (EFECP) is incorporated into building elements (*e.i.* wall, wind catcher/solar chimney, shutter, etc.) which provides multi-functionality to the building elements. The integration of cooling methods into building elements provide multi-functionality for each architectural design elements.

As seen above, the conceptual design ideas of evaporative cooling system into building elements are described and illustrated by using three-dimensional modelling. The integration of eucalyptus fibres based evaporative cooling panel can be named as multifunctional building elements which makes the traditional building elements such as wall, window, shutter, etc. to have many functions. Due to the flexible functions of the building elements, the various thermal requirements can be provided in order to increase the thermal comfort of the people. Thus, the building element turns into an individual cooling supply.

In architectural design project, the functional, constructive and formal integration of the building elements with cooling system should be considered. Besides of providing cooling effect, the integration of evaporative cooling into building elements provides a shell of the building based on architectural approach. This shell provides protection from environmental conditions and it also separates the indoor living space from outside. In addition to these, the conceptual integration ideas mostly provides daylighting, cooling, air ventilation and shading in the building physics point of view. However, some of the integrated design ideas, in particular shutters are not simple structures since they are moveable and thus, some additional structural systems are required in order to withstand live loads. Generally speaking, these ideas are easy to integrate into the existing building. Moreover, these cannot require extra space since they are articulated into the part of the building elements. The system is a simple construction and includes few components which make the system easy to clean and maintain.

In this chapter, it is presented that these conceptual design ideas of evaporative cooling system into building elements can fit in building design while providing both cooling effect and architectural requirements. This causes to reduce energy consumption by using of vapour compression AC, to enhance the indoor thermal comfort conditions and lastly, to give less harm to the environment as mentioned in Chapter 1.

In the following chapter, the monthly cooling load of an existing residential building located in Northern Cyprus is investigated by using Ecotect Analysis 2011 by predicting the saving of annual energy consumption of the existing building. Afterwards, economic and environmental emissions savings with the use of eucalyptus fibres based evaporative cooling system compared to vapour compression air conditioning have performed.

CHAPTER 5: Application of evaporative cooling for a house in Cyprus

5.1 Introduction

This stage of the study represents the computer simulation by using Ecotect to further investigate the performance of eucalyptus fibres material by predicting the saving of annual energy consumption of the existing building. According to the testing results as stated in chapter 4, a house was modelled in Cyprus to determine the size and the cost of the eucalyptus fibres.

5.2 Building Simulation Programmes

Many building simulation programmes have been created and continued to be used for the last 50 years in the energy area (Crawley et al., 2008). A computer-based simulation has a deterministic role in predicting the energy performance of any building and human thermal comfort. Nowadays, computer simulations based on energy efficiency are useful in analysing building performance. Architects, engineers, students, researchers and others have been using many computer simulation programmes at an early stage and during the design process to observe building energy performance.

In this work, Ecotect was used to calculate the monthly cooling loads of a house in Cyprus. According to the cooling capacity of the proposed material for evaporative cooling (eucalyptus fibres), the coverage ratio of cooling load for modelled house has been calculated.

5.3 Autodesk Ecotect

The Ecotect was first developed by Dr. Andrew Marsh. It provides many performance analysis functions such as solar control, thermal performance, acoustic analyses, lighting simulation and cost evaluation in the conceptual stage of building design (Marsh, 2003).

Autodesk Ecotect™ has a wide variety of options for building design based on weather conditions, heat loss or gain and heating or cooling loads. In the analysis section, some screens which show the energy performance and indoor temperature on the visual graphs are presented. One of the parameters is the "Hourly Temperature Profile" which gives the indoor temperature of spaces in the building. Another parameter is "Hourly Heat Gains/Losses" which shows the main source of heat gains and losses by conduction, internal gains by lighting,etc. of all zones in the building. "Monthly Loads/Discomfort" is another parameter related to total heating and cooling loads of all zones.

Energy consumption of buildings is mostly based on its use for heating, cooling and lighting. This consumption can be minimized by the consideration of building design and climatic condition factors in the pre-design stage. On some occasions, a comfortable indoor environment can be provided by using HVAC system. It is important to size the cooling equipment for indoor thermal comfort conditions. Cooling or heating loads of the building should therefore be calculated, these represent the amount of energy removed from a building to keep optimum indoor environmental conditions (Santamouris, Asimakopoulos, 1996).

5.4 Description of Modelled House in Kyrenia, Cyprus

A house in Cyprus was modelled and discussed based on environmental, geometrical, constructional and thermal conditions.

5.4.1 Climatic Zones of Cyprus

After Sicily and Sardinia, Cyprus is the third largest island located in the Mediterranean Sea. It is on latitude 35°N and longitude 33°E. It has a subtropical, intense Mediterranean climate which is hot and dry in summer (June to September), mild and rainy in winter (November to March). It is formed by two dominant mountains, Troodos and Kyrenia (Five Fingers), the Mesaoria Plain and the narrow coastal areas. These different topographical

characteristics play an important role on the climate of Cyprus and make the island as “multi-climate” region, particularly in the distribution of wind speeds, directions, rainfalls, humidity and solar radiation (Abohorlu, 2010).

Daily greater temperature difference between day and night is due to the very long, excess sunshine and very clear sky creates local effects near the coastal and central plain of the island.

There are two distinctive mountain ranges on Cyprus, which play an important role in the meteorology of the island. The Troodos range, rising to 1,952 m, covers the south and west part, whereas Kyrenia Mountains (at 1,024 m) are in the northern part of the island (Figure 98). Together they prevent moisture from the Mediterranean Sea from reaching the inside of the island. The temperature in the mountains is around 5 ºC and rainfall is 457 mm in winter, but they reach over 40 ºC and 295 mm rainfall in summer (Qi, 2008).



Figure 98. Cyprus

The plain is bordered from the west part of the island to the east in between two distinctive mountains. Although it acts as a bowl in terms of water collection coming from top of the hills, it is poorer in underground water resources. As mountains play an important role in terms of preventing humidity to reach into Mesaoria, the air is drier than the coastal region. The Westerlies,

the prevailing winds over the Mesaoria plain are very strong because of the funnelling-effect (Pashardes, Christofides, 1995).

5.4.2 Climatic Data of Cyprus

The first meteorological measurement was started in 1866 during the Ottoman Period. After 1878, Cyprus was ruled by British Colony and some meteorological stations were installed in Nicosia, Kyrenia, Famagusta, Larnaka, Pafos and Limassol. Totally, 42 climatological stations and 136 precipitation stations were in operation in the Cyprus Department of Meteorology of the Ministry of Agriculture, Natural Resources and Environment in the Republic of Cyprus.

After 1974, Turkish Republic of Northern Cyprus (TRNC) Department of Meteorology was also established. Today, there is two different meteorological centre to measure different location of the island. Therefore, there are some differences in the average measurement.

Cyprus has a very hot summer and mild winter. In summer and winter, the temperatures range from 18 C° in central plain to 14 C° in the coastal area. The temperature differences in between day and night are 8-10 C° in the lowlands in winter, 5-6 C° in the mountain areas and 16 C° in the central plain in summer.

According to the Cyprus Department of Meteorology, temperature is 36C° on the central plain and 27C° on the mountains in summer. In winter, temperature drops to 10C° on the central plain and 3C° on the mountains.

The average temperature of the island was approximately 27.6 C° for July in between 2013-2014 (Figure 99). Before 1998, the temperature in July is below the normal temperature; however, it increased above the normal temperature from 1998 to the present (TRNC Department of Meteorology). NASA and National Oceanic and Atmospheric Administration (NOAA) reported that 2014 is the warmest among all year since 1880. The highest temperature was measured in August of 2010 at Athalassa with a temperature of 45.6 C°. It is

believed that the temperature will increase by 1.0 – 1.5^{0}C by 2030 (Cyprus Department of Meteorology, 2014).

	2014 July (°C)	2013 July (°C)
Maximum Temperature	42.7	39.9
Max. Average Temperature	32.7	33.4
Average Temperature	27.4	27.9
Min. Average Temperature	22.5	22.6
Minimum Temperature	15.7	15.1

Figure 99. Average Annual Temperature for July (adapted from Department of Meteorology, TRNC, 2014)

Although the main direction of wind is coming from west into Cyprus, the temperature differences between land and sea which is named as land and sea breeze effect, anabatic and katabatic winds; the upslope heat driven by the temperature contrast of land and the topography control the wind direction over Cyprus (Pashardes, Christofides, 1995). According to Cyprus Department of Meteorology, the annual wind velocity is 2.8 m/s.

5.4.3 Environmental Conditions of Modelled House

In this study, one of the 2-storey apartment blocks designed by the architect Kazım Doğramacı, is chosen for the simulation study. The apartment block consists of four flats per floor. One of the flat is chosen for modelling. It is located in Kyrenia, Cyprus at latitude 35° N and longitude 33° E and was built in 2016. It also lies at 37 m above sea level. As seen from the aerial view in Figure 100, there is a road in front of the building, and nearby, there is a large park area which shows that there will be no obstructions from neighbouring dwellings.



Figure 100. Aerial view of Modelled House in Kyrenia (Source: Google Earth)

The climatic conditions of Kyrenia are expressed by the minimum and maximum air temperatures and relative humidity charts shown in Figure 101. This weather data for Kyrenia was obtained from the Energy Plus in .epw format and converted to .wea format for Ecotect.

The first graph as seen in Figure 101, represents monthly diurnal averages of temperature with diffuse and direct solar. The red grading represents the air temperature and the yellow continuous line represents direct solar radiation. It is obvious that the hottest months are June, July and August with maximum air temperatures of 41 to 46 °C. As seen in the second graph in Figure 101, the relative humidity in summer is lower than in the winter. The prevailing wind is mostly from East and West, at 9 am and 3 pm respectively, as shown in the third graph.

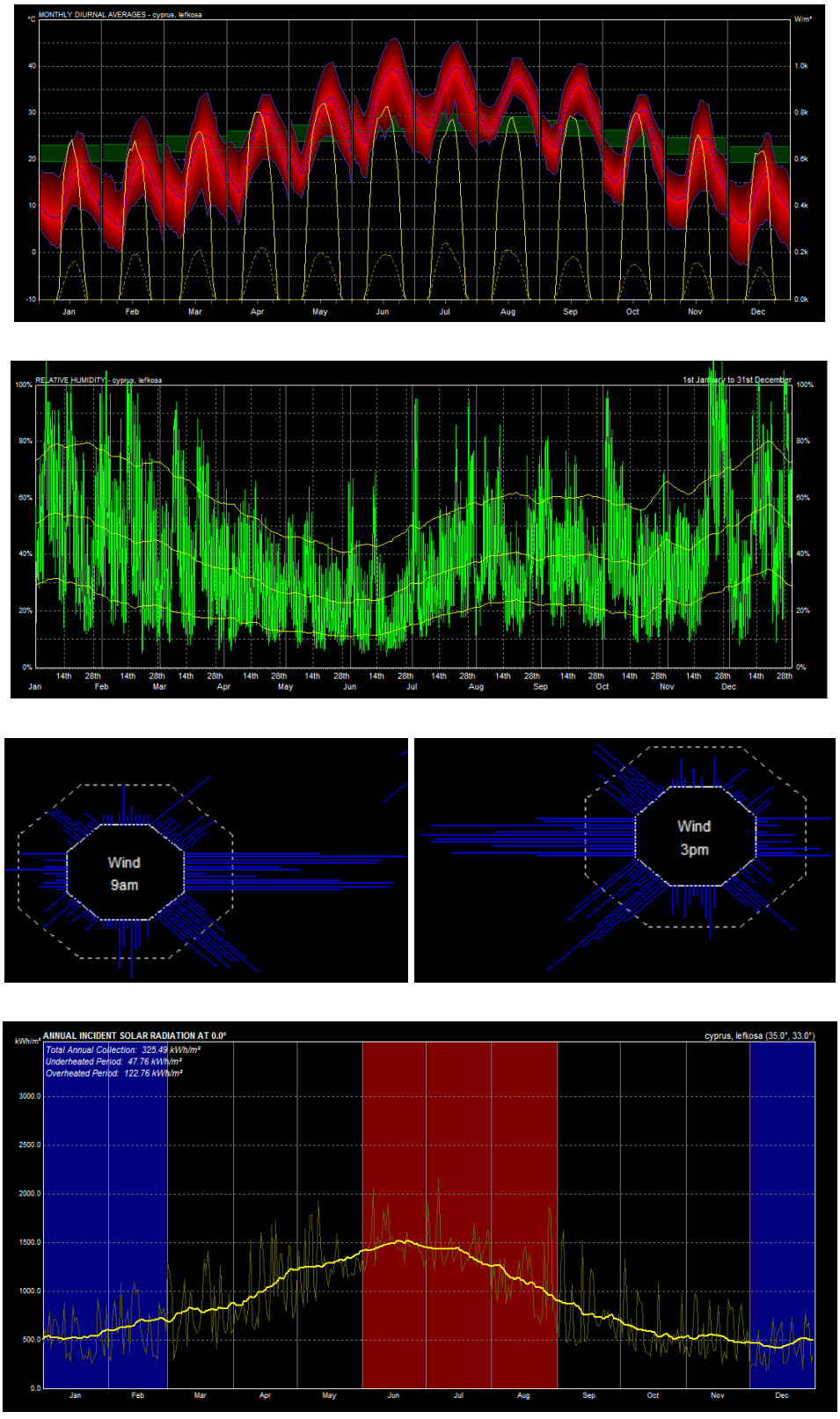


Figure 101. Monthly average temperature, relative humidity, wind analysis and incident solar radiation for Cyprus (Kyrenia) generated from Ecotect

5.4.4 Geometrical Model of House

The building is a double-storey apartment block which includes four separate flats in each floor, with 8 flats in total as seen in Figure 102.



Figure 102. General view of apartment block

The building is a rectangular shape with a flat roof. Each floor contains a bedroom, a toilet and an open plan kitchen which is a continuation of the living room with 21.45 m^2 floor area. Each floor height is 3.0 metres and the total height of the apartment block is 7.5 metres. Each flat has a volume of 107.48 m^3. The modelled flat in the block faces the south which means it is exposed to more sunlight during the day than the flats facing north (Figure 103).

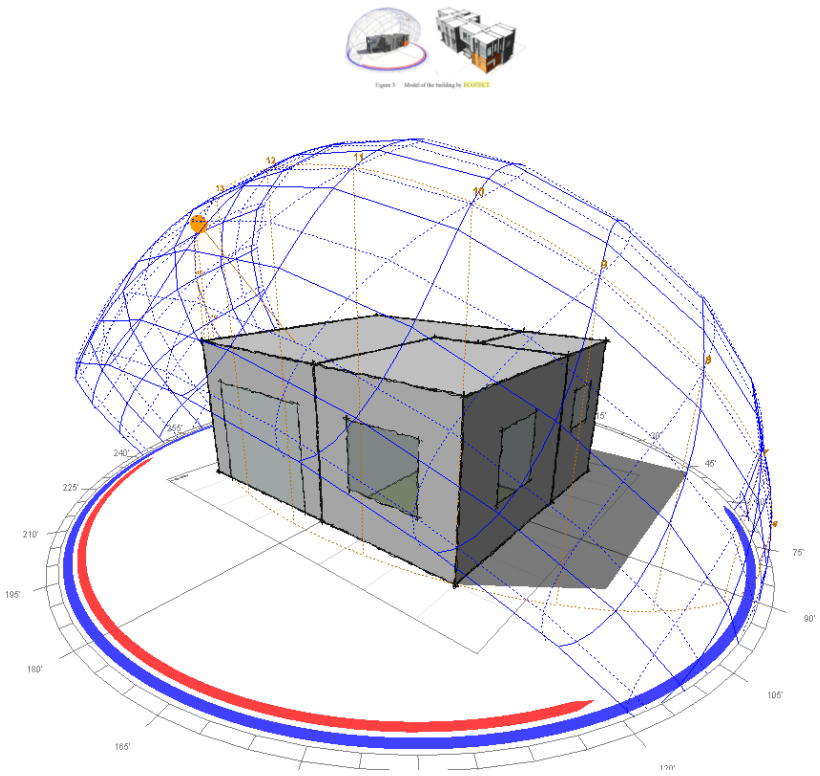
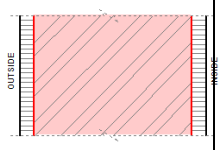
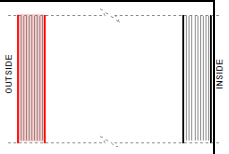
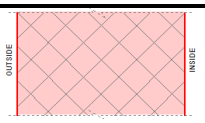
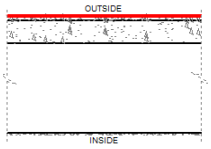
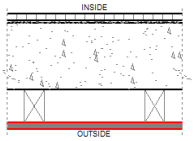


Figure 103. Sun path diagram of the case area with Ecotect v 5.50

5.4.5 Building Components and Constructional Conditions

The modelled building is reinforced concrete building with a 190 mm brick wall with 10mm plaster either side. The ceiling is a suspended concrete structure. The windows are double glazed with a PVC frame. The components of the modelled house are shown in Table 19 with thermal properties and schematic views.

Table 19. Implemented Settings for Modelled House

Building Element	Material	Thickness (mm)	λ-value (W/mK)	U-value (W/m 2K)	Admittance (W/m2 K)	Schematic Section
Wall	Plaster Building (Molded Dry)	10	0.43	2.620	4.380	
	Brick Masonry Medium	110	0.71			
	Plaster Building (Molded Dry)	10	0.43			
Window	Glass Standard	6	1.05	2.410	2.380	
	Air Gap	30	5.56			
	Glass Standard	6	1.05			
Door	Wood Pine	40	0.34	2.31	3.54	
Ceiling	Ceramic Tiles	12	2.09	2.56	4.20	
	Screed	25	0.21			
	Concrete Floors	150	0.75			
	Air Gap	600	5.56			
	Gypsum	12	1.297			
Floor	Plaster Board	10	0.431	2.90	5.21	
	Air Gap	50	5.56			
	Concrete	100	0.7530			
	Concrete Screed	5	0.753			
	Ceramic Tiles	10	0.309			

5.4.6 Thermal Conditions

The thermal performance of any building is dependent on the personal and environmental factors (Taleghani et al., 2013). Therefore, it is important to identify the conditions of the building. Personal factors are related to the profile of the occupants. The behaviour of the users and their relation to the building define the performance of the heating or cooling load which are directly affected by internal heat sources. The function of the building, the user profile, passive and active systems used for cooling, heating or lighting and the relation of building with the user are some criteria which should be discussed during the simulation stage (Hoes et al., 2009).

Two people aged over 40 are living in this modelled house which is used 24 hours a day during the weekdays and at the weekends.

The cooling period begins in June and lasts till September since in the winter period the average temperature is lower than 18°C. Thus, air conditioning systems are working from June to September in the living room. They are set to cooling mode and their operational hours are mostly during the day and in the evening. Thus, it operates from approximately 10am to 10pm on weekdays and at the weekends.

Due to the activity of the occupants, the heat production in the building is set as sedentary – 70W. The sensible heat is set at 5W/m² and the latent heat is at 2W/m². The values for the exchange of air between the inside and outside were set at 0.50/hr and wind sensitivity was 0.25/hr.

According to the ASHRAE Standard 55-2013, Thermal Environmental Conditions for Human Occupancy, the indoor air temperature should be set up in the range of 19-27°C for thermal comfort purposes. In addition to this, relative humidity should be set below 65% according to the ASHRAE Standard 62.1-2013, "Ventilation for Acceptable Indoor Air Quality".

5.4.7 Zoning of Modelled Building

Zoning in Ecotect is used to evaluate the thermal simulations and heating and/or cooling loads of a modelled project. Each zone is different in the building as the operation hours for each space are different. In addition, the optimum temperature for different activities, in particular sleeping or sitting, is different (Bradshaw, 2006). According to the ASHRAE Standard 55, Thermal Environmental Conditions for Human Occupancy, the temperature range for winter can be described as 20 to 23.5 °C and 22 to 26 °C for summer. ASHRAE Standard 62-2001, Ventilation for Acceptable Indoor Air Quality recommends relative humidity level in should be between 30-60%.

In this simulation, the thermal zones are categorized in terms of spaces, thermal requirements and hours of operation for cooling (Table 20).

Table 20. Implemented Zoning for Modelled House

Zone No	Space	Temp. for Winter & Summer (°C)	Humidity (%)	Hours of operation
Zone 1	Bedroom 1	20-26	30-60	On: 22
Zone 2	Living R. Kitchen	18-27	30-60	On:22

As seen in floor plan layout in Figure 104, the modelled house consists of a living room, kitchen, bedroom and bathroom. One side of the living room wall is shared with the neighbouring flat. The other side of the living room and bedroom are south-facing. The rest of the façade is east-facing.

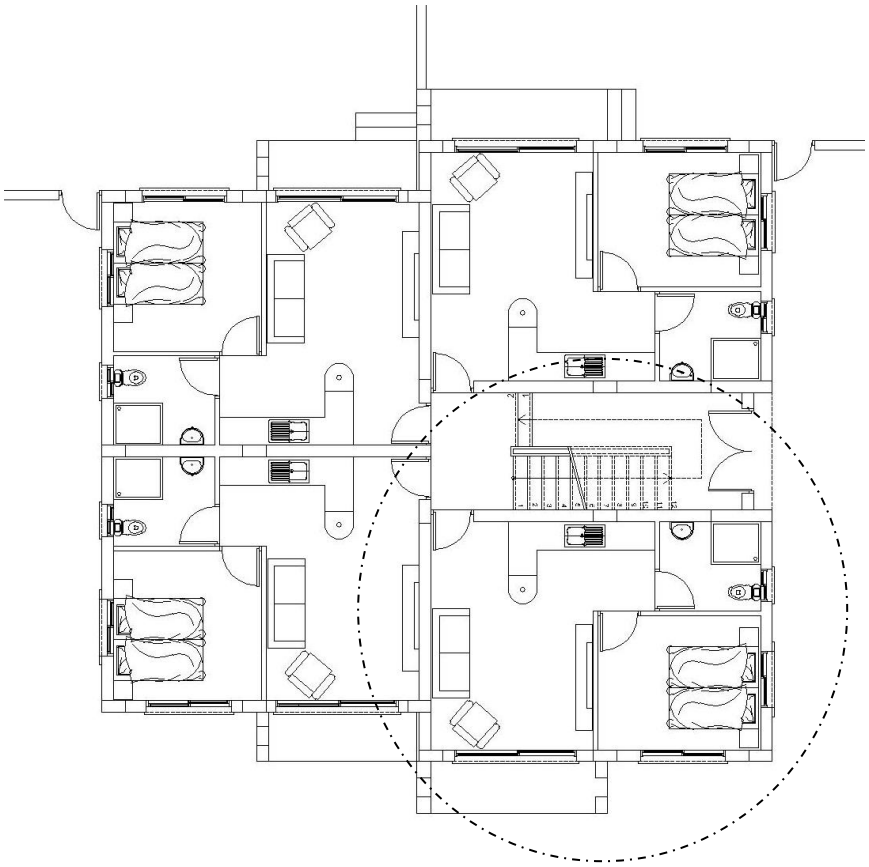


Figure 104. Floor plan layout of modelled house

5.5 Analyses of Modelled House in Nicosia, Cyprus

In this part of the study, the results of energy simulation and environmental information, which are carried out by the computer-based simulation programme, Ecotect, are analysed for the hottest day of the year in Cyprus (1st of August). This day is indicated by Ecotect due to the fact that it had the highest solar radiation in Cyprus. Environmental information related to hourly temperatures is separately analysed for all thermal zones, which are the living room and kitchen and bedroom.

5.5.1 Hourly Temperatures for all Visible Thermal Zones

Hourly temperature graphs show the temperature in °C in the Y-axis and the time from 0 to 23 hours in the X-axis. The solar radiation in W/m² is also shown on the vertical axis on the right-hand side. The different line types and colours represent the weather data of Cyprus and the indoor temperatures of different zones. The coloured lines show each zone's indoor temperature for the hottest day of the year. The climatic factors are shown with different coloured dashed lines. The blue dashed line is related to the outside temperature. The wind speed and solar radiation are also shown as different coloured of dashed lines.

The graph in Figure 105 shows the hourly temperatures which represents the outdoor and indoor temperature of the thermal zones for the hottest day of the year when the air-conditioning unit is turned on and off. In this way, the indoor temperatures of the zones which are already cooled by AC at 10am to 10 pm can be indicated for the hottest period of the day. The hourly temperature graphs clearly show that the highest outdoor temperature is from 10am to 10pm. Therefore, the operation hour for the AC is set in that period to provide a comfortable indoor environment.

As clearly seen from Figure 105, the outdoor temperature starts to increase gradually at 7am and reaches peak point at around 2-4pm. This is due to the higher level of solar radiation shown on the vertical axis on the right-hand side of the graph. After 4pm, the temperature starts to drop until 11pm as the solar radiation reduces.

The indoor temperature suddenly falls to about 24°C when the AC is turned on at 10am. This indoor temperature is kept constant until 10pm. As seen in the graph, the maximum outdoor temperature for 1st of August is 46°C, whereas the indoor temperature of the building is around 24°C, which is quite low compared to the outdoor temperature.

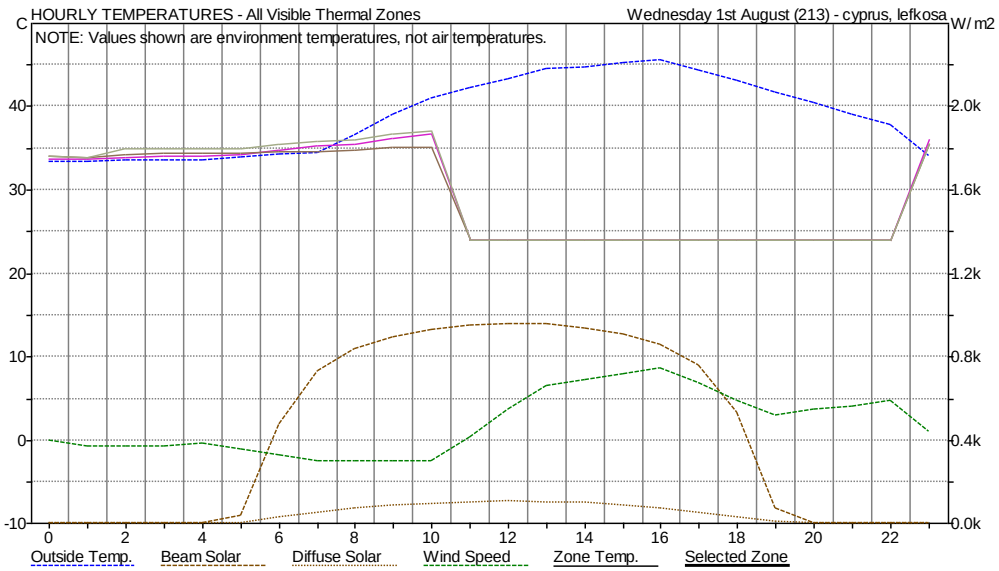


Figure 105. Hourly Temperature for all Thermal Zones

The thermal comfort level by colour gradient band (red, blue and white) can be indicated by using the highlighted zone sections. The specific zone can also be highlighted in each graph by a bold line. The white band represents the thermal comfort level which is the ideal gradient for human comfort. The indoor temperature of the zones should fall into the white band to provide a thermally comfortable environment. As shown in Figure 106, the indoor temperature of the selected zone which represents the bedroom, is within the upper comfort level of around 24°C. During the operation hours of the AC, the comfort level is stabilized from 10am to 10pm. When the three zones are compared in terms of indoor temperatures, it can clearly be seen from graphs (a) and (b) that the indoor temperatures of zones 1 (bedroom) are higher when compared to zone 2 (the living room and kitchen). This is due to the fact that zones 1 has east-facing windows which are exposed to more solar radiation in the morning. The living room and kitchen have south-facing windows which are exposed to less solar radiation since the angle of sun is higher in the summer compared to the winter.

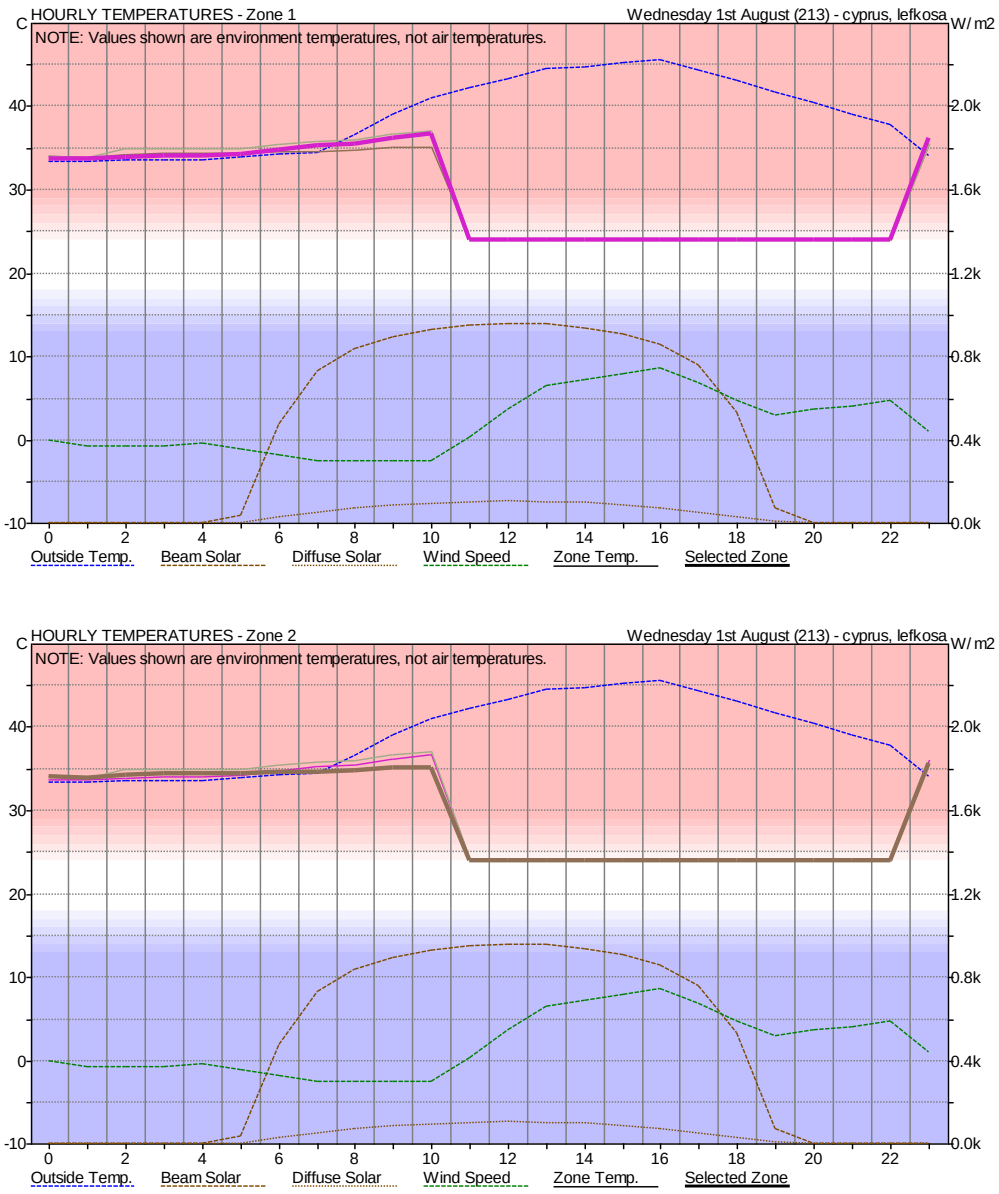


Figure 106. (a) Hourly Temperature for Zone 1 (Bedroom) and (b) 2 (Living Room and Kitchen)

5.5.2 Hourly Gains and Losses for all Visible Thermal Zones

The hourly heat gains and losses graph shows the indoor air temperature changes according to the heat transfer through the building fabric. The graph indicates the time in the X-axis and energy in Watts in the Y-axis. Some parameters, such as HVAC load, conduction, SolAir, etc. are represented in this graph.

As can be seen in the hourly temperature profile graphs, the curve of the outdoor temperature almost correlates with the curve of HVAC (Figure 107). The outdoor temperature starts to increase around 7am and peaks at around 46°C at around 5pm and falls again to 35°C at 11pm. During this time period, the load of HVAC also shows the same trend, with the outdoor temperature indicating that indoor cooling is required. The loads of HVAC system in August reach a peak by around 7650W. It is also obvious that the heat gains by conduction around 4500W through the envelope of the building are also increased as the outdoor temperature and solar radiation increase. There is no any significant change in heat gains by ventilation and internal gains.

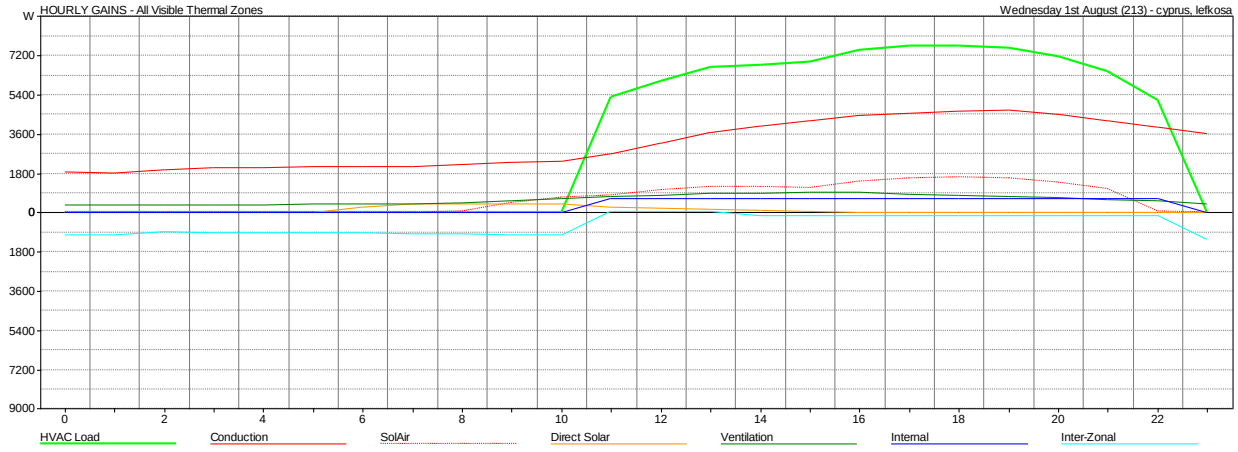


Figure 107. Hourly gains and losses for the hottest month

5.5.3 Gains Breakdown for all Visible Thermal Zones

The gains breakdown graph shows the heat transfer mechanisms in Wh/m². The heat gains are shown above the X-axis and heat losses are below this axis. On the right-hand side, the heat gains and losses are represented by percentage values. As can be seen in Figure 108, the main part of heat gains during the summer is responsible for conduction at 37.6% through the fabric (Table 21). It is then followed by SolAir and internal contributors by 24.4% and 16.1%, respectively. It is evident that heat gains and losses mostly occur by conduction.

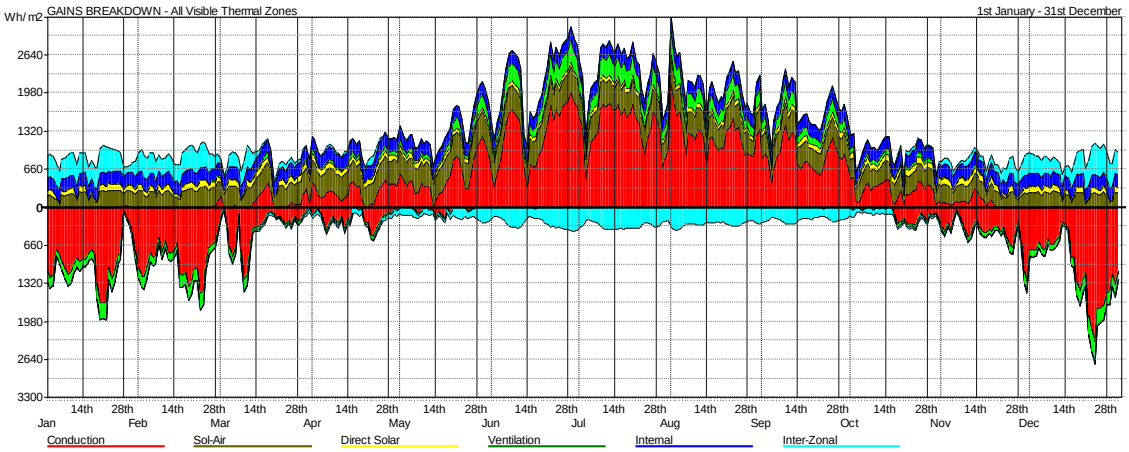


Figure 108. Gains breakdown for all thermal zones

Table 21. Gains breakdown for period 1st January to 31st December

CATEGORY	LOSSES	GAINS
FABRIC	65.7%	37.6%
SOL-AIR	0.0%	24.4%
SOLAR	0.0%	6.5%
VENTILATION	11.4%	7.0%
INTERNAL	0.0%	16.1%
INTER-ZONAL	22.9%	8.4%

5.5.4 Monthly Heating and Cooling Loads

These loads are mostly defined as the amount of heat energy which needs to be added or removed from a building in order to keep the indoor temperature at thermostat settings (18-24°C). The graph of monthly heating and cooling loads

represents the discomfort level for the zones and the amount of energy needed to heat and cool the building. It displays the months of the year in the X-axis and the loads in W (watt) in the Y-axis. The red bar which projects above the X-axes and blue bar which projects below the X-axes indicates heating and cooling load, respectively.

The annual cooling and heating load of the modelled house is calculated when the AC is on. According to this, the annual cooling loads of a AC system for bedroom (zone 1), living room + kitchen (zone 2) are 4323kWh and 4790kWh, respectively (Table 22).

Table 22. Annual cooling load of each zone

Spaces (Zone No)	**Floor Area (m²)**	**Annual Cooling Loads (Wh)**
Bedroom (Zone 1)	10.50	4323744
Living R. + Kitchen (Zone 2)	21.45	4790888

As seen in Figure 109, the monthly cooling load for each zone is calculated to indicate how much energy is required for each space. The amount of energy needed for cooling is dependent on the surface area of the spaces. As the living room and kitchen have larger surface areas, a higher cooling load is needed to provide a comfortable indoor environment.

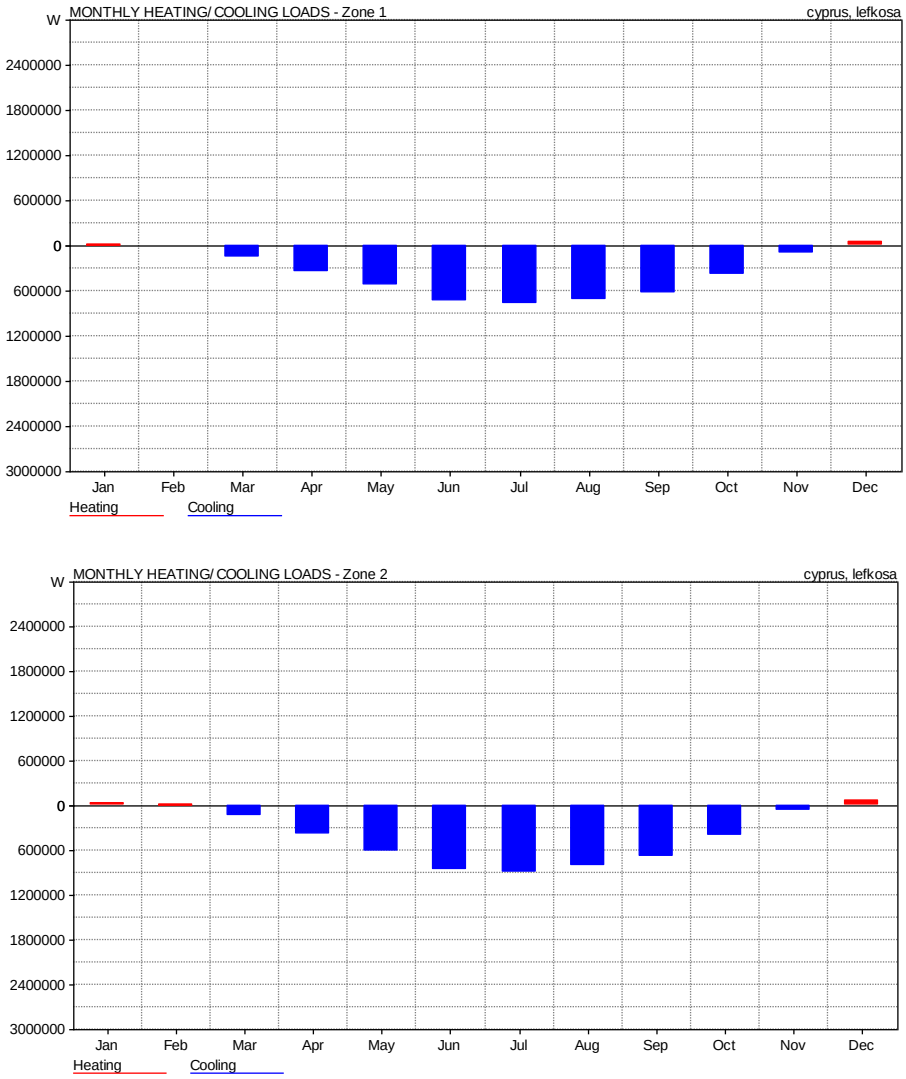


Figure 109. Monthly cooling and heating loads for Zone 1 and 2

In Figure 110, the monthly cooling and heating loads are calculated for all the thermal zones. Each bar represents the amount of energy required each month for heating or cooling the building. The different colours represent the spaces in the building. It is clearly evident that the brown which represents the living room and kitchen consumed more energy than the other spaces. In addition to this, a significant amount of cooling load is required to keep a thermally comfortable indoor environment compared to the heating loads.

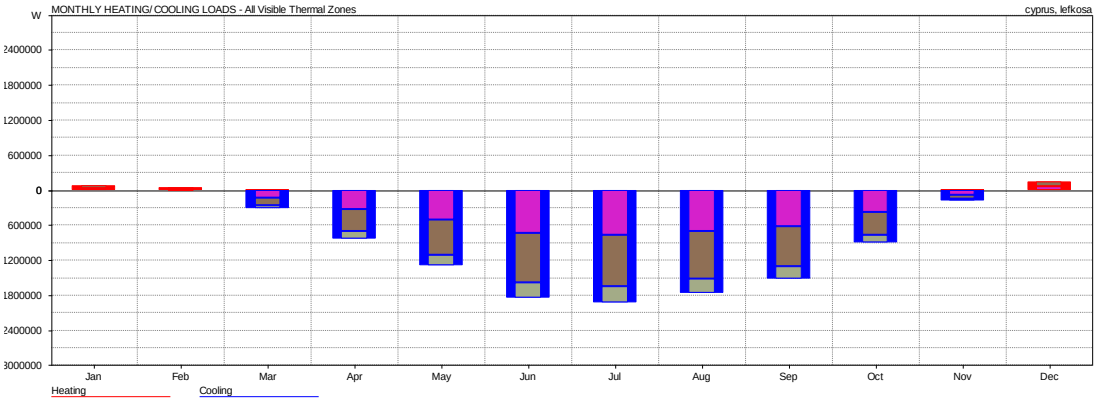


Figure 110. Monthly cooling and heating loads of AC system for all thermal zones

According to the result of the simulation, the need for cooling is lasts from March to November and in total 10626kWh and heating loads are 280kWh. The need for cooling for the hottest month of the year (July) is approximately 1932kWh. This is then followed by 1850kWh in June and 1770kWh in August (Table 23).

Table 23. Monthly cooling loads of modelled house

	COOLING	HEATING
MONTH	(Wh)	(Wh)
Jan	0	74813
Feb	0	40470
Mar	324078	10697
Apr	838976	0
May	1301103	0
Jun	1850533	0
Jul	1932867	0
Aug	1770219	0
Sep	1519546	0
Oct	908115	0
Nov	181417	8332
Dec	0	146188
TOTAL	10626854	280500

} 5553.62kWh

5.5.5 Simulation Results

As mentioned above, the first requirement is to provide cooling due to the climatic properties of Cyprus. In Table 24, the variation of cooling months can be seen. The monthly cooling capacity of the proposed system through eucalyptus fibres, the total cooling capacity of 1 m^2 eucalyptus fibres evaporative pad and the percentage of the coverage ratio of the cooling load are presented. It should be noted that the cooling need is extended into late autumn and mid spring. In the first three months, the cooling load is gradually increased and reaches a peak in July at 1932kWh. It is then gradually reduced to 908.1kWh by October.

According to the test results, the cooling capacity of the system condition was found to be around 0.4kW for 0.07 m^2 surface area of eucalyptus fibres. 5.7kW was then calculated for 1 m^2 surface area of eucalyptus fibres. The surface area is indicated as 1 m^2 to give a general indication of the system performance. As a result, the monthly cooling capacity of the system operation for eucalyptus fibres was found to be 1710 kWh per m^2 (5.7kW x 30 days x 10 hours).

When this system is operated to meet the cooling loads in the summer, it is found that the system mostly covers the cooling load for each month. This system covers the peak load in July as 88% of cooling load. The next highest is the coverage of the cooling load as 92% and 96% in June and August, respectively as seen in Table 24.

Table 24. Monthly cooling loads of AC system for all thermal zones with cooling capacity of system operation

Months	Monthly Cooling Load (kWh)	Total cooling capacity of 1 m^2 eucalyptus fibres evaporative pad (kWh)	Percentage cooling covered
April	838.976	1710	100%
May	1301.103	1710	100%
June	1850.533	1710	92%
July	1932.867	1710	88%
August	1770.219	1710	96%
September	1519.546	1710	100%
October	908.115	1710	100%

Based on the cooling load of 5.7kW of 1 m^2 eucalyptus fibres, the mass flow rate was calculated as 0.58kg/s when the outdoor temperature was reduced from 36°C to 26°C. Thus, the air velocity through 1 m^2 eucalyptus fibres panel was found as 0.48m/s.

5.5.6 Economic and Environmental Analyses

In this part of the study, the level and amount of environmental and economic performances were studied for the proposed evaporative cooling system. It is required to identify if this proposed system is environmentally friendly, economically profitable and commercially viable.

Economic Analyses

An evaporative cooling method using local material of eucalyptus fibres was used to reduce the energy consumption and environmental impact of the proposed cooling system. Thus, the economic and environmental analyses of the system were carried out in order to evaluate the potential of this evaporative cooling method. In the first part, the economic feasibility of the system was investigated through the use of the Present Worth method. In the analyses, the discount rate and the inflation rate were used to calculate the rate of interest. Later, the present worth factor was calculated to find the present value of the cost. Thereby, potential and cost savings through the replacement of EC with AC was investigated over a certain period. In the analyses, the total cost of the proposed evaporative cooling system including capital cost, operational cost and maintenance cost was considered in order to calculate the payback period (Aydın et al., 2015).

The reason for studying these economic analyses is to determine the feasibility of the proposed system for a specific project (Moaveni, 2010). It is aims to identify the advantages of the cooling system in terms of its economic approach.

Based on the testing results, the cooling capacity of 1m² eucalyptus fibres is 5.7kW and the monthly cooling capacity of the system operation for eucalyptus fibres was found to be 1710 kWh. The cooling loads of the considered building were found to be between 1301-1519Wh, in May and September, respectively. In order to evaluate the adequate number of panels required to meet the cooling load, the system sizing should be considered. Therefore, for system sizing 1m², eucalyptus fibres panels can be used to cover the monthly cooling load. The

operational parameters of the system were determined based on the obtained experimental results (Table 25).

Table 25. Optimum design conditions for using 1 m² eucalyptus fibres

Design condition for 1 m² proposed evaporative cooling system by eucalyptus fibres:
$\dot{m}$: 0.07 kg/s
SCC : 0.44 - 0.48
COP : 3.65
Cooling Capacity : 5.7 kW
ϑ : 0.75 m/s
Evaporation rate: 0.27 g/s

The total cost of the system was approximately calculated as €500 as seen in Table 26. These prices are taken from retail shops in Cyprus.

Table 26. The cost of system components

Cooling System Components	Price (€)	Reference
Fan	81	Argos.co.uk (http://www.argos.co.uk/product/4250454)
Pump	34	Amazon.com
Ducting and Fittings	85	Amazon.com
Installation costs	300	
Capital Total	500	

The present value of the cost for a specific year should be calculated in order to analyse the total savings of the system considered. Thus, the rate of interest should be calculated by using the following Equation 8 which is important to make calculations according to the inflation rate:

$$r = \frac{(i+g)}{(1-g)} \tag{8}$$

Where i is the inflation rate (14.5%) and the discount rate is represented by g (11.4%). Thus, r is found as 2.7% (Aydın et al., 2015). The present worth factor is calculated by using the following Equation 9 in order to find the present value of the money for specific year:

$$PWF = \frac{1}{(1+r)^N} \tag{9}$$

The potential saving with using EC instead of AC over 25 years is calculated by the following Equation 10 and 11:

$$\gamma_{AC} = \sum_{N=0}^{N=25} \xi_{AC} \times \frac{fe}{2.5} \times PWF \quad (10)$$

$$\gamma_{EFECP} = \sum_{N=0}^{N=25} \xi_{EFECP} \times \frac{fe}{3.65} \times PWF \quad (11)$$

Where γ is the total operational cost and ξ is the total yearly energy consumption. f_e is the unit of electricity in Cyprus which is €0.10/kWh for domestic usage. The COP for AC and EC is 2.5 and 3.65, respectively.

The total cost of the Eucalyptus Fibre Based Evaporative Cooling Panel (EFECP), γ_{EFECP}, for 25 years is calculated by using Equation 11 where C, O, M represent the capital cost, operational cost and maintenance cost, respectively.

$$\gamma_{EFECP} = \gamma_C + \sum_{N=0}^{N=25} (\gamma_O + \gamma_M) \times PWF \quad (10)$$

The payback period represents the length of time needed to recover the initial investment and the unit is the number of years (Eiffert, 2003). It is the ratio of initial cost to annual savings which is shown in Figure 111.

The results of the economic analysis of using AC and EC based on the cumulative sum of these systems are shown in Figure 111. The cumulative sum of AC represents the sum of operational and maintenance costs. The cumulative sum of EC represents the sum of capital, operational and maintenance costs of the system.

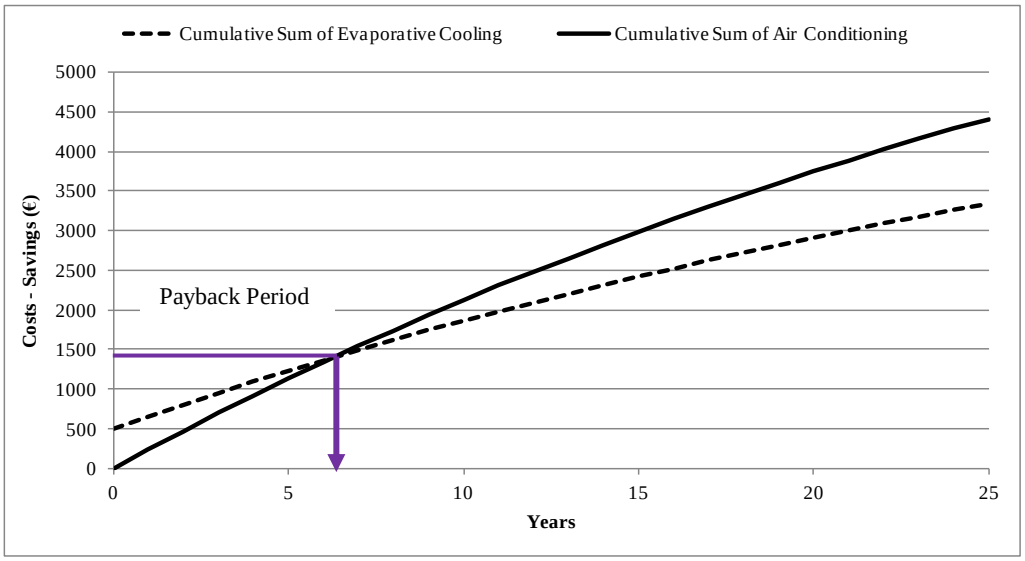


Figure 111. Payback period of the integrated eucalyptus fibre based evaporative cooling panel (EFECP)

The graph clearly shows that payback period would be 6.5 years. It is obvious that the time required for the system to pay back for itself is less than 7 years.

At first 6.5 years, the cumulative sum of EC exceeds the cumulative sum of AC since the capital cost (€500) is also added for EC in order to find the cumulative sum. After that time periods, the sum of AC starts to exceed the sum of EC. It was found that the integrated eucalyptus fibre based evaporative cooling panel (EFECP) could provide a saving of average €625 at the year of 16 (Table 27 and 28).

Table 27. The results of economic analysis of AC

ECONOMIC ANALYSIS OF AC				
Years	Total Operational Cost (€)	Maintenance Cost	Total (O + M)	Cumulative Sum of Air Conditioning
0	227.1198053	11.35599026	238.4757955	238.4757955
1	205.4893476	10.27446738	215.763815	238.4757955
2	200.0869987	10.00434993	210.0913486	470.6820229
3	194.8266783	9.741333917	204.5680123	696.7835101
4	189.7046527	9.485232636	199.1898853	916.9407518
5	184.717286	9.2358643	193.9531503	1131.310023
6	179.861038	8.993051898	188.8540899	1340.043491
7	175.1324615	8.756623075	183.8890846	1543.289321
8	170.5282001	8.526410005	179.0546101	1741.191785
9	166.0449855	8.302249275	174.3472348	1933.89136
10	161.6796353	8.083981767	169.7636171	2121.524832
11	157.429051	7.871452548	165.3005035	2304.225388
12	153.2902152	7.664510758	160.9547259	2482.122717
13	149.26019	7.463009501	156.7231995	2655.343095
14	145.3361149	7.266805746	152.6029207	2824.009481
15	141.5152044	7.07576022	148.5909646	2988.2416
16	137.7947463	6.889737313	144.6844836	3148.156029
17	134.1720996	6.708604978	140.8807045	3303.866282
18	130.6446929	6.532234643	137.1769275	3455.482886
19	127.2100223	6.360501113	133.5705234	3603.113464
20	123.8656497	6.193282486	130.0589322	3746.862811
21	120.6092013	6.030460064	126.6396613	3886.832963
22	117.4383654	5.871918271	123.3102837	4023.123276
23	114.3508913	5.717544567	120.0684359	4155.830495
24	111.3445875	5.567229374	116.9118169	4285.048819
25	108.4173198	5.420865992	113.8381858	4410.869971

Table 28. The results of economic analysis of EC

ECONOMIC ANALYSIS OF EC						
Years	Capital Cost	Total Operational Cost (€)	Maintenance Cost	Total (O + M)	Cumulative (O + M)	Cumulative Sum of Air Conditioning
0	500					500
1		146.0055891	7.300279455	153.3058685	153.3058685	653.3058685
2		142.167078	7.108353899	149.2754319	302.5813004	802.5813004
3		138.429482	6.921474099	145.3509561	447.9322565	947.9322565
4		134.790148	6.739507399	141.5296554	589.4619119	1089.461912
5		131.2464927	6.562324634	137.8088173	727.2707292	1227.270729
6		127.7960007	6.389800033	134.1858007	861.4565299	1361.45653
7		124.4362226	6.221811132	130.6580338	992.1145637	1492.114564
8		121.1647738	6.058238688	127.2230124	1119.337576	1619.337576
9		117.9793318	5.89896659	123.8782984	1243.215875	1743.215875
10		114.8776356	5.743881782	120.6215174	1363.837392	1863.837392
11		111.8574836	5.592874179	117.4503578	1481.28775	1981.28775
12		108.9167318	5.445836591	114.3625684	1595.650318	2095.650318
13		106.0532929	5.302664646	111.3559576	1707.006276	2207.006276
14		103.2651343	5.163256714	108.428391	1815.434667	2315.434667
15		100.5502768	5.027513841	105.5777907	1921.012457	2421.012457
16		97.90679339	4.89533967	102.8021331	2023.81459	2523.81459
17		95.33280759	4.766640379	100.099448	2123.914038	2623.914038
18		92.82649229	4.641324615	97.46781691	2221.381855	2721.381855
19		90.38606845	4.519303422	94.90537187	2316.287227	2816.287227
20		88.00980374	4.400490187	92.41029393	2408.697521	2908.697521
21		85.69601144	4.284800572	89.98081201	2498.678333	2998.678333
22		83.44304911	4.172152455	87.61520157	2586.293535	3086.293535
23		81.24931754	4.062465877	85.31178341	2671.605318	3171.605318
24		79.11325953	3.955662976	83.06892251	2754.674241	3254.674241
25		77.03335884	3.851667942	80.88502678	2835.559267	3335.559267

Over the full 25 years, the cumulative sum of evaporative cooling and air conditioning would be €3335 and €4410, respectively. Thus, the annual energy saving is found as €1075.

Environmental Analyses

Since ozone depletion and global warming have negatively affected by greenhouse gases (GHGs) and CO_2 emissions, the savings of these have gained significant attention for environment.

Previous section had studied the total energy savings of proposed eucalyptus fibre based evaporative cooling panel (EFECP) over air conditioning system, through the 25 years of period. By using the following equations, the carbon dioxide emissions (SCO_2) of air conditioning and EFECP can be found by Eq.11 and Eq.12, respectively.

$$Sco_{2,AC} = \sum_{N=0}^{N=25} \xi_{AC} \times \varsigma_e \quad (11)$$

$$Sco_{2,EFECP} = \sum_{N=0}^{N=25} \xi_{EFECP} \times \varsigma_e \quad (12)$$

Where ςe is the conversion factor of electricity per kWh consumption, which is 0.87 in Cyprus. ξ is the total yearly energy consumption, which is 5553.62 kWh. It represents the cooling loads of a modelled house for June, July and August. Total yearly consumption value was divided by COP of AC and EFECP, respectively as done for economic analysis.

In accordance to these calculations, the CO_2 emissions with the usage of eucalyptus fibres integrated evaporative cooling system is found 430.2 ton CO_2 and 628.1 ton CO_2 for AC at first year. Therefore, the yearly CO_2 savings of the investigated building with the usage of eucalyptus fibre based evaporative cooling panel (EFECP) is estimated as 197.9 tons of CO_2 per year (Table 29).

The CO_2 emissions for eucalyptus fibres integrated evaporative cooling system and AC are 10755 and 15702.5 ton CO_2 for 25 years which is assumed that the lifetime of both systems can be 25 years. The total saving is calculated as 4.9 ton CO_2 (Figure 112).

Table 29. The results of CO_2 Emissions of EFECP and AC

CO_2 Emissions of EFECP and AC		
Years	EFECP (tons CO2 / year)	AC (tons CO2 / year)
0	0	0
1	430,2	628,1
2	860,4	1256,2
3	1290,6	1884,3
4	1720,8	2512,4
5	2151	3140,5
6	2581,2	3768,6
7	3011,4	4396,7
8	3441,6	5024,8
9	3871,8	5652,9
10	4302	6281
11	4732,2	6909,1
12	5162,4	7537,2
13	5592,6	8165,3
14	6022,8	8793,4
15	6453	9421,5
16	6883,2	10049,6
17	7313,4	10677,7
18	7743,6	11305,8
19	8173,8	11933,9
20	8604	12562
21	9034,2	13190,1
22	9464,4	13818,2
23	9894,6	14446,3
24	10324,8	15074,4
25	10755	15702,5

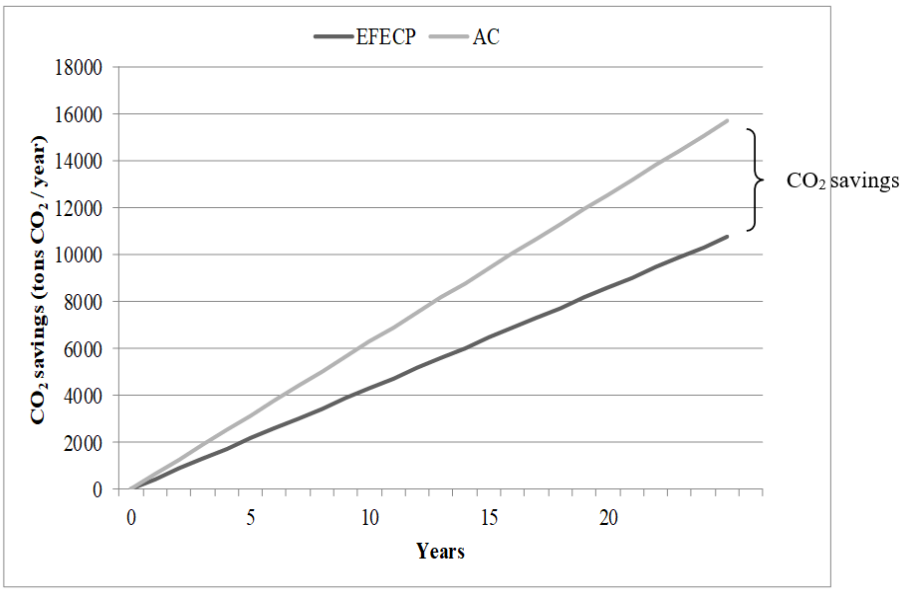


Figure 112. CO_2 savings using EFECP in comparison with AC

CHAPTER 6: Hollow fibre used for evaporative cooling performances through experimental investigations

6.1 Introduction

Cyprus has a variation of different climate: hot-dry and hot-humid. Thus, different evaporative pads should be used for different climatic zones in Cyprus. The relative humidity is around 23% for inland in July which is suitable area for using direct evaporative cooling system. On the other hand, the direct evaporative cooling method by using eucalyptus fibres pad cannot be used in hot-humid regions as the relative humidity level is around 56% in July, 2017. Due to this, the vapour compression AC system is predominantly used in order to enhance the thermal comfort of the occupants. The high level of temperature and moisture should be controlled in such regions. This discomfort of high humidity level can be minimized by using desiccant based evaporative cooling system in humid regions. In this respect HF, as an alternative pad, are used to test the performance of cooling by using water and potassium formate as working fluids for hot-dry and hot-humid climates, respectively. For hot and dry inland, the temperature can be reduced and the additional relative humidity can be added to the indoor by using direct evaporative cooling method. As water is an environmentally friendly source, it is used as a working fluid for evaporative cooling method (Chen et al., 2018). Whereas, the temperature and relative humidity can be reduced by using desiccant (potassium formate) based evaporative cooling system. Several local materials mentioned in section 2.6 are studied and used for the evaporative cooling method, however man-made materials can also be tested as they consists of various advantages compared to local materials. In this chapter, hollow fibres have been experimentally studied since these are light weight, corrosion resistant and low cost materials. In addition to this, the fibres prevent the bacteria and fungi penetration while allowing the water vapour transfer (Chen et al., 2017).

These hollow fibres module can be used for the humidifier, dehumidifier and the evaporative cooler. Meaning, this system can be used for hot-dry and hot-

humid areas. These fibres were tested under different testing modules. These are:

Hollow fibre integrated evaporative cooling system with bundles in a horizontal cylinder test module,

Hollow fibre integrated evaporative cooling system with bundles in circular module (with liquid)

*Hollow fibre integrated evaporative cooling system with potassium formate (*KCOOH*) desiccant dehumidification.*

The cooling performances of the proposed novel polymer hollow fibre integrated evaporative cooling system were experimentally investigated under the incoming air temperature in the range of 30 ˚C to 40 ˚C and relative humidity of 23% to 40%. The effects of air velocities on temperature difference, relative humidity, cooling efficiency, cooling capacity, COP and evaporation rate were analysed. In addition to this, the performance of the dehumidifier is evaluated based on moisture removal rate, dehumidifier effectiveness and cooling output. During dehumidification testing, it was focused on dehumidification, and regeneration process of the desiccant solution has not been investigated within the research.

These fibres were allowed to have alternative materials for the evaporative cooling pad resulting in energy conservation through the cooling of buildings.

6.2 Hollow fibre integrated evaporative cooling system with bundles in a horizontal cylinder test module

In this part of the study, the hollow fibres were tested in a test rig which was designed in a laboratory in the University of Nottingham. Formerly, local materials were tested as new pad materials for the evaporative cooling process. Following this, artificial hollow fibres were tested in the laboratory in order to evaluate the behaviour of the material under different environmental conditions. Since the hollow fibres are light weight and low cost, hollow fibre integrated evaporative cooling system was studied.

6.2.1 Test rig description for hollow fibre material

A small scale experimental test rig was designed to ascertain the cooling efficiency of the hollow fibre integrated evaporative cooling system. The dimensions of the laboratory test rig for testing the hollow fibres as wet media for evaporative cooling process are 150x250x1000mm. As seen in detailed schematic diagram in Figure 113, the rig consists of a cylinder shaped aluminium air tunnel (tube) and air blower (fan). A 5-litre water tank and pump were also added to the rig system in order to provide water circulation inside the fibre. A ball valve and a flow meter were also used to control the water flow through the fibres.

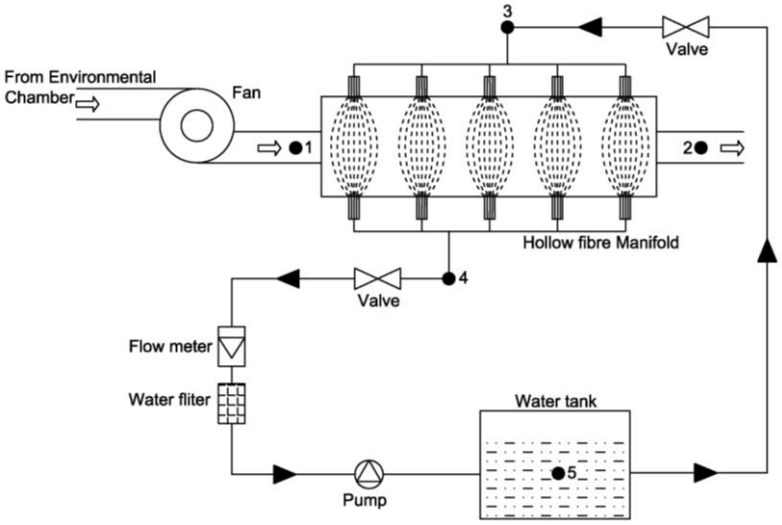


Figure 113. Diagram of the hollow fibre integrated evaporative cooling system

The tube was drilled from the top and bottom in order to place the hollow fibres diagonally through the gaps (Figure 114). The hollow fibres were placed into the tube which has 0.15 m diameter of flow cross section area and 1000 mm in length. For the fabrication of the polymer hollow fibre manifold, polyvinylidene fluoride (PVDF) hollow fibres (manufactured by ZENA Ltd.) were used with an effective pore size of 0.5μm and a porosity of 50%. The size of hollow fibres is 150 mm in length. The fibre inside/outside diameter is 0.6/0.8 mm. The air was supplied by a 25W air blower.



Figure 114. The flow cross section of aluminium tunnel

The experiment was carried out in May 2016 in the Marmont Laboratory. The environmental chamber was used to control the temperature and relative humidity during experimentation in a more controlled condition. It was also used to simulate the different climatic conditions of different regions. The environmental chamber was directly linked with the aluminium tunnel which was connected by fan.

The hollow fibres manifold was created as hollow fibre bundle for testing in the rig system. Thus, 5 fibre bundles of hollow fibres (each contains 100 fibres) were glued with silicon from the upper and lower ends. After they were dried, the excess fibres were cut. The bundles were then inserted into a T piece plastic tubing which were all connected to each other to form a round-shaped pipe circulation as shown in Figure 115. The round pipe system was placed at the lower and upper sides of the hollow fibres bundles. The five fibre

bundles with the distance of 5 cm were placed as is shown in Figure 115 and 116.

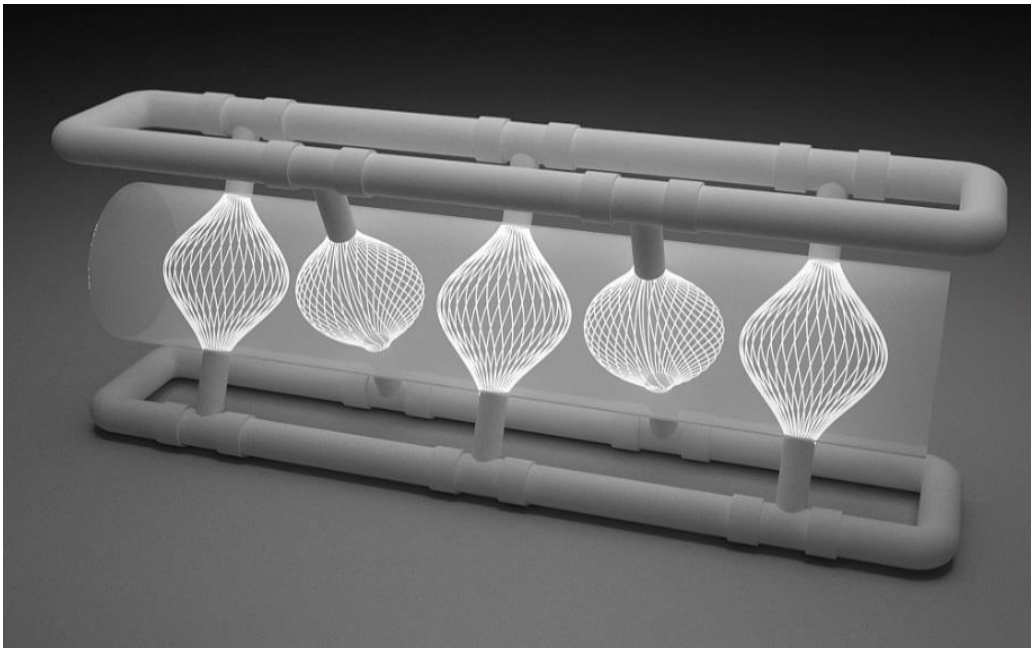


Figure 115. Detailed 3D model of testing



Figure 116. The actual testing prototype

Water was supplied by using 20W water pump through the plastic pipe system which was integrated into the aluminium tunnel. When water from the pipe was passed via the plastic fibres, it was collected in the water tank which was then re-circulated through the pipe onto the material. As a result, the system was designed to keep the materials wet during experimentation (Figure 117).



Figure 117. General view of the test rig

Instruments such as the datalogger and anemometer were used in the laboratory. A DT500 model data taker which was connected to a computer was used to record air temperatures and the relative humidity of the materials. The inlet, outlet temperature and RH measurements were recorded by Evaluation Kit EK-H4. In order to minimize the testing errors, four temperature and humidity sensors were located at the inlet and outlet air flow as shown in Figure 118. The water temperature was measured by K-type thermocouples which the water entering and leaving the manifold (Point 3 and 4). An anemometer was also used to measure the inlet and outlet air velocity. From the Table 30, the instruments used during the tests can be seen.

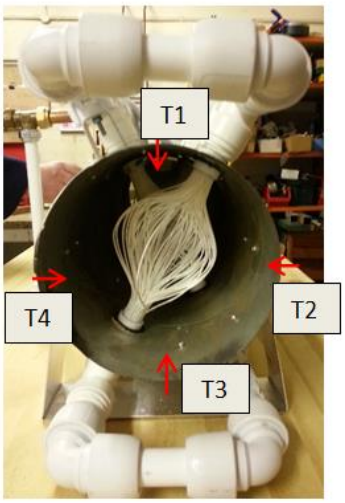


Figure 118. The cross section of the duct showing thermocouple locations as T1-T4

Table 30. Properties of experimental sensors used in the test

Sensor type	**Sensor model**	**Sensor accuracy**	**Specification range**
Temperature	Evaluation Kit EK-H4, Sensirion, UK	± 0.2%	-20 ~ + 70 °C
Relative humidity	Evaluation Kit EK-H4, Sensirion, UK	± 2%	0 ~ + 100 %
Air flow	Testo 405 V1 anemometer	± 2 %	0 ~ 10 m/s
Water temperature	Multi-thermometer	± 1 °C	-50 ~ + 300 °C

6.2.2 Procedure of the test rig

At the beginning of each test, the air temperature and RH were adjusted at the laboratory by using an environmental chamber. When the temperature and relative humidity reached the desired values, the fan and the pump were switched on. The air temperature was set at 30°C, 36°C and 40°C which represent the average and maximum air temperature in August on Cyprus Island. In addition to this, the air velocity was set at 0.6 m/s, 0.9 m/s, 1.2 m/s and 1.5 m/s to compare the performance of material at different air velocities. The air velocity is measured at the five different points of the outlet tunnel.

For each test, the values were recorded every 20 seconds until the system reach steady states conditions. The readings were taken into consideration after there was no longer any change in temperature and RH. The test started after 30 minutes when the indoor environmental condition was established by the help of the environmental chamber.

The measurements were recorded every minute and in total, 60 readings were recorded over one hour. As there were no longer significant changes in the readings, only 10 readings were illustrated as graphs.

6.2.3 Results of the test for hollow fibres

The cooling performance of the hollow fibres integrated evaporative cooling system was carried out in the laboratory at temperatures 30°C, 36°C, 40°C and relative humidity of 23-26, 40%. In accordance with the tests, the performance of hollow fibres was evaluated based on the effects of relative humidity, cooling efficiency, cooling capacity and COP. As seen in Table 31, three different testing conditions are summarized to show the measured inlet and outlet dry bulb temperature, relative humidity and inlet wet bulb temperature at different air velocities.

Table 31. Testing data for three different experimental conditions

Testing conditions	Air velocity (m/s)	DBT_{in} (◦C)	WBT_{in} (◦C)	RH_{in} (%)	DBT_{out} (◦C)	RH_{out} (%)
Condition 1	0.6	30.43	17.81	26.25	28.58	30.95
	0.9	30.45	17.81	26.16	28.57	30.78
	1.2	30.66	17.86	25.79	28.96	29.65
	1.5	30.69	17.81	25.48	28.99	29.20
Condition 2	0.6	36.38	21.64	24.49	32.35	31.83
	0.9	36.67	21.75	24.15	33.34	29.85
	1.2	36.64	21.71	24.08	33.44	29.43
	1.5	37.64	21.91	22.46	35.0	26.65
Condition 3	0.6	39.96	23.11	21.24	35.34	27.81
	0.9	40.45	23.28	20.81	35.85	26.77
	1.2	40.94	23.26	19.78	36.86	24.8
	1.5	40.77	22.54	18.98	36.99	23.62

6.2.3.1 Temperature difference at different air velocity

The temperature difference trends at different air speeds and at different inlet temperatures are shown in Figs. 119, 120 and 121. The tests were repeated for air temperature at 30°C, 36°C and 40°C with 0.6 m/s, 0.9 m/s, 1.2 m/s and 1.5 m/s air velocity. It is obvious that at the lower air speed, 0.6 m/s, the temperature difference was higher compared to the higher air velocity; in particular, 0.9 m/s - 1.5 m/s. At a lower air velocity, the longer the time of exposure to air, the more the evaporation. In other words, by decreasing the air velocity, there is more time for heat transfer and thus, the cooling efficiency will be higher.

As depicted in Figure 119, the temperature difference at 30°C inlet air temperature is approximately 1.86-1.53°C which is not a remarkable change for the cooling performance of plastic fibres. The range of temperature reduction at 36°C and 40°C inlet air temperature was from 2.9 to 4.06 and from 3.76 to 4.65°C, respectively (Figure 120 and 121).

The temperature differences were 1.42°C, 3.65°C and 4.66°C when the inlet air temperature was set at 30°C, 36°C and 40°C, respectively at 0.6 m/s air velocity. It can be concluded that at 0.6 m/s air velocity and at 40°C, the highest temperature difference was observed as shown in Figure 121. The temperature decreased from 40°C to 35.34°C, from 36°C to 32.35°C and from 30°C to 28.58°C at air velocity, 0.6 m/s (Table 31).

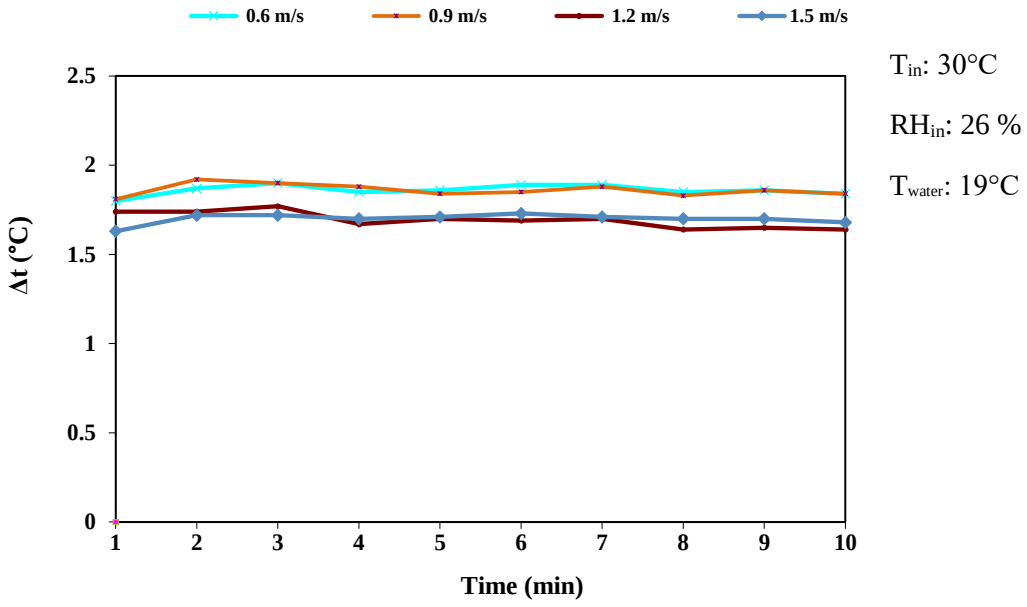


Figure 119. Temperature difference trends for hollow fibres at 0.6 - 1.5 m/s at 30°C

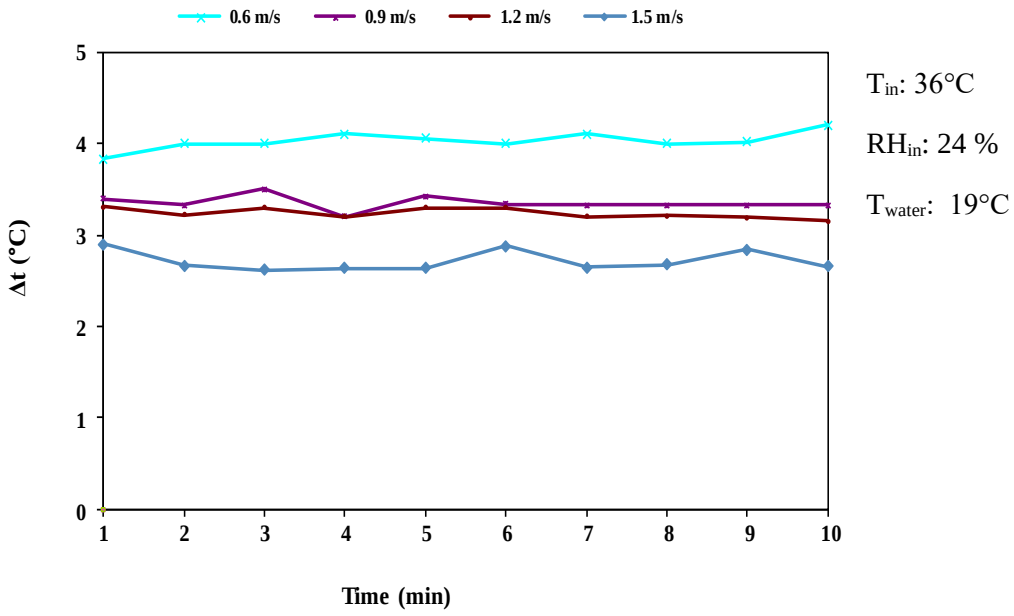


Figure 120. Temperature difference trends for hollow fibres at 0.6 - 1.5 m/s at 36°C

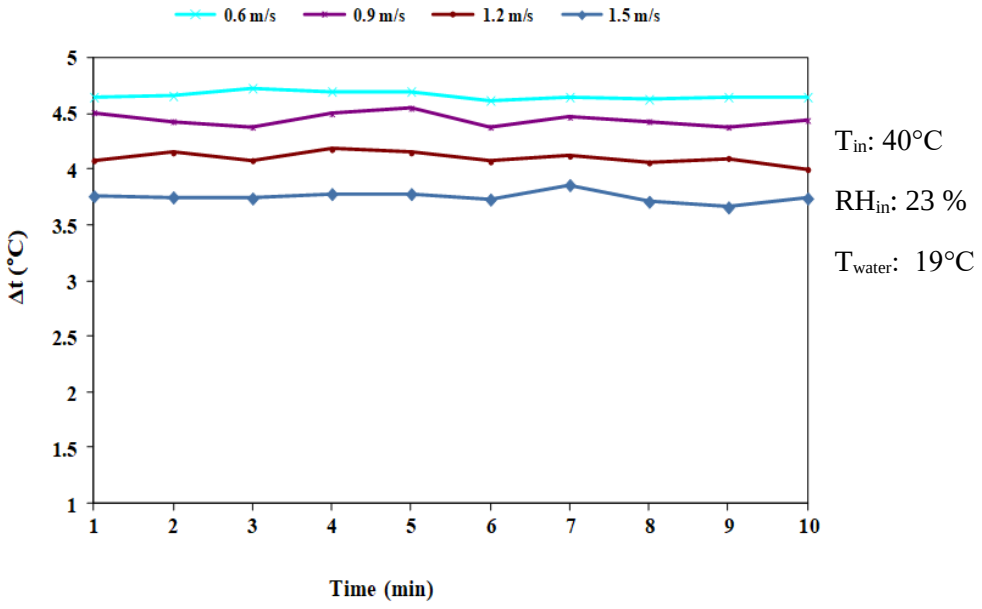


Figure 121. Temperature difference trends for hollow fibres at 0.6 - 1.5 m/s at 40°C

6.2.3.2 Relative humidity at different air velocity

As relative humidity affects the human comfort level, it is crucial to observe the effect of hollow fibres for evaporative cooling from that point of view. In accordance with the literature, at lower air flow, relative humidity at the outlet is higher since more evaporation occurs at lower air flow. However, according to the readings of outlet RH ratio at 24% inlet RH, it was seen that the ratio remained almost constant in between 29-32% at different air velocity, 0.6-1.5 m/s. At 50% inlet RH, the results for outlet RH were around 58-61% at air velocity 1.2-1.9 m/s.

As a result, it can be seen from Figure 122 that the outlet RH was increased by 25% when the inlet RH was set as 24% with constant air flow, 1.2 m/s. On the other hand, the outlet RH was increased by 20% at inlet of 50% RH to 61.5% with the same constant air flow. It can be concluded that hollow fibres can be used in dry climatic regions with a lower inlet RH ratio. In humid regions, the first air can be dried by using desiccant dehumidification.

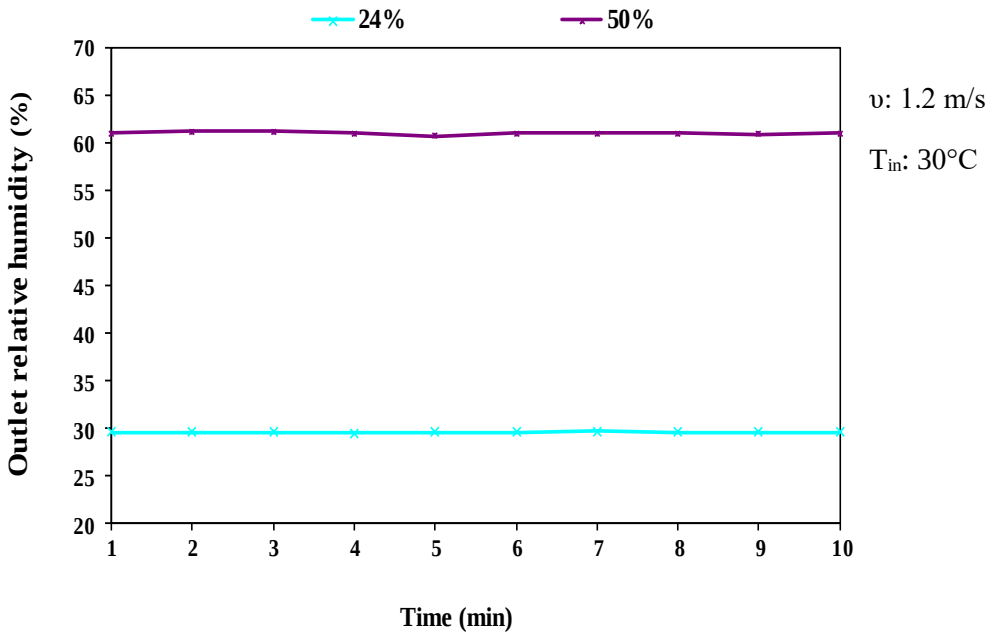


Figure 122. Outlet relative humidity trends at 1.2 m/s

6.2.3.3 Cooling efficiency at different air velocity

The potential of hollow fibres for evaporative cooling material was evaluated in terms of their cooling efficiency. As seen in Fig. 123, 124 and 125, the cooling efficiency is shown for different air velocities at different air temperatures. The graphs represent the trends of cooling efficiency at 30°C, 36°C and 40°C inlet air temperatures.

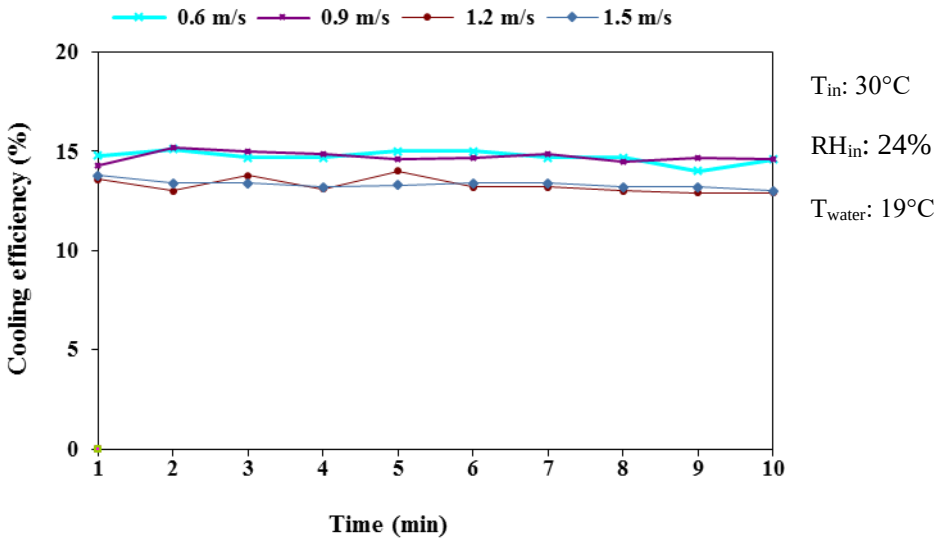


Figure 123. Cooling efficiency trends for hollow fibres at 0.6 - 1.5 m/s at 30°C

The maximum cooling efficiency at 30°C, 36°C and 40°C was 13, 25 and 26%, respectively. The maximum cooling efficiency of the hollow fibres was increased by reducing air velocity from 1.5 to 0.6 m/s at 20% and 26% when the inlet air temperature was set at 40°C. As seen from Figures 124 and 125, the cooling efficiency is around 25-26% at 36°C and 40°C compared to 14% at 30°C inlet air temperature. This is because at higher temperature but with the same absolute moisture value, air has a larger potential for evaporation and so the cooling efficiency will be higher. As temperature drop is directly proportional to cooling efficiency, the ratio of cooling efficiency becomes higher.

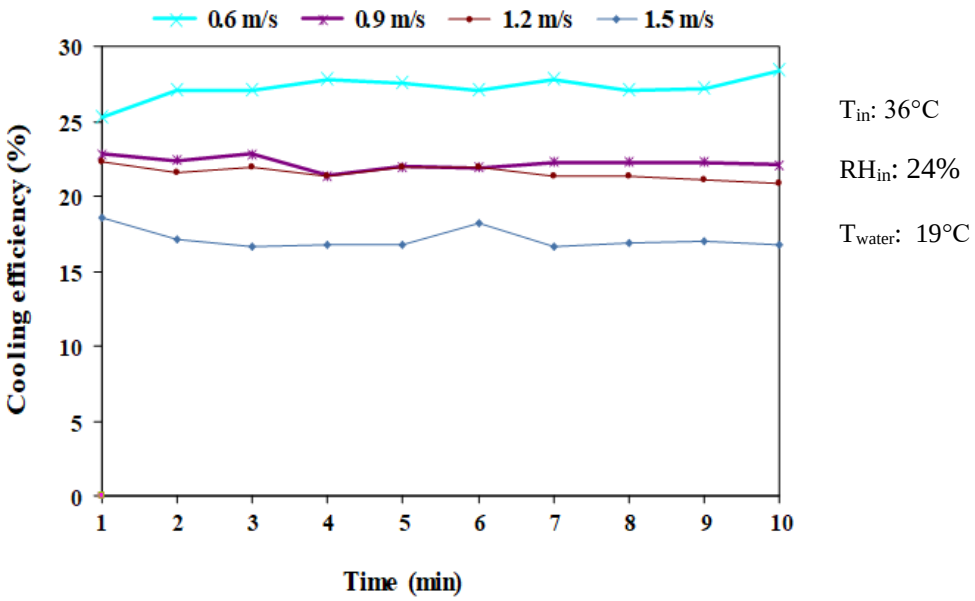


Figure 124. Cooling efficiency trends for hollow fibres at 0.6 - 1.5 m/s at 36°C

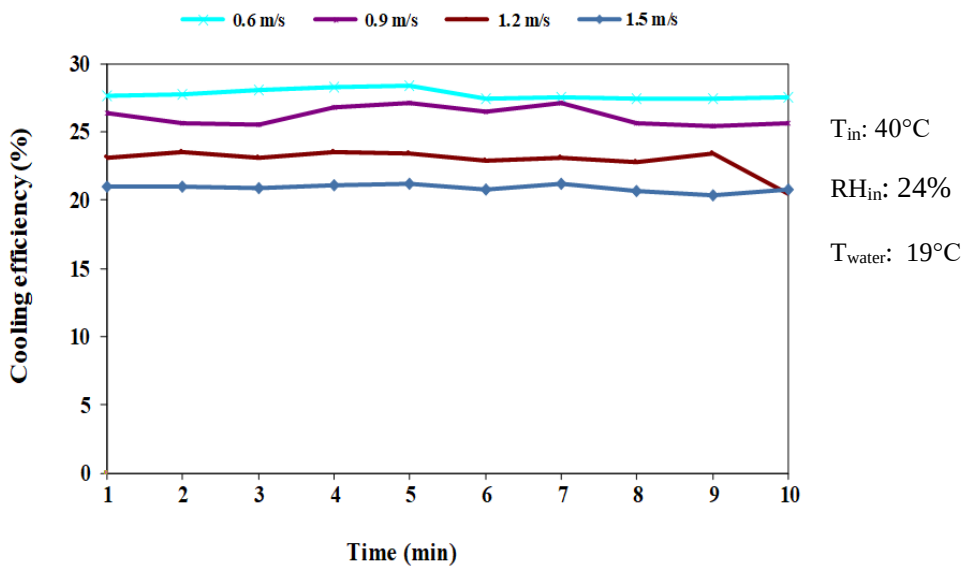


Figure 125. Cooling efficiency trends for hollow fibres at 0.6 - 1.5 m/s at 40°C

6.2.3.4 Cooling capacity at different air velocity

The performance of hollow fibres is related to the release of heat energy during the evaporative cooling process. In Fig. 126, the variation of cooling capacity versus air velocity for hollow fibres is illustrated. The cooling capacity was raised by increasing air velocity as compatible with the literature. According to the literature, the cooling capacity is increased by increasing the mass flow rate of water with air velocity. The cooling capacity was increased to **99W, 118W, 121W, 132W, 152W and 167W** by increasing the air velocity at 1.2, 1.5, 1.7, 1.9, 2.2 and 2.5 m/s, respectively.

The increased inlet RH will result in the decreasing of cooling capacity according to the Eq(3). Since cooling capacity is directly proportional to the temperature difference, the higher of temperature difference affects the cooling capacity to increase more. When the inlet relative humidity is increased, the air has less time to get in contact with the water circulating inside the hollow fibre, therefore, temperature difference tends to decrease, and thus reduce cooling capacity since cooling capacity is directly proportional to the temperature difference.

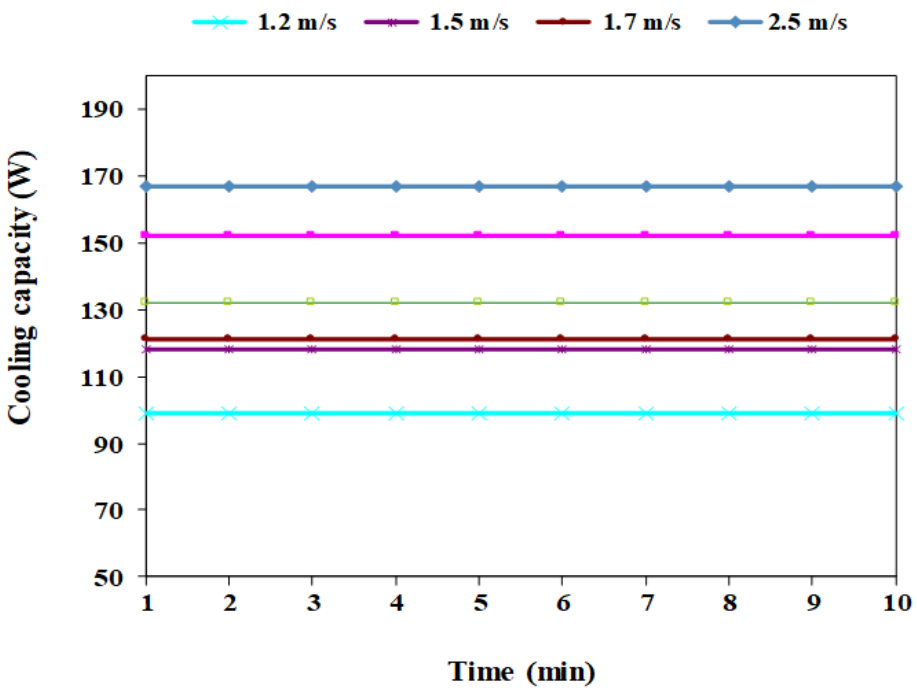


Figure 126. Cooling capacity trends at 1.2 – 2.5 m/s

6.2.3.5 COP at different air velocity

The overall COP at different air velocities is shown in Figure 127. As seen in the graph, a highest COP value occurred at 2.5 m/s air velocity with 2.6 and the minimum COP value was observed at 1.2 m/s air velocity as 1.7 which had lower water consumption as 0.00005 g/s as shown in Figure 109.

The COP value is increased by increasing of air velocity and thus the cooling capacity of the material up to a certain velocity. Since COP is also affected by the fan power which increases strongly with velocity.

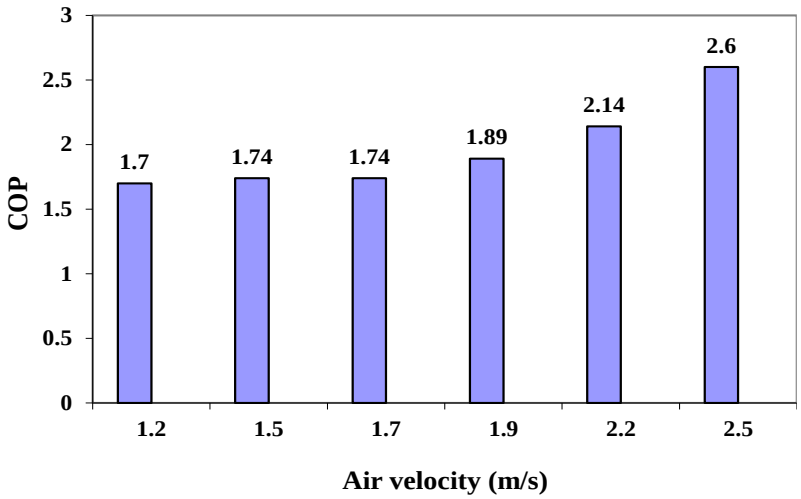


Figure 127. COP trends

6.2.3.6 The effect of air velocity on evaporation rate

Fig. 128 shows the variation of water consumption according to the different air velocities. As shown in the graph, the maximum water consumption is obtained at higher air flow, in particular 2.2 and 2.5 m/s with 0.00036 and 0.0004 g/s, respectively.

Consequently, it was observed that the water consumption rate is higher when air mass flow rate are increased.

The lowest water consumption is observed at 0.1 m/s air velocity with 0.00005 g/s for hollow fibres since water consumption increased with increasing air velocity as expected (Franco et al., 2014).

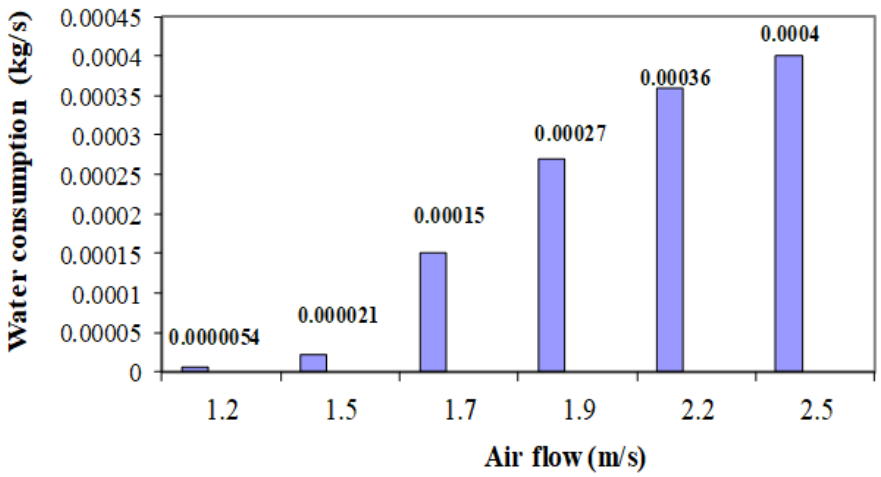


Figure 128. Water consumption trends at 1.2 - 2.5 m/s

6.3 Hollow fibre integrated evaporative cooling system with bundles in circular module

In this part of the study, the configuration of hollow fibre manifold was changed in order to test the performance of hollow fibres. The hollow fibres were tested in a laboratory in the University of Nottingham. The air temperature was experimentally investigated under the incoming air temperature in the range of 34°C -35°C. In addition to this, the air velocity was set from the range 0.25 m/s to 3.5 m/s and relative humidity in the range of 23%-40% to compare the performance of material at different air velocities.

6.3.1 System description for hollow fibres material

A large scale experimental test rig was designed to ascertain the cooling efficiency of the hollow fibre integrated evaporative cooling system with bundles in circular module. The dimensions of the laboratory test rig are 400x600x2000mm. As seen in detailed schematic diagram in Figure 129, the manifold consists of a circular shape polymer hollow fibre module, air tunnel, air blower, 8-litre water tanks, water filter and water pump. A glass box is located in the middle of the manifold where the hollow fibres are located

inside. The system also consists of a ball valve and a flow meter to control the water flow inside the fibres.

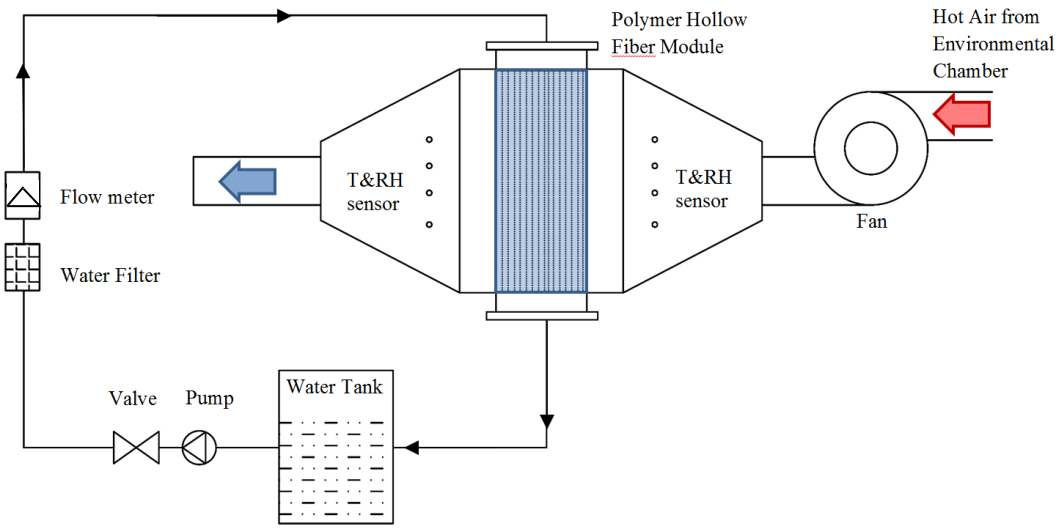


Figure 129. Diagram of the hollow fibre manifold

The hollow fibre integrated evaporative cooling system manifold experiment was carried out in March 2017 in the Marmont Laboratory. In order to control the temperature and relative humidity during experimentation, the environmental chamber was used. It was also set to the required climatic conditions.

The hollow fibres manifold was designed by using many fibres for testing. The module approximately consists of 5000 fibres as one large bundle of hollow fibres. Both lower and upper ends were connected to the water pipes which provide to transfer of water inside of the fibres (Figure 130).



Figure 130. Detailed view of the glass box

This manifold was incorporated into an aluminium tunnel, whose cross section diameter was 400mm. The prototype image and detailed 3D model of the system is shown in Figure 131 and 132. A large bundle consisting of 5000 fibres was placed in a glass box facing air flow from one side by a variable frequency drive centrifugal fan. The size of Polyvinylidene fluoride (PVDF) hollow fibres (manufactured by ZENA Ltd.) is 1.6mm of outside diameter and 1.4mm of inside diameter with the pore size of 0.5μm and a porosity of 50%. The height of the hollow fibres module is 600mm in length and the cross section is 400mm. In order to achieve uniform air flow, blades/flow guiders were integrated to inlet port across the chamber.

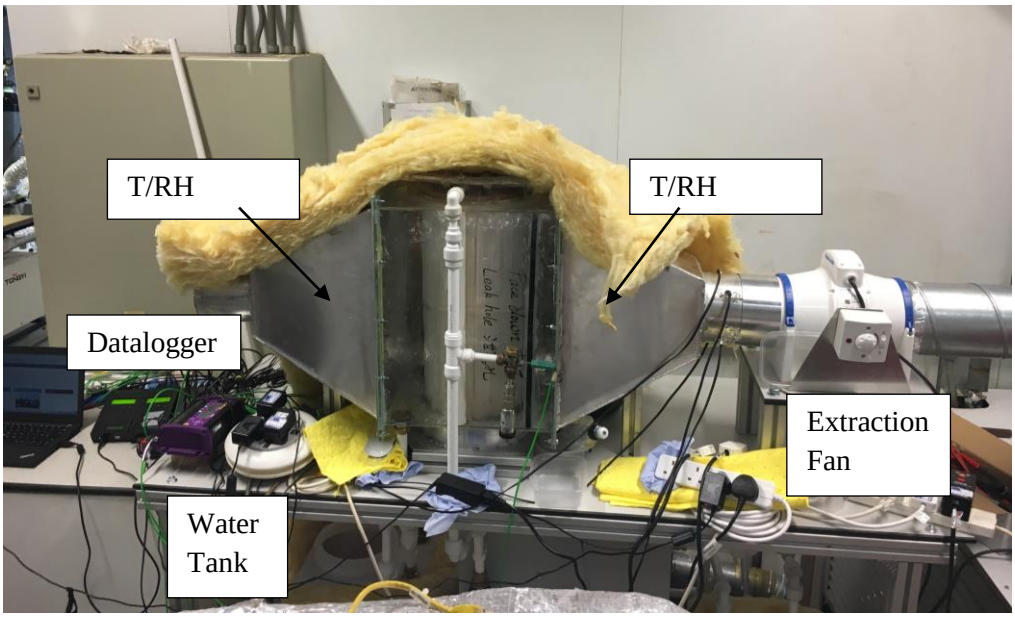


Figure 131. The actual testing prototype

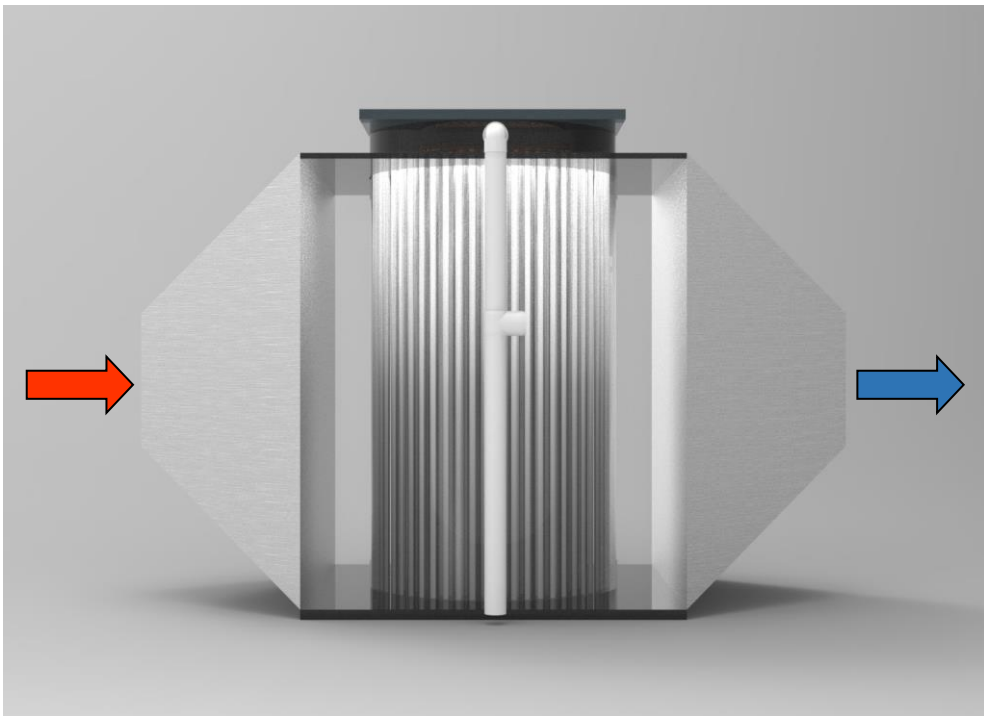


Figure 132. Detailed 3D model of testing

Water was supplied through the plastic pipe system by using 20W water pump which was integrated into the tunnel. When water from the pipe was passed via the plastic fibres, it was collected in the water tank which was then re-circulated through the pipe onto the material (Figure 133). As a result, the system was designed to keep the materials wet during experimentation.

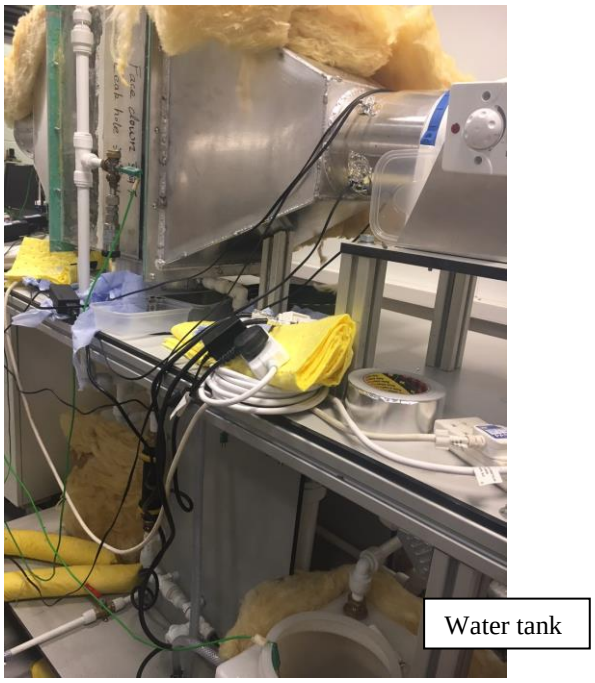


Figure 133. Side image of the system

A DT500 model data taker, Evaluation Kit EK-H4 and Testo 405 V1 anemometer were used to record air temperatures, the relative humidity of the materials and the air velocity at the inlet and outlet. Four humidity and temperature sensors (EK-H4, Sensirion, UK) were located at the inlet and outlet of the air stream (Figure 134). In addition to this, to measure the water temperature entering and leaving the hollow fibre module, K-type thermocouples were used. The instruments used during the tests can be seen from the Table 15.

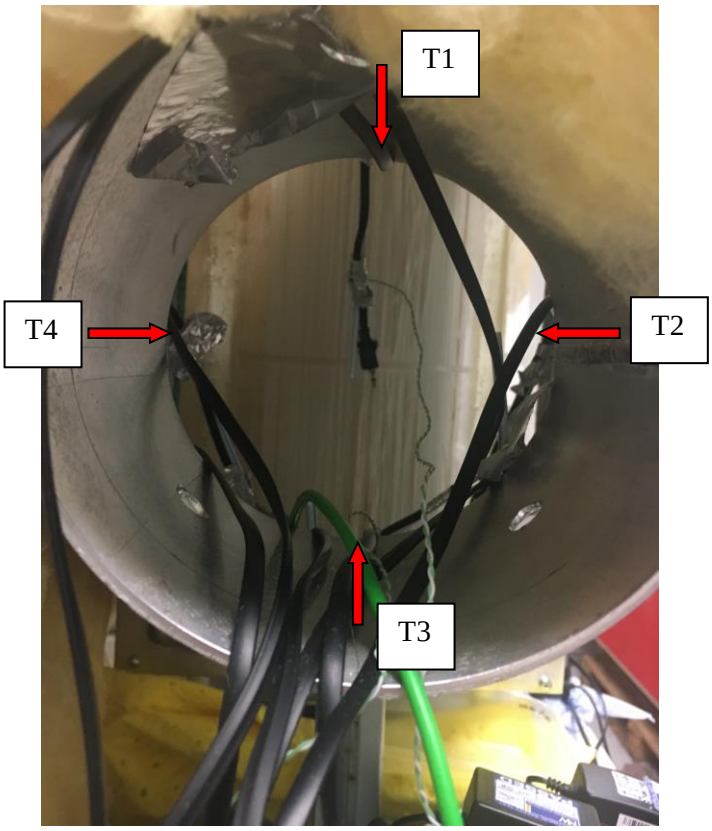


Figure 134. The cross section of the duct showing thermocouple locations as T1-T4

Table 15. Properties of experimental sensors used in the test

Sensor type	**Sensor model**	**Sensor accuracy**	**Specification range**
Temperature	Evaluation Kit EK-H4, Sensirion, UK	± 0.3%	-40 ~ + 125 °C
Relative humidity	Evaluation Kit EK-H4, Sensirion, UK	± 2%	0 ~ + 90 %
Air flow	Testo 454 anemometer	± 5 %	0 ~ 10 m/s

6.3.2 Procedure of the test rig

The RH and air temperature were adjusted at the laboratory by using an environmental chamber at the beginning of each test. The fan and the water circulation pump were switched on, when the inlet relative humidity and temperature reached the desired values. The air temperature was experimentally investigated under the incoming air temperature in the range of 34-35°C. In addition to this, the air velocity was set from the range 0.25 to 3.5 m/s to compare the performance of material at different air velocities.

For each test, the values were recorded every 20 seconds until the system reach steady states conditions. The readings were taken into consideration after there was no longer any change in temperature and RH. The test was started after 30 minutes when the indoor environmental condition was established by the help of the environmental chamber.

The measurements were recorded every minute and in total, 60 readings were recorded over one hour. As there were no longer significant changes in the readings, only 10 readings were illustrated as graphs.

6.3.3 Results of the test for hollow fibre

The cooling performance of the hollow fibres integrated evaporative cooling system was carried out with the temperature in the range of 34°C -35°C and relative humidity in the range of 23%-40%. Three different testing conditions are summarized as seen in Table 32 which shows the measured inlet and outlet dry bulb temperature, relative humidity and inlet wet bulb temperature at different air velocities. As a result, the performance of hollow fibres was evaluated based on the effects of air velocity on the temperature, relative humidity, cooling efficiency, cooling capacity and COP.

Table 32. Data for three different experimental conditions

Testing conditions	Air velocity (m/s)	**Inlet Dry-bulb temperature (◦C)**	**Inlet Air relative humidity (%)**	Inlet Wet-bulb temperature (◦C)	Outlet Dry-bulb temperature (◦C)	Outlet Air Relative Humidity (%)
Condition 1	0.16	**34.63**	**22.48**	18.72	19.42	92.68
	0.37	**34.52**	**22.4**	19.31	20.01	90.2
	0.92	**34.63**	**22.73**	19.58	20.71	86.62
	1.48	**34.71**	**22.63**	19.6	21.54	84.36
	1.86	**34.68**	**22.53**	19.56	22.16	81.1
	3.24	**34.58**	**22.35**	19.44	23.45	76.9
Condition 2	0.23	**34.57**	**31.67**	21.84	21.68	88.5
	0.45	**34.71**	**31.58**	21.88	22.01	86.6
	0.64	**34.65**	**31.45**	21.8	22.32	84.5
	1.52	**34.74**	**31.25**	21.82	23.05	79.41
	2.03	**34.58**	**31.56**	21.78	23.85	76.6
	3.22	**34.62**	**31.42**	21.77	24.65	71.5
Condition 3	0.27	**34.65**	**39.5**	23.69	23.28	84.3
	0.51	**34.74**	**39.42**	23.74	23.56	80.5
	0.72	**34.82**	**39.61**	23.85	23.94	77.8
	1.73	**34.53**	**39.78**	23.66	24.62	75.5
	2.51	**34.62**	**39.69**	23.71	25.34	70.4
	3.55	**34.78**	**39.85**	23.87	26.12	64.2

6.3.3.1 Outlet temperature at different air velocity

The outlet air dry bulb temperature trend at different air velocity is shown in Fig 135. The incoming air temperature was kept at 35ºC, while the relative humidity was kept as 23%, 32% and 40%, the experiments were conducted when the air velocity was changed from 0.25m/s to 3.6m/s.

It is obvious that when the incoming air velocity increases, the outlet air dry bulb temperature will increases. At lower air speed, 0.25 m/s, the outlet air dry bulb temperature was lower compared to the higher air velocity. This is due to the fact that when air velocity reduced, the air have more contact with the fibres. Thus, the heat transfer will lead to the lower outlet air dry bulb temperature. In other words, by increasing the air velocity, the heat transfer becomes less effective and thus, the cooling efficiency will be lower.

As depicted in Figure 116, the temperature difference at 35°C inlet air temperature is approximately 11.8-9°C at 40% RH, 13-10.2°C at 32% RH and 15.5-11.5°C at 23% RH. It is observed that when the incoming relative humidity is increased from 23% to 40%, the outlet air dry bulb temperature is increased because the incoming air with lower relative humidity will lead to greater driving force for the water evaporation, which result in better cooling performance.

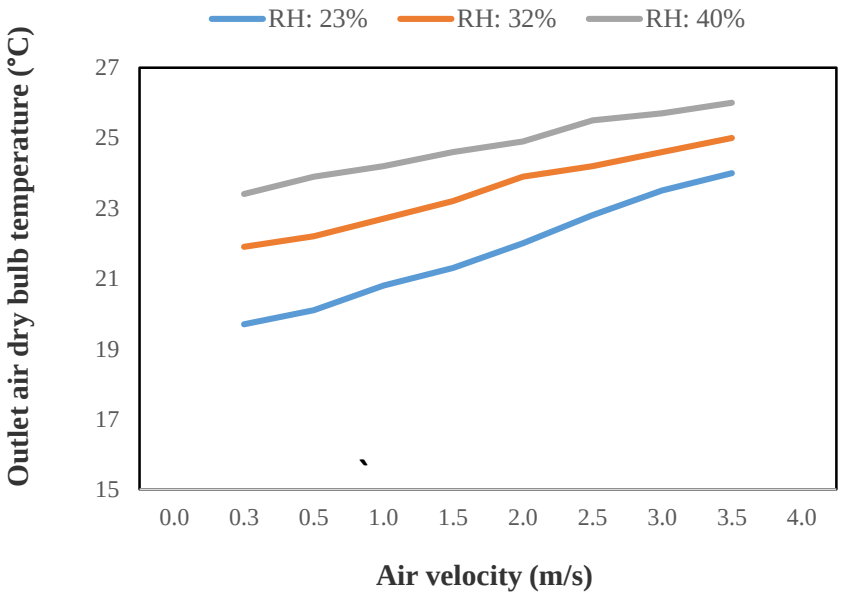


Figure 135. Outlet air dry temperature at 0.25 - 3.5 m/s at 35°C

6.3.3.2 Relative humidity at different air velocity

In accordance with the literature, at higher air velocity, relative humidity at the outlet is lower since less evaporation occurs at higher air velocity (Figure 136).

As a result, it can be seen from Figure 136 that at air velocity, 3.5m/s the outlet RH decreased from 83% to 65% RH when inlet RH increased from 23% to 40%. It can be concluded that hollow fibres can be used in dry climatic regions with a lower inlet RH ratio. In humid regions, the air can be dried by using desiccant dehumidification.

In Figure 137, it is also depicted that when the incoming air RH is increased from 23% to 32% and to 40%, less moisture addition will be occurred which due to the lower incoming air RH represents great potential of the air to absorb moisture from the water (Figure 137). It is obvious that at lower inlet RH, more temperature reduction occurred as seen in Figure 135.

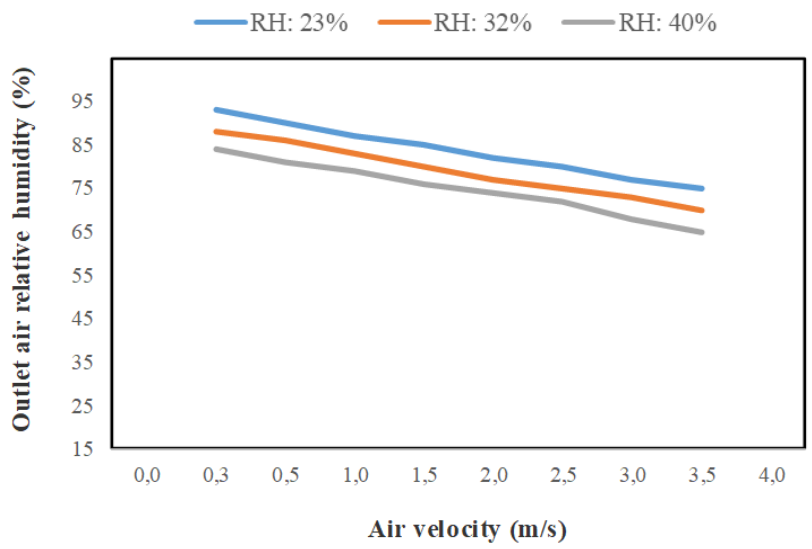


Figure 136. Outlet relative humidity at different air velocities for different inlet air humidity conditions

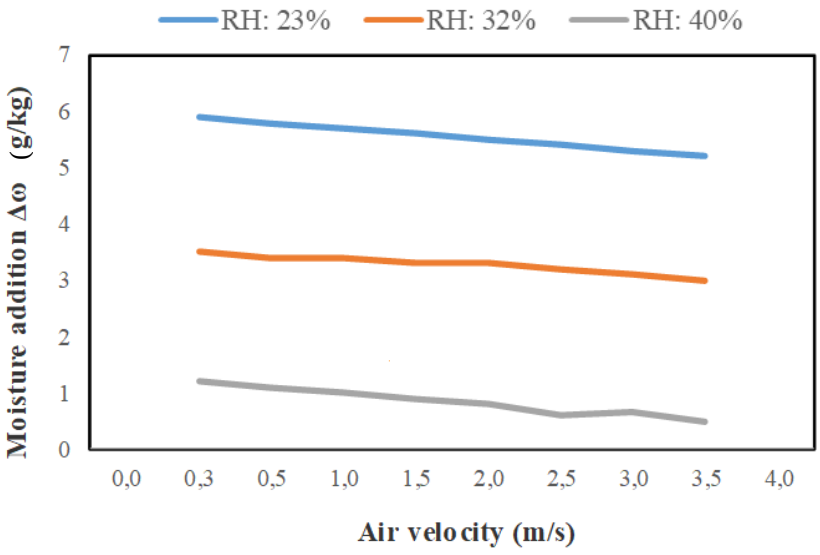


Figure 137. Absolute humidity change at different velocities for different inlet air humidity conditions

6.3.3.3 Cooling efficiency at different air velocity

As seen in Fig. 138, the cooling efficiency is shown for different air velocities at different inlet RH. The graphs represent the trends of cooling efficiency at 35°C inlet air temperatures. The inlet RH varied between 23-35 and 40%.

As it is observed from the graph, cooling efficiency is reduced by increasing air velocity from 0.3 to 3.5m/s consistent with previous results. This is due to at higher air velocity, the cooling efficiency will be lower since greater amount of air is contact with the air. According to the Eq(2), cooling efficiency is the ratio of the inlet and outlet air dry bulb temperature difference to the inlet air dry bulb and wet bulb difference. When the incoming air relative humidity increases, the wet-bulb effectiveness is increased as the incoming air relative humidity increases.

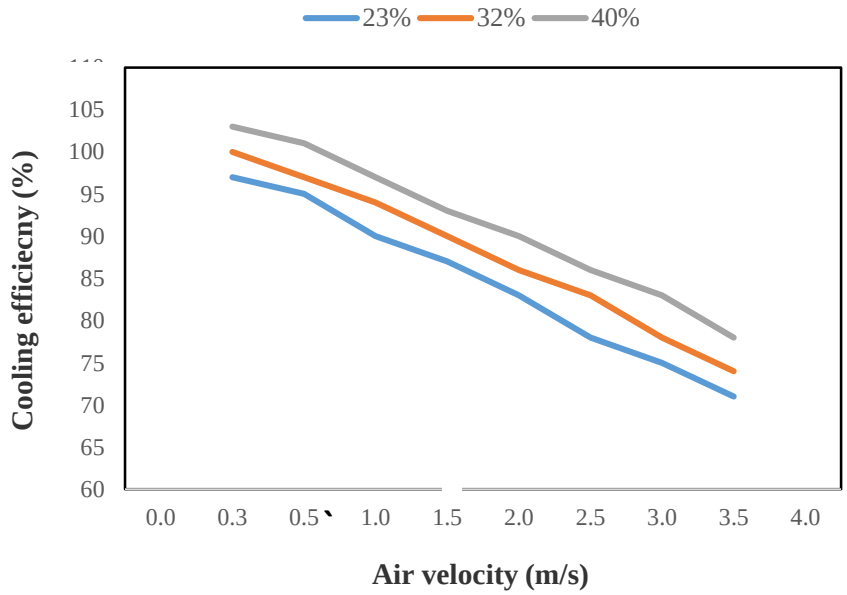


Figure 138. Cooling efficiency at different air velocities

6.3.3.4 Cooling capacity at different air velocity

In Fig. 139, the variation of cooling capacity versus air velocity for hollow fibres is seen under different inlet RH (23%, 32%, 40%). The cooling capacity was raised by increasing air velocity from 0.25m/s to 3.5m/s. As seen in the graph, at 3m/s, the cooling capacity are 1500W, 1700W and 2000W respectively for the incoming air relative humidity of 40%, 32% and 23%. Meaning that when RH is increased, the cooling capacity is decreased due to the Eq(3). Since cooling capacity is directly proportional to the temperature difference, the higher of temperature difference affects the cooling capacity to increase. When the inlet relative humidity is increased, the air has less time to get in contact with the water circulating inside the hollow fibre, therefore, temperature difference tends to decrease, and thus reduce cooling capacity since cooling capacity is directly proportional to the temperature difference.

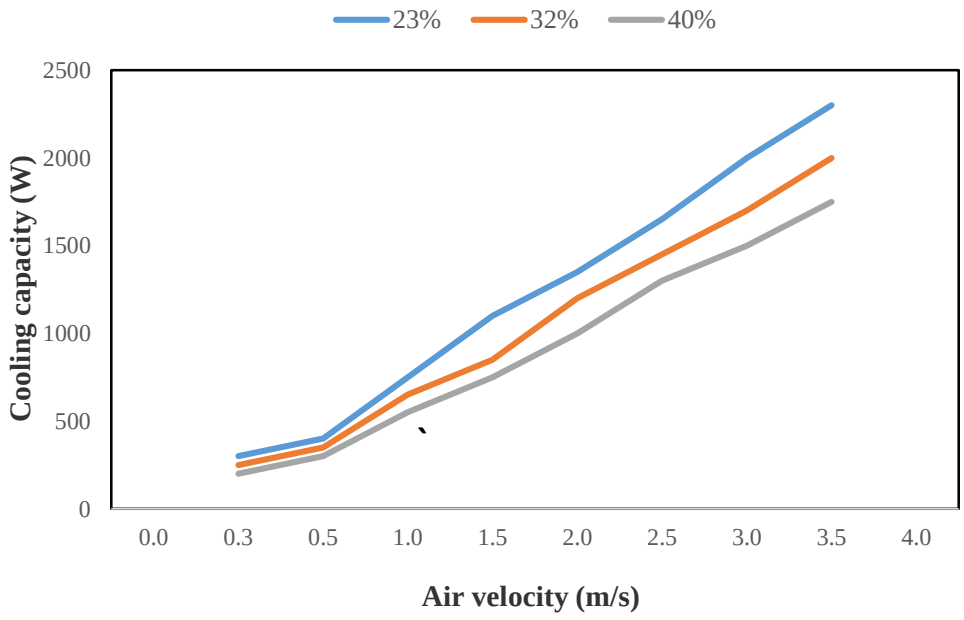


Figure 139. Cooling capacity at different air velocities

6.3.3.5 COP at different air velocity

The system energy efficiency or COP is rated as the ratio of the cooling capacity to power. The power consumption of proposed hollow fibre integrated evaporative cooling system with bundles in circular module by using water is limited by the power used for water pump and fan.

The proposed system's cooling capacity ranged from 0.3 to 2.3kW as seen in Figure 139 and the COP is between 1.72 and 13.8 (Figure 140). The performance of the proposed system increases with an increase in air velocity as depicted in Figure 140. However, it is observed that the COP drops at 3.24 m/s due to the sudden increase of air velocity during the experiment. At 1.86 m/s air reaches to moisture equilibrium and above that velocity level rate of water evaporation is constant. On the other hand, as the pump power increases with the increasing air velocity, the COP cooling shows a decreasing trend at velocities >1.86 m/s. Consequently, it can be seen that the cooling capacity and COP increase with reducing relative humidity and increasing air velocity as seen in Figure 139 and 140. Therefore, it can be concluded that this system is suitable for hot and dry locations.

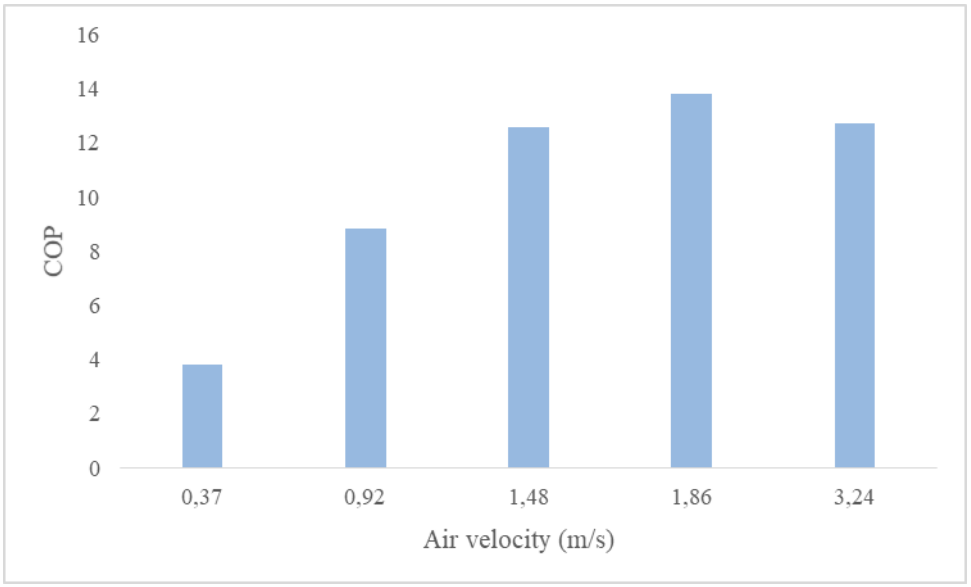


Figure 140. COP at different air velocities

6.4 Hollow fibre integrated evaporative cooling system with potassium formate desiccant dehumidification

In this section of the study, hollow fibres have been studied by the application of potassium formate (KCOOH) solution as the liquid desiccant in hollow fibre integrated liquid dessicant cooling system. The hollow fibre integrated liquid desiccant cooling system, with 3000 hollow fibres formed into a circular module was analysed under the incoming air temperature in the range of 30ºC to 45 ºC and relative humidity of 55% to 75%. The variations of dehumidifier effectiveness, cooling capacity and moisture removal rates were studied by varying the incoming air velocity from 0.1m/s to 4.5m/s. In addition to this, the effects of various incoming air relative humidity and solution concentration ratios on the system performance were experimentally studied as well.

6.4.1 System description for hollow fibres material

A large scale experimental test rig was designed to investigate the dehumidification performance of the hollow fibre integrated liquid desiccant cooling system. The dimensions of the laboratory test rig are 400x600x2000mm. As seen in detailed schematic diagram in Figure 141, the manifold consists of a polymer hollow fibre dehumidifier, an air tunnel, a circulation pump, a fan, a water filter and two solution tanks (weak and strong solution). A glass box is located in the middle of the manifold where the hollow fibres are located inside. The system also consists of a ball valve and a flow meter to control the water flow inside the fibres.

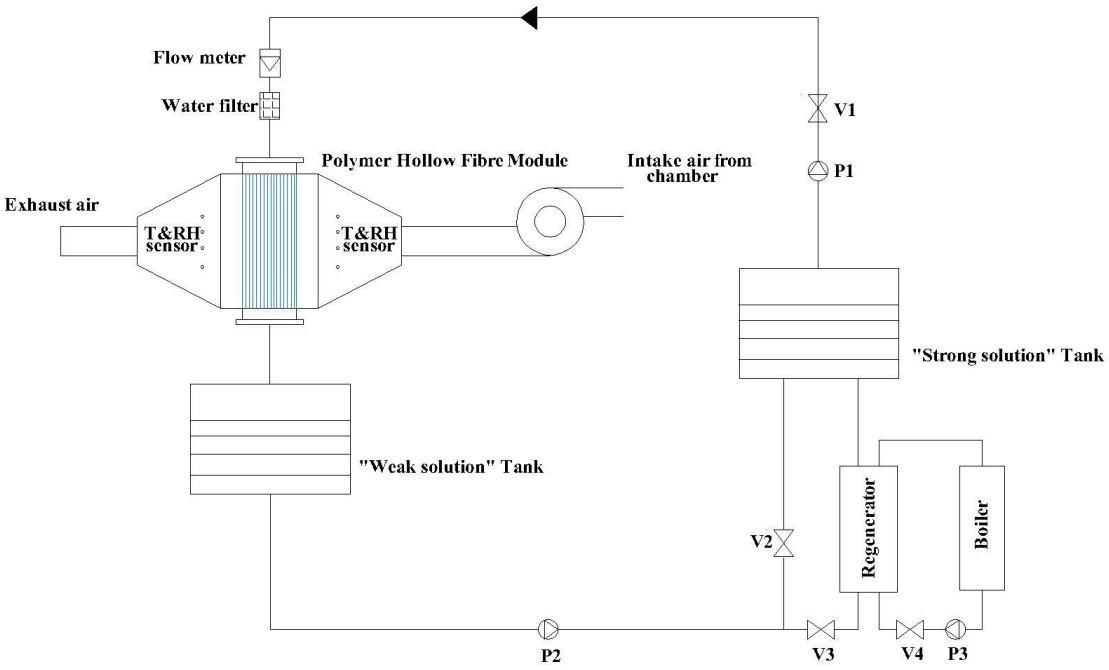


Figure 141. Schematic diagram of polymer hollow fibre integrated evaporative cooling system with desiccant dehumidification

The hollow fibre integrated evaporative cooling system manifold experiment was carried out in March 2017 in the Marmont Laboratory. In order to control the temperature and relative humidity during experimentation, the environmental chamber was used. It was also set to the required climatic conditions.

The hollow fibres manifold was designed by using many fibres for testing. The system approximately consists of 5000 fibres as one large bundle of hollow fibres. Both lower and upper ends were connected to the water pipes which provide to transfer of water inside of the fibres (Figure 142).



Figure 142. Detailed view of the glass box

This manifold was incorporated into an aluminium tunnel, whose cross section diameter was 400mm. The prototype image and detailed 3D model of the system is shown in Figure 143. A large bundle consisting of 5000 fibres was placed in a glass box facing air flow from one side by a variable frequency drive centrifugal fan. The size of Polyvinylidene fluoride (PVDF) hollow fibres (manufactured by ZENA Ltd.) is 1.6mm of outside diameter and 1.4mm of inside diameter with the pore size of 0.5µm and a porosity of 50%. The height of the hollow fibres module is 600mm in length and the cross section is 400mm.

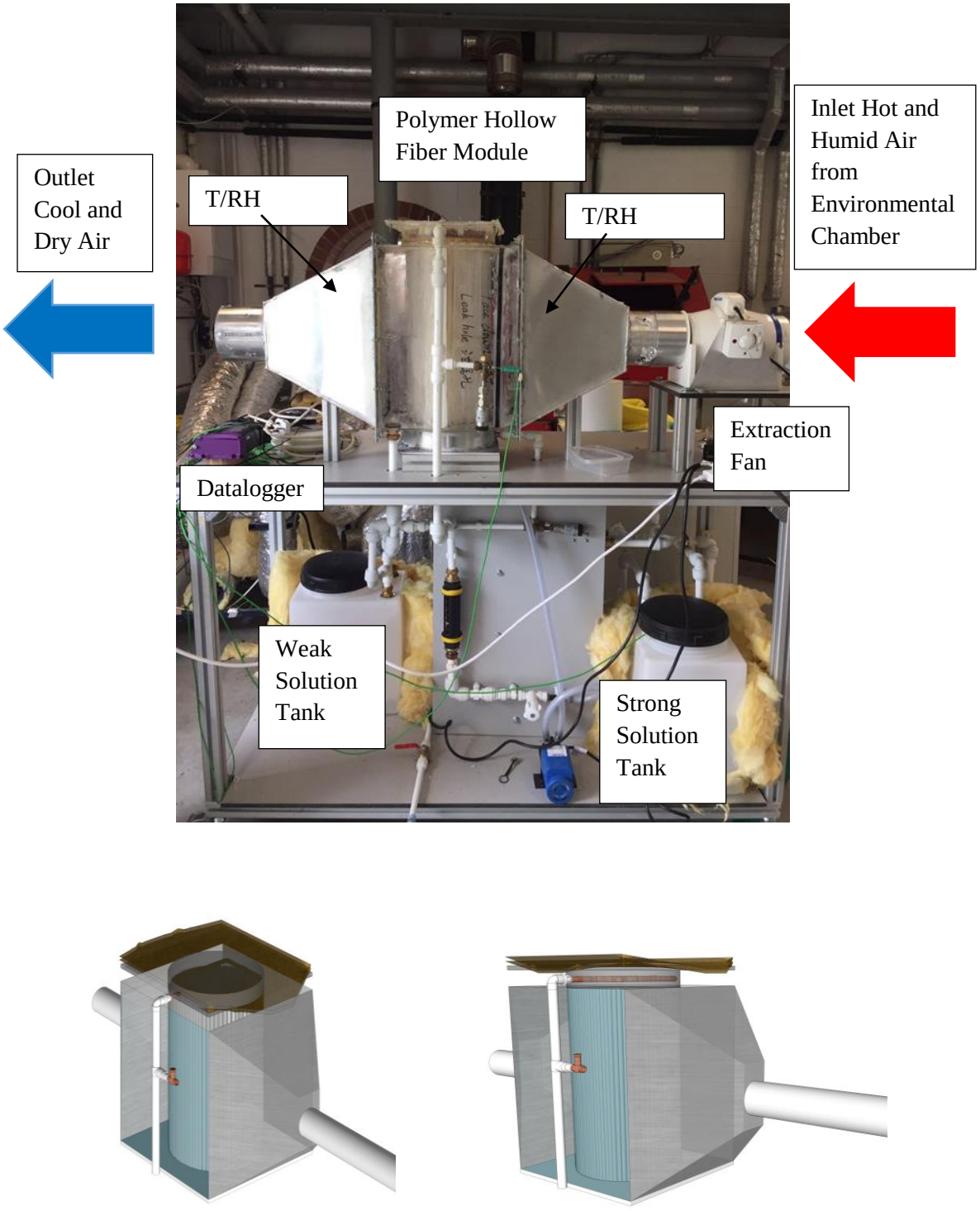


Figure 143. The actual and 3D view testing prototype

The strong solution was supplied through the plastic pipe system by using 25W single phase pump, from the solution tank to the top of the hollow fibre dehumidifier. A rectangular shape copper frame with 1mm holes on the sides of the frame was placed on top of the hollow fibre dehumidifier inn order to ensure the uniform distribution of the liquid desiccant solution into the hollow fibre module. Liquid desiccant was passed through the fibres from the holes of the copper frame and flew down the hollow fibre dehumidifier by gravity. After getting contact with the incoming air, the weak solution was directed into another weak solution tank via a T-piece tubing. The weak solution was then pumped into the regenerator, which was made from an aluminium plate heat exchanger. The regenerator was connected up with a 3kW electrical boiler. This boiler could provide hot water up to 80ºC, with the purpose to regenerate the liquid desiccant. After the regeneration, the concentration ratio of the diluted solution was increased to a higher level. It was finally pumped back by a 25 W single phase centrifugal pump to the strong solution tank to complete the cycle.

A DT500 model data taker, Evaluation Kit EK-H4 and Testo 405 V1 anemometer were used to record air temperatures, the relative humidity of the materials and the air velocity at the inlet and outlet. Four humidity and temperature sensors (EK-H4, Sensirion, UK) were located at the inlet and outlet of the air stream (Figure 144). Additional K type thermocouples were used to measure the temperature of liquid desiccant solution entering and leaving the hollow fibre module. The air velocity was taken for the five points across the outlet of the air tunnel, and the average value was taken. The dynamic pressures in the upstream and downstream of the liquid desiccant were recorded using Pressure transducers (Ge UNIK 5000). The instruments used during the tests can be seen from the Table 33.

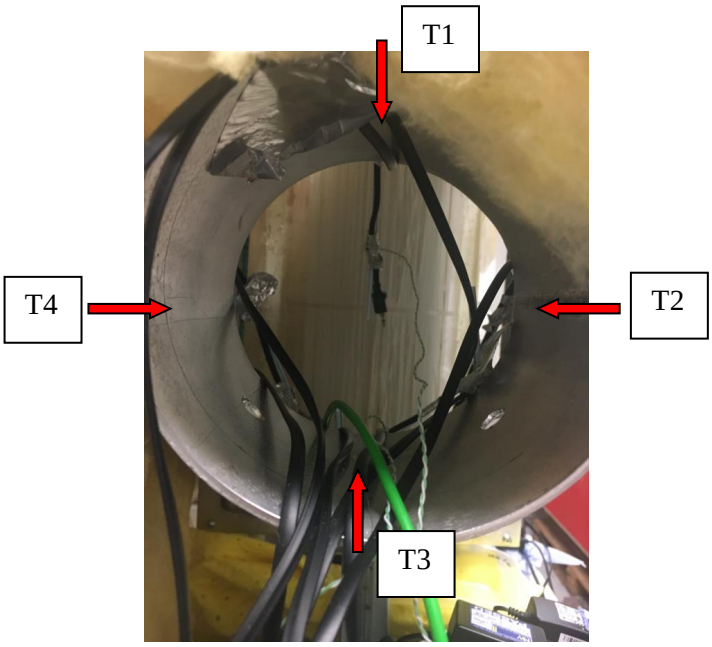


Figure 144. The cross section of the duct showing thermocouple locations as T1-T4

Table 33. Properties of experimental sensors used in the test

Sensor type	**Sensor model**	**Sensor accuracy**	**Specification range**
Temperature	Evaluation Kit EK-H4, Sensirion, UK	± 0.3%	-40 ~ + 125 °C
Relative humidity	Evaluation Kit EK-H4, Sensirion, UK	± 2%	0 ~ + 90 %
K-type thermocouple	Desiccant solution temperature		
Air flow	Testo 454 anemometer	± 5 %	0 ~ 10 m/s

6.4.2 Procedure of the test rig

The RH and air temperature were adjusted at the laboratory by using an environmental chamber at the beginning of each test. The fan and the water circulation pump were switched on, when the inlet relative humidity and temperature reached the desired values. The air temperature was experimentally investigated under the incoming air temperature in the range of 30ºC to 45ºC and relative humidity of 55% to 75%. The variations of dehumidifier effectiveness, cooling capacity and moisture removal rates were studied by varying the incoming air velocity from 0.1m/s to 4.5m/s.

For each test, the values were recorded every 20 seconds until the system reach steady states conditions. The readings were taken into consideration after there was no longer any change in temperature and RH. In this light, the test was started after 30 minutes when the indoor environmental condition was established by the help of the environmental chamber.

The measurements were recorded every minute and in total, 60 readings were recorded over one hour. As there were no longer significant changes in the readings, only 10 readings were illustrated as graphs.

6.4.3 Results of the test for plastic fibre

Dehumidification experiments were carried out in order to analyse the performance of the hollow fibre integrated liquid desiccant evaporative system. During the tests, the inlet air temperature was set to 35ºC and 40ºC and RH was kept in the range of 60-70%. Throughout the tests, the volumetric flow rate of desiccant solution was kept 2Lmin^{-1} in order to provide sufficient wetting of the fibres. If the volumetric flow rate is kept below 1.5Lmin^{-1}, there is not any sufficient wetting of the fibres inside the dehumidifier (Elmer et al., 2016). The results were analysed based on different inlet air velocity and inlet relative humidity with respect to inlet air temperature and humidity, in order to evaluate the performances of fibres in terms of moisture removal rate, cooling capacity and dehumidifier effectiveness. The condition of different tests can be seen based on the different effects of air velocity on the change in absolute humidity, moısture removal rate, dehumidifier cooling output and dehumidifier effectiveness in Table 34.

Table 34. Testing data of dehumidifier performance for various experimental conditions

Test number	Xsol (%)	$\nu_{air,in}$ (m/s)	$T_{air,in}$ (◦C)	$RH_{air,in}$ (%)	$T_{air,out}$ (◦C)	$\Delta\omega$ (kg/kg)	MRR (g/s)	$Q_{cooling}$ (kW)	η (%)
1	62	0,7	35.35	55.23	33.56	0.0029	0.11774	0.58	0.263
2	62	0,65	34.83	60.12	33,84	0,0055	0,207	0,44	0,296
3	62	0,7	35.38	65.56	33,42	0,0059	0,241	0,64	0,324
4	62	0,7	35.29	70.26	32,88	0,0064	0,260	0,87	0,367
5	62	0,7	35.36	75.18	32.65	0.0068	0,276	0,958	0,39

6.4.3.1 The effect of different inlet air temperature and RH at different air velocity

The dehumidifier effectiveness was evaluated for inlet air temperature at 35ºC and 40ºC and RH in the range of 55-75%. As can be seen in Figure 145 and 146, the MRR is increased by increasing of inlet air dry bulb temperature from 35ºC to 40ºC and RH from 55% to 75%. When both values increase, the vapour pressure of the air is also increased. As the difference of vapour pressure between the humid air and desiccant solution is increased, higher mass transfer occurred which means that solution attract moisture from the humid air. It is worth mentioning that this type of dehumidifier can be used in hot and humid regions. Considering the MRR at 55% RH and air velocity at 0,7m/s, it was increased from 0,117g/s to 0,248g/s as the inlet air dry bulb temperature is increased from 35ºC to 40ºC and from 0,227g/s to 0,382gr/s at 75% RH (Figure 146).

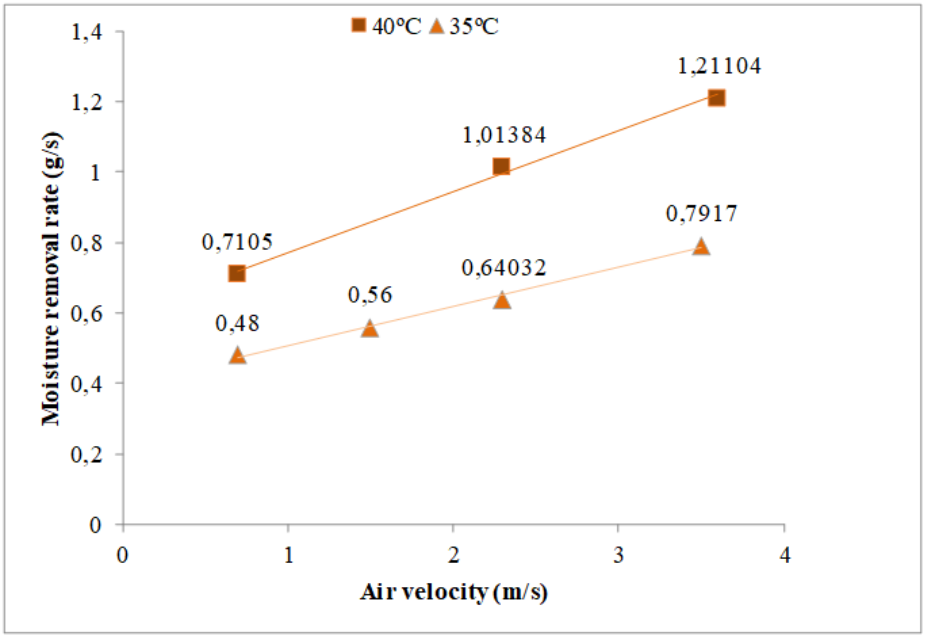


Figure 145. The dehumidifier moisture removal rate trends at different air temperature (T_{in}= 35-40ºC at 70%RH)

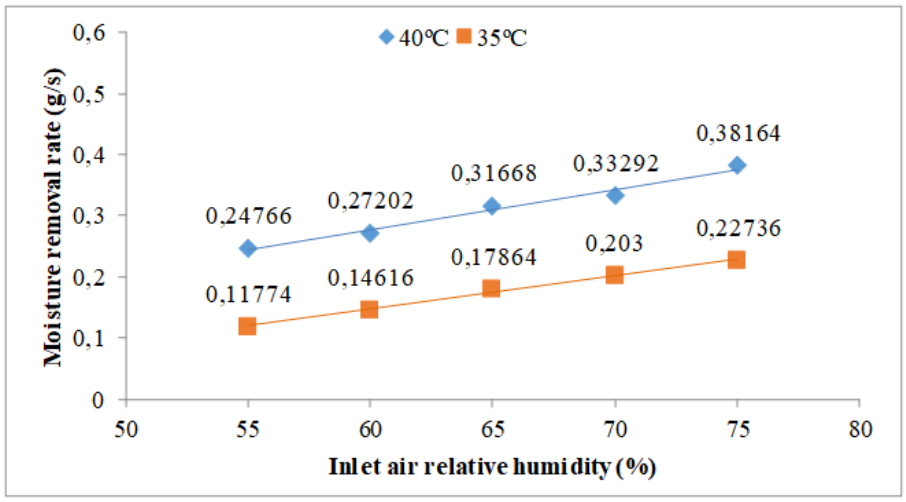


Figure 146. The dehumidifier moisture removal rate trends at different relative humidity (RH=55-75%, velocity: 0,7m/s)

Figure 147 and 148 show the cooling capacity of the dehumidifier based on the inlet air temperature at 35ºC and 40ºC and RH in the range of 55-75%. As can be seen from the graphs the cooling capacity is increased by increasing of air temperature and RH. This is related to the increase of MRR and thus the latent

cooling. In addition to this, the sensible cooling is also increased as the higher temperature difference occurred between the air and desiccant solution. The cooling capacity of dehumidifier is increased from 0,84kW to 1,92kW from 0,7m/s to 3,6m/s at 35ºC inlet air temperature and 70%RH.

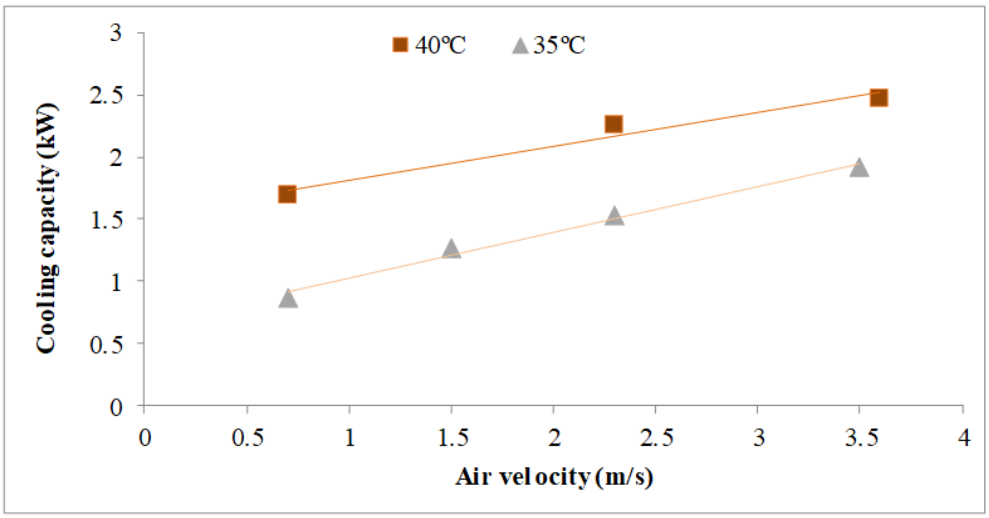


Figure 147. The cooling capacity trends at different air temperature and relative humidity (T_{in}= 35-40ºC, RH=70%)

The increasing of cooling capacity is also observed with increasing inlet air temperature and RH in Figure 147. The cooling capacity is increased from 0,59kW to 0,96kW with RH from 55% to 75% (Figure 129).

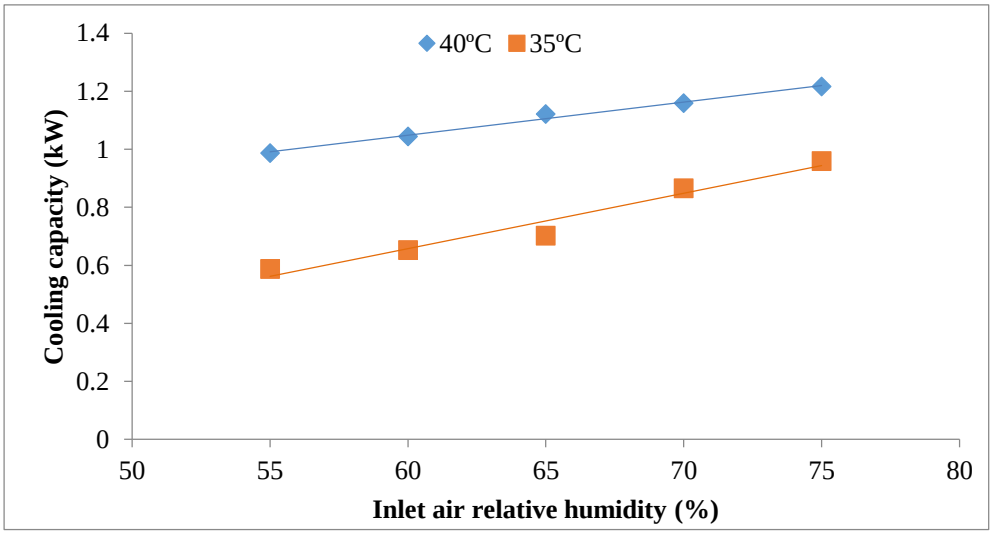


Figure 148. The cooling capacity trends at different relative humidity (RH=55-75%, velocity: 0,7m/s)

As seen in Figure 149 and 150, the dehumidifier effectiveness is increased by increasing inlet air temperature and inlet relative humidity. However, at higher incoming air velocity, dehumidifier effectiveness declined from 0,41% to 0,30% at 40ºC and from 0,37 to 0,25 at 35ºC. As aforementioned above, this is due to the less contact time of the air with the solution inside of the fibres while increasing air velocity.

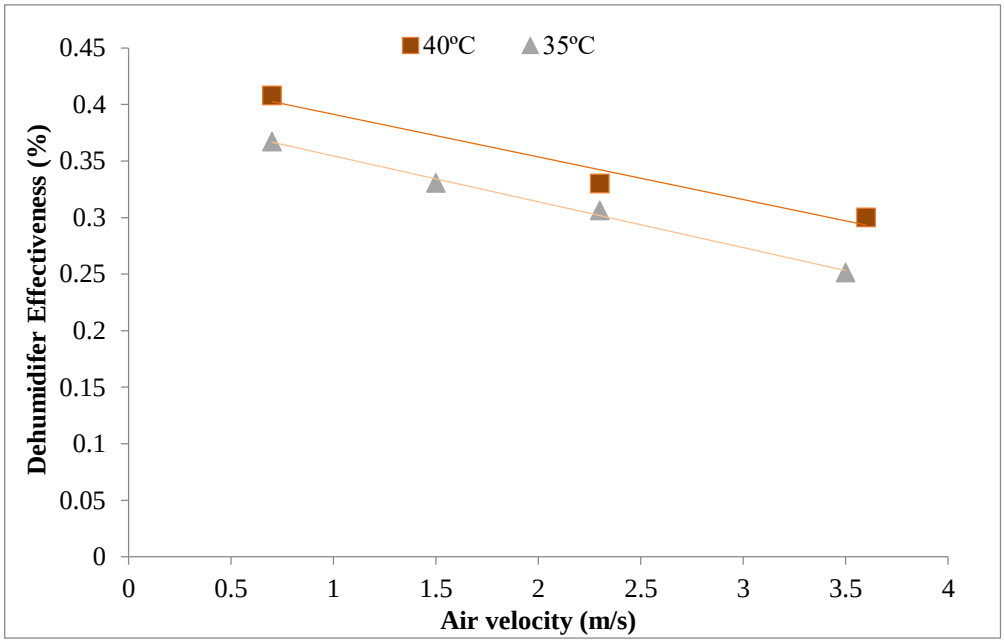


Figure 149. The dehumidifier effectiveness trends at different air temperature (T_{in}= 35-40ºC, RH=70%)

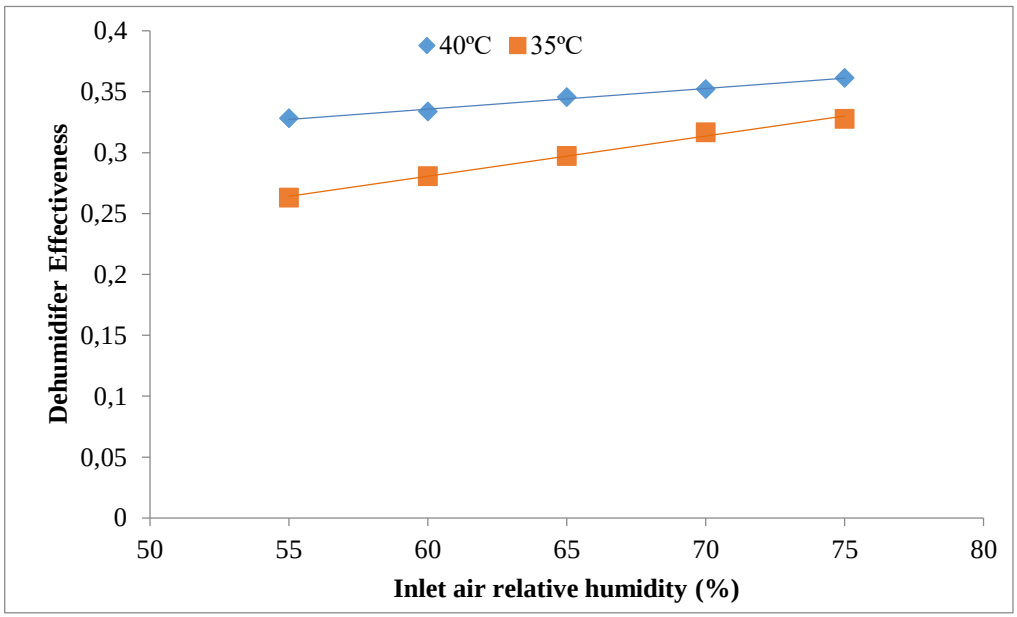


Figure 150. The dehumidifier effectiveness trends at different relative humidity (RH=55-75%, velocity: 0,7m/s)

6.4.3.2 The effect of different inlet RH at different air velocity

In the following Figures, the variations of the moisture removal rate, the cooling capacity and the dehumidifier effectiveness are shown with respect to different air velocity (0.5 m/s-3.5 m/s) and relative humidity (60%-65%-70%). During the dehumidification experiments, the concentration ratio of potassium formate is tested for 62% and inlet temperature is tested as 35ºC.

As seen in Figure 151, the moisture removal rate is increased as the air velocity is increased from 0.5m/s to 3.5m/s and inlet RH are increased from 60% to 70%. With higher inlet RH, higher vapour pressure occurred which provides greater amount of moisture removal rate. When there is a higher vapour pressure difference, larger moisture transfer occurred which leads to improve moisture removal rate. Take the air velocity at 3.5m/s, the moisture removal rate is 0.42g/s, 0.56g/s and 0.79g/s respectively for incoming air relative humidity of 60%, 65% and 70%. Elmer et al., 2016 demonstrated the novel integrated desiccant air conditioning system by using potassium formate. They have found that at 60% RH and 70% RH, the MRR is 0.36g/s and 0.45g/s at 35ºC inlet air temperature and %62 solution concentration ratio. From this point of view, the moisture removal effects of proposed system is obviously better than what is presented by Elmer et al., 2016, although the solution concentration rate is 5% higher than proposed study.

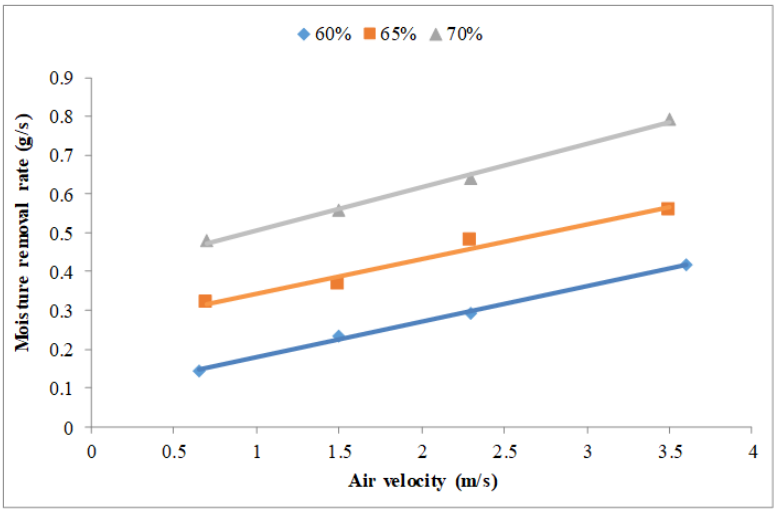


Figure 151. The dehumidifier moisture removal rate trends at different air velocity (T_{in}= 35ºC, sol=62%)

In Figure 152, the cooling capacity trends at different air velocity is shown under same solution concentration ratio of 62% and inlet air dry bulb temperature of 35ºC. As it is obvious that, the cooling capacity is increased as the air velocity is increased. In addition to this, inlet RH has also an effect on higher cooling capacity. The increase of dehumidifier cooling output together with inlet temperature and RH is related to the higher MRR and thus, the higher latent cooling together with higher temperature difference which leads to increase sensible cooling. Take the air velocity at 3.5m/s, the cooling capacity is 1340W, 1530W and 1920W respectively for incoming air relative humidity of 60%, 65% and 70%. Elmer et al., 2016 have found that at 60% RH and 70% RH, the cooling capacity is 1150W and 1350W at 35ºC inlet air temperature and %67 solution concentration ratio. The cooling capacity of proposed system is thus better than what is presented by Elmer et al., 2016.

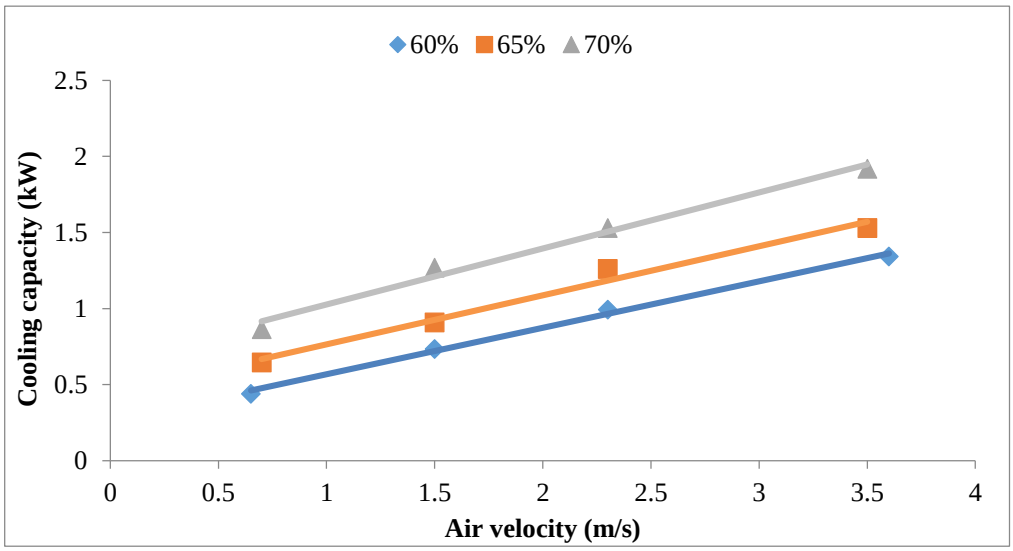


Figure 152. The cooling capacity trends at different air velocity (T_{in}= 35ºC, sol=62%)

In Figure 153, the latent (dehumidifier) effectiveness trends at different air velocity is shown under same solution concentration ratio of 62% and inlet air dry bulb temperature of 35ºC. As it is easily depicted from the graph, the humidifier effectiveness is reduced as the air velocity is increased and inlet RH is reduced. Since at higher incoming air velocity, the solution inside the polymer hollow has less time to get in contact with the incoming air. This leads

to reduce change in the absolute humidity (Δω). According to Eq. (8), Δω is proportionally related to the dehumidifier effectives. Hence, higher air velocity is associated with lower dehumidifier effectiveness. The experimental results presented by Elmer et al., (2016) indicated that, at incoming air temperature 35ºC and RH at 60% and 70%, the dehumidifier effectiveness was around 0.32% and 0.34%, which is actually lower than the proposed hollow fibre integrated evaporative cooling system.

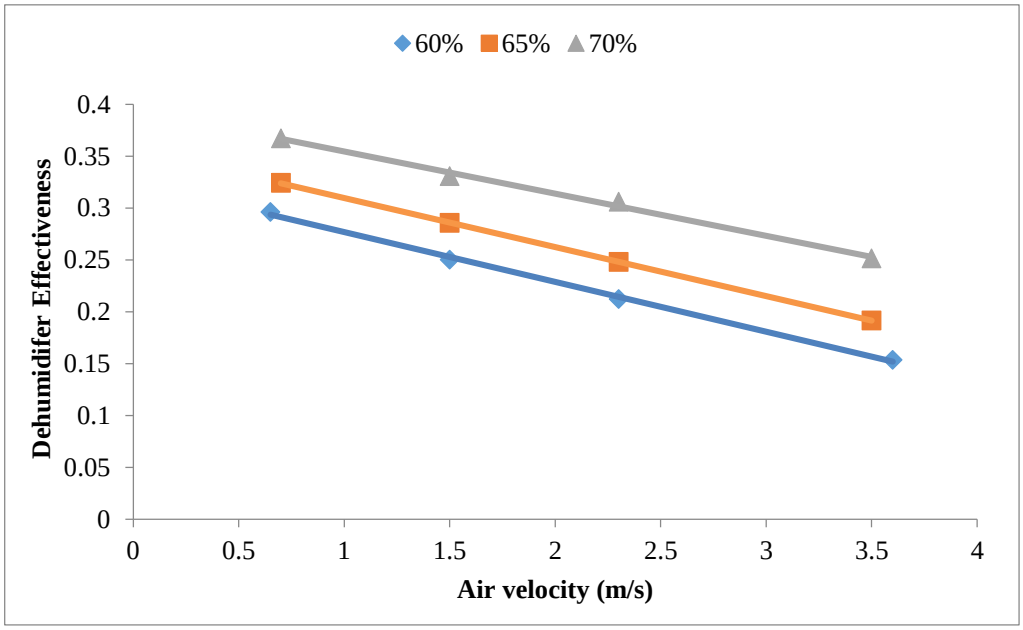


Figure 153. The dehumidifier effectiveness trends at different air velocity (T_{in}= 35ºC, sol=62%)

6.4.3.3 The effect of different solution concentration at different air velocity

In this part of the testing, the effect of different solution concentration ratio (62%, 49%, 36%) on moisture removal rate, cooling effects and dehumidifier effectiveness were investigated under 35ºC inlet air dry bulb temperature and 60% RH. As can be seen in Figure 154, at higher air velocity and at higher concentration solution, the moisture removal rate is higher. At lowest air velocity (0,7m/s), the MRR is 0,11g/s, 0,13g/s and 0,14g/s for solution concentration 36%, 49% and 62%, respectively. Compared the study of Elmer et al., (2016) the MRR was found 0,28 g/s at incoming air temperature 35ºC and RH at 60% when the solution concentration was 66%. In this study, the MRR is increased from 0,14g/s to 0,47g/s from 0,7-4,5m/s at the same conditions.

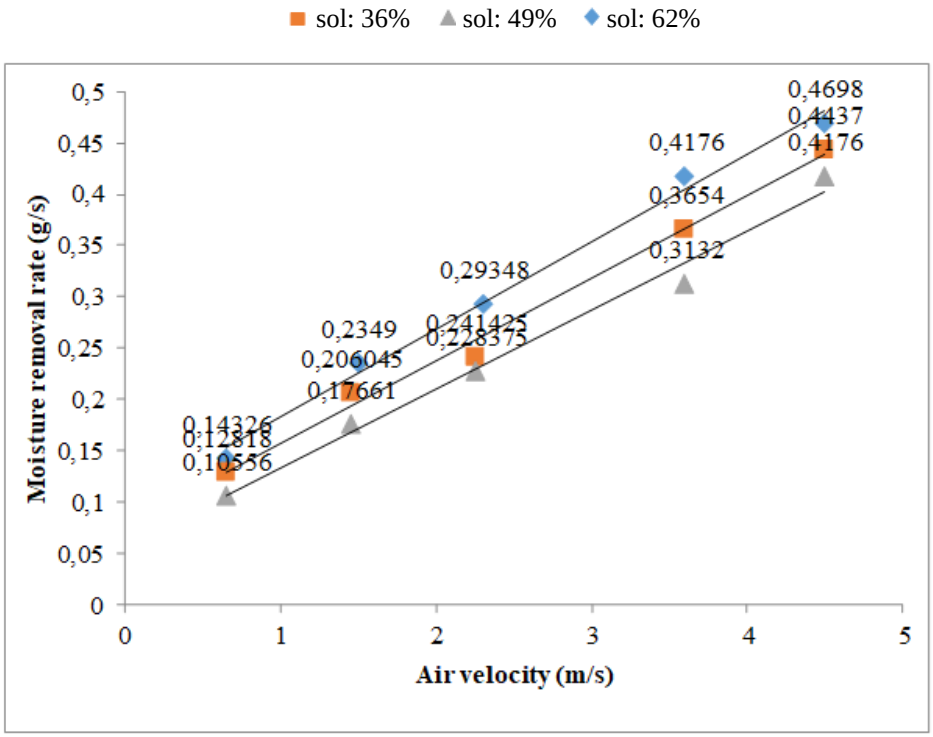


Figure 154. The dehumidifier moisture removal rate trends at solution concentration (T_{in}= 35ºC, RH=60%)

Figure 155 shows the variations of cooling capacity with respect to various inlet air velocities under different solution concentration ratio for T_{in} = 35ºC, inlet RH=60%. It can be found that as the air velocity is increased, the cooling capacity increases together by increasing of absolute humidity difference. The increasing of solution concentration ratio also causes to increase cooling capacity. For example, at air velocity of 1.5m/s, the cooling capacity increases from 0.31kW to 0.53kW and finally 0.74kW (average 58.2% increase) as the solution concentration improves from 36% to 49% and 62%.

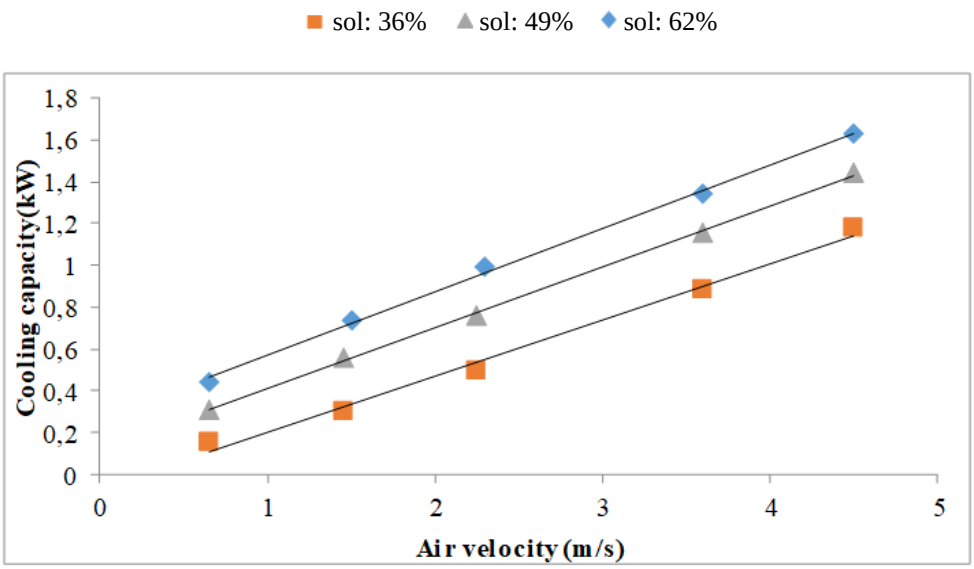


Figure 155. The cooling capacity trends at different solution concentration (T_{in}= 35ºC, RH=60%)

Higher solution concentration ratio also leads to better dehumidifier effectiveness, as demonstrated in Figure 156. The increasing of the desiccant solution mass concentration from 36%, 49% and to 62%, increases the latent effectiveness from 0.084 to 0.197, 0.118 to 0.25 and 0.156 to 0.296, respectively.

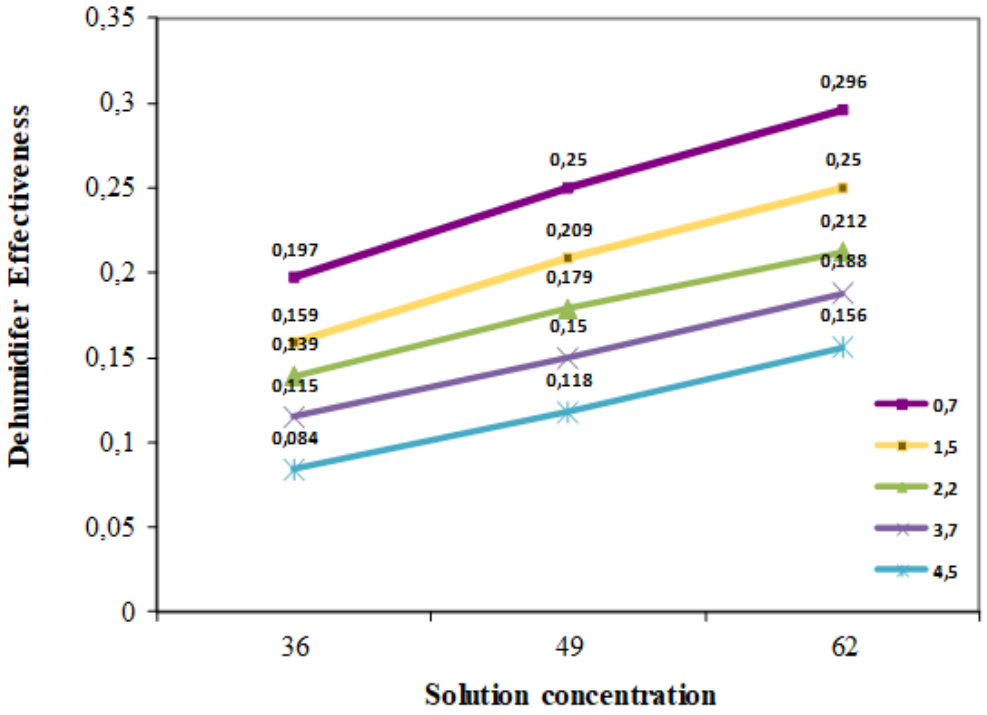


Figure 156. The cooling capacity trends at solution concentration (Tin= 35ºC, RH=60%)

6.5 A comparison of experimental study on eucalyptus fibres and hollow fibres

The evaporative cooling method is an environment-friendly technology which has been proposed as an alternative to vapour compression AC system. The direct evaporative cooling system is used in hot and dry regions where the relative humidity is low. However, the direct evaporative cooling system is less effective in humid regions, thus it can be used in conjunction with desiccant dehumidification. In accordance to literature, the researchers are interested in investigating the potential of the direct evaporative cooling system and desiccant based evaporative cooling system in different climatic conditions. In this part of the chapter, the experimental results are compared in between direct evaporative cooling system and desiccant-based evaporative cooling system. In this respect, eucalyptus fibres based evaporative cooling system, hollow fibres based evaporative cooling system by using water and hollow fibres based

desiccant evaporative cooling system by using potassium formate are compared for different climatic regions of Cyprus.

In hot Cyprus climate, it is important to reduce the air temperature in order to enhance thermal comfort level. For humid regions, reducing the moisture level of the air is as necessary as cooling. High level of moisture affects both the occupant health condition and building itself by the mildew and mould growth. In this study, the water is used as a working fluid in direct evaporative cooling system in two different testing module. In these modules, eucalyptus fibres and polymer hollow fibres were used as pad in direct evaporative cooling system. These can be suggested to be used in hot and dry regions of Cyprus where it is in inland regions (Figure 157). For hot and humid coastal regions, the dehumidification and cooling of ambient air should be proposed to remove the moisture from the air. Thus, desiccant should be used in order to dehumidify the air by absorbing moisture and the air is then cooled by direct evaporative cooling system. As a working fluids, the potassium formate is used in desiccant based evaporative cooling system where it is suggested to be used in coastal regions of Cyprus (Figure 157).

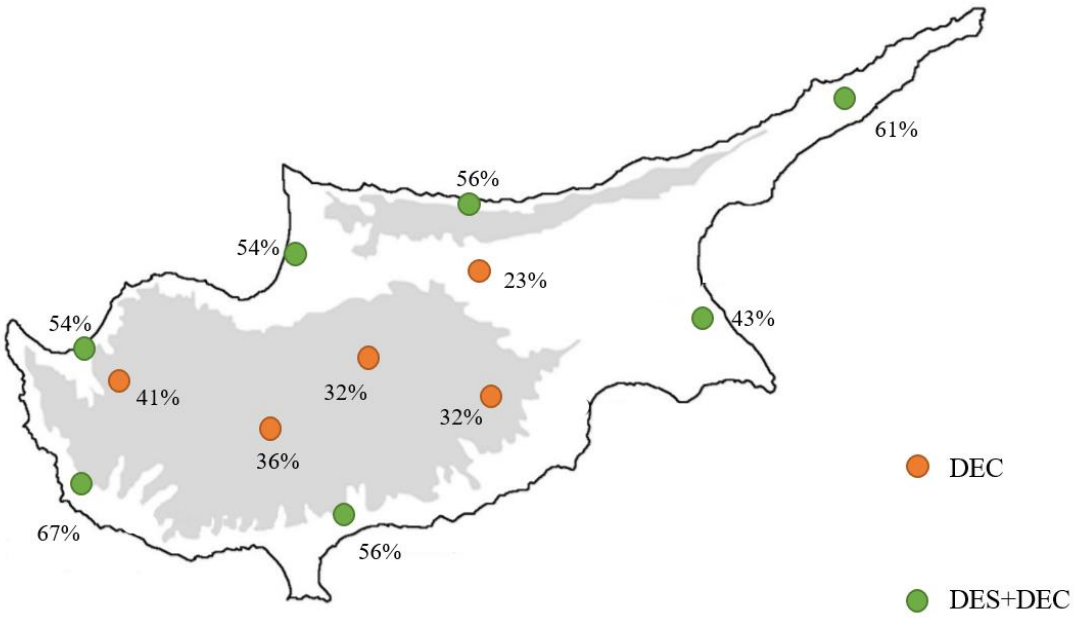


Figure 157. Suggestion of EC strategies on different geographic location of Cyprus

As seen in Table 35, the testing results of direct evaporative cooling system by using eucalyptus fibres and hollow fibres for hot and dry regions and the testing results of desiccant based evaporative cooling system by using potassium formate are presented. The cooling performance of these testing includes temperature difference, cooling efficiency and cooling capacity. The moisture removal rate is also shown for desiccant based evaporative cooling system since reducing of moisture is as important as cooling. These various performance factors are experimentally evaluated.

According to the testing results, it is seen that hollow fibres based EC system has better performance than local eucalyptus fibres based EC system. This is due to the surface area of the hollow fibres bundle are larger than eucalyptus fibres panel. The surface area of both materials are not the same as they are different structural combinations. The components and fittings of the materials are differently combined as they are natural and man-made materials. Their geometrical configuration, size and thickness are in different shape and scale which makes the testing panel not easy to develop a standard testing unit. Therefore, they can be both suggested for hot and dry inland. The area of application may be differ due to the cost of manufacturing of the systems and the size of the buildings that are used. The local based DEC can be used in residential buildings, whereas the man-made DEC can be suggested to use in commercial and industrial buildings. For desiccant based evaporative cooling system, MRR becomes higher by increasing air velocity since the mass flow rate is a function of moisture removal rate.

Table 35. Testing results of the experimentations

	Air velocity (m/s)	**ΔT (°C)**	**ης (%)**	**Q (W)**
Eucalyptus fibres based DEC (water) **hot-dry**	0.3	8.1	52	239
	0.6	5.7	42	350
	0.9	4.1	24	404
	1.2	3.1	27	518
Hollow fibres based DEC (water) **hot-dry**	0.3	19.9	96	330
	0.6	20.2	94	480
	0.9	20.7	91	700
	1.2	21.05	88	840
	Air velocity (m/s)	**MRR (g/s)**	**ης (%)**	**Q (W)**
Hollow fibres Desiccant EC (KCOOH) **hot-humid**	0.3	0.43	39	745
	0.6	0.46	37	870
	0.9	0.49	35	1050
	1.2	0.57	34	1120

Table 36 provides the experimental results of eucalyptus fibres based evaporative cooling, hollow fibres based evaporative cooling by using water and desiccant based evaporative cooling by using potassium formate. The summary of the comparison indicates that local eucalyptus fibres based evaporative cooling system has an overall advantage compared to hollow fibres based evaporative cooling. However, it is worth mentioning that the cooling performance is higher for hollow fibres in both cooling systems. Thus, it can be concluded that direct evaporative cooling system by using eucalyptus fibres and hollow fibres can be used in hot and dry inland regions. Whereas,

desiccant based evaporative cooling system by using potassium formate can be sued in hot and humid coastal regions in Cyprus.

Table 36. Comparative summary of evaporative cooling systems

	EF based EC	***HF* based EC**	**HF based desiccant EC**
Cooling fluid	water	water	potassium formate
Climate	hot-dry	hot-dry	hot-humid
Material replacement	easy to replace	not easy to replace	not easy to replace
Cost	cheap	not very cheap	not very cheap
System instalment	easy to install	not easy to install	not easy to install
Humidity control	moisture is added	moisture is added	moisture is dehumidified
Energy source	very low grade heat source	low grade heat source	low grade heat source

6.6 Conclusion

The cooling pad plays a vital role in cooling performance of the evaporative cooling systems. Different types of evaporative pads can be used in different climatic conditions. As Cyprus is hot and dry climates in inland regions and hot and humid climates in coastal regions, the same material cannot be available for different climatic conditions. In this chapter, polymer hollow fibres are experimentally tested in a module of direct evaporative cooling system by using water as a working fluids for hot and dry regions. In addition to this, polymer hollow fibres are tested by using potassium formate as a desiccant in order to dehumidify the ambient air for hot and humid regions. Following that section, the experimental results of local material, eucalyptus fibres and hollow plastic fibres were evaluated by comparing the results of temperature difference, cooling efficiency and cooling capacity of the materials for evaporative cooling method. Thus, the experimental results of both evaporative cooling materials (pads) are compared to present the cooling performances in different climatic regions in this chapter.

Regarding the testing of hollow fibre integrated evaporative cooling system, it constitutes as the evaporative cooler and as dehumidifier. Since hollow fibre is light weight, corrosion resistant and low cost materials, it is used to ascertain the performance of the material under different conditions. The performance of the fibres are analysed based on the effects of inlet air velocity, temperature and humidity on temperature difference, relative humidity, cooling efficiency, cooling capacity, COP and evaporation rate. According to this, the main conclusions in these 3 different test results conclusions are:

1. *Hollow fibre integrated evaporative cooling system with bundles in a horizontal cylinder test module*

- Increase the inlet air dry bulb temperature will lead to the increase of the outlet air dry bulb temperature, cooling efficiency and cooling capacity. At the same inlet air dry bulb temperature, increase the inlet air relative humidity will lead to the decrease of cooling capacity, wet bulb effectiveness and dew point effectiveness. At inlet dry bulb air

temperature of 30°C, 35°C and 40°C, the average temperature differences are 1.86°C, 4.03°C and 4.66°C at the 25%inlet air RH and at 0.6 m/s constant air velocity respectively.

- By increasing air velocity from 0.6m/s to 2.5m/s, the outlet air RH is increased to 29-32% at 24% inlet air RH, increased to 58-61% at 50%. This shows that the air velocity had a small effect on relative humidity ratio.

- When inlet air dry bulb temperature is increased from 30-40°C, the cooling efficiency is increased from 35% to 39% at 40% inlet air RH, from 38% to 45% at 23% inlet air. In other words, the cooling efficiency is reduced by increasing inlet RH.

- The cooling capacity was increased to 99 W, 118, 121, 132, 152 and 167 W at 1.2, 1.5, 1.7, 1.9, 2.2 and 2.5 m/s, respectively by increasing the air flow.

- The highest COP value occurred at 2.5 m/s air velocity with 2.6 and the minimum COP value was observed at 1.2 m/s air velocity as 1.7.

2. *Hollow fibre integrated evaporative cooling system with bundles in circular module*

- At inlet dry bulb air temperature of 35°C, the temperature differences are 15.2°C, 9.97°C and 8.66°C at 23%, 32% and 40% inlet air RH, respectively.

- By increasing air velocity from 0.25m/s to 3.5m/s, the outlet air RH is reduced from 93% to 75% at 23% inlet air RH, 88% to 70% at 32% inlet air RH and 84% to 65% at 40% inlet air RH.

- When air velocity is increased from 0.25m/s to 3.5m/s, the cooling efficiency is reduced from 97% to 71% at 23% inlet air RH, 100% to 74% at 32% inlet air RH and 103% to 78% at 40% inlet air RH.

- The cooling capacity is increased by increasing air velocity at 3.5m/s to 2300W, 2000W and 1750W, at inlet RH of 23%, 32% and 40%.
- The COP is between 1.72 and 13.8.

3. *Hollow fibre integrated evaporative cooling system with potassium formate (*KCOOH*) desiccant dehumidification.*

- Evaluation at different inlet air dry bulb temperature and RH

  The MRR is increased by higher of inlet air dry bulb temperature from 35ºC to 40ºC and by increasing of RH from 55% to 75%. It is increased from 0.48g/s to 0.79g/s at 35ºC inlet air temperature and at 70% RH.

  The cooling capacity of dehumidifier is increased from 0,84kW to 1,92kW from 0,7m/s to 3,6m/s at 35ºC inlet air temperature and 70%RH.

  At higher incoming air velocity, the dehumidifier effectiveness is declined from 0,37 to 0,25 at 35ºC. It is also increased by increasing of RH.

- Evaluation at different air velocity

  The moisture removal rate is increased as the air velocity from 0.5m/s to 3.5m/s and inlet RH are increased from 60% to 70%. Take the air velocity at 3.5m/s, the moisture removal rate is 0.42g/s, 0.56g/s and 0.79g/s respectively for incoming air relative humidity of 60%, 65% and 70%.

  The cooling capacity is also increased as the air velocity is increased. At 3.5m/s, the cooling capacity is 1340 W, 1530 W and 1920 W respectively for incoming air relative humidity of 60%, 65% and 70%.

  The humidifier effectiveness is also reduced as the air velocity is increased and inlet RH is reduced.

- Evaluation at different mass concentration solution

  At higher air velocity and at higher concentration solution, the moisture removal rate is increased. At lowest air velocity (0,7m/s), the MRR is 0,11g/s, 0,13g/s and 0,14g/s for solution concentration 36%, 49% and 62%, respectively.

  As the air velocity is increased, the cooling capacity increases together by increasing of absolute humidity difference.

  The increasing of solution concentration ratio also causes to increase cooling capacity. For example, at air velocity of 1.5m/s, the cooling capacity increases from 0.31kW to 0.53kW and finally 0.74kW (average 58.2% increase) as the solution concentration improves from 36% to 49% and 62%. Higher solution concentration ratio also leads to better dehumidifier effectiveness. The increasing of the desiccant solution mass concentration from 36%, 49% and to 62%, increases the latent effectiveness from 0.084 to 0.197, 0.118 to 0.25 and 0.156 to 0.296, respectively.

This chapter was based on experimental work on evaporative cooling using polymer hollow fibres for three types of system module. Each tests were conducted in a controlled environment with various inlet air dry bulb temperature, relative humidity and air velocity. It was found that with the first test module (*Hollow fibre integrated evaporative cooling system with bundles in a horizontal cylinder test module*), little temperature reduction was found compared to *Hollow fibre integrated evaporative cooling system with bundles in circular module (with water)* and *Hollow fibre integrated evaporative cooling system with potassium formate (*KCOOH*) desiccant dehumidification.* There were significant temperature drop at both systems. The hollow fibre module used with water can be suggested for hot and dry regions whereas the system used by desiccant liquid can be suggested to be used in hot-humid regions.

Chapter 7: Conclusion and Recommendations

The application, research and development of evaporative cooling process have been using since pre-scientific eras. Many theoretical and experimental research are still continuing on the feasibility of the process for different climatic conditions. The cooling process is occurred by the evaporation of water which makes the process environmentally-friendly cooling method since water is used as a working fluid. This reduces the using of chorofluorocarbon (CFCs) and hydrochlorofluorocarbon (HCFCs) in the vapour compression systems as they have negative impacts on global warming and ozone layer depletion.

In this respect, the aim of this study was to reduce the energy consumption and environmental problems by investigating the potential of evaporative cooling process based on direct evaporative cooling and as explained in Chapter 1.

The research firstly began with the literature review of one of the passive cooling methods of evaporation cooling including direct, indirect, direct/indirect and desiccant evaporative cooling in different climates. The literature review of DEC covered the using of local and artificial materials in particular porous, non-porous, fibres materials, etc. as an evaporative pad and integration of this material into building elements. The review of desiccant based evaporative cooling system mostly covered the experiments done by using liquid desiccant evaporative cooling system such as LiBr, LiCl, $CaCl_2$, etc.

Following that, the potential of water harvesting methods were reviewed to study and compare the new development of obtaining water in some regions with Cyprus condition. Since water is essentially required for evaporative cooling process, the new technologies and potential of using it for Cyprus should be reviewed before proposing new materials and systems for the process in Cyprus.

The study then continued with the experimental investigations which were carried out at the laboratory to investigate the potential of evaporative cooling. The experimental investigations were done in respect to parameters which affect their cooling performance. Experimental investigations have been conducted by two types of experimental units including different local materials for evaporative cooling process. At first, local materials were tested under small scale preliminary testing. The eucalyptus fibres and yellow stone have chosen to be tested under the wind tunnel experiments. Since they had higher cooling efficiency compared to other local materials. The wind tunnel experiment were carried out under two stages: the first one was the comparison of two local materials and selection of better candidate of material. The second one is for focusing one of them which had higher cooling efficiency and investigating the effect of operating parameters for eucalyptus fibres performance. The average cooling efficiency of eucalyptus fibres was 42% and produced 350W cooling capacity, water consumption rate of 0,203g/s at 0.6m/s air velocity and achieved a COP of 3.54 under more controlled conditions. Specific cooling capacity was reduced by increasing air velocity, meaning the air velocity should be lower to save more water for the process.

During experimentation, it was found that the cooling performance was higher at higher inlet air dry bulb temperature and lower RH. As a result, it had been found that inlet dry air temperature, RH and inlet air velocity influenced the cooling performance of the materials. It can be concluded that this material can works better in hot and drier part of Cyprus. According to the performance evaluation of eucalyptus fibres in terms of SCC, CC, COP, mass flow rate and evaporation rate, the optimum design conditions were obtained as stated in section 3.3.4. Following this, the conceptual design ideas of integrated eucalyptus fibres based evaporative cooling into building elements were studied in particular, shutter, fenestration, toplighting elements, wind cather/solar chimney and wall.

Based on the results, evaporative cooling works well for climates where the air is hot and relative humidity is low. Therefore, direct evaporative cooling system by using eucalyptus fibres could be proposed for hot and dry region of

Cyprus. The various factors such as availability, saturation efficiency, cost, application and environment should be considered during the selection of pad materials. Compared to commercial pads such as celdek pad, aspen pad, cellulosic pad, rigid pad, etc. the local material, eucalyptus fibres are local, cheap and light weight. Although commercial materials have good saturation efficiency, they are more expensive due to their preparation, material and fabrication processing costs. Eucalyptus fibres provides good cooling efficiency and high cooling capacity per kg of water consumption. Since this local material is abundant, environmentally friendly, has higher water holding capacity and long life span, it can be an alternative material that can be used as evaporation pad in evaporative cooling systems.

During the testing, hollow fibre was used to evaluate the cooling performance for evaporative cooling. Hollow fibres were integrated into evaporative cooling system as a humidifier. Through the hollow fibres, the water vapour can pass effectively and the liquid water droplets will be prevented from mixing with the air. In order to prevent flow channelling and covering of the adjacent fibres, the fibres inside each bundle were made of spindle shape to provide maximum contact of water inside the fibres with air.

Three different testing have been conducted at the laboratory in order to evaluate the performance of hollow fibres. The first experiment was a small scale test rig resulting lower cooling efficiency of 15-27% at 30-40°C inlet air dry bulb temperature. It produced 99W to 167W cooling capacity with lower COP of 1.7 to 2.6. It can be concluded that the test module could be developed to improve the cooling efficiency and COP.

In the following testing, the fibre manifold configuration was changed by increasing the number and size of fibres to evaluate the cooling performance of hollow fibres. In achieving this, hollow fibres were integrated with bundles in large scale circular module. The water was used as a working fluid through the fibres. Based on the result, the temperature difference were 15.2°C, 9.97°C and 8.66°C at the 23%, 32% and 40% inlet air RH, respectively. Cooling efficiency was also increased by reducing air velocity and inlet RH. Thus, the hollow

fibre integrated evaporative cooling system with bundles in circular module could be proposed to be used for hot-dry region in Cyprus.

At the third testing, the previous module (bundles with circular module) had been carried out, but potassium formate was used as a working fluid instead of water. In this testing, desiccant based evaporative cooling system was tested for hot-humid region of Cyprus since it was considered that the performance of cooling system can be improved by using desiccant. The results showed that the MRR of hollow fibres was increased by higher inlet air dry bulb temperature, air velocity and at higher concentration solution. It was increased to 0.79g/s at 35°C inlet air temperature and at 70% RH. The cooling capacity was also increased as the air velocity was increased. It should be noticed that by increasing of mass concentration to 62%, the latent effectiveness was increased from 0.084 to 0.296.

The results showed that hollow fibre integrated desiccant based evaporative cooling can provide better thermal comfort in hot and humid regions of Cyprus whereas direct evaporative cooling by using eucalyptus fibres as a pad material are not applicable in hot-humid regions. The liquid desiccant system could be used to achieve comfort where DEC could not provide optimum thermal comfort conditions in hot and humid regions.

A house in Cyprus was modelled by using Ecotect to calculate the monthly cooling loads of the house. After brief description of climatic condition of Cyprus, the environmental geometrical, constructional and thermal conditions of modelled house were reviewed. According to the test results, the cooling capacity of $1m^2$ of eucalyptus fibres panel was calculated as 5.7kW monthly cooling capacity was found to be 1710kWh per m^2. It was found that this system mostly covered the cooling load for each month. In addition to this, the payback period was calculated as 6.5 years. When compared to the cumulative sum of air conditioning with evaporative cooling by eucalyptus fibre, the total saving was €1075. Results show that evaporative cooling system using eucalyptus fibres has a reasonable payback period. Thus, it has the potential to be replaced with vapour compression AC system. This would provide both cost

saving and reduction in GHGs emissions in AC application for buildings. Regarding the environmental analysis, CO_2 savings would be 4.9475 tonnes.

Although the water scarcity is not a major problem in Cyprus, there is a water shortage problem in regions such as Africa and some parts of Asia. However, there are many developing technology for water harvesting to be used in evaporative cooling system. Since water is a significant requirement for evaporative cooling process, it should be continuously provided to supply water to the process. Thus, some water harvesting methods or technologies should be incorporated to the evaporative cooling system to keep the pads wet. The application and feasibility of evaporative cooling system can be improved in such locations by "integrated water harvesting-evaporative cooling technologies". In this context, atmospheric water generation technologies, desalination system for seawater and rainwater harvesting systems could be used to produce required water for evaporative cooling system.

The improvements of water quality should also be considered to lower maintenance cost of the system. In addition to this, the quality of air is related to the water quality thus, the water should be filtered or cleaned for the process in order to improve indoor air quality.

Evaporative cooling works better in drier region. However, less efficient in humid regions. Liquid desiccant based evaporative cooling could solve this problem in order to dry the humid air. Since high humidity causes some problems such as mould growth, limitation of evaporation from the body for occupants and buildings in Cyprus during hot seasons, the liquid desiccant evaporative cooling system could be proposed in order to dehumidify the air by absorbing water vapour and prevent the problem related to high humidity. DEC by using local material could also be proposed in conjunction with the desiccant based evaporative cooling system in order to improve thermal conditions in humid regions. The experimental investigation could be improved to combine both process in order to evaluate the performance for Cyprus condition.

The development of conceptual design ideas of integrated evaporative cooling system into building design is aimed to increase the public awareness of the role of architectural design on cooling method. This architectural perspective provides opportunities for widening the knowledge of the integration of evaporative cooling system into architecture which is one of the old technology. It should be emphasized that the old and traditional evaporative cooling idea is combined with the new technological opportunities for architectural building design. As an architect, it is believed that the application of such ideas increases the attention of several designers and public. These proposed ideas can be easily integrated into existing and new buildings. It can be concluded that these simple and practical ideas reduce the demand of energy on cooling by introducing effective cooling methods into architecture.

As final recommendations, the application of eucalyptus fibres can be improved by compressing the material inside of the meshed structure in order to prevent dropping of the fibres in the fabrication process. For desiccant system, since energy is required for the system, the solar energy can be integrated to the evaporative cooling system as Cyprus has a remarkable solar potential. This potential can be used to meet the cooling demand in summer by utilizing this system. In addition to this, both DEC and desiccant based EC system can be powered by photovoltaic panels in particular for regions where electricity is not available.

The future works on proposed evaporative cooling systems can includes further experimentations by modifying material's size, thickness, shape, etc. and structural configurations. In addition to this, public awareness can be promoted in order to encourage people to use these systems for sustainable development. The development and application of evaporative cooling systems can also be increased by government regulations. Finally, the manufacturing and marketing of evaporative cooling system can be supported for cooling industry.

REFERENCES

A

ABOHORLU, P., (2010). *Investigation of Traditional Cypriot Houses In The Areas Around The "Five Fingers" Mountain Range Of North Cyprus Regarding The Climatic Parameters*, unpublished master thesis, Near East University, Cyprus, pp. 3-92.

ABOHORLU, P., KURT, S., (2017). *Traditional Earth Sheltered Buildings on Five Finger Mountain (Cyprus) Evaluation of the Energy Efficiency by Computer Simulating the Rectangular Plan Typology*, Prostor: a scholarly journal of architecture and urban planning, Vol. 25, No. 1(53), 98-111.

AHMAD, M. I., ISMAIL, M., & RIFFAT, S. (2016). *Renewable Energy and Sustainable Technologies for Building and Environmental Applications:* Options for a Greener Future.

AL-FAHED, S. F., ALASFOUR, F. N., & QUADRI, M. M. (2014). *Pottery Evaporative Cooling System: A Novel Approach to Cool Inlet Air with Minimal Change in Relative Humidity and Low Water Consumption.* Experimental Heat Transfer, 27(2), 144-159. doi:10.1080/08916152.2012.757675.

AL-HASSAN, G. A. (2009). Fog Water Collection Evaluation in Asir Region– Saudi Arabia. *Water Resources Management*, *23*(13), 2805-2813.

AL-SULAIMAN, F. (2002). *Evaluation of the performance of local fibers in evaporative cooling*. Energy Conversion and Management, 43(16), 2267-2273.

ALI, M. T., FATH, H. E., ARMSTRONG, P. R. (2011). *A comprehensive techno-economical review of indirect solar desalination*. Renewable and Sustainable Energy Reviews, 15(8), 4187-4199.

American Society of Heating, Refrigeration and Air-conditioning Engineers (ASHRAE), Inc. Standard S19 - *Evaporative Air Cooling Equipment*, 2000.

American Society of Heating, Refrigeration and Air-conditioning Engineers (ASHRAE), Inc. Standard A50 – *Evaporative Cooling Applications*, 1999.

American Society of Heating, Refrigeration and Air-conditioning Engineers (ASHRAE), Inc. Standard F3 – *Heat Transfer*, 1997.

American Society of Heating, Refrigeration and Air-conditioning Engineers (ASHRAE), Inc. Standard F6 – *Psychrometrics*, 1997.

ANON, (2017). [online] Available at: http://www.cyi.ac.cy/system/files/Manfred%20Lange_Abstract.pdf [Accessed 18 May 2017].

ASHRAE Standard 55 (2004). *Thermal Environmental Conditions for Human Occupancy*, Atlanta, ASHRAE Inc.

ASHRAE Standard 62-2001, Ventilation for Acceptable Indoor Air Quality.

ATIKOL, U., HACIŞEVKI, H., (2001). *Lefkoşa Bölgesi için Evaporatif Soğutma Fizibilite Çalışması.* İzmir, Turkey, KTMMOB Chamber of Mechanical Engineers.

AYDIN, D., CASEY, S. P., & RIFFAT, S. (2015). *Theoretical analysis of the potential for thermochemical heat storage under Mediterranean climate conditions: Northern Cyprus Case. Future Cities and Environment, 1(1).*

B

BACA, I. M., TUR, M., GONZALEZ, J. N., ROMÁN, C. A., (2011). *Evaporative cooling efficiency according to climate Conditions,* Procedia Engineering, Vol. 21 pp. 283 – 290.

BAHADORI, M. N., SAYIGH, A., DEHGHANI-SANIJ, A., (2014). *Wind Towers: Architecture, Climate and Sustainability*. (Springer eBooks.) Cham: Springer International Publishing.

BAKER, N., (1987). *Passive and Low Energy Building Design for Tropical Island Climates,* Commonwealth Secretariat Publications, London, p. 114.

BANIK, P., GANGULY, A. (2017). *Performance and economic analysis of a floricultural greenhouse with distributed fan-pad evaporative cooling coupled with solar desiccation*. Solar Energy, 147, 439-447.

BATISHA, A. F., (2003). *Fog Collection As A Complementary Water Resource In Egypt,* Seventh International Water Technology Conference IWTC7, Egypt.

BERGMAIR, D., METZ, S., DE LANGE, H., & VAN STEENHOVEN, A. (2014). *System analysis of membrane facilitated water generation from air humidity.* Desalination, 339, 26-33.

BEYER R, STEIGER M. (2010). *Vapor Pressure Measurements of NaHCOO + H(2)O and KHCOO + H(2)O from 278 to 308K and Representation with an Ion Interaction (Pitzer) Model*. J Chem Eng Data;55:830–8.

BRADSHAW, V., (2006). *The Building Environment: Active and Passive Control Systems,* John Wiley & Sons, Canada, pp. 4-216.

BROOKS, D. B., MEHMET, O. (2014). *Water Balances in the Eastern Mediterranean*. International Development Research Center, IDRC Books / Les editions du CRDI.

BROWN, G. Z., DEKAY M., (2001). *Sun, Wind and Light: Architectural Design Strategies,* John Wiley & Sons, Canada, pp. 18-79.

BROWN, P. S., BHUSHAN, B. (2016). *Bioinspired materials for water supply and management: water collection, water purification and separation of water from oil*. Philosophical Transactions of the Royal Society A: Mathematical, Physical and Engineering Sciences, 374(2073), 20160135.

BUI, D. T., NIDA, A., NG, K., CHUA, K. (2016). Water vapor permeation and dehumidification performance of poly(vinyl alcohol)/lithium chloride composite membranes. Journal of Membrane Science, 498, 254-262.

C

CALAUTIT, J. K., HUGHES, B. R., O'CONNOR, D., SHAHZAD, S. S. (2017). *Numerical and experimental analysis of a multi-directional wind tower integrated with vertically-arranged heat transfer devices (VHTD).* Applied Energy, 185, 1120-1135.

CAMARGO, J. R., EBINUMA, C. D., SILVEIRA, J. L., (2005). *Experimental performance of a direct evaporative cooler operating during summer in a Brazilian city*, International Journal of Refrigeration, Vol.28, pp. 1124–1132.

CAO, M., XIAO, J., YU, C., LI, K., JIANG, L. (2015). *Hydrophobic/Hydrophilic Cooperative Janus System for Enhancement of Fog Collection.* Small, 11(34), 4379-4384.

CELdek*5090-15 Evaporative cooling. http://www.Munters.com [accessed on 15/06/2018].

CELdek*7090-15 Evaporative cooling. http://www.Munters.com [15/06/2018].

CHAIBI, M. T. (2000). *An overview of solar desalination for domestic and agriculture water needs in remote arid areas.* Desalination, 127(2), 119–133.

CHAN, H., RIFFAT, S. B., & ZHU, J. (2010). *Review of passive solar heating and cooling technologies.* Renewable and Sustainable Energy Reviews, 14(2), 781-789.

CHANDRASHEKARA, C., YADAV, A. (2017). *Water desalination system using solar heat: A review*. Renewable and Sustainable Energy Reviews, 67, 1308-1330.

CHEN, W., (2011). *Thermal analysis on the cooling performance of a wet porous evaporative plate for building,* Energy Conversion and Management, Vol.52 pp. 2217-2226.

CHEN, Z., ZHU, J., & BAI, H. (2017). *Performance assessment of a membrane liquid desiccant dehumidification cooling system based on experimental investigations.* Energy and Buildings, 139, 665-679.

CHEN, X., et al., (2016). *Recent research developments in polymer heat exchangers – A review.* Renewable and Sustainable Energy Reviews, 60: p. 1367-1386.

CHEN, X., et al., (2016). *Experimental investigations of polymer hollow fibre heat exchangers for building heat recovery application*. Energy and Buildings, 125: p. 99-108.

CHEN, X., SU, Y., AYDIN, D., ZHANG, X., DING, Y., REAY, D., RIFFAT, S. (2017). *Experimental investigations of polymer hollow fibre*

integrated evaporative cooling system with the fibre bundles in a spindle shape. Energy and Buildings, 154, 166-174.

CHEN, X., SU, Y., AYDIN, D., DING, Y., ZHANG, S., REAY, D., RIFFAT, S. (2018). *A novel evaporative cooling system with a polymer hollow fibre spindle*. Applied Thermal Engineering, 132, 665-675.

CHIARI, A., (2000). *Air humidification with membrane contactors: experimental and theoretical results.* International journal of ambient energy, 21(4): p. 187-195.

CHOI, W. K., YOO, K. D., SUH, S. J., (2004). *Application of Suncatcher System for the North in Building.* Proceedings ISEA Asia-Pacific, 2004.10, 882-891.

CONNELLY, K., WU, Y., CHEN, J., & LEI, Y. (2016). *Design and development of a reflective membrane for a novel Building Integrated Concentrating Photovoltaic (BICPV) 'Smart Window' system*. Applied Energy, 182, 331-339.

COUPPIS, T. A., (1956). *Reclamation of sand dunes with particular reference to Ayia Erini sand drifts, Cyprus.* Empire Forestry Rev: 77-84.

CRAWLEY, D. B., HAND, J. W., KUMMERT, M., GRIFFITH, B. T. (2008). *Contrasting the capabilities of building energy performance simulation programs.* Building and Environment, 43(4), 661-673.

D

DAGTEKIN, M., KARACA, C., YILDIZ, Y., BASCELIK, A., PAYDAK, O., (2011). *The effects of air velocity on the performance of pad evaporative cooling systems*. African Journal of Agricultural Research, Vol. 6(7) pp. 1813-1822.

DAI, Y. J., ZHANG, H. F., (2004). *Numerical simulation and theoretical analysis of heat and mass transfer in a cross flow liquid desiccant air dehumidifier packed with honeycomb paper*. Energy Conversion and Management 45, 1343-1356.

DAOU, K., WANG, R., & XIA, Z. (2006). *Desiccant cooling air conditioning: a review*. Renewable and Sustainable Energy Reviews, 10(2), 55-77.

DE MARCHI, B., FUNTOWICZ, S., LO CASCIO, S., & MUNDA, G. (2000). *Combining participative and institutional approaches with multicriteria evaluation. An empirical study for water issues in Troina, Sicily*. Ecological Economics, 34*(2),* 267-282.

DEHGHANI-SANIJ, A., SOLTANI, M., RAAHEMIFAR, K. (2015). *A new design of wind tower for passive ventilation in buildings to reduce energy consumption in windy regions.* Renewable and Sustainable Energy Reviews, 42, 182-195.

DEMETRIOU, C., GEORGIOU, A., (2004). *Management of groundwater resources in Cyprus—Harmonisation with the EU Water Framework Directive.* In Proceedings of the BALWOIS 2004 Ohrid, FY Republic of Macedonia.

Directive 2010/30/EU of the European Parliament and of the Council of 19 May 2010 on the indication by labelling and standard product information of the consumption of energy and other resources by energy-related products.

DOMÈNECH, L., MARCH, H., SAURÍ, D. (2013). *Degrowth initiatives in the urban water sector? A social multi-criteria evaluation of non-conventional water alternatives in Metropolitan Barcelona*. Journal of Cleaner Production, 38, 44-55.

DUBE, D. K., REDDY, R. U., & YADAV, R. H. (2013). *Ground Water Harvesting through Traditional Water Harvesting Technology: Adopting Himalayan Practices in Ethiopian Highlands*. International Journal of Geosciences, 04(06), 30-37.

DUKES, (2017). *Energy Consumption in the UK*, Available from: https://assets.publishing.service.gov.uk/government/uploads/system/uploads/attachment_data/file/633503/ECUK_2017.pdf [Accessed: 4 May 2018].

E

EBNER, M., MIRANDA, T., ROTH-NEBELSICK, A. (2011). *Efficient fog harvesting by Stipagrostis sabulicola (Namib dune bushman grass).* Journal of Arid Environments, 75(6), 524-531.

EIFFERT, P., (2003). G*uidelines for the economic evaluation of building-integrated photovoltaic power system.* National Renewable Energy Laboratory: Colorado (USA). NREL/TP-550-31977.

ELMER, T., WORALL, M., WU, S., & RIFFAT, S. (2016). *An experimental study of a novel integrated desiccant air conditioning system for building applications.* Energy and Buildings, 111, 434-445.

ELSARRAG, E., IGOBO, O. N., ALHORR, Y., & DAVIES, P. A. (2016). *Solar pond powered liquid desiccant evaporative cooling*. Renewable and Sustainable Energy Reviews, 58, 124-140.

F

FANG, L., CLAUSEN, G., AND FANGER, P.O., (1998) *Impact of Temperature and Humidity on the Perception of Indoor Air Quality,* Indoor Air, 8: 80–90.

FARMER, A., AUFENANGER, V., BASSİ, S., BRİNK, P., ANDERSON, J., (2006). *Strategic Evaluation on Innovation and the knowledge based economy in relation to the Structural and Cohesion Funds, for the programming period 2007-2013:* Country report Cyprus.

FARRENY, R., MORALES-PINZÓN, T., GUISASOLA, A., TAYÀ, C., RIERADEVALL, J., GABARRELL, X. (2011). *Roof selection for rainwater harvesting: Quantity and quality assessments in Spain.* Water Research, 45(10), 3245-3254.

FATHY, H., (1986). *Natural Energy and Vernacular Architecture: Principles and Examples with Reference to Hot-Arid Climates*, The University of Chicago Press Ltd., London, pp. 404.

FLORIDES G.A., TASSOU, S.A. KALOGIROU, S.A., WROBEL, L.C., (2001). Evolution of domestic dwellings in Cyprus and energy analysis, *Renewable Energy 23, pp. 219–234.*

FREEWAN, A. A. (2015). *Developing daylight devices matrix with special integration with building design process.* Sustainable Cities and Society, 15, 144-152.

FOURIER, J., (1824). "*Remarques Générales sur les Températures Du Globe Terrestre et des Espaces Planétaires." Annales de Chemie et de Physique* 27: 136-67. Translation by Ebeneser Burgess, "General Remarks on the Temperature of the Earth and Outer Space," *American Journal of Science* 32: 1-20 (1837).

FRANCO, A., VALERA, D. L., PENA, A., (2014). *Energy Efficiency in Greenhouse Evaporative Cooling Techniques: Cooling Boxes versus Cellulose Pads,* Energies, Vol. 7(3), pp. 1427-1447

FRANCO, A., VALERA, D. L., PENA, A., PEREZ, A. M., (2011). *Aerodynamic analysis and CFD simulation of several cellulose evaporative cooling pads used in Mediterranean greenhouses*, Computers and Electronics in Agriculture, Vol. 76, pp. 218–230.

FUMO, N. & GOSWAMI, D. Y., (2002). *Study of an aqueous lithium chloride desiccant system: air dehumidification and desiccant regeneration*. Solar Energy 72, 351-361.

FYLAKTOS, N., MITRA, I., TZAMTZIS, G., PAPANICOLAS, C. (2014). *Economic analysis of an electricity and desalinated water cogeneration plant in Cyprus*. Desalination and Water Treatment, 55(9), 2453-2470.

G

GARCIA NIETO, P., MARTINEZ TORRES, J., DE COS JUEZ, F., & SÁNCHEZ LASHERAS, F. (2012). Using multivariate adaptive regression splines and multilayer perceptron networks to evaluate paper manufactured using Eucalyptus globulus. Applied Mathematics and Computation,219(2), 755-763.

GHARAKHANI, A., SEDIADI, E., ROSHAN, M., SABZEVAR, HB., (2017). *Experimental Study On Perfomance Of Wind Catcher In Tropical Climate*, ARPN Journal of Engineering and Applied Sciences, Vol. 12, No. 8.

GIVONI, B., (1994). *Passive and Low Energy Cooling of Buildings,* John Wiley and Sons. Inc., Canada, pp. 3-139.

GIVONI, B., (1998). *Climate Considerations in Building and Urban Design,* John Wiley and Sons. Inc., Canada, pp. 36-37.

GIVONI, B., (2011). Indoor Temperature Reduction by Passive Cooling Systems, Solar Energy 85, pp. 1692–1726.

GIVONI, B., M.E. HOFFMAN, (1968). *Effect of Building Materials on Internal* Temperatures, Research Report, Building Research Station, Technion Haifa.

GOG, L., (1955). *Cooling with solar energy*. Congress on Solar Energy, Tucson, Arizona, 73-78.

GOMES, U. A., HELLER, L., PENA, J. L. (2012). A National Program for Large Scale Rainwater Harvesting: An Individual or Public Responsibility? Water Resources Management, 26(9), 2703-2714.

GÓMEZ, C. M., TIRADO, D., REY-MAQUIEIRA, J. (2004). *Water exchanges versus water works: Insights from a computable general equilibrium model for the Balearic Islands.* Water Resources Research, 40(10), n/a-n/a.

GRUNDMANN, R., *MEGS Seminar Series The Future of Climate Policies,* The University of Nottingham, UK, November 2013.

GUNHAN, T., DEMIR, V., & YAGCIOGLU, A., 2007. *Evaluation of the Suitability of Some Local Materials as Cooling Pads.* Biosystems Engineering, 96(3), 369-377.

H

HAGHIGHI, A.P., GOLSHAAHI, S.S., ABDINEJAD, M., (2015). *A study of vaulted roof assisted evaporative cooling channel for natural cooling of 1-floor building,* Sustainable Cities and Society, Vol.14, pp. 89-98.

HAMED, A. M., A. E. KABEEL, E-SHEFEI B. ZEIDAN, AND AYMAN A. ALY. 2010. *A Technical Review on the Extraction of Water from Atmospheric Air in Arid Zones*. JP Journal of Heat and Mass Transfer 4 (3):213–228.

HAN, J., LU, L., YANG, H. (2010). *Numerical evaluation of the mixed convective heat transfer in a double-pane window integrated with see-through a-Si PV cells with low-e coatings.* Applied Energy, 87(11), 3431-3437.

HARB, R., (2015). *Assessing The Potential Of Rainwater Harvesting System At The Middle East Technical University – Northern Cyprus Campus.* PhD. Thesis, METU.

HE, J., HOYANO, A., (2011). *Experimental study of cooling effects of a passive evaporative cooling wall constructed of porous ceramics with high water soaking-up ability*, Building and Environment, Vol.45, pp.461-472.

HE, S., GUAN, Z., GURGENCI, H., HOOMAN, K., LU, Y., & ALKHEDHAIR, A. M. (2014). *Experimental study of film media used for evaporative pre-cooling of air*. Energy Conversion and Management, 874-884. doi:101016/jenconman201407084.

HEIDARINEJAD, G., HEIDARINEJAD, M., DELFANI, S., & ESMAEELIAN, J., (2008). *Feasibility of using various kinds of cooling systems in a multi-climates country*. Energy and Buildings, Vol. 40, 1946–1953.

HOES, P., HENSEN, J., LOOMANS, M., DE VRIES, B., & BOURGEOIS, D. (2009). *User behavior in whole building simulation*. Energy and Buildings, 41(3), 295-302.

I

IESNA. (1984). IES *Lighting handbook reference volume.* New York: Illuminating Engineering Society of North America.

IOANNOU, I., ANDREOU, A., TSIKOURAS, B., & HATZIPANAGIOTOU, K. (2009). *Application of the Sharp Front Model to capillary absorption in a vuggy limestone*. Engineering Geology, 105(1-2), 20-23.

IU, J., ZHANG, T., LIU, X., JIANG, J., (2015). *Experimental analysis of an internally-cooled/heated liquid desiccant dehumidifier/regenerator made of thermally conductive plastic.* Energy and Buildings 99, 75-86.

J

JABER, S., & AJIB, S., (2011). *Evaporative cooling as an efficient system in Mediterranean region*. Applied Thermal Engineering, Vol. 31, pp. 2590-2596.

JAIN, J.K., HINDOLIYA, D.A., (2011). *Experimental performance of new evaporative cooling pad materials, Sustainable Cities and Society*, Vol.1 pp. 252-256.

JOHNSON, D.W., C. YAVUZTURK, AND J. PRUIS, (2003). *Analysis of heat and mass transfer phenomena in hollow fiber membranes used for evaporative cooling.* Journal of Membrane Science, 227(1–2): p. 159-171.

K

KABEEL, A., EL-SAMADONY, Y., KHİERA, M. (2017). *Performance evaluation of energy efficient evaporatively air-cooled chiller*. Applied Thermal Engineering, 122, 204-213.

KACHHWAHA, S.S., S. PRABHAKAR, (2010). Heat and mass transfer study in a direct evaporative cooler. Journal of Scientific & Industrial Research, 69: p. 705-710.

KADIR, A. A., ISMAIL, LH., KASIM, N., (2015). *Optimization of daylighting system by using light pipe system in a building.*

KARAGIANNIS, I. C., SOLDATOS, P. G. (2007). *Current status of water desalination in the Aegean Islands.* Desalination, 203(1-3), 56-61.

KARAGIANNIS, I. C., SOLDATOS, P. G. (2008). *Water desalination cost literature: review and assessment.* Desalination, 223(1-3), 448-456.

KARKEE, M.B. (2005) *Harvesting of atmospheric water: a promising low cost technology.* Ninth International Water Technology Conference, IWTC9 2005, Sharm El-Sheikh, Egypt. 3: 3–14.

KLEMM, O., SCHEMENAUER, R. S., LUMMERICH, A., CERECEDA, P., MARZOL, V., CORELL, D., FESSEHAYE, G. M. (2012). *Fog as a Fresh-Water Resource: Overview and Perspectives.* AMBIO, 41(3), 221-234.

KONYA, A., (1996). *Design Primer for Hot Climates*, The Architectural Press Ltd. London, pp. 39-302.

KORONAKI, I. P., CHRISTODOULAKI, R. I., PAPAEFTHIMIOU, V. D., ROGDAKIS, E. D., (2013). *Thermodynamic analysis of a counter flow adiabatic dehumidifier with different liquid desiccant materials*. Applied Thermal Engineering 50, 361-373.

KOUTSAKOS, E., SAVVIDES, K., & SAVVA, K. (2005). *Larnaca desalination plant operation—a client and contractor perspective.* Desalination, 184*(1-3*), 157-164.

KOVAČEVİĆ, I., SOURBRON, M. (2017). *The numerical model for direct evaporative cooler.* Applied Thermal Engineering, 113, 8-19.

KULKARNI, R.K., RAJPUT, S.P.S., (2010). *Theoretical performance analysis of jute fiber rope bank as media in evaporative coolers*, Indian J Sci Technol, 3 (2010), pp. 1075–1080.

KULKARNI, R.K., RAJPUT, S.P.S., 2013. *Comparative performance analysis of evaporative cooling pads of alternative configurations and materials*, International Journal of Advances in Engineering & Technology, Vol. 6, Issue 4, pp. 1524-1534.

L

LECHNER, N., (2009). *Heating, Cooling, Lighting: Sustainable Design Methods for Architects*, John Wiley & Sons, Inc., Canada, p. 43-290.

LEITE DIDONÉ, E., WAGNER, A. (2013). *Semi-transparent PV windows: A study for office buildings in Brazil.* Energy and Buildings, 67, 136-142.

LI, H., HARVEY, J., GE, Z., (2014). *Experimental investigation on evaporation rate for enhancing evaporative cooling effect of permeable pavement materials*, Journal of Construction and Building Materials, Vol. 65, pp. 367-375.

LIAO, C. M., CHIU, K.H., (2002). *Wind tunnel modelling the system performance of alternative evaporative cooling pads in Taiwan region*, Building and Environment, Vol. 37, pp. 177–187.

LING, E., BENHAM, B. (2014). *Rainwater Harvesting Systems*, VCE Publications, Virginia Tech. (15.05.2017). Retrieved from https://www.pubs.ext.vt.edu/BSE/BSE-116/BSE-116.html

LIOR, N., (2012). Sustainable energy development (May 2011) with some game-changers. *Energy* 40, 3-18.

LONGO, G. A., GASPARELLA, A., (2015). *Three years experimental comparative analysis of a desiccant based air conditioning system for a flower greenhouse: Assessment of different desiccants.* Applied Thermal Engineering 78, 584-590.

LOTFIZADEH, H., RAZZAGHI, H., & LAYEGHI, M. (2013*). Experimental performance analysis of a solar evaporative cooler with three different types of pads*. J. Renewable Sustainable Energy, 5(6), 063113. doi:10.1063/1.4831779.

LOUCAIDES, A., KOUTSAKOS, E. (2015). *Fluctuations in potable water quality in Cyprus during the past two decades – the role of seawater desalination.* Desalination and Water Treatment, 55(9), 2270-2277.

M

MA, Y., GUAN, L. (2015). *Performance Analysis of Solar Desiccant-Evaporative Cooling for a Commercial Building under Different Australian Climates*. Procedia Engineering, 121, 528-535.

MAEREFAT, M., HAGHIGHI, A.P., (2010). *Natural cooling of stand-alone houses using solar chimney and evaporative cooling cavity*, Renewable Energy, Vol.35 pp. 2040-2052.

MAHMOUD, W. H., ELAGIB, N. A., GAESE, H., HEINRICH, J. (2014). *Rainfall conditions and rainwater harvesting potential in the urban area of Khartoum*. Resources, Conservation and Recycling, 91, 89-99.

MALLİ, A., SEYF, H. R., LAYEGHİ, M., SHARİFİAN, S., BEHRAVESH, H. (2011). *Investigating the performance of cellulosic evaporative cooling pads.* Energy Conversion and Management, 52(7), 2598-2603.

MANİOĞLU, Gülten, *Enerji Etkin Binalar: Pasif Ev Örnekleri,* Tasarım Dergisi 198, İstanbul, February 2010, pp. 76-79.

MANJU, S., SAGAR, N. (2017). *Renewable energy integrated desalination: A sustainable solution to overcome future fresh-water scarcity in India.* Renewable and Sustainable Energy Reviews, 73, 594-609.

MANOLI, E., ASSIMACOPOULOS, D., KARAVITIS, C. A. (2004). *Water supply management approaches using RES on the island of Rhodes, Greece*, Desalination, 161, 179–189.

MARANGOU, V. S., & SAVVIDES, K. (2001). *First desalination plant in Cyprus — product water aggresivity and corrosion control*. Desalination, 138*(1-3), 251-258.*

MARC EL BEYROUTHY, D. E. (2015). *How Emerging Technologies and Biomimicry can Help Solving Water Problems: Desert case Studies*. Advances in Crop Science and Technology, 03(04).

MARSH, Andrew, (2003). *Ecotect and Energy Plus*. The Building Energy Simulation User News, Vol. 24, No. 6.

MARTINEZ, F. J. R., GOMEZ, E. V., GONZALEZ, A. T., MURRIETA, F. E. F., (2010). *Comparative study between aceramic evaporati*ve *cooler (CEC) and an air-source heat pump applied to a dwelling in Spain*, Energy and Buildings, Vol.42 pp. 1815-1822.

MARZOL JAÉN, M. V. (2002). *Fog water collection in a rural park in the Canary Islands (Spain).* Atmospheric Research, 64(1-4), 239-250.

MATHIOULAKIS, E., BELESSIOTIS, V., DELYANNIS, E. (2007). *Desalination by using alternative energy: Review and state-of-the-art.* Desalination, 203(1-3), 346-365.

MCMULLEN, R., (2007), *Environmental Science in Building*, 6. Edition, McMullen, UK, p. 316.

MENTIS, D., KARALIS, G., ZERVOS, A., HOWELLS, M., TALIOTIS, C., BAZILIAN, M., ROGNER, H. (2016). *Desalination using renewable energy sources on the arid islands of South Aegean Sea*. Energy, 94, 262-272.

MILLER, S., SHEMER, H., & SEMIAT, R. (2015). *Energy and environmental issues in desalination*. Desalination, 366, 2-8.

MILNES, E., (2011), Process-based groundwater salinisation risk assessment methodology: Application to the Akrotiri aquifer (Southern Cyprus). Journal of Hydrology, Vol. *399*(1-2), pp. 29-47.

MIYAZAKI, T., AKISAWA, A., NIKAI, I., (2011). The cooling performance of a building integrated evaporative cooling system driven by solar energy, Energy and Buildings, Vol.43 pp. 2211-2218.

MOAVENI, H. (2010), '*Technical and Economic Analysis of Solar Cooling Systems in a Hot and Humid Climate'*, Proceedings of the 17th Symposium for Improving Building Systems in Hot and Humid Climates, Austin TX, 24–25 August.

MODESTOU, S., THEODORIDOU, M., FOURNARI, R., & IOANNOU, I. (2015). Physico-mechanical properties and durability performance of natural

building and decorative carbonate stones from Cyprus. Geological Society, London, Special Publications.

MOFFAT, R. J. (1988). *Describing the uncertainties in experimental results.* Experimental Thermal and Fluid Science, 1(1), 3-17.

MOHAMMAD A, MAT S, SULAIMAN MY, SOPIAN K., (2013). *Experimental performance of a direct evaporative cooler operating in Kuala Lumpur.* Int J Therm Environ Eng;6(1):15–20.

MONTAZERI, H. (2011). Experimental and numerical study on natural ventilation performance of various multi-opening wind catchers. Building and Environment, 46(2), 370-378.

MONTREAL PROTOCOL, (1987). Montreal Protocol on Substances That Deplete the Ozone Layer United Nations (UN), New York, NY, USA.

MOORE, F., (1993). Environmental Control Systems (heating, cooling, lighting), McGraw-Hill, Inc., United States of America, pp. 30-202.

MUNARI PROBST, MC., ROECKER, C., (2011). *Architectural integration and design of solar thermal systems.* Milton Park, Abingdon: Routledge, p.p. 27-51.

MUNARI PROBST, MC., ROECKER, C., (editors). *Solar Energy Systems in Architecture - integration criteria and guidelines.* Report T.41.A.2. IEA SHC Task 41, Subtask A; 2012.

MURAD, A. A., (2010). *An Overview of Conventional and Non-Conventional Water Resources in Arid Region: Assessment and Constrains of the United Arab Emirates (UAE).* Journal of Water Resource and Protection, 02*(02),* 181-190.

MUSA, M., (2008). *Novel evaporative cooling systems for building* applications. PhD thesis, University of Nottingham, p. 42-63.

N

NATICCHIA, B., D'ORAZIO, M., CARBONARI, A., PERSICO, I., (2010). *Energy performance evaluation of a novel evaporative cooling technique*, Energy and Buildings, Vol.42 pp. 1926-1938.

NGUYEN, T. C. (5 May 2017). Retrieved from SMITHSONIAN.COM http://www.smithsonianmag.com/innovation/this-tower-pulls-drinking-water-out-of-thin-air-180950399/?no-ist

NOTT, K., SAVAGE, M. (1985). *Observations on the utilization of a dune succulent by Namib faunae*. South African Journal of Zoology, 20(4), 269-271.

NURAJE, N., KHAN, W. S., LEI, Y., CEYLAN, M., ASMATULU, R. (2013). *Superhydrophobic electrospun nanofibers*. J. Mater. Chem. A, 1(6), 1929-1946.

O

OJEMBARRENA, J., CHANAMPA, M., RIVAS, P., OLIVIERI, F., ARAGONÉS, R., NEILA GONZÁLEZ, F., FRUTOS, C. (2013). *Thermal and Illuminance Performance of a Translucent Green Wall*, J. Archit. Eng., Vol. 19(4), pp. 256–264.

OLGYAY, A., OLGYAY, V., (1957). *Solar Control & Shading Devices*, Princeton University Press, Princeton, p. 64.

OLIVIER, J., (2004). *Fog-water harvesting along the West Coast of South Africa: a feasibility study.* Water SA;28(4):349–60.

OMORPHOS, C., IOANNOU, E., (2000), *Southern Conveyor Project*, Ministry of Agriculture, Natural Resources and Environment, Cyprus.

ORTIZ, J., EXPOSITO, E., GALLUD, F., GARCIAGARCIA, V., MONTIEL, V., & ALDAZ, A. (2008). *Desalination of underground brackish waters using an electrodialysis system powered directly by photovoltaic energy*. Solar Energy Materials and Solar Cells, 92(12), 1677-1688.

P

PARK, K., CHHATRE, S. S., SRINIVASAN, S., COHEN, R. E., MCKINLEY, G. H. (2013). *Optimal Design of Permeable Fiber Network Structures for Fog Harvesting.* Langmuir, 29(43), 13269-13277.

PASHARDES, S., CHRISTOFIDES, C., (1995). *Statistical analysis of wind speed and direction in Cyprus*. Solar Energy, Vol.55 pp.405-414.

PHAN, R. S., *The Development of Passive Downdraught Evaporative Cooling Systems Using Porous Ceramic Evaporators and their application in residential Buildings,* The 21th Conference on Passive and Low Energy Architecture. Eindhoven, The Netherlands, 2004.

POHL, J., (2011). *Building Science: concepts & application*, Wiley-Blackwell, UK, p. 51.

POSHTIRI, A. H., MOHABBATI, S. M. (2017). *Performance analysis of wind catcher integrated with shower cooling system to meet thermal comfort conditions in buildings.* Journal of Cleaner Production, 148, 452-466.

Q

QIBLAWEY, H. M., & BANAT, F. (2008). *Solar thermal desalination technologies.* Desalination, 220(1-3), 633-644.

QIU G. Q, RIFFAT S. B., (2010). *Experimental investigation on a novel air dehumidifier using liquid desiccant.* Int J Green Energy; 7:174–80.

QIU G. Q, RIFFAT S. B., ZHU J., (2008). *Novel liquid regeneration system with solar evacuated tubes and evaporative bed.* J Energy Institute; 81:92 –6.

R

RAFIQUE, M.M., GANDHIDASAN, P., REHMAN, S. AND ALHEMS, L.M., (2016). *Performance analysis of a desiccant evaporative cooling system under hot and humid conditions.* Environmental Progress & Sustainable Energy, 35(5), pp.1476-1484.

RAFIQUE, M. M., GANDHIDASAN, P., BAHAIDARAH, H. M. (2016). *Liquid desiccant materials and dehumidifiers – A review*. Renewable and Sustainable Energy Reviews, 56, 179-195.

RAPOPORT, A., (1969). *House, form and culture*, Prentice-Hall, USA, pp. 18-19.

RASHIDI MEHRABADI, M. H., SAGHAFIAN, B., HAGHIGHI FASHI, F. (2013). *Assessment of residential rainwater harvesting efficiency for meeting non-potable water demands in three climate conditions*. Resources, Conservation and Recycling, 73, 86-93.

RAWANGKUL, R., KHEDARI, J., HIRUNLABH, J., ZEGHMATI, B., (2008). *Performance analysis of a new suitable evaporative cooling pad made from coconut coir.* Int J Sustainable Eng;1:117–31.

REDDY, P. J., (2010). *Science Technology of Photovoltaics*, New Delhi: BS Publications, p. 199.

REINHART, C. F., WIENOLD, J. (2011). *The Daylighting Dashboard - A Simulation-Based Design Analysis for Daylit Spaces.* Building and Environment. Vol. 46: 386–396.

RIEBEEK, H., (2010). Global Warming. Available from: *http://earthobservatory.nasa.gov/Features/GlobalWarming/* [Accessed: 1 November 2014].

ROGDAKIS, E.D., KORONAKI, I.P., TERTIPIS, D.N. (2013). Estimation of the water temperature Influence on direct evaporative cooler operation, Int. J. Thermodynam. 16/4, p.p. 172–178.

ROGDAKIS, E. D., KORONAKI, I. P., TERTIPIS, D.N., (2014). *Experimental and computational evaluation of a Maisotsenkoevaporative cooler at Greek climate,* Energy and Buildings, Vol. 70, pp. 497–506.

ROTH, L. M., 2007. *Understanding Architecture: Its Elements, History, And Meaning*, Perseus-Westview Books, UK, pp. 1-9.

S

SAHLOT, M., RIFFAT, S. B. (2016). *Desiccant cooling systems: a review*. Int J Low-Carbon Tech, 11 (4): 489-505.

SANTAMOURIS, M., ASIMAKOPOULOS, D. N. (1996). *Passive cooling of buildings*. London: James & James.

SAVVIDES, L., DÖRFLINGER, G. AND ALEXANDROU, K. (2001). *The Assessment of Water Demand of Cyprus', in: Reassessment of the Island's Water Resources and Demand*. Water Development Department and Food and Agricultural Organisation. Nicosia, Cyprus.

SHALABY, S. (2017). *Reverse osmosis desalination powered by photovoltaic and solar Rankine cycle power systems: A review*. Renewable and Sustainable Energy Reviews, 73, 789-797.

SHATAT, M., WORALL, M., RIFFAT, S. (2013). *Opportunities for solar water desalination worldwide:* Review. Sustainable Cities and Society, 9, 67-80.

SHRIVASTAVA, K., DESHMUKH, D., RAWLANI, M. V., (2014). *Experimental Analysis of Coconut Coir Pad Evaporative Cooler,* International Journal of Innovative Research in Science, Engineering and Technology, Vol. 3, pp. 8346-8351.

SILVA, C. M., SOUSA, V., CARVALHO, N. V. (2015). *Evaluation of rainwater harvesting in Portugal: Application to single-family residences.* Resources, Conservation and Recycling, 94, 21-34.

SIMBERLOFF, D., REJMÁNEK, M., 2011. *Encyclopedia of biological invasions*. Berkeley: University of California Press.

SOCRATOUS, G., (2011). *Integrated Water Resources Planning in Cyprus. Water Resources Allocation,* 111-124.

SODHA, M.S., BANSAL, N.K., BANSAL, P.K., KUMAR, A., MALIK, M. A. S., (1986). Solar Passive Building: Science and Design, Pergamon Press, Vol. 2, UK, p. 127-302.

SOFRONIOU, A., BISHOP, S. (2014). *Water Scarcity in Cyprus: A Review and Call for Integrated Policy*. Water, 6(10), 2898-2928.

SOHANI, A., SAYYAADI, H., HASANI BALYANI, H., & HOSEINPOORI, S. (2016). *A novel approach using predictive models for performance analysis of desiccant enhanced evaporative cooling systems.* Applied Thermal Engineering, 107, 227-252.

SOPONPONGPIPAT, N., KOSITCHAIMONGKOL, S., (2011). *Recycled High-Density Polyethylene and Rice Husk as a Wetted Pad in Evaporative Cooling System*. American Journal of Applied Sciences, 8(2), 186-191.

SULAIMAN, F. A., (2002). *Evaluation of the performance of local fibres in evaporative cooling,* Energy Conversion and Management, Vol. 43, pp. 2267–2273.

SZOKOLAY, Steven V., (2008). *Introduction to Architectural Science: The Basis of Sustainable Design,* Architectural Press, p. 63.

T

TABOR, H., 1966. *Mirror boosters for solar collectors*. Solar Energy 10 (3), 111–118.

TALEGHANI, M., TENPIERIK, M., KURVERS, S., & VAN DEN DOBBELSTEEN, A. (2013). *A review into thermal comfort in buildings*. Renewable and Sustainable Energy Reviews, 26, 201-215.

TAYLOR, J.R., (1997). *An Introduction to Error Analysis: The Study of Uncertainties in Physical Measurements*, second ed., University Science Books, Sausalito, CA.

TSIOURTIS, N. X. (2003). *Small Islands Water Resources Development-a holistic approach*, Water Development Department, Nicosia, Cyprus.

TOMASZKIEWICZ, M., ABOU NAJM, M., ZURAYK, R., & EL-FADEL, M. (2017). *Dew as an adaptation measure to meet water demand in agriculture and reforestation.* Agricultural and Forest Meteorology, 232, 411-421.

TORCELLINI, P., PLESS, S., DERU, M., GRIFFITH, B., LONG, N., JUDKOFF, R. (2006). *Lessons Learned from Case Studies of Six High-Performance Buildings.* **U**

UNEP, (2007a). *Adopted by the Nineteenth Meeting of the Parties to the Montreal Protocol on Substances that Deplete the Ozone Layer*. United Nations Environment Programme (UNEP) Ozone Secretariat, Nairobi, Kenya (2007).

V

VALA, K., KUMPAVAT, M., & NEMA, A. (2016). *Comparative Performance Evaluation of Evaporative Cooling Local Pad materials with Commercial Pads.* International Journal of Engineering Trends and Technology, 39(4), 198-203.

W

WANPHEN, S., & NAGANO, K. (2009). *Experimental study of the performance of porous materials to moderate the roof surface temperature by its evaporative cooling effect.* Building and Environment, 44(2), 338-351.

WARKE, D. A., DESHMUKH, S. J., (2017). *Experimental Analysis of Cellulose Cooling Pads Used in Evaporative Coolers*. International Journal of Energy Science and Engineering, 3(4), pp. 37-43.

WATER RESEARCH AND MANAGEMENT - THE CYPRUS INSTITUTE. Retrieved from https://www.cyi.ac.cy/index.php/eewrc/eewrc-research-projects/water-research-management.html [05 May 2017].

WICKRAMASINGHE, S.R., M.J. SEMMENS, AND E.L. CUSSLER, (1993). *Hollow fiber modules made with hollow fiber fabric.* Journal of Membrane Science, 84(1): p. 1-14.

WONG, N. H., TAN, A. Y., CHEN, Y., SEKAR, K., TAN, P. Y., CHAN, D., WONG, N. C. (2010). *Thermal evaluation of vertical greenery systems for building walls.* Building and Environment, Vol. 45, pp. 663-672.

WU, J., HUANG, X., ZHANG, H. (2009). *Theoretical analysis on heat and mass transfer in a direct evaporative cooler*. Applied Thermal Engineering, 29(5-6), 980-984.

X

XUE, P., MAK, C., CHEUNG, H. (2014). *New static lightshelf system design of clerestory windows for Hong Kong.* Building and Environment, 72, 368-376.

Z

ZHANG, L.-Z., (2012). *Coupled heat and mass transfer in an application-scale cross-flow hollow fiber membrane module for air humidification*. International Journal of Heat and Mass Transfer, 55(21–22): p. 5861-5869.

ZHANG, S., HUANG, J., CHEN, Z., LAI, Y. (2017). *Bioinspired Special Wettability Surfaces: From Fundamental Research to Water Harvesting Applications.* Small, 13(3), 1602992.

ZEILER, W., VISSERS, D., (2012). *Active Roof Cooling of Atria*. PLEA2012 – 28th Conference, Opportunities, Limits & Needs Towards an environmentally responsible architecture Lima, Peru.

ZUBERI, M. J. S., KHAN, M. A. A., AKINTUG, B., (2013). *Rainwater Harvesting System for Dormitories of METU - Northern Cyprus Campus,* Istanbul: Seventeenth International Water Technology Conference, IWTC17, Session 5: Purification, Plants and Networks (PP)